University of Wollongong

Research Online

University of Wollongong Thesis Collection 1954-2016

University of Wollongong Thesis Collections

2016

Walking With Indonesian elephants: attribution of isolated proboscidean femurs and tibias to genus based on morphological differences

Unggul Prasetyo Wibowo
University of Wollongong

Follow this and additional works at: https://ro.uow.edu.au/theses

University of Wollongong

Copyright Warning

You may print or download ONE copy of this document for the purpose of your own research or study. The University does not authorise you to copy, communicate or otherwise make available electronically to any other person any copyright material contained on this site.

You are reminded of the following: This work is copyright. Apart from any use permitted under the Copyright Act 1968, no part of this work may be reproduced by any process, nor may any other exclusive right be exercised, without the permission of the author. Copyright owners are entitled to take legal action against persons who infringe their copyright. A reproduction of material that is protected by copyright may be a copyright infringement. A court may impose penalties and award damages in relation to offences and infringements relating to copyright material. Higher penalties may apply, and higher damages may be awarded, for offences and infringements involving the conversion of material into digital or electronic form.

Unless otherwise indicated, the views expressed in this thesis are those of the author and do not necessarily represent the views of the University of Wollongong.

Recommended Citation

Wibowo, Unggul Prasetyo, Walking With Indonesian elephants: attribution of isolated proboscidean femurs and tibias to genus based on morphological differences, Master of Philosophy thesis, School of Earth and Environmental Sciences, University of Wollongong, 2016. https://ro.uow.edu.au/theses/4803

Research Online is the open access institutional repository for the University of Wollongong. For further information contact the UOW Library: research-pubs@uow.edu.au

UNIVERSITY OF WOLLONGONG

Walking With Indonesian Elephants: Attribution of Isolated Proboscidean Femurs and Tibias to Genus Based on Morphological Differences

A thesis submitted in fulfilment of the requirements for the award of the degree

Master of Philosophy

From

University of Wollongong

by
Unggul Prasetyo Wibowo

Department of Science, Medicine and Health

2016

CERTIFICATE OF ORIGINALITY

I hereby declare that this submission is my own work and that, to the best of my knowledge and belief, it contains no material previously published or written by another person nor material which to a substantial extent has been accepted for the award of any other degree or diploma of a university or other institute of higher learning except where due acknowledgment is made in the text.

I also declare that the intellectual content of this thesis is the product of my own work, even though I may have received assistance from others on style, presentation and language expression.

Unggul Prasetyo Wibowo

(Signed)…….....

Date: 25/08/2016

ABSTRACT

Direct comparison and biometric measurement analysis of homologue skeletal elements pertaining to distinct members of closely related vertebrate taxa (genera and species) can reveal qualitative diagnostic distinctive characteristics that reflect phylogeny and that may be related to differences in functional morphology. Apart from morphological differences, size can be an important factor in distinguishing taxa, especially when considering dwarfed insular proboscideans. Dwarfed proboscideans were once present on several islands of Indonesia during the Quaternary, but their postcranial remains have hardly been studied in detail. Most studies on fossil proboscideans focus on cranial and dental elements, which are comparatively easy to distinguish. In the case of proboscidean limb bones, morphological differences may be associated with different types of locomotion and could represent specific adaptations to insular environments. In order to investigate such adaptive morphologies in detail, a first step is to assess which differences exist between closely related genera. Establishing a list of diagnostic criteria to distinguish limb bones of different proboscidean genera and species will also aid in identifying isolated specimens of these elements.

This study applied biometric analysis combined with 3D Geometric Morphometric (GM) analysis of fossil and recent skeletal parts of Indonesian proboscideans. The study aimed at characterizing the morphological differences between proboscidean taxonomic groups of two skeletal elements, the femur and the tibia. These elements were chosen because complete specimens of femur (n=10) and tibia (n=10) of known identity (based on associated dental elements) are relatively common in Indonesian fossil collections and were easily accessible. The studied sample comprises a recently excavated femur and tibia of a single adult individual of the very small-sized *Stegodon sondaari* from Flores. This offered the opportunity for the first time to investigate if this insular dwarf proboscidean possessed specific adaptations (apart from its small size) that are frequently encountered in insular megafauna, such as shortened distal limbs.

First a surface morphology assessment and Principal Component Analysis (PCA) of biometric variables taken from the literature were performed on femurs and tibias of known species pertaining to the genera *Stegodon*, *Elephas* and *Sinomastodon*. PCA resulted in only a weak grouping predominantly according to size. Because dwarfed proboscidean taxa were included in the PCAs, size differences rather than morphological differences tended to

dominate the grouping outcome. Next, a Geometric Morphometric (GM) analysis was performed on the same specimens to investigate additional shape differences of femurs and tibias. All specimens were 3D scanned and a set of meaningful 3D landmarks was defined. Following size and orientation adjustments of the 3D coordinates (procrustes registration) a PCA was performed on the 3D shapes combined with visualization of the outcome with wireframe images. This revealed a set of additional distinctive morphological features for both the femur and the tibia. *Stegodon* and *Sinomastodon* both have a more robust femur and tibia than *Elephas*. This is expressed by the new composite variable Total Length/Minimum Circumference, which is significantly smaller in *Stegodon* and *Sinomastodon* than in *Elephas.* For the femur other new variables that separate genera are the length of the third trochanter and the angle of shaft rotation. The third trochanter is longer and more flaring outward in *Stegodon* and *Sinomastodon* than in *Elephas*, which has a weakly developed third trochanter and as a result a more columnar femur. The angle of femur rotation in *Elephas* shows greater values than in most S*tegodon* and *Sinomastodon*, with the exception of *Stegodon sondaari*, which has a rotational angle even greater than in *Elephas*. Regarding the tibia, all *Stegodon* specimens have a markedly deeper and longer medial collateral ligament (MCL) attachment scar than in *Elephas* (no *Sinomastodon* tibia was available for study).

The differences between *Stegodon* and *Elephas* suggest that the *Elephas* hindlimb is designed to restrict movement and reduce energy consumption, while the *Stegodon* hindlimb is more flexible in movement during locomotion and has a higher strength and robustness. The more slender and columnar hindlimb of *Elephas* is shared with *Mammuthus* and supports a shared close common ancestry for these genera, while the more robust hindlimb bones of *Stegodon* and *Sinomastodon* are the primitive character state that is shared with *Mammut.* These results support classification of *Elephas* and *Stegodon* into distinct subfamilies. The *Stegodon sondaari* hindlimb is morphologically different from all other *Stegodon* species examined, in showing a mixture of advanced and primitive morphologies. The *S. sondaari* femur has the longest and most widely flaring third trochanter of all taxa investigated, and its femur rotation angle is even greater than in *Elephas*. Although *S. sondaari* does not appear to exhibit a relative shortening of the distal hindlimb, its specific hindlimb morphology may reflect an adaptation to locomotion in a rugged and steep mountainous terrain. However, more fossil material would be required to verify this hypothesis, particularly of the pelvis.

ACKNOWLEDGEMENTS

I gratefully acknowledge the University of Wollongong for providing me with a scholarship for this research. Fieldwork in Flores and visits to the various museums in Central Java were financed by an Australian Research Council (ARC) Discovery grant to Mike Morwood/Gert van den Bergh (DP1093342).

I would like to express my deep appreciation to my supervisors Dr. Gerrit van den Bergh and Dr. Susan Hayes for their help, encouragement and guidance during the study.

I'm also indebted to the Head of Postgraduate Studies, Dr. Samuel Marx, the former Head of the School of Earth & Environmental Sciences of the University of Wollongong, Professor Colin Murray Wallace and Professor Zenobia Jacobs. Special gratitude also goes to all academic, administrative and technical staff of the department.

Special thanks are forwarded to the former Head of the Geological Agency, Energy and Mineral Resources Ministry (EMRM) of Indonesia, Dr. Surono; the Expert Staff for Spatial Planning and Environment of EMRM, Dr. Yunus Kusumahbrata; the Secretary of the Geological Agency, Ir. Imam Sinulingga; the former Director of the Geological Survey Institute, Ir. Agung Pribadi M.Sc.; the former Director of the Geology Museum in Bandung, Ir. Sinung Baskoro, M.T.; and the Manager of the Documentation and Conservation Section of the Geology Museum, Iwan Kurniawan, S.T.

My sincere appreciation is also extended to the following people for granting me permission to use their facilities and generously spending time and efforts with me: Mr. Jamin of the Patiayam Museum, Pati, Central Java, for access to fossil specimens in the collection under his care; Mr. Donan Satria Yudha, S.Si., M.Sc. of the Biology Museum of Gajah Mada University, Yogyakarta, for granting me access to recent *Elephas maximus* skeletons; Mr. Sukronedi, S.Si., M.A. of the Centre for Ancient Human Preservation Sites of Sangiran, Sragen, Central Java, for access to fossil proboscidean specimens.

Many thanks are also forwarded to my colleagues, Mas Ruli, Mas Dida, Pak Thomas, Mika, Mba Wulan and to all researchers and administrative and technical staff of the Geological Museum of Bandung.

Finally, I would especially like to thank my wife Windi Restyana Rahayu for her love and support and both our parents for their support and encouragement throughout my studies.

TABLE OF CONTENTS

LIST OF FIGURES

LIST OF TABLES

1. INTRODUCTION

1.1. Background

Palaeontology is concerned with understanding what fossil remains indicate regarding the adaptations and evolutionary processes of organisms, either as individuals or as populations (Pojeta & Springer 2001). In the past, paleontological research was mostly descriptive of the fossils, and used qualitative and quantitative measures (e.g. van der Maarel 1932; Hooijer 1964). Current palaeontological research includes quantitative statistical analyses, such as Principle Components Analyses (PCA), which compare fossil measures (Bonnan 2004; Hammer & Harper 2006), and Geometric Morphometric analysis (GM) which registers differences in fossil shapes (e.g. O'Higgins 2000; Finlay & Cooper 2015).

Exploration and research related to Indonesian proboscidean fossils have been done by many researchers. These fossils were sometimes found associated with stone artefacts and hominin fossils, and so far fossil proboscidea have been recovered from Java (Leinders et al. 1985), Sulawesi (van Heekeren 1958), and the islands of Eastern Nusa Tenggara, Flores, and Timor (Glover & Glover 1970; Maringer & Verhoeven 1975; van den Bergh et al. 2009). Many other fossil vertebrate remains have been recovered from these Indonesian islands, but proboscidean fossils usually represent a significant proportion of the finds (van den Bergh 1999). Fossil vertebrates, and in particular proboscidean fossils, have become an important tool in the reconstruction of fauna migration routes, adaptation to environmental change and evolution in the region (Audley-Charles & Hooijer 1973; van den Bergh 1999).

A primary objective of palaeontological studies is to distinguish and identify taxa based on morphological distinctive features. Distinctive features used to identify and recognise proboscidean taxa are predominantly based on dental characteristics and/or distinctive features from the skull (Todd 2010). The teeth and skulls are good to identify proboscidean taxa, because they have comparatively clear and distinctive morphological features. However, identification is limited when only postcranial proboscidean fossils are recovered, or if the associated dental/skull remains are not in a good and complete condition. Proboscidean hindlimb bones (the femur and tibia) are the kind of

proboscidean fossils that seem to be most frequently discovered in a good condition. The focus of this palaeontological research is all of the documented and reasonably complete fossil hindlimb bones of proboscidea discovered or excavated from the Indonesian Archipelago, and currently stored in Indonesian research institutions. While stored in Indonesian research institutions like Museums and Universities, they often remain ignored.

Because of their good preservation and because many are recovered without associated teeth and skulls and cannot be identified, this research tests whether the isolated proboscidean hindlimb bones can be used to distinguish the proboscidean taxa. If so, this would mean that the hindlimb bones could be used as an alternative or additional identification tool other than identification that is based on dental and skull elements alone. The aim of this research is therefore to try to find and characterise features of hindlimb bone morphology to distinguish proboscidean taxa, using qualitative features and quantitative measures that can be easily applied using standard techniques.

The qualitative features are those characteristic features of the femur and tibia from each taxa. The quantitative features are those used in biometric analyses. Biometrics is the study of measurable biological characteristics of a species (Hammond & Kenchington 1978), and are used to identify individuals as belonging to a certain species (Pesquero et al. 2006). Biometric parameters (e.g. lengths, widths, measures of circumferences, angles, etc.) are the anatomical features that are measured and their values are used to quantify the features of proboscidea. These measurements also produce data that can be used to do statistical analyses.

Additional measurements that may assist in assigning a genera or species can be explored using 3D geometric morphometrics (GM). GM uses 3D landmarks (defined points on a bone) and the relationship between all of the 3D landmarks are used in the statistical analyses. Because all of the landmarks are analyzed, and not just the anatomical landmarks used in previously published biometric parameters of proboscidea (Pevzner & Vangengeim 2001), the GM analyses may indicate new biometric parameters or features of shapes that can be used to identify proboscidean fossils.

Using qualitative, quantitative and GM analyses, this study addresses the following question:

> Anatomically, are there any quantifiable morphological differences as well as similarities in the hindlimb bones amongst proboscidean taxa that are known to have been present in Indonesia during the Quaternary (~ 2.58 million years ago to present): *Elephas maximus*, *Elephas hysudrindicus*, *Stegodon trigonocephalus*, *Stegodon florensis*, *Stegodon sondaari* and *Sinomastodon bumiajuensis*?

If there are quantifiable morphological differences, then this will lead to further research. For example, a verification study using a larger sample including Indonesian fossil proboscidea currently stored outside of Indonesia (Hooijer 1955; de Vos & Aziz 1989); whether the results of this study are applicable to other fossil proboscidea recovered outside of Indonesia; and, how the morphological differences identified in this study reflect adaptation in locomotion and/or if they reflect taxonomic affinities within the family of the proboscidea.

1.2. Thesis Objectives

The goal of this thesis is to provide information and methods that will help identify isolated proboscidean hindlimb bones that have been discovered in the Indonesian Archipelago (e.g. van der Maarel 1932; Setiyabudi et al. 2012), and future discoveries. This goal contains the following specific objectives:

1) A review of the literature on proboscidea, particularly as it relates to the morphology of the proboscidean hindlimb;
2) To gain new information about proboscidean hindlimb morphology, and in particular the extinct proboscidea from the Indonesian Archipelago;
3) To examine the biometric and landmark variability in extant and fossil Indonesian proboscidean hindlimb bones;
4) To identify possible proboscidean hindlimb bone determination methods that agree with the dental and skull methods, and as a result, to make a recommendation of potentially key characteristics that will assist in determining the genera and species of Indonesian proboscidean hindlimb fossils;
5) To provide a summary of this new information and make recommendations for future research.

1.3. Thesis Structure

The organization of the thesis is shown in detail in the Table of Contents and described briefly as follows:

Chapter 1. Brief introduction and thesis outline

Chapter 2. Literature Review: Proboscidea

A summary of research into proboscidea in the general areas relevant to the research, with a focus on Indonesian fossil proboscidea, and the anatomy and morphology of the proboscidean hindlimb.

Chapter 3. Materials and Methods

A description of the specimens: genera and species (where known), source, geo-chronological context (where known), preservation, and the methods used to analyse the specimens that are common to both of the experiments undertaken.

Chapter 4. Results

This study has two experiments. The first involves a statistical analysis of Indonesian proboscidean specimens that have been designated a genus and species on the basis of associated dental and/or skull characteristics (10 femur and 10 tibia from identified specimens). The second experiment is an initial trial to see whether the results of the first experiment are able to predict the genus (and possibly species) of a collection of unidentified Indonesian proboscidean hindlimb bone fossils (7 femurs and 1 tibia from unidentified specimens).

Chapter 5. Discussion

The main focus is what the experiments indicate regarding how to distinguish Indonesian proboscidea from the hindlimb bones so that they have the agreement with classifications determined from dental and/or skull characteristics, and how these findings relate to current and past research.

Chapter 6. Conclusions and Recommendations

A summary of the findings and recommendations resulting from this study, and what these results indicate for further research.

2. PROBOSCIDEA

The order proboscidea includes the largest ever terrestrial mammals in history following the re-examination of a very large *Palaeoloxodon namadicus* femur specimen in the collections of the British Museum (Larramendi 2016). The smallest member of the order, *Paleoloxodon falconeri*, was only 80 cm high (Larramendi & Palombo 2015). People commonly recognise these mammals by their distinctive trunk and call them an elephant. However, the earliest known proboscidea (*Eritherium azzouzorum*) lived at least 60 million years ago and did not have a trunk, but only a prototrunk; a nose with nostrils in its tip (Andrews 1906). The word proboscidea comes from the Latin word 'proboscis', meaning trunk (Osborn 1936), and so the proboscidea (see Figure 2.1) is the order of mammals with trunks, and this includes their more primitive relatives with prototrunks. This order was first described by Illiger in 1811 (Shoshani & Tassy 2005; Vergiev & Markov 2010).

Proboscidea is classified into the clade Tethytheria, together with their extant sister group Sirenia, and the extinct order Desmostylia (Gohlich 1999). Proboscidea consists of several families, but there is only one extant family, *Elephantidae*, and within this family, there are only two extant genera, *Loxodonta* in Africa and *Elephas* in Asia (see Figure 2.2). The three extant species within these genera are: the forest African elephant (*Loxodonta cyclotis*), the bush African elephant (*Loxodonta africana*) (Laursen & Bekoff 1978), and the Asian elephant (*Elephas maximus*, which has three subspecies) (Shoshani & Eisenberg 1982).

Osborn produced the first comprehensive description of the order of proboscidea in monographs he published in 1936 and 1942 (Shoshani & Tassy 2005). These monographs embrace the discovery, evolution, migration, extinction and classification of the proboscidean order. Over time many researchers have further developed the classification of proboscidea and provided more detail. The proboscidean classification has risen to the level of genus and been compiled by several authors (Shoshani & Tassy 2005; Shoshani et al. 2006; Gheerbrant 2009) and can be seen in Table 2.2.

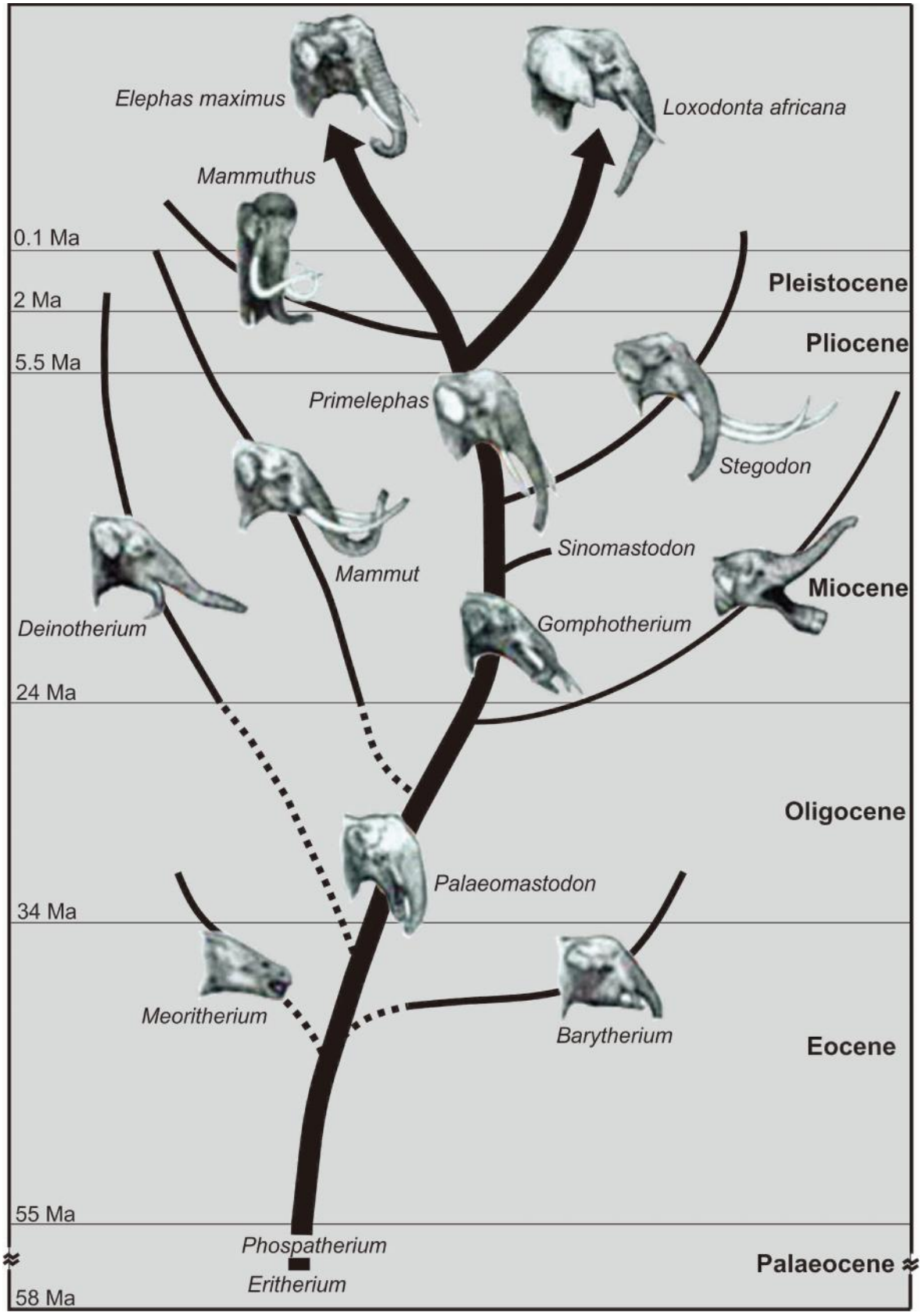

Figure 2.1. General review of the proboscidea from the Early Tertiary to the Holocene period, including Sinomastodon (modified from Shoshani 2002).

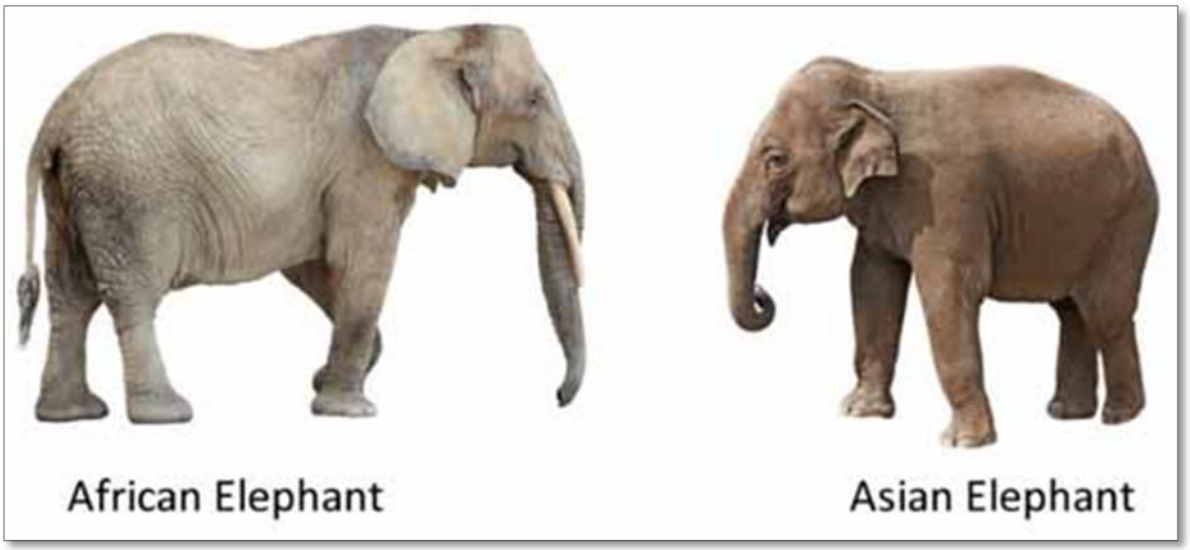

Figure 2.2. The two extant Elephantidae genera (International Elephant Foundation 2014).

2.1. Proboscidean Evolutionary History

The distribution history of proboscidea from a geological perspective starts from the Early Tertiary period, about 60 million years ago (see Figure 2.1). This earliest known proboscidean, *Eritherium azzouzorum* (Gheerbrant 2009), was excavated from Dogali in Eritrea, Africa, and is from the early Late Paleocene period (Gheerbrant 2009). In the Early Eocene period, *Eritherium* was then followed by a small proboscidea which was about the size of a fox, named *Phosphatherium* (Gheerbrant, Sudre & Cappetta 1996) (see Figure 2.1). Other proboscidean fossils that originate from Eocene deposits in Africa are *Numidotherium* (Mahboubi et al. 1986) from El Kohol in Algeria, *Daouitherium* from Ouled Abdoun in Morocco (Gheerbrant et al. 2002) and *Moeritherium* from El-Fayum, Egypt (Andrews 1904; Andrews, 1906).

Based on *Moeritherium* fossils, Andrews (1904) proposed that Africa was the evolutionary origin of proboscideans (see Figure 2.3). Also based on the *Moeritherium* fossil morphology and the geological context of where the *Moeritherium* was discovered, some researchers have argued that proboscidea had a semi-aquatic ancestor (Andrews 1906; Matsumoto 1923; Osborn 1936; Gaeth, Short & Renfree 1999) and that proboscidea have an aquatic adaptation; for example, the position of the eye sockets, are located high up on the skull like in Hippopotamus, which to accommodate underwater activity (Andrews 1904; Janis 1988). As will be discussed in the next section, proboscidea are good swimmers and can cross water

barriers. However, the aquatic adaptation hypothesis still need further research, to get a clearer picture about whether this is indeed the case.

During the Early Tertiary period, proboscidea are thought to have first evolved in the African continent. *Mastodons* were the first group to leave Africa and migrated through Eurasia to the northern part of the American continent in the Late Miocene (Fiedel 2009), and some members of the family eventually continued their migratory path to the South American continent during the Late Pliocene (Mothe, Avilla & Cozzuol 2012). During Pleistocene, *Stegodon* migrated from southern Asia to the Indonesian and Philippine Archipelagos, to then become extinct in the Pleistocene age (van den Bergh, de Vos & Sondaar 2001). During this Pleistocene, the elephants that expanded in Africa and Asia were spread out into northern America and western Europe (see Figure 2.3) (Shoshani 1998; Shoshani 2002).

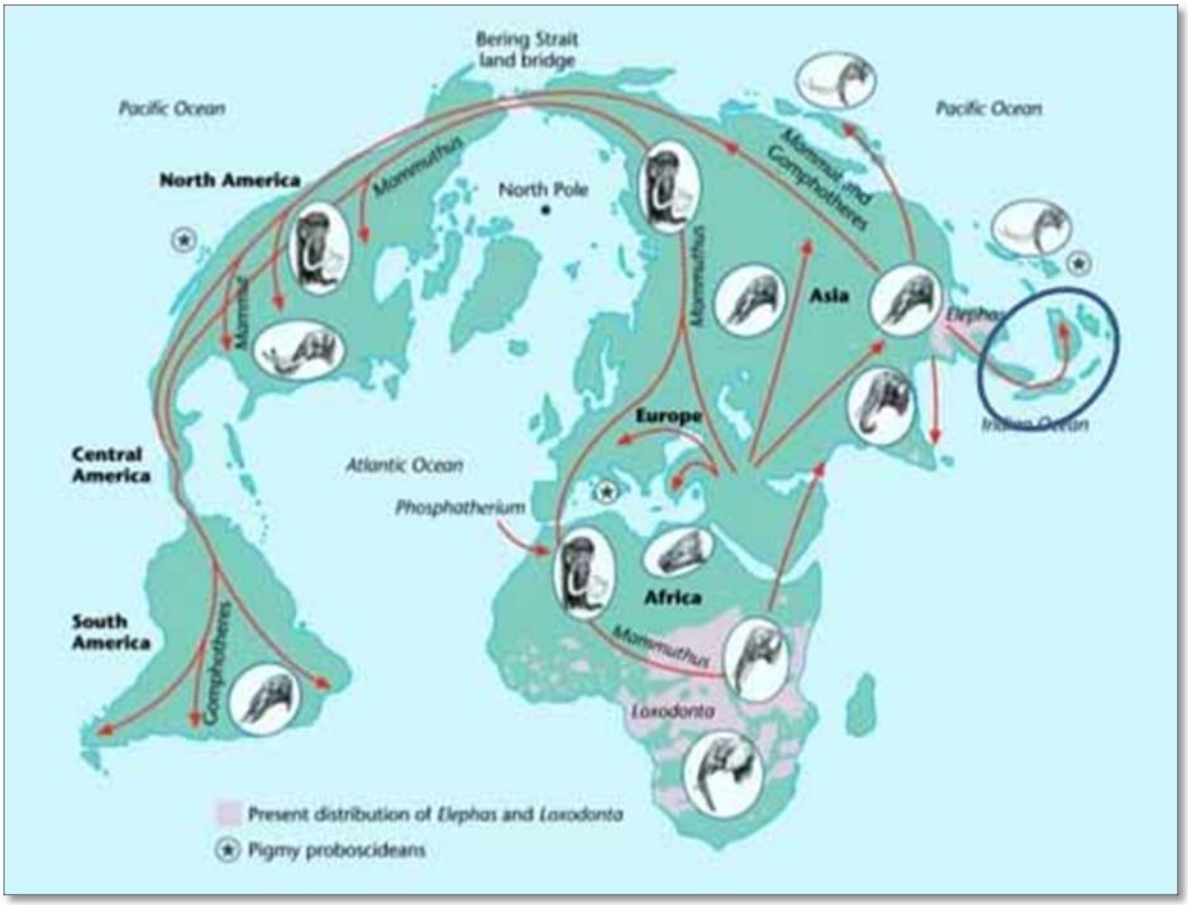

Figure 2.3. The paths of distribution of proboscidea during the geological times of their existence. The Indonesian Archipelago is shown within a blue oval (modified from Shoshani 2002).

2.1.1. Indonesian Proboscidea

The proboscidean migration and dispersal into the Indonesian Archipelago is highly related to the geological context of the archipelago, which had a strong influence on the distribution of terrestrial biota. The biogeography of the Indonesian Archipelago is typically divided into three areas. These are: Sundaland in the western part, Wallacea in the middle, and Sahulland in the eastern part (see Figure 2.4). Sunda and Sahul formed widely connected land masses during times of low sea levels in the Quaternary period (de Vos 1997; Voris 2000; van den Bergh, de Vos & Sondaar 2001). All researchers recognise the important role of land bridges intermittently connecting Sunda and Sahul with Asia and Australia, respectively during low sea-level stands of the Pleistocene. The Wallacea islands were never connected to either of these continental land masses.

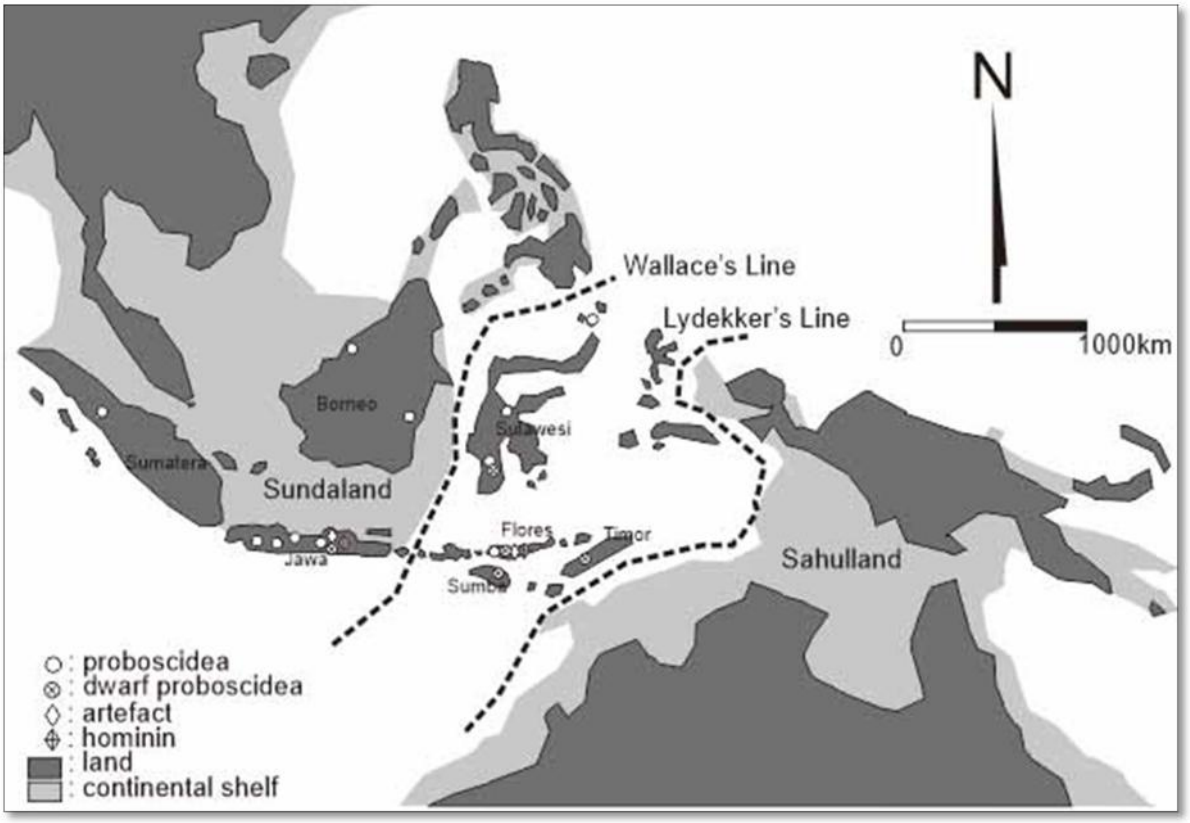

Figure 2.4. Proboscidean site locations in the Indonesian Archipelago.

Glaciation and deglaciation during the Pleistocene were accompanied by declining and rising sea levels, which had a major effect on the configurations of the land mass in Southeast Asia (van Bemmelen 1949; Gibbons & Clunie 1986; Rainboth 1991). Voris (2000) depicted how

the regional coastline may have appeared during the Pleistocene period when the sea levels dropped several times. The Voris maps show that extensive land bridges formed to the mainland continents of Asia and between the main Sundaland Islands, Sumatra, Java and Borneo. The significance of sea levels changing over geological time in Sunda, Wallacea and Sahul has long been assumed to be important in understanding terrestrial organism distributions (Wallace 1881; Darlington 1957). This phenomenon is considered to be one of many aspects that allowed terrestrial animals to migrate from mainland Southeast Asia to Sumatra, Java and Borneo during the Pleistocene period. Early megafaunal migration to Java is understood to have come from the north part of India (Siwaliks), the west part of India (Narmada beds) and via Burma (now known as Myanmar) via what de Vos (1997) refers to as the Siva-Malayan route (see Figure 2.5), and this migration route included proboscidea.

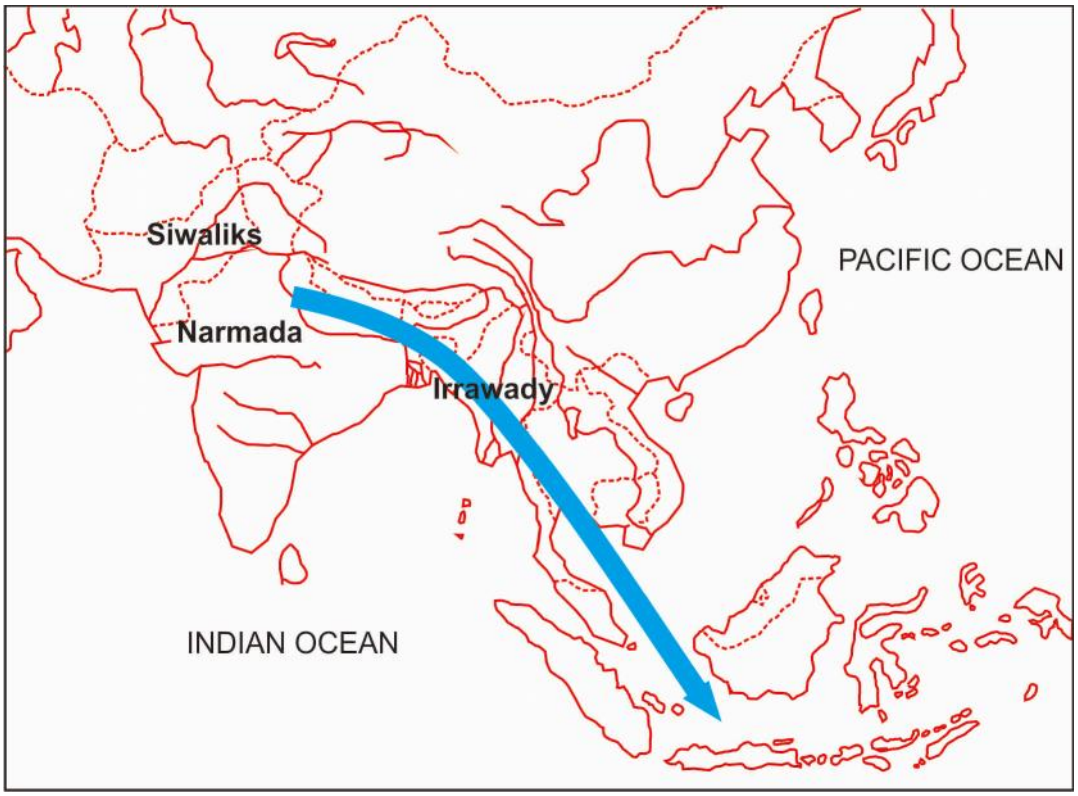

Figure 2.5. Siva-Malayan fauna migration route during the Pleistocene period (modified from de Vos 1997).

The first recorded excavation that yielded fossils of megafauna in Indonesia was by Raden Saleh in 1865-1866, who then published descriptions of the specimens. One of the fossils from Saleh's collection, a juvenile skull of a proboscidean, became the holotype of *Stegodon trigonocephalus* (Martin 1887). After that, many proboscidean fossils were discovered in

Quaternary deposits of Java, Sulawesi, Flores, Timor and Borneo, representing a number of genera: *Sinomastodon, Stegodon* and *Elephas* (Hooijer 1975; van den Bergh 1999). Markov & Saegusa (2008) inferred that *Stegoloxodon* also occurred in Java and Sulawesi during the Quaternary.

Indonesian proboscideans can be divided into three clusters according to their arival in geological age (van den Bergh, de Vos & Sondaar 2001). These are the Early Pleistocene, Middle-Late Pleistocene and Late Pleistocene-Holocene periods (see Table 2.1). Below is a summary of the known excavations and contexts that have resulted in the recovery of Indonesian fossil proboscidea that are currently stored in Indonesian research institutions, grouped according to their geological age:

Early Pleistocene Period

Proboscidea of this age are *Sinomastodon bumiajuensis* from the Bumiayu area (van der Maarel 1932), *Sinomastodon* spec. (de Vos 1997) and *Stegodon elephantoides* from the Sangiran site (van den Bergh 1999). *Palaeoloxodon* is also from the Bumiayu site (van der Maarel 1932), but was later to become classified as *Stegoloxodon indonesicus* (Kretzoi 1950; Markov & Saegusa 2008). All of these sites are located in Central Java. Early Pleistocene proboscidea that have been discovered outside of Java are from Sulawesi and the Lesser Sunda Islands, and are represented by *Stegodon sompoensis* and *Stegoloxodon celebensis* from Sulawesi, and *Stegodon sondaari* from Flores (van den Bergh 1999).

Middle Pleistocene-Late Pleistocene Period

de Vos and Sondaar (1982) noted the presence of two proboscideans in the Middle Pleistocene faunas of Java. These were *Elephas hysudrindicus* and *Stegodon trigonocephalus.* Some researchers have claimed that large-bodied *Stegodon* from Sulawesi, Flores and Timor belong to *Stegodon trigonocephalus* as well (Hooijer 1975; Sondaar 1981). Wallacean islands that are known to proboscidean fossils from the Middle and Late Pleistocene are Sulawesi, Flores, Sumba and Timor. These proboscidea are *Stegodon florensis florensis* and *Stegodon florensis insularis* from Flores (van den Bergh et al. 2008), *Stegodon sumbaensis* from Sumba (Sartono 1979), and *Stegodon timorensis* from Timor (Sartono 1969). The age of *Stegodon sumbaensis*

and *Stegodon timorensis* is not clear but, based on the development of the teeth in comparison to the other *Stegodon*, it is assumed that both are from the Middle to Late Pleistocene (van den Bergh 1999).

Table 2.1. Summary of Indonesian proboscidea stratigraphy.

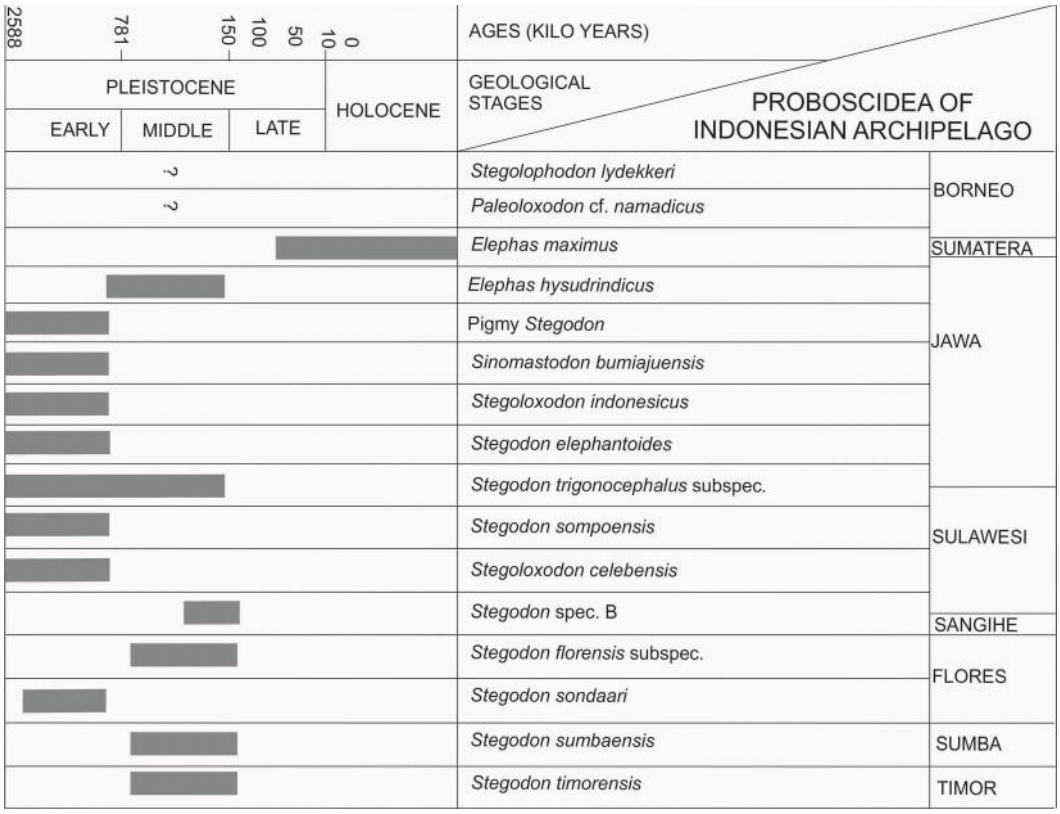

Late Pleistocene-Holocene Period

Two species of *Elephas* have been recognised in Java. These are *Elephas hysudrindicus* and *Elephas maximus* (Hooijer 1955; Hooijer 1974). *E. hysudrindicus* originated from several Middle and Late Pleistocene localities, and *E. maximus* is known from Late Pleistocene and Holocene localities, but they have never been found together. *E. maximus* fossils originate from Cipeundeuy, West Java (van den Bergh 1999) and the caves of Lida Ajer, Djambu and Sibrambang in West Sumatra (Hooijer 1955). Some subfossil remains of *Elephas* have also reportedly been discovered in Malaysia's Niah Cave in Borneo (Medway 1979) and Bangka, a small island that is located in the northern part of Sumatera (Martin 1884).

2.1.2. Insular Dwarfism and Evolution

Among the documented Indonesian proboscideans are various species and subspecies of small body size, which represent dwarfed proboscideans (van der Geer et al. 2016). These exhibit insular dwarfism (Hooijer 1975; Aziz et al. 1995). The degree of dwarfing is variable (van den Bergh 1999). *S. florensis*, and even *S. trigonocephalus* from Trinil, are much smaller than their mainland ancestor, *S. ganesa*. *S. trigonocephalus* from Kedung Brubus or Ngandong is larger then *S. trigonocephalus* from Trinil (van den Bergh 1999). *S. florensis* from the So'a Basin in Flores is also dwarfed, although not as much as *S. sondaari*, or its descendent from Liang Bua (van den Bergh et al. 2009; van der Geer et al. 2010).

Current thinking is that this phenomenon is closely related to the tectonic and climatic evolution changes over time that provided Java with more land and connections to the mainland when the sea levels were low, but led to isolation with less land mass when sea levels rose (de Vos 1997; Voris 2000; van den Bergh, de Vos & Sondaar 2001) (see Figure 2.4). Large-bodied proboscideans had to adapt to reduced land and resources or become extinct during periods of high sea-level and isolation. It is thought that dwarfing is an evolutionary response to these reductions in land mass (van der Geer et al. 2010; van der Geer et al. 2010).

Insular dwarfism is the process of the size reduction that occurs over many generations in large animals. This occurs primarily on islands when a population's level is limited to a small and restricted environment (Prothero & Sereno 1982). Generally, mammals in an insular environment will change their body mass and limb bone structure over many generations. Usually, large herbivores and medium-sized omnivores become smaller because of competition and lack of food resources, whereas small mammals tend to become larger (van der Geer et al. 2010). Sondaar (1977) noted that on islands, the lower limb bones of big mammals will shorten in response to the environmental pressure on the island. Short limbs in tetrapods make the body more stable to deal with steep terrain due to the centre of gravity of the body becoming lower (Agenbroad 2003).

The Indonesian fossil proboscidea that display some degree of insular dwarfism are the dwarf *Stegodon* sp. from Sambungmacan in Java, *Stegodon sondaari* and *Stegodon florensis insularis* from Flores, *Stegodon sumbaensis* from Sumba Island and *Stegodon timorensis*

from Timor (van den Bergh 1999; van den Bergh et al. 2008). Of all these dwarf proboscideans, only a single *Stegodon sondaari* individual has been discovered with associated limb bones, and therefore could be included in this study. This specimen of *Stegodon sondaari* displays strong insular dwarfism.

2.2. Proboscidean Anatomy and Morphology

The earliest publication of elephant morphology was by Linnaeus (1758) using his binominal classification system of organisms (Shoshani & Eisenberg 1982). The Linnaeus classification system pushed scientists to develop description keys for taxonomy. These description keys are based on morphology. Morphology is the study of an organism's form and function; how a structure and its function become an integrated part of an interconnected design, and how this design itself becomes a factor in the evolution of new forms (Kardong 2012). Anatomy is part of the study of an organism's morphology and both are the main tools that are used to describe an organism (Kardong 2012).

In their living appearance, proboscidea from different genera sometimes have a very similar appearance. Most of the diagnostic characteristics are found in their teeth, and this is especially the case for fossil specimens. Proboscidean teeth have a distinct shape and, because the teeth are covered by enamel, the potential for preservation and fossilisation is higher compared other the skeletal elements.

2.2.1. Genera, Species and Dental Morphology

Mammalian teeth are the main anatomical features that are used to distinguish their taxon, and especially the characteristics of their molar tooth crowns. For example (see Figure 2.6), humans and pigs have a low molar crown (brachydont) and horses have a high crown (hypsodont). When the cusps of the molar have rounded peaks, then it is called bunodont. If the cusps are predominantly straight ridges, such as with elephants, rodents and horses, then these are called lophodont teeth. Some mammals, have crescent-shaped cusps and are called selenodont (Kardong 2012).

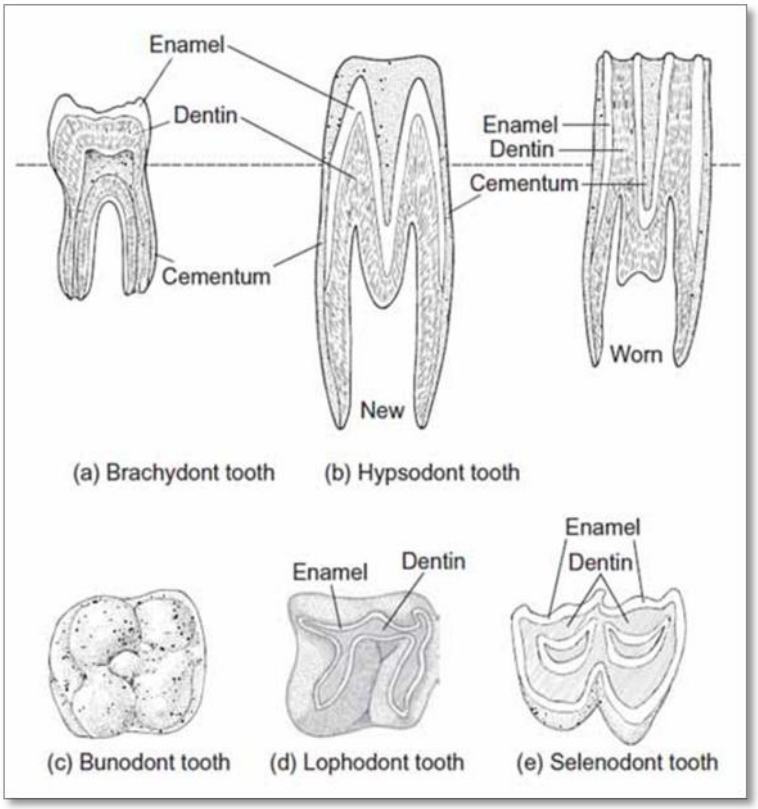

Figure 2.6. Mammalian molar tooth types (Kardong 2012).

Dental measurements are commonly used in the diagnosis of fossil elephant species (Roth 1992). Their size, pattern, position and shape are the main parameters for clustering the species of the same genus based on their teeth (see Figure 2.7) (Hooijer 1974; Saegusa, Thasod & Ratanasthien 2005). For examples: *E. maximus* is characterised by its 21-29 plates in its lower M3s (Prothero & Sereno 1982), which is just within the range observed for *E. hysudrindicus* (18-21 plates) (Hooijer 1955); *Stegodon* is characterised by the shape of the valleys in between the molar ridges or lamellae (van den Bergh, 1999); and *Sinomastodon* is characterised by bunolophodont molar shape (Saegusa 1995). Furthermore, some researchers inferred that the advanced dental stages of proboscidea are characterized by the higher hypsodonty and thinner enamel (Dubrovo 1977; Athanassiou 2012; Baigusheva & Titov 2010).

Different genera and species of proboscidea have been recognised and put into a family tree based on their dental characteristics (see Figure 2.7), and this includes the proboscideans of

Indonesia. The genera and species (extant and extinct) that are known to have lived in Indonesia are:

1. *Elephas*:

   The genus *Elephas* is characterised by a lophodont and hypsodont molar type (see Figure 2.8). Species of this genus that are part of this study are *Elephas maximus* and *Elephas hysudrindicus.*

2. *Stegodon*:

   The genus *Stegodon* has a lophodont and brachyodont molar type (see Figure 2.8). The species of this genus that are included in this study are *Stegodon trigonocephalus, Stegodon florensis* and *Stegodon sondaari.*

3. *Sinomastodon*:

   The genus *Sinomastodon* has a bunolophodont tooth type (see Figure 2.8). Just one species from this genus is used in this research: *Sinomastodon bumiajuensis*.

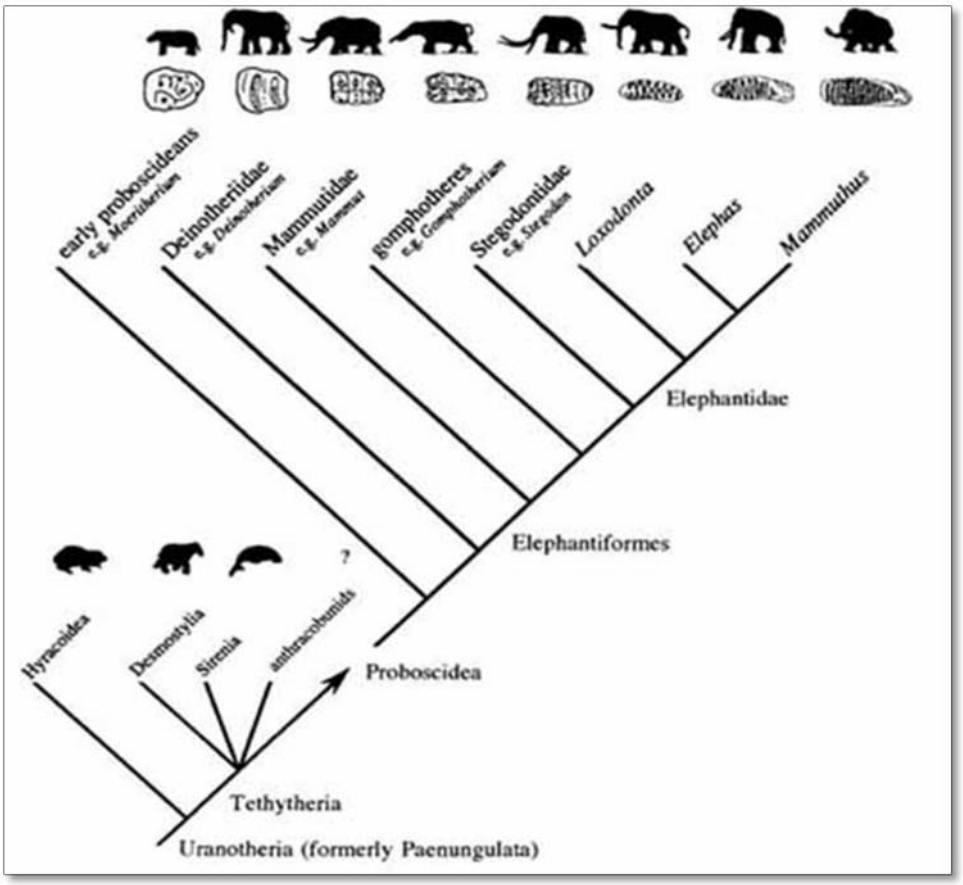

Figure 2.7. Simplified cladogram of proboscidea, with representative third upper molars (Shoshani 1998). The genus *Sinomastodon* is usually considered as a member of the family *Gomphoteriidae*

2.2.2. Tooth Replacement

Primitive elephants had one incisor in both the lower and upper jaw (tusks), no canines, three deciduous molars in both the lower and upper jaws, and three molars in both the lower and upper jaws. In advanced proboscideans such as the African and Asian elephant, the age estimates can be made based on dental wear patterns and used to estimate age at death of extinct species.

One to two molariform teeth were in use in every part of the jaw at any one time during life (Lee et al. 2011). In more advanced genera, such as the three genera that form part of this study, the lower incisors or tusks have disappeared and their dental formula is:

I 1/0, C 0/0, dp 3/3, M 3/3

I: Incisor (tusk)
C: Canine
dp: deciduous premolar
M: Molar

dp2 and dp3 are in use following birth and during the juvenile stage; dp4 and M1 appear successively and are in use until worn down completely during the young adult stage; and M2 and M3 appear and are worn during the adult stage (Lee et al. 2011). Each tooth used will be pushed forward and gradually replaced by a tooth which has formed at the back of both the lower and upper jaws. When an elephant reaches a very old age, the occlusal tooth surfaces of the last molars are worn down to the root. This makes it difficult for the animal to grind plant/grass material and eventually it starves to death (Scheid 2012).

Molar teeth, especially in grazing animals, have limitations in endurance with regard to diet. Silica particles in grasses (but not leafy plants) make the diet of grazers more abrasive than for browsers. The process of tooth abrasion experienced during mastication usually creates an uneven occlusal surface, exposing three different hard tissues that have different resistance to wear: enamel, dentine and cementum. Uneven occlusal surfaces are functionally important as they act as grinding stones. A flat occlusal surface, such as that found in very old individuals where the last molar is abraded to the root mass, makes the food unable to be ground anymore (Scheid 2012).

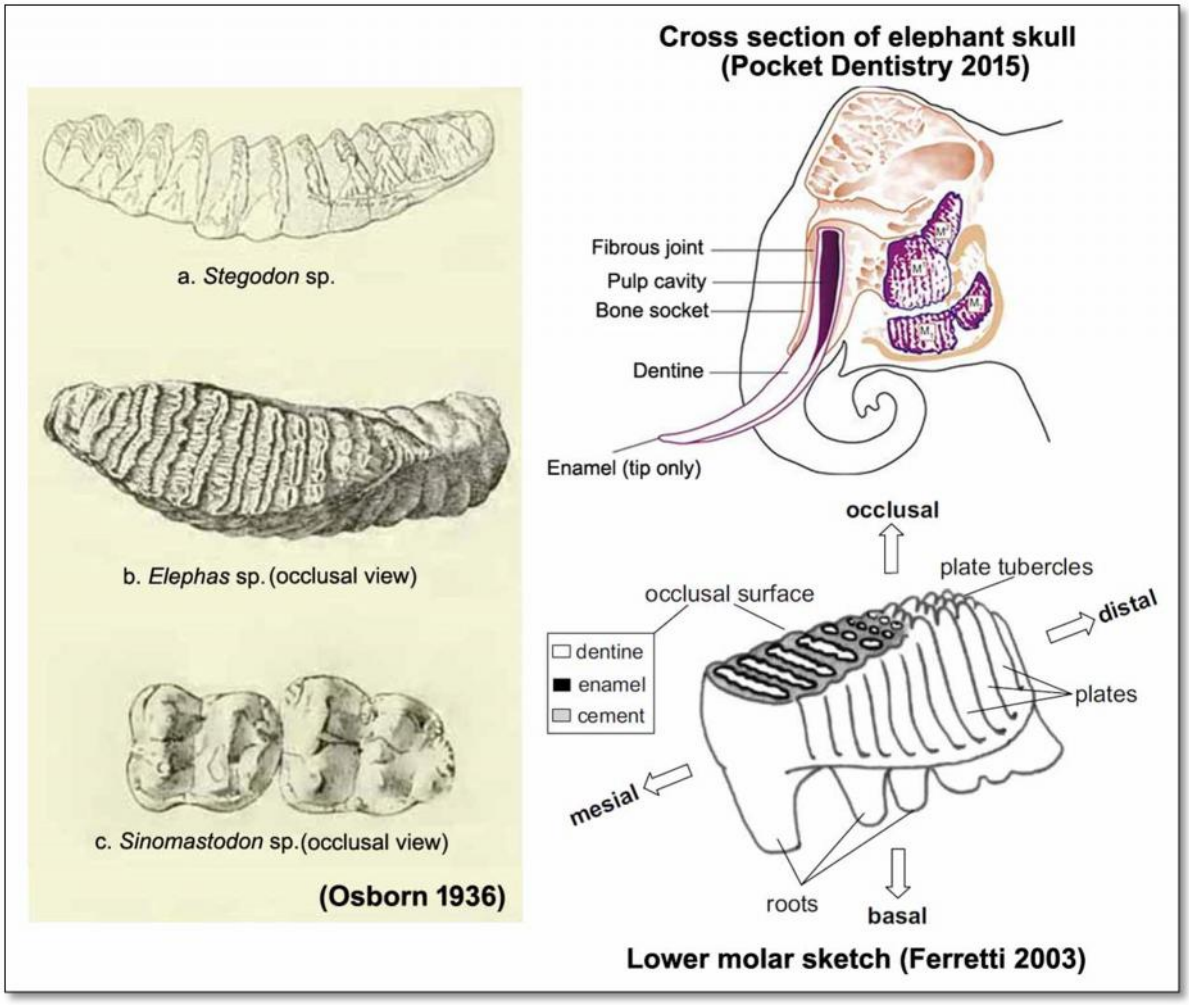

Figure 2.8. Sketches of the proboscidean molar.

2.2.3. Proboscidean Body Structure

The elephant is a large terrestrial mammal. With its large size and proboscis its trademark, this mammal is easy to recognise. Regardless of this fact, proboscidea still need a systematic description regarding anatomy. The researchers who have studied proboscidean anatomy are Miall and Greenwood (1878) and Shindo and Mori (1956). Proboscidean anatomy has also been studied to understand bone scaling and allometry within different proboscidean genera (Christiansen 2007), biomechanics (Ren & Hutchinson 2008) and adaptation (Ferretti & Croiter 2001; Agenbroad 2003; Bonnan 2004).

In order to describe, in three dimensions, the orientations and positions of the structures of large vertebrate mammals like proboscidea, the body needs to be in a standing position

(Figure 2.9). Some of the most useful of these studies address similarity and symmetry, and discuss how these characteristics are relevant to proboscidea. The details are summarised below:

Similarity

When comparing organs in different animals, some segments may be considered identical to each other by appearance, function and ancestry (Kardong 2012). The terms that usually appear in similar forms and/or functions are homology and analogy. The term 'homology' applies to two or more characteristics that share a common ancestry. The forelimb and hindlimb of an elephant are homologous with the forelimb and hindlimb of other mammals, such as humans or bats. Only their functions are different. The forelimbs of the elephant are used to support locomotion, whereas the forelimbs in humans are used for handling objects, and the forelimbs in bats enable them to fly. The term 'analogy' refers to features that have a similar function but a distinct evolutionary origin; e.g., the fin in a fish and the fin in an aquatic mammal, such as the dolphin. A fish fin has a different structure than a dolphin fin, but they have the same function. The tusk of an elephant (which evolved from an incisor) could be considered as analogous with the tusk of a pig (which evolved from a canine).

Symmetry

Symmetry defines the way in which an organism's form meets its surrounding environment (Kardong 2012). Because proboscidea have bilateral symmetry (see Figure 2.9), the left (sinistral) hindlimb bone can be flipped to the right (dextral) view to make the bones comparable, when applying geometric morphometric analyses.

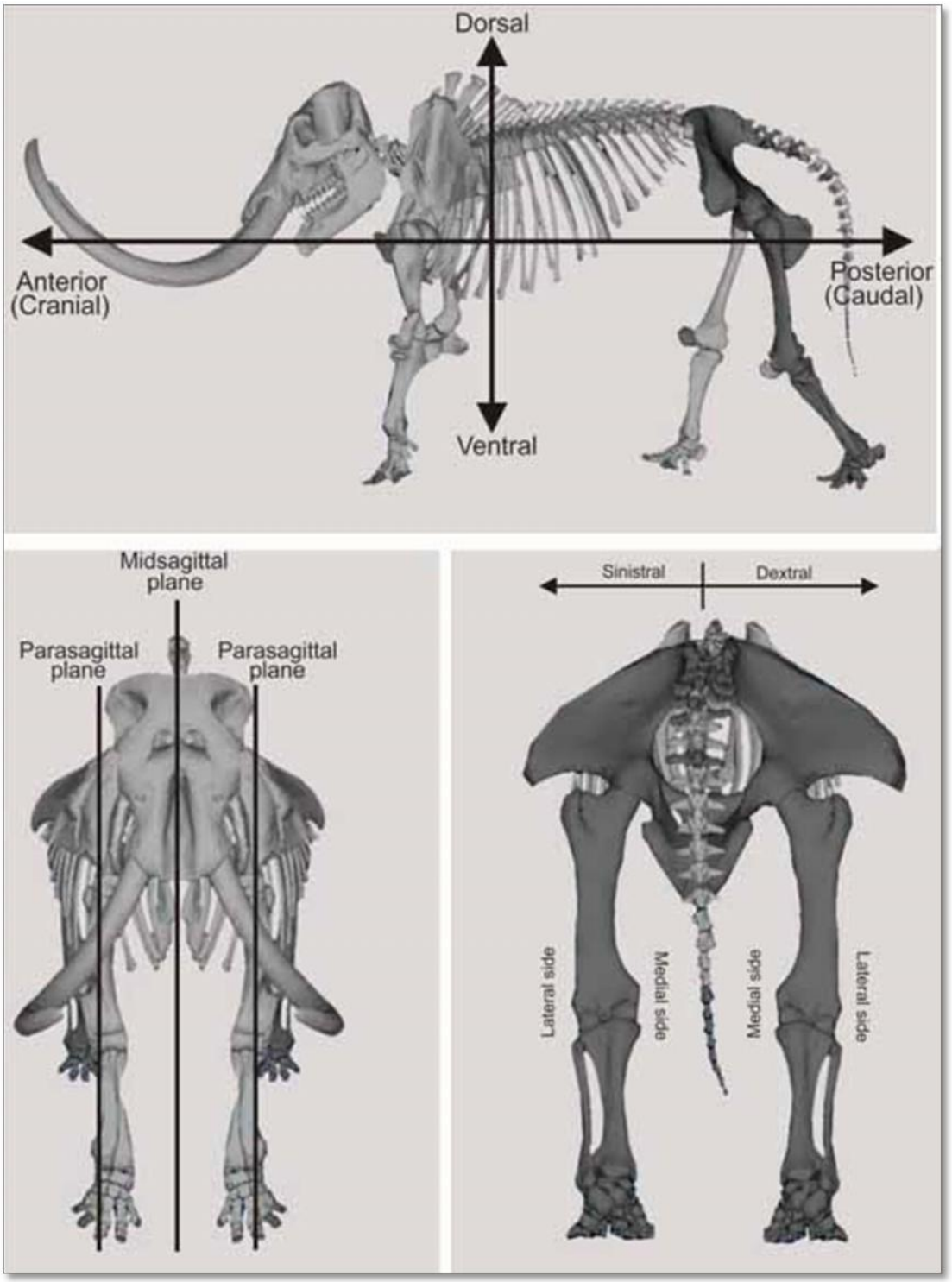

Figure 2.9. Body regions and bilateral body symmetry of proboscidea (image from: Museum of Paleontology University of Michigan 2014)

2.2.4. Hindlimb Bones

The hindlimbs of three long bones (*ossa longa*), the femur, the tibia and the fibula (see Figure 2.10). A long bone is characterised by its long tubular shape and has two ends (see Figure 2.11). The main structure of a long bone is shown in Figure 2.11 and is divided into the following anatomical regions:

- *Epiphysis*

  The epiphysis is present at each end of the long limb bones and located between the articular cartilages and the growth plate. The inside of this region contains spongy trabecular bone tissue covered by an external thin layer of compact bone.

- *Diaphysis*

  The diaphysis is the shaft of the long bone. It is characterised by an inner cavity (*cavitas medullaris*) filled with bone marrow and covered by compact bone walls.

- *Metaphysis*

  The metaphysis is located between the diaphysis and the growth plate. It is also characterised by thin layer of cortical bone, as with the diaphysis.

- *Ephypiseal Plate*

  The ephypiseal plates is only found in actively growing bones.

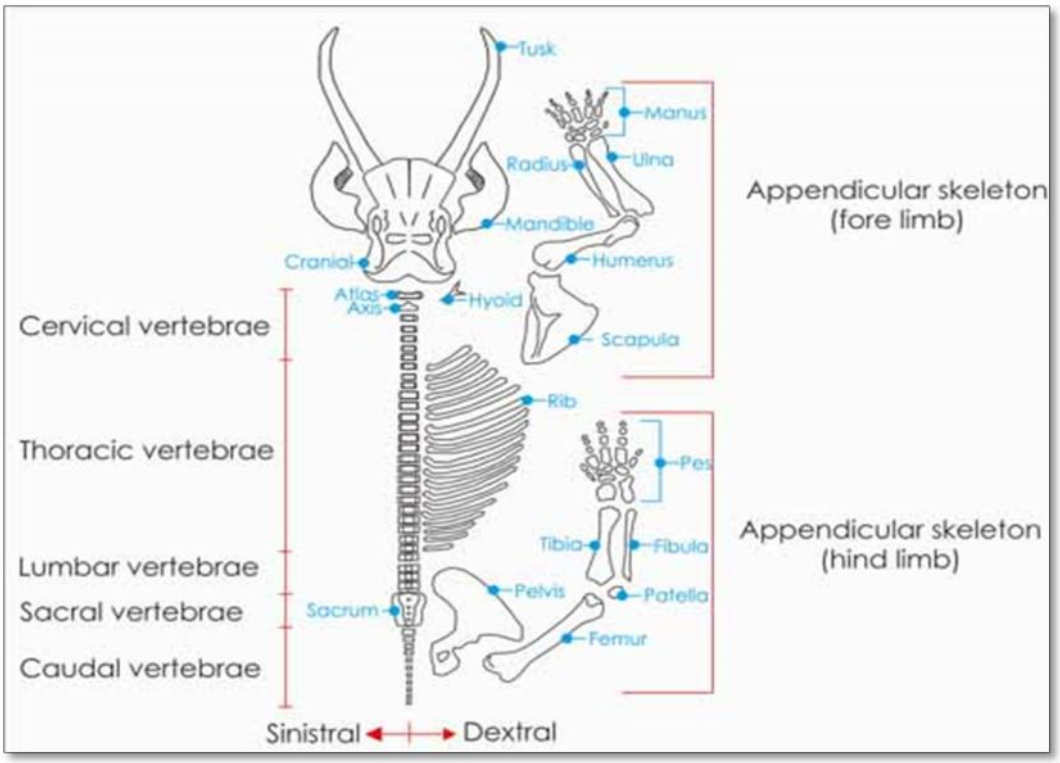

Figure 2.10. A schematic depiction of the proboscidea skeleton (modified from Villa et al. 2005).

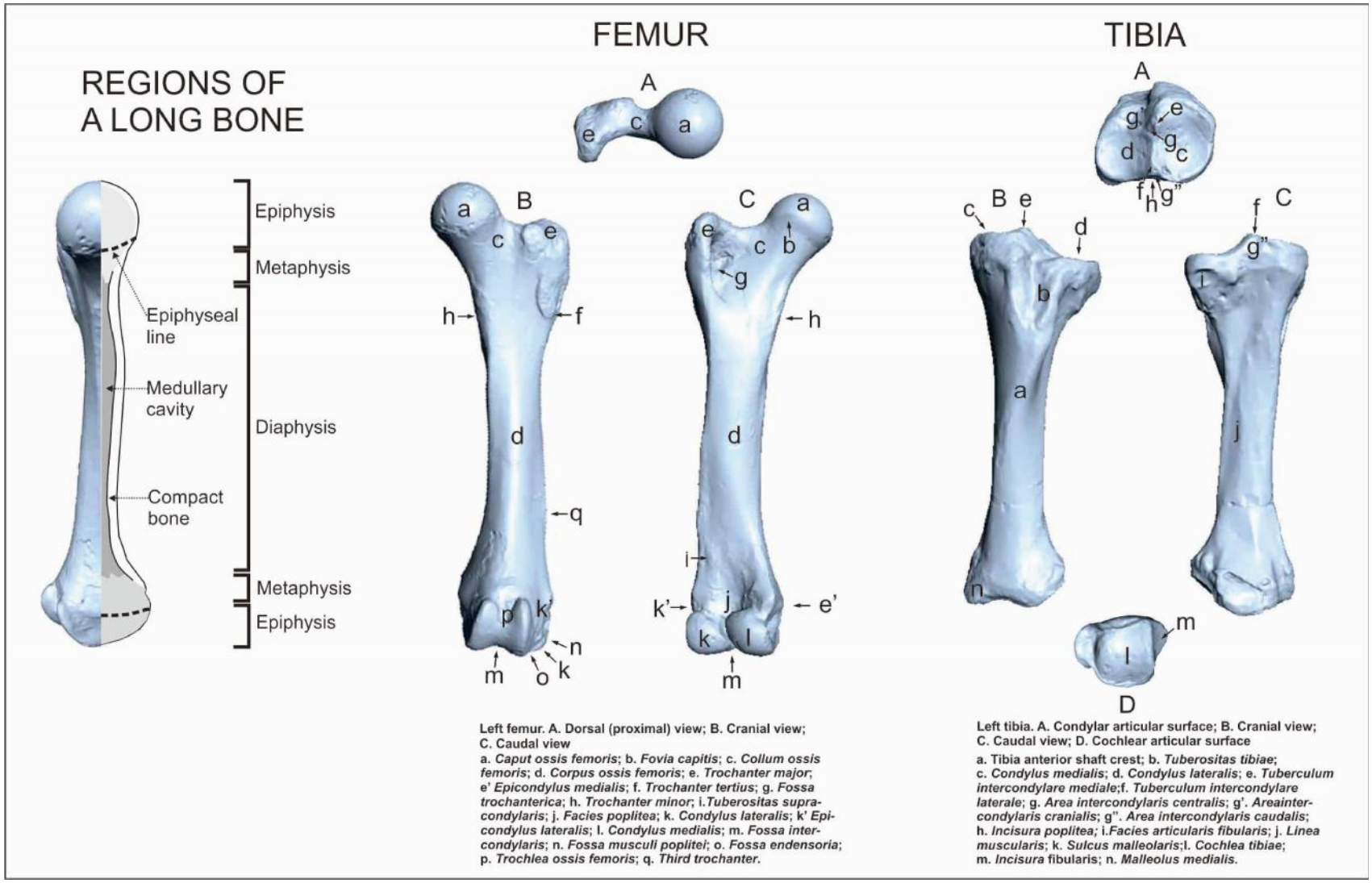

Figure 2.11. Regions of a long bone based on Kardong (2002). Anatomy of the proboscidea hindlimb based on Smuts and Bezuidenhout (1994).

2.2.5. Age and Long Bones

The age of a fossil elephant is usually estimated by looking at the teeth and examining their wear condition (Athanassiou 2012). This cannot provide an absolute estimation of age. Age can also be assessed by looking at the condition of the epiphyseal fusion. Since bone growth essentially occurs between the epiphyses and the diaphysis, some epiphyseal sutures remain open until late in life. Because the ephipyseal plate is only present in bones that are still growing, it is useful for estimating the age of an individual.

The degree of epiphyseal fusion in animals with determinate growth is an important anatomical feature. In many mammals, and this includes proboscidea, epiphyseal fusion, where the growth plate cartilage (or 'metaphysis') is completely ossified, indicates the end of longitudinal growth in that bone, and it can then be inferred to be in the full-grown age stage (Nilsson & Baron 2004). In the case of age estimation, Herridge (2010) developed the fusion stage by the order of epiphysis fusion in the elephant forelimb and hindlimb (see Figure 2.12).

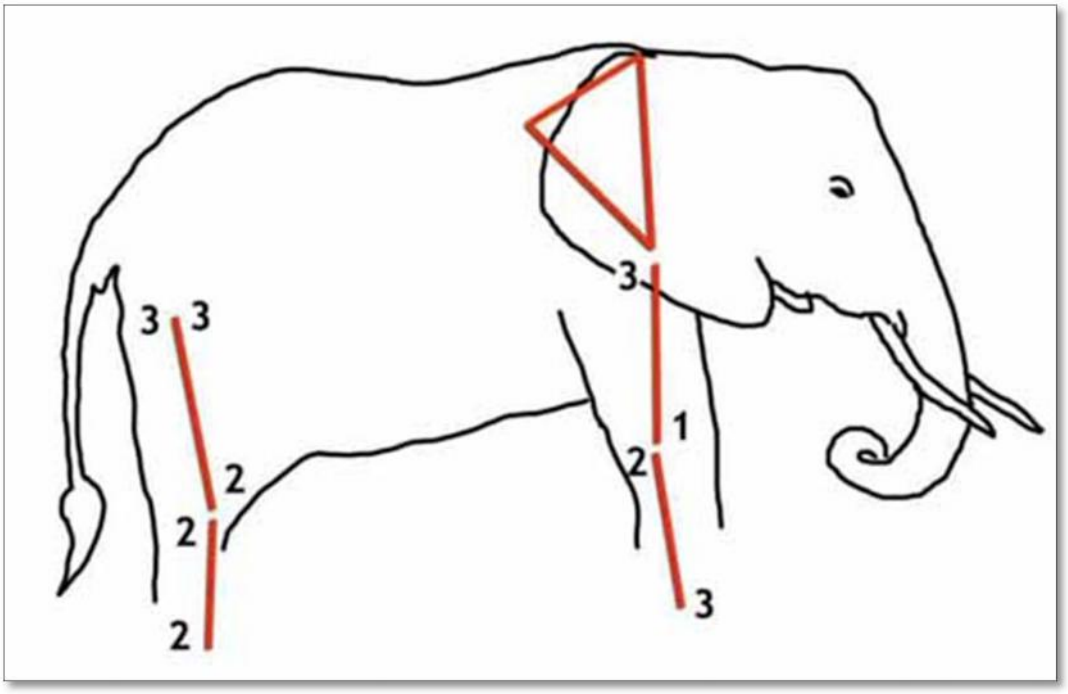

Figure 2.12. The generalised order of epiphysis fusion in the elephant (Herridge 2010).

Herridge (2010) distinguished three elephant age stages based on the ephypises fusion state in its limb bones. In stage 1, the distal part of humerus fused; in stage 2, the proximal part

of ulna, the distal part of femur, the proximal part of tibia and the distal part of tibia fused; in stage 3 (adult), in the proximal part of the humerus, the distal part of ulna and the proximal part of femur fused.

2.2.6. Sexual Dimorphism

Sexual dimorphism in mammals is often recognisable by the degree of robusticity. Male mammals tend to be larger than females. The elephant is a mammal that shows clear sexual dimorphism. In linear size, the males are about 20-40% larger than females and can be nearly two times as heavy (Sukumar 2003; Haynes 1991). Among the extant modern elephants, the male African bush elephants (*Loxodonta Africana*) are usually 23% taller than females on average, whereas Asian elephant (*Elephas maximus*) males are around 15% taller than females (Larramendi 2016).

In mammalian post-cranial bones, the sex can be identified based on pelvis shape (Athanassiou 2012). In females, the pelvic hole is wider than in males to accommodate the baby when the female gives birth (Athanassiou 2012). Unfortunately, because its shape is wide and thin compared to other post-cranial proboscidean bones, it is rare to find a pelvis fossil in good condition. The post-cranial bone that is articulating with the pelvis and has a better potential to be preserved in good condition is the femur.

2.2.7. Muscles, Tendons and Ligaments

Muscles, tendons and ligaments work within the skeletal system to enable an animal to move. Each has a specific function that is related to specific actions and motions. Muscles supply force for movement and tendons connect muscles to bones (Kardong 2012). Ligaments are dense bands of collagenous tissue (fibres) that extend a joint and then become stuck to the bone at either end. In other words, ligaments are a type of solid network of fibres connecting bones to other bones (see Figure 2.13) (Kardong 2012).

The knee has two collateral ligaments and also two cruciate ligaments. The cruciate (*crossed*) ligaments are located in the femur's intercondylar fossa and are named based on where they attach. The **posterior cruciate ligament** (PCL) is stronger than the **anterior**

cruciate ligament (ACL). The location on the tibia where the PCL is attached is on the posterior intercondyle. On the lateral surface of the medial femoral condyle, the PCL is attached and extends anteriorly, superiorly and medially. On the femur, the anterior cruciate and posterior cruciate ligaments resist anterior and posterior displacement of the tibia, respectively. The location of the ACL on the tibia is on the anterior intercondylar area. Furthermore, on the medial aspect of the lateral femoral condyle, the ACL is attached and extends posteriorly, superiorly and laterally. Inside the knee joint capsule, an 'X' pattern is formed by these two ligaments (Zhang, Brian & Wang 2015).

The side ligaments of the knee that have the function of reinforcing the knee joint are called **collateral ligaments** (CL). The lateral CL ligament comes from the lateral condyle of the femur and extends to the head of the fibula. The ligament that has the function of stabilising the joint to prevent it from breaking open inside the aspect of the knee on the medial position is called the **medial collateral ligament** (MCL). The MCL extends from the medial epicondyle of the femur to the upper medial shaft and medial condyle of the tibia (Zhang, Brian & Wang 2015).

Every attachment of muscle, tendon or ligament usually makes a scar on the bones. From the size and robustness of the attachment scars, it can be concluded that the muscle is robust or gracile. The muscles and their attachments to the bones of the proboscidean hindlimb can be seen in Figures 2.14, 2.15 and 2.16. For a diagram of the main hindlimb muscles, see Figure 2.17.

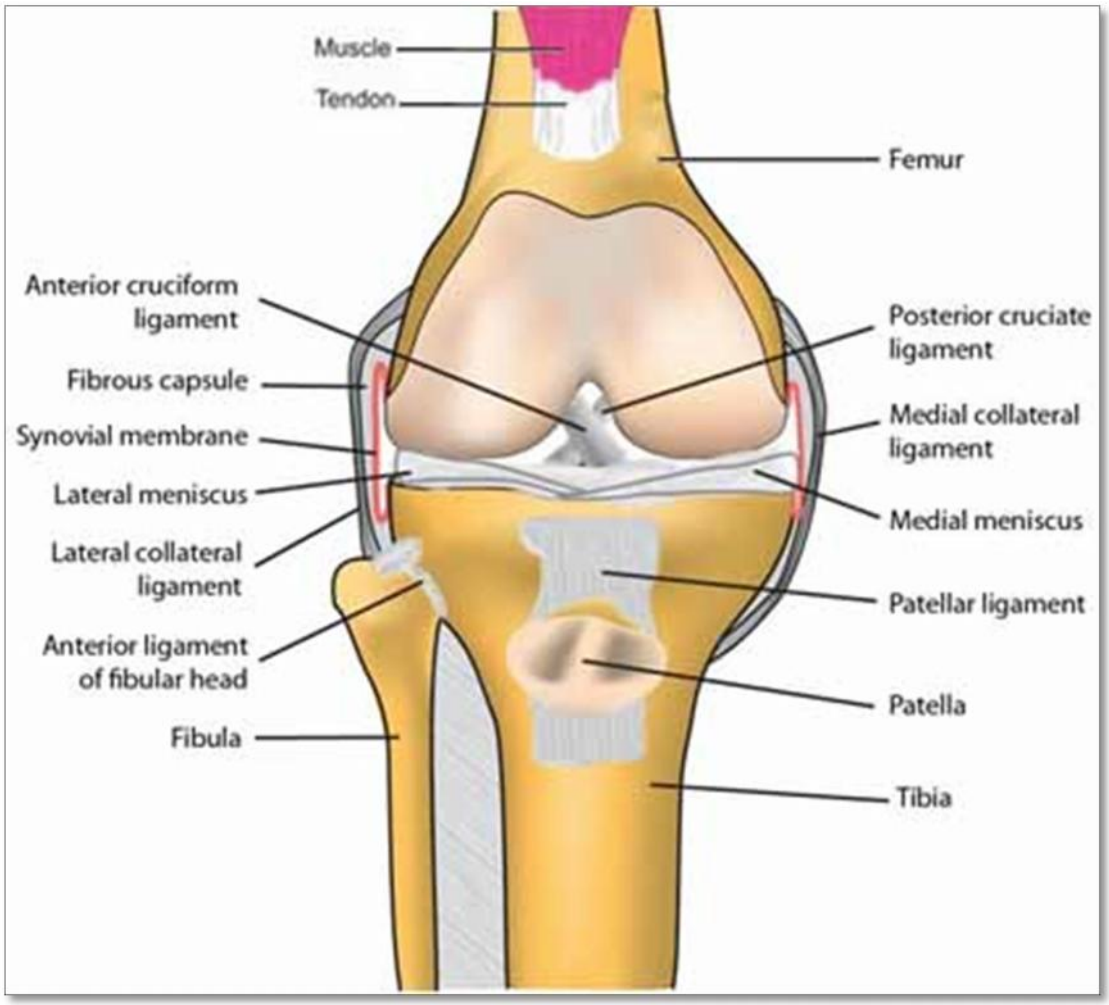

Figure 2.13. The anatomy of the right knee joint in the anterior view (modified from Zhang, Brian & Wang 2015).

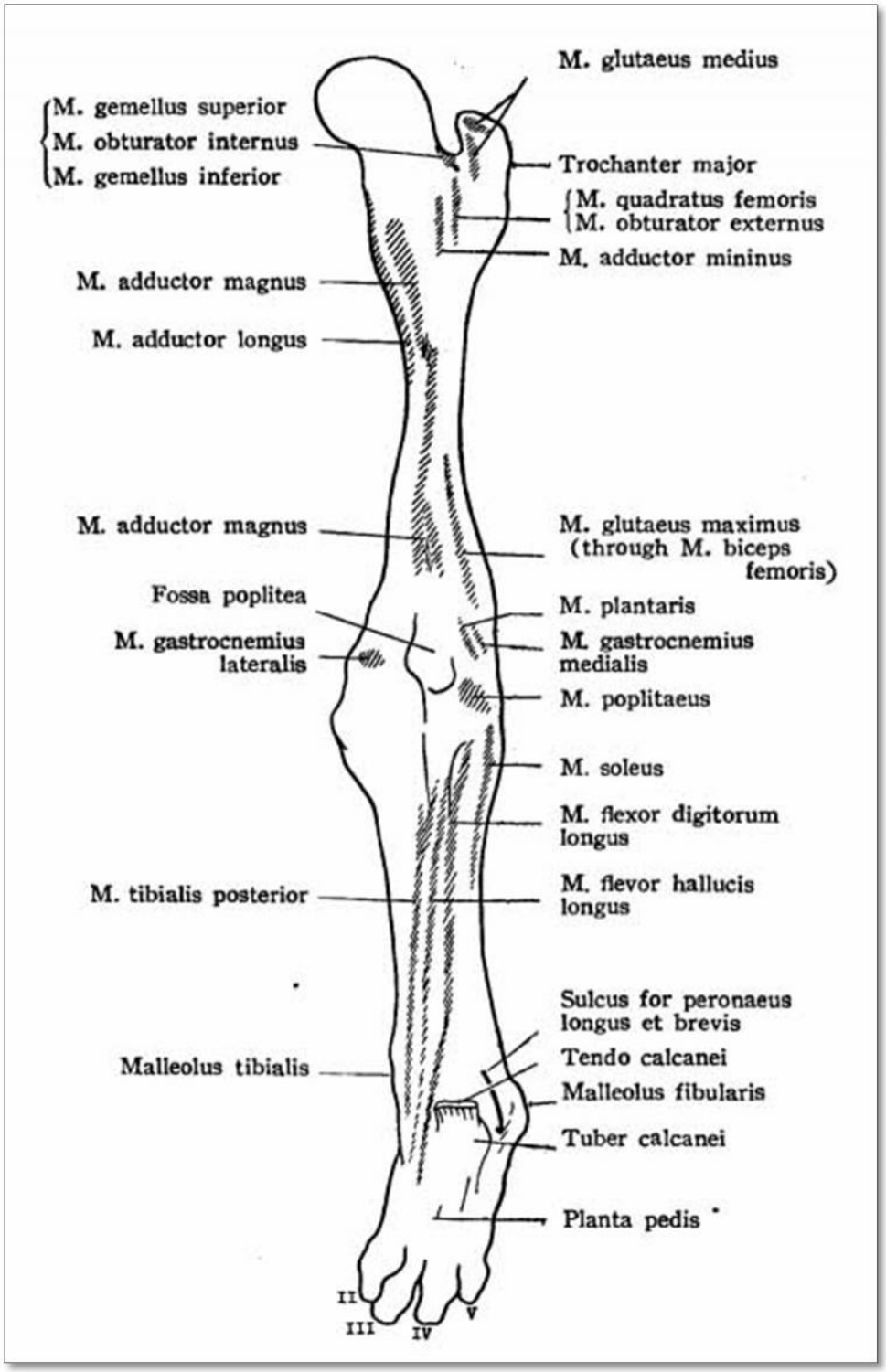

Figure 2.14. The muscle attachments of the right proboscidean hindlimb in the dorsal view (Shindo & Mori 1956).

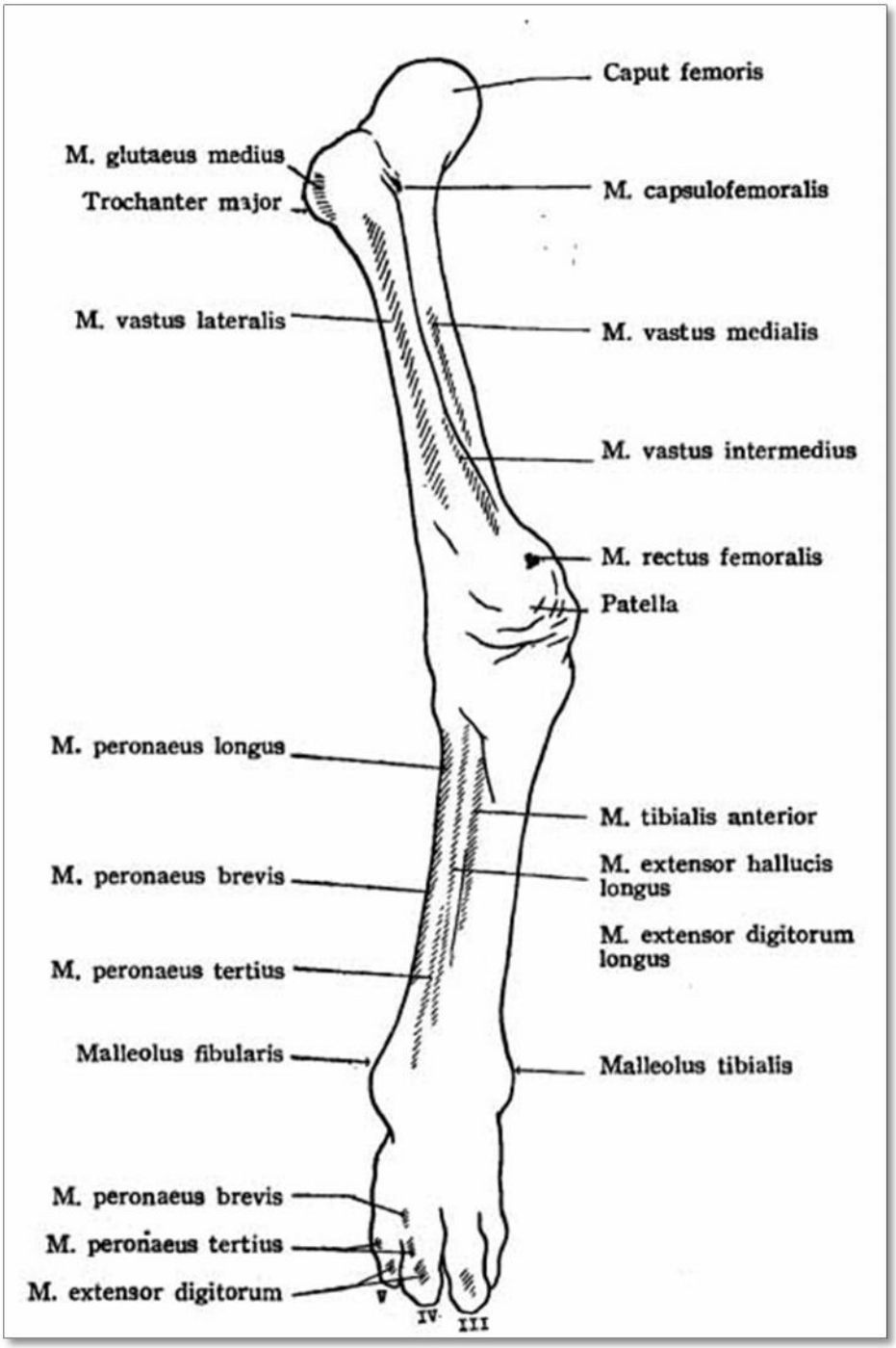

Figure 2.15. The muscle attachments of the right proboscidean hindlimb in the anterior view surface (Shindo & Mori 1956).

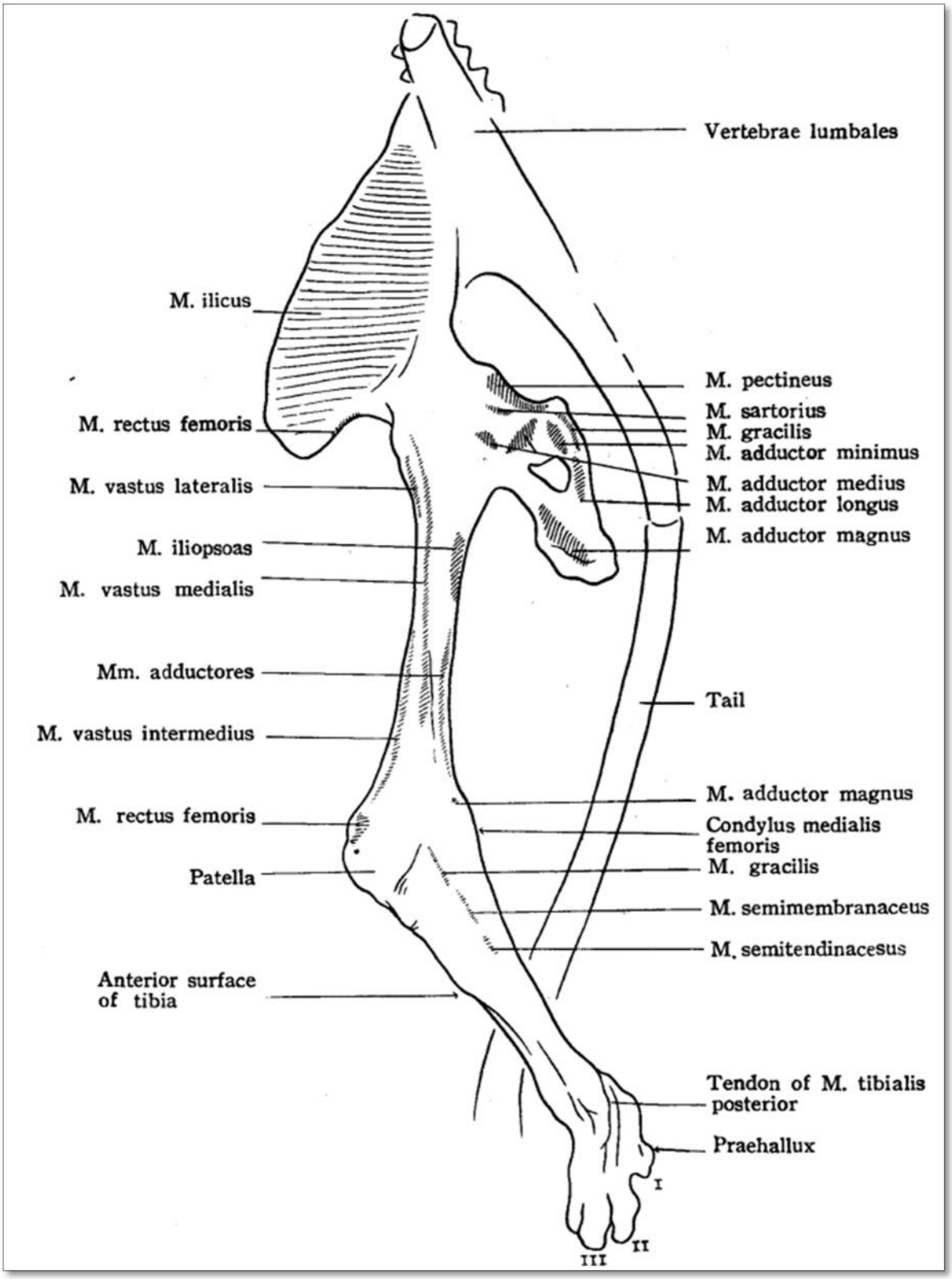

Figure 2.16. The muscle attachment of the proboscidean hindlimb in the medial view (Shindo & Mori 1956).

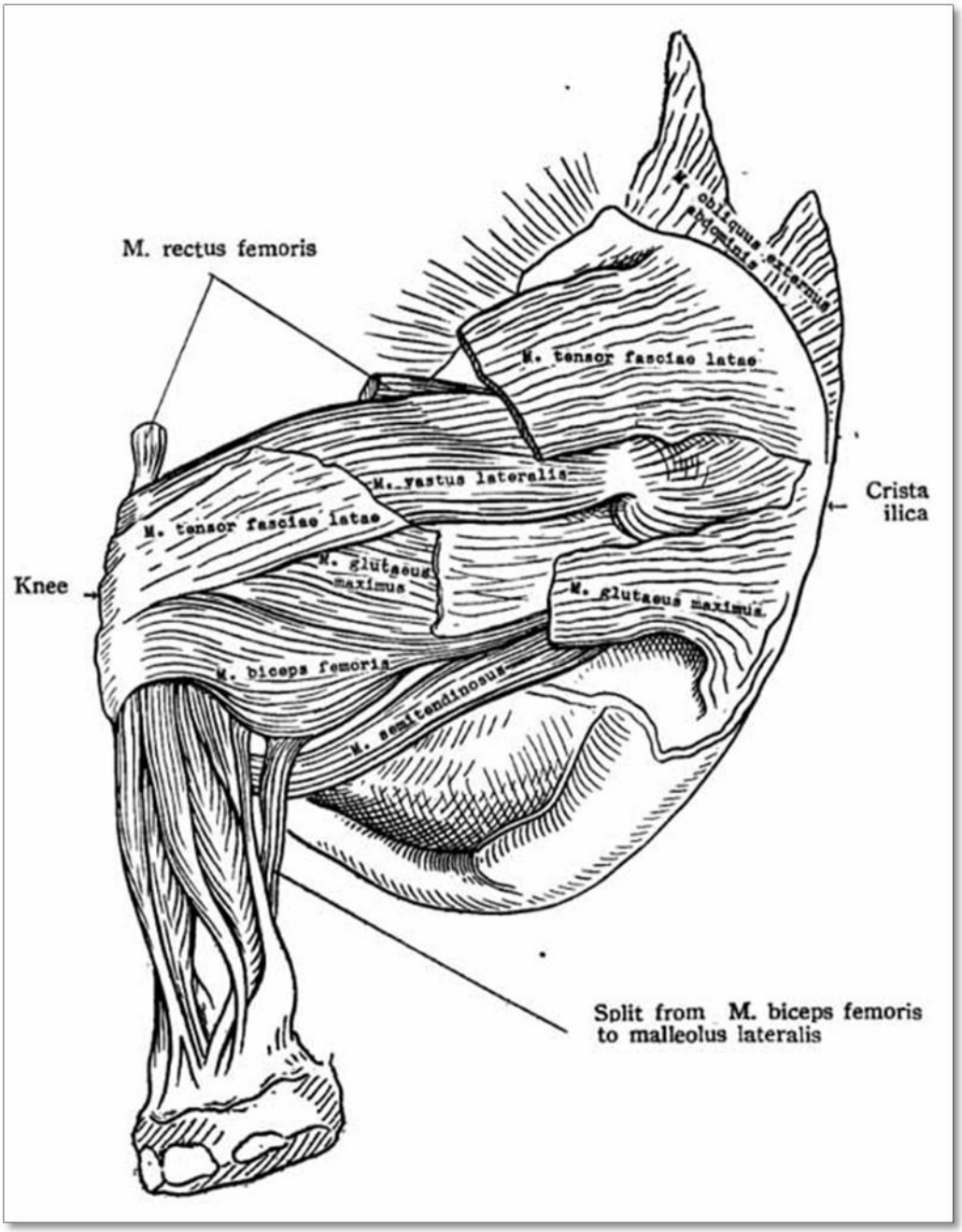

Figure 2.17. The lateral muscles of the proboscidean thigh (Shindo & Mori 1956).

2.3. Locomotion

Proboscidea are tetrapods and use their limbs for terrestrial locomotion, and this locomotion is called a walk. A *walk* is described as "a gait whereby each foot is on the ground for more than half the time of one stride cycle, and during a walk there are no unsupported (aerial) phases during which all feet are off the ground" (Matheus 2003, p. 8).

Proboscidea, as with all quadrupeds, divide the labour between their forelimbs and hindlimbs during their terrestrial locomotion. The forelimbs usually brake the animal (slow it down) and the hindlimbs mainly propel it (make it move). In locomotion, terrestrial vertebrates are divided into cursorial and graviportal groups based on their limb structure (Ren & Hutchinson 2008). Cursorial animals are those whose anatomical structures provide them with speed or endurance. Examples of these animals are the tiger (speed) and the horse (endurance) (Hildebrand 1985; Hildebrand 1995). Graviportal animals are the opposite of cursorial animals. Graviportal animals are usually large, relatively slow in their locomotion and have long proximal and short distal limb segments (Gregory 1912). The archetype of the graviportal animal is the elephant (and all proboscidea) (Hutchinson et al. 2006; Kokshenev & Christiansen 2010).

Even though proboscidea are slow in their locomotion in a terrestrial environment compared to the other large terrestrial mammals, when they meet with a body of water, proboscidea are more able to deal with it. They have the capability of crossing a body of water, such as a river or small strait that separates land masses, by swimming and using their trunk as a snorkel. This capability provides proboscideans with a relatively high potential to reach islands (Sondaar 1977). This is why proboscidean fossils are found on islands even when the island, such as the Indonesian island of Flores, has never been connected to another land mass (Aziz & Morwood 2009).

The shape of a bone is highly influenced in response to the structural environment and the mechanical strains to which the bones are subjected during the development of an individual from juvenile to adult, such as locomotion and muscle contractions (Mosley et al. 1997; Curray 2003). Locomotion in tetrapods is based on alternating limb displacements at normal rates and depends on modifications of the musculature that powers them. The performance of a muscle may depend on how it is attached to the bones of the limb (Kardong 2012).

Proboscidea, being tetrapods, also have modifications to the musculature of limbs to support heavy body mass.

2.4. Summary

The oldest known proboscideans were discovered in Early Tertiary sedimentary deposits from Africa (at least 60 million years ago). The proboscidean migrated into the Indonesian Archipelago during the Quaternary. Proboscidean fossils are among the most commonly found megafauna fossils in Indonesia compared to the other kinds of large-bodied fossil vertebrates.

Proboscidean teeth are the main characteristics that distinguish genera among proboscidea. Other parts of proboscidean skeletons that are sometimes well-preserved are proboscidean limb bones. Sometimes the bone features are also well-preserved, such as the fusion stage of the epiphyses and the scars formed by muscle attachments. Proboscidean limb bones are usually recognised because of their large size. As large tetrapods, proboscideans are slow movers (graviportal locomotion) because they must support a heavy body mass. As a consequence, the limb structure, both the bone and its muscles, are specially adapted. In the case of insular dwarf proboscideans, it would be interesting to see if they maintained graviportal limb structure, or developed shorter limbs like documented in other island mammals.

Sometimes proboscidean limb fossils represent isolated finds, this study intends to explore morphological differences between proboscidean hindlimb bones with the aim of defining biometric parameters that can help identifying the specimens that would otherwise remain unidentified.

Table 2.2. The Proboscidean classification system adopted in this thesis (to the level of genus) compiled from Shoshani and Tassy 2005; Soshani et al. 2006; Gheerbrant 2009.

Mammalia, Linnaeus 1758
Theria, Parker and Haswell 1897; Placentalia, Owen 1837 (=Eutheria, Huxley 1880)
Epitheria, McKenna 1975
Ungulata, Linnaeus 1766
Uranotheria, McKenna et al. 1997 (=Paenungulata, Simpson 1945, in part)
Tethytheria, McKenna 1975
Tethytheria incertae sedis; Genus Anthracobune, Pilgrim 1906†
Proboscidea, Illiger 1811
Proboscidea incertae sedis
Genus Eritherium, Gheerbrant 2009†
Proboscidea incertae sedis; Family Moeritheriidae, Andrews 1906†
Genus Moeritherium, Andrews 1901†
Plesielephantiformes, Shoshani et al. 2001
Family Numidotheriidae, Shoshani and Tassy, 1992†
Genus Phosphatherium, Gheerbrant et al. 1996†
Genus Daouitherium, Gheerbrant and Sudre 2002 in Gheerbrant et al. 2002
Genus Numidotherium, Mahboubi et al. 1986†
Family Barytheriidae, Andrews 1906†
Genus Barytherium, Andrews 1901†
Family Deinotheriidae, Bonaparte 1841†
Genus Prodeinotherium, Ehik 1930†
Genus Deinotherium, Kaup 1829†
Elephantiformes, Tassy 1988
Elephantiformes incertae sedis; Genus Hemimastodon, Pilgrim 1912†
Family Palaeomastodontidae, Andrews 1906†
Genus Palaeomastodon, Andrews 1901†
Family Phiomiidae, Kalandadze and Rautian 1992†
Genus Phiomia, Andrews and Beadnell 1902†
Elephantimorpha, Tassy and Shoshani 1997 in Shoshani 1998
Family incertae sedis
Eritreum melakeghebrekristosi gen. et sp. nov.†, Shoshani et al 2006
Mammutida, Tassy and Shoshani 1997 in Shoshani 1998†
Superfamily Mammutoidea, Hay 1922†
Family Mammutidae, Hay 1922†
Subfamily Eozygodontinae, McKenna, Bell and Shoshani, 1997 in McKenna et al. 1997†
Genus Eozygodon, Tassy and Pickford 1983†
Subfamily Mammutinae, Hay 1922†
Genus Zygolophodon, Vacek 1877†
Genus Mammut, Blumenbach 1799†
Elephantida, Tassy and Shoshani 1997 in Shoshani 1998
Superfamily Gomphotherioidea, Hay 1922†
Family Gomphotheriidae, Hay 1922 (trilophodont gomphotheres)†
Gomphotheriidae incertae sedis; Genus Gnathabelodon, Barbour and Sternberg 1935†
Subfamily Choerolophodontinae, Gaziry 1976†
Genus Afrochoerodon, Pickford 2001†
Genus Choerolophodon, Schlesinger 1917†
Subfamily Gomphotheriinae, Hay 1922†
Genus Gomphotherium, Burmeister 1837†
Subfamily Amebelodontinae, Barbour 1927†
Genus Archaeobelodon, Tassy 1984†
Genus Serbelodon, Frick 1933†
Genus Protanancus, Arambourg 1945†

Genus Amebelodon, Barbour 1927†
Genus Platybelodon, Borissiak 1928†
Subfamily incertae sedis; Genus Sinomastodon, Tobien, Chen, and Li 1986†
Subfamily incertae sedis; Genus Eubelodon, Barbour 1914†
Subfamily Rhynchotheriinae, Hay 1922†
Genus Rhynchotherium, Falconer 1868†
Subfamily Cuvieroniinae, Cabrera 1929†
Genus Cuvieronius, Osborn 1923†
Genus Stegomastodon, Pohlig 1912†
Genus Haplomastodon, Hoffstetter 1950†
Genus Notiomastodon, Cabrera 1929†
Superfamily Elephantoidea, Gray 1821
Family incertae sedis; Genus Tetralophodon, Falconer 1857 (tetralophodont gomphothere) †
Family incertae sedis; Genus Morrillia, Osborn 1924 (tetralophodont gomphothere) †
Family incertae sedis; Genus Anancus, Aymard 1855 (tetralophodont gomphothere) †
Family incertae sedis; Genus Paratetralophodon, Tassy 1983 (tetralophodont gomphothere) †
Family Stegodontidae, Osborn 1918†
Genus Stegolophodon, Schlesinger 1917†
Genus Stegodon, Falconer 1857†
Family Elephantidae, Gray 1821
Subfamily Stegotetrabelodontinae, Aguirre 1969†
Genus Stegotetrabelodon, Petrocchi 1941†
Genus Stegodibelodon, Coppens 1972†
Subfamily Elephantinae, Gray, 1821
Genus Primelephas, Maglio 1970†
Tribe Loxodontini, Osborn 1918
Genus Loxodonta, Anonymous 1827
Tribe Elephantini, Gray 1821
Genus Palaeoloxodon, Matsumoto 1924†
Genus Elephas, Linnaeus 1758
Genus Mammuthus, Brookes 1828†

Remarks:
†: extinct taxon
Taxas that used in this study are marked with bold letter.

3. MATERIALS AND METHODS

This chapter describes the specimens used in this study, their surface morphology and biometric characteristics, the 3D scanning process and landmark coordinate data acquisition, and the statistical methods used to analyse the biometric and 3D landmark coordinate data.

3.1. Specimens

The materials used in this study are the hind limb long bones (the femur and tibia) of 23 individual proboscidea, and all are sourced from islands in the Indonesian Archipelago. Limb bones of two of the proboscidea are recent specimens of the extant species (*Elephas maximus),* the other 21 are fossil specimens. 17 specimens come from excavation projects and six were donated by individuals and institutions to research institutions in Indonesia. The materials are housed in the following institutions, and all of these institutions are located in Java: the Geology Museum Bandung (GMB), the Sangiran Museum, the Patiayam Museum and the Biology Museum of Gajah Mada University. Taxonomic identifications of the specimens were based on the associated dental characteristics, and in some cases the long bones are from nearly complete skeletal specimens.

The extant *Elephas maximus* specimens are from a male and a female. The male hind limb bones come from a skeleton that was dug up at the Elephant Conservation Centre in Waykambas, Sumatra, and now housed in the GMB. The female was a pet of the Mataram/Yogyakarta Kingdom, which is a part of Yogyakarta Province, and after its death in 2000 the skeleton was donated to the Biology Museum of Gajah Mada University, Yogyakarta.

The proboscidean hind limb fossils that were excavated or donated from Java and that are housed in the Geology Museum Bandung predominantly come from the Dutch colonial period of Indonesia, and were collected around 1930-1934 (Brill 1935). *Sinomastodon bumiajuensis* comes from the collection described by (van der Maarel 1932) and *Stegodon trigonocephalus* comes from the von Koenigswald collection (Brill 1935). These specimens are from a variety of different sites, though most come from Central Java (Bumiayu Regency: Satir excavations with an Early Pleistocene age) and terraces of the Bengawan Solo River (Ngandong, Pitu, Watualang, with a late Middle or Late Pleistocene age).

Unfortunately, the geological information from this material was destroyed during World War II, but the stratigraphic period from which this material is derived is of Pleistocene age.

Two proboscidean hind limb fossils housed in the Sangiran Museum are donations by local villagers. They were one tibia found by Mr. Siswanto in Grogolan, Manyarejo and one femur found by Mr. Wasimin. Two proboscidean hind limb fossils housed in the Patiayam Museum also are donations by local villagers. They are one tibia found by Mr. Supeno and one femur found by Mr. Karmijan, both of them were found at Slumprit hill, Patiayam area. One femur from Bekasi also represents a donated specimen. It was donated by SMP 3 Setu, Bekasi (the junior high school institution from near the discovery site Setu).

Stegodon florensis is from the geoarcheology excavation sites in the So'a Basin of Flores. This research and excavation project commenced in 2004 and is still ongoing. The project is a cooperation involving the Geological Agency (Indonesia) and the University of Wollongong (Australia), and the specimens are housed in the Geology Museum Bandung. The *Stegodon florensis* specimens are mostly from the Mata Menge excavation site, where the fossil bearing layer age is of Middle Pleistocene age, more precisely ~0.8 million years old (Myr) kyr based on various radioisotopic dating techniques on underlying and overlying volcanic tephra beds (Brumm et al. 2016). The other species of *Stegodon* that originates from the So'a Basin is *Stegodon sondaari*. It was from the chronologically oldest locality in the So'a Basin. This specimen was excavated from the Tangi Talo site and the fossil bearing layer's age is Early Pleistocene (~1.4 Myr, unpublished data).

The 23 individual proboscidea and associated hind bone specimens are illustrated and described in Appendix B organized according to their genera (where the genus could be identified based on association with skeletal and or dental remains) and the individual proboscideans from which the specimens were sourced. The illustrations are extracted from the 3D scans that were undertaken for this study (refer section 3.7 3D Scanning). The femur and tibia are scaled and orientated in the anterior and posterior view. The site location of the specimens is shown in Figure 3.1, and a summary of the materials is shown in Table 3.1 and 3.2 for femur specimens and Table 3.3 and 3.4 for tibia specimens.

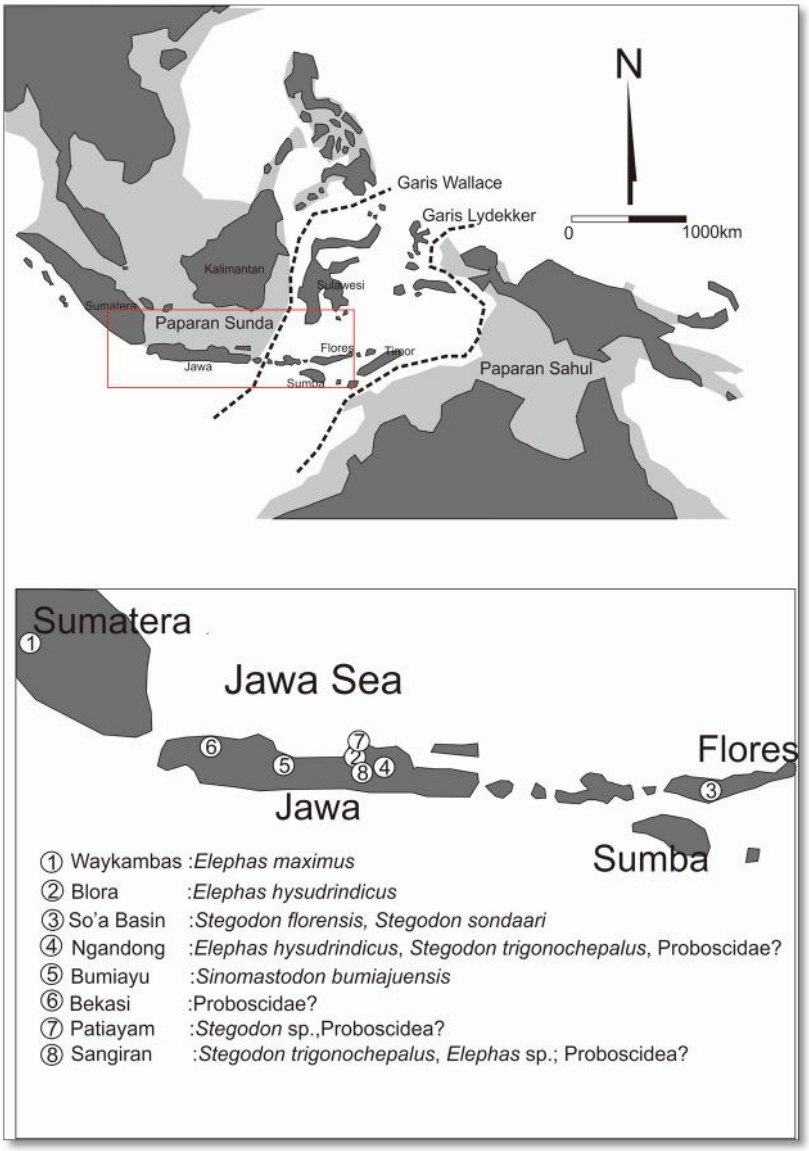

Figure 3.1. The discovery locations of Indonesian proboscidean hindlimb bones used in this study.

Table 3.1. Femur specimens identified based on associated fossils (n=10).

No.	GENERA AND SPECIES	SPECIMEN CODE	REFERENCE COLLECTION	Sinistral / Dextral	COLLECTION	LOCATION	GEOLOGICAL FORMATION	GEOLOGICAL AGE	REMARKS
1	*Elephas maximus* 1	EM1	MGB-EM	D	Museum Geology Bandung	Way Kambas, South Sumatra Province	-	Recent	from 15 years old male skeleton
2	*Elephas maximus* 2	EM2	MB-UGM-EM	D	Museum Biology of Gajah Mada University	Sumatra	-	Recent	from 29 years old female skeleton
3	*Elephas hysudrindicus*	EH	*MGB-EH	D	Museum Geology Bandung	Sunggun village, Blora Regency, Central Java Province	Menden Terrace of the Solo River	late Middle Pleistocene	from skeleton
4	*Stegodon florensis* 1	SF1	MM14-F619	S	Museum Geology Bandung	Mata Menge, So'a Basin, Ngada District, Flores, NTT Province	Middle Sandstone Member of the Ola Bula Formation	~800 kyr	Isolated, but found associated with *S. florensis* dental remains from multiple individuals
5	*Stegodon florensis* 2	SF2	MM11-T23BF176	D	Museum Geology Bandung	Mata Menge, So'a Basin, Ngada District, Flores, NTT Province	Middle Sandstone Member of the Ola Bula Formation	~800 kyr	Isolated, but found associated with *S. florensis* dental remains from multiple individuals
6	*Stegodon florensis* 3	SF3	MGB DD4188	D	Museum Geology Bandung	Dozodalu, So'a Basin, Nage Keo District, Flores, NTT Province	Middle Sandstone Member of the Ola Bula Formation	~800 kyr	Isolated, but found associated with *S. florensis* dental remains from multiple individuals
7	*Stegodon sondaari*	SS	TT12-FF3A	D	Museum Geology Bandung	Tangi Talo, So'a Basin, Nage Keo District, Flores, NTT Province	Basal Tuff member of the Ola Bula Formation	Early Pleistocene	Isolated, from single partial skeleton found associated with tibia and *S. sondaari* dental remains
8	*Stegodon trigonocephalus* 1	ST1	*MGB-K-ST-FS	S	Museum Geology Bandung	Ngandong, Central Java	Terrace of Solo River	late Middle – early Late Pleistocene	Isolated, but found associated with *S. trigonocephalus* dental remains

9	*Stegodon trigonocephalus* 2	ST2	*MGB-K-ST-FD	D	Museum Geology Bandung	Ngandong, Central Java	Terrace of Bengawan Solo River	late Middle – early Late Pleistocene	Isolated, but found associated with *S. trigonocephalus*
10	*Sinomastodon bumiajuensis*	SINO	MGB-M	D	Museum Geology Bandung	Satir, Bumiayu, Java,	base of Kali Glagah Formation	Early Pleistocene	from skeleton

*:because the original catalogue is damaged and the specimen has not yet been re-catalogued, a temporary reference collection number was assigned in agreement with the museum management.

Table 3.2. Unidentified femur specimens (n=7).

No.	SPECIMEN	SPECIMEN CODE	REFERENCE COLLECTION	Sinistral / Dextral	COLLECTION	LOCATION	GEOLOGICAL FORMATION	GEOLOGICAL AGE	REMARKS
1	Bekasi femur	uBF	MGB-Bekasi	D	Museum Geology Bandung	Bekasi, West Java Province	Unknown	Pleistocene	Isolated
2	Patiayam femur	uPT	MPT-FS	S	Museum Patiayam	Bukit Slumprit, Pati, Central Java Province	Slumprit Formation	early Middle Pleistocene	Isolated
3	Sangiran femur 1	uSang1	Reg225inv1388	S	Museum Sangiran	Sangiran, Central Java, Province	Unknown	Pleistocene	Isolated
4	Sangiran femur 2	uSang2	Elp0183	D	Museum Sangiran	Sangiran, Central Java, Province	Unknown	Pleistocene	Isolated
5	Sangiran femur 3	uSang3	Inv1712	S	Museum Sangiran	Sangiran, Central Java, Province	Unknown	Pleistocene	Isolated
6	Sangiran femur 4	uSang4	Reg485inv1327	D	Museum Sangiran	Pucung, Dayu, Gondangrejo, Central Java Province	Kabuh Formation	Pleistocene	Isolated
7	Ngandong femur	uNG	*MGB-K-FNG	D	Museum Geology Bandung	Ngandong, Central Java Province	Ngandong	late Middle - early Late Pleistocene -	from mounted hind leg, same as tibia uNG

*:because the original catalogue is damaged and the specimen has not yet been re-catalogued, a temporary reference collection number was assigned in agreement with the museum management.

Table 3.3. Tibia specimens identified based on associated fossils (n=10).

NO	GENERA AND SPECIES	SPECIMEN CODE	REFERENCE COLLECTION	Sinistral / Dextral	COLLECTION	LOCATION	GEOLOGICAL FORMATION	GEOLOGICAL AGE	REMARKS
1	*Elephas maximus* 1	EM1	MGB-EM	D	Museum Geology Bandung	Way Kambas, South Sumatra Province	-	Recent	from same skeleton as femur MGB-EM
2	*Elephas maximus* 2	EM2	MB-UGM-EM	D	Museum Biology of Gajah Mada University	Sumatra	-	Recent	from same skeleton as femur MB-UGM-EM
3	*Elephas hysudrindicus*	EH	MGB-EH	S	Museum Geology Bandung	Sunggu village, Blora Regency, Central Java Province	Menden Terrace of the Solo River	late Middle or early Late Pleistocene	from same skeleton as femur MGB-EH
4	*Stegodon florensis* 4	SF4	MM05-1	S	Museum Geology Bandung	Mata Menge, So'a Basin, Ngada District, Flores, NTT Province	Middle Sandstone Member of the Ola Bula Formation	~800 kyr	Isolated, but found associated with *S. florensis* dental remains from multiple individuals
5	*Stegodon sondaari*	SS	TT12-FF18	D	Museum Geology Bandung	Tangi Talo, So'a Basin, Nage Keo District, Flores, NTT Province	Basal Tuff member of the Ola Bula Formation	Early Pleistocene	from single skeleton found associated with femur and dental remains
6	*Stegodon trigonocephalus* 3	ST3	MGB-K-ST-TS	S	Museum Geology Bandung	Ngandong, Central Java Province	Terrace of the Solo River	late Middle - early Late Pleistocene -	Isolated, but found associated with *S. trigonocephalus* dental
7	*Stegodon trigonocephalus* 4	ST4	MGB-K-ST-TD	D	Museum Geology Bandung	Ngandong, Central Java Province	Terrace of the Solo River	late Middle – early Late Pleistocene	Isolated, but found associated with *S. trigonocephalus* dental remains
8	*Elephas* sp.	ESang5	ELP0983	D	Museum Sangiran	Sangiran, Central Java Province	Unknown	Pleistocene	Isolated, but found associated with *Elephas* dental remains
9	*Stegodon* sp. Sangiran	SSang6	Reg1965 Inv187	D	Museum Sangiran	Grogolan, Manyarejo, Sangiran, Central Java Province	Unknown	Pleistocene	Isolated, but found associated with *S. trigonocephalus* dental remains
10	*Stegodon* sp. Patiayam	SPT	MPT-TS	S	Museum Patiayam	Bukit Slumprit, Pati, Central Java Province	Slumprit Formation	early Middle Pleistocene	Isolated

Table 3.4. Unidentified tibia specimens (n=1).

No.	SPECIMEN	SPECIMEN CODE	REFERENCE COLLECTION	Sinistral / Dextral	COLLECTION	LOCATION	GEOLOGICAL FORMATION	GEOLOGICAL AGE	REMARKS
1	Ngandong Tibia	uNG	MGB-K-TNG	D	Museum Geology Bandung	Ngandong, Central Java Province	Terrace of Solo River	late Middle – early Late Pleistocene -	from mounted hind leg, the same with femur uNG

3.2. Surface Morphology

Surface morphology is a qualitative analysis to distinguish the differences between specimens based on visual assessment. The differences that are visibly present in the extant and fossil hind limb bones are described and, where possible, recorded biometrically. Once all of the data had been recorded, the specimens that were identified by genera and species, or just genera, are compared. Visual assessment is also linked to identifying landmark points that have been used in past publications regarding the hind limb bones, and also to other points that are not mentioned in the literature but have the potential to be homologous landmark points.

A description of the surface morphology is important to assess the condition of the specimens. The specimens involved in this study are predominantly fossils, and the fossilised condition makes some features and landmarks unclear. For example, the scar of muscle attachment sometimes cannot be identified because the surface of the fossil is abraded. In these cases, only the big scars can sometimes be recognised. This is also the case with the landmark points on the peak or tip of the fossil bone. This area is also sometimes not in a complete condition because the epiphyses are the most fragile areas and are more often damaged by taphonomic processes.

Because of this reasons, not all the observation points that have been used by studies of recent bone can be applied in this study. Only the observation points that have a strong and clear appearance and so can be distinguished are applied in this study. These observation points are illustrated in Figure 3.2. The results of the surface morphology assessments are listed in Table 3.5 (femur) and Table 3.6 (tibia), and are described below.

3.2.1. Femur

Six distinctive features were recognised based on surface observations: 1) At the distal articulation of the knee joint, all *Elephas* specimens have an opening between the medial and lateral condyles that are wider than in *Stegodon* and *Sinomastodon*; 2) The *Elephas* femur's indentation between the condyles is narrower and shallower than in *Stegodon* and *Sinomastodon*; 3) The lateral and medial borders of the central part of the diaphysis of *Elephas* tend to be more straight and parallel compared to *Stegodon* and *Sinomastodon*; 4) The medial crest in *Stegodon* specimens has a more robust and strong appearance, especially

in *Stegodon sondaari* that has the strongest and widest medial crest compared to all other specimens; 5) In the third trochanter (see Figure 3.3), *Stegodon sondaari* also has a significantly distinct appearance. Its third trochanter is extremely wide compared to all *Stegodon* specimens, and even more so when compared with *Elephas* specimens, which tend to be more gracile in appearance; and 6) In the most laterally protruding point of the proximal epiphysis, all *Stegodon* specimens are located proximally and more robust compared with all *Elephas* specimens (see Figure 3.3). Based on these six distinctive surface observation points recognised in identified taxa, it follows that six of the isolated and unidentified femur specimens resemble *Stegodon* genera, whereas one (Ngandong specimen MGB-K-FNG) shows more similarity with the identified *Elephas* specimens.

In summary, the surface morphology assessment of the femurs shows that all *Stegodon* specimens typically look more robust than *Elephas* specimens. Among the *Stegodon* specimens, there is only *Stegodon sondaari* that has a markedly different appearance, apart from its much smaller size. *Stegodon sondaari* has the third trochanter much wider than in the other large-sized *Stegodon* specimens. *Sinomastodon bumiajuensis* is quite similar to *Stegodon*. The length of its third trochanter, however, appears to be longer compared to *Stegodon.*

3.2.2. Tibia

Five distinctive features were recognised based on surface observations: 1) All *Elephas* tibias have a small tuberculum intercondylare mediale (see Figure 3.3), contrary to *Stegodon* specimens that have a big tuberculum intercondylare mediale. 2) In *Elephas* tibias the anterior shaft crest is relatively shorter than in *Stegodon* specimens; 3) The medial collateral ligament attachment scar (see Figure 3.3) in *Stegodon* is deeper and more robust than in all *Elephas* specimens; 4) In lateral view the longitudinal appearance of *Stegodon* tibias is more robust than in *Elephas* specimens; and 5) The inferior articular surface of *Elephas* tibias appear flatter than in *Stegodon* specimens (see Figure 3.3). Based on these five distinctive surface observation characteristics, the unidentified Ngandong specimen (MGB-K-FNG) shows similarity in shape with *Elephas* specimens. In short, as with the femur results, the surface morphology assessment of the tibias indicates that *Stegodon* specimens demonstrate a more robust appearance than *Elephas* specimens.

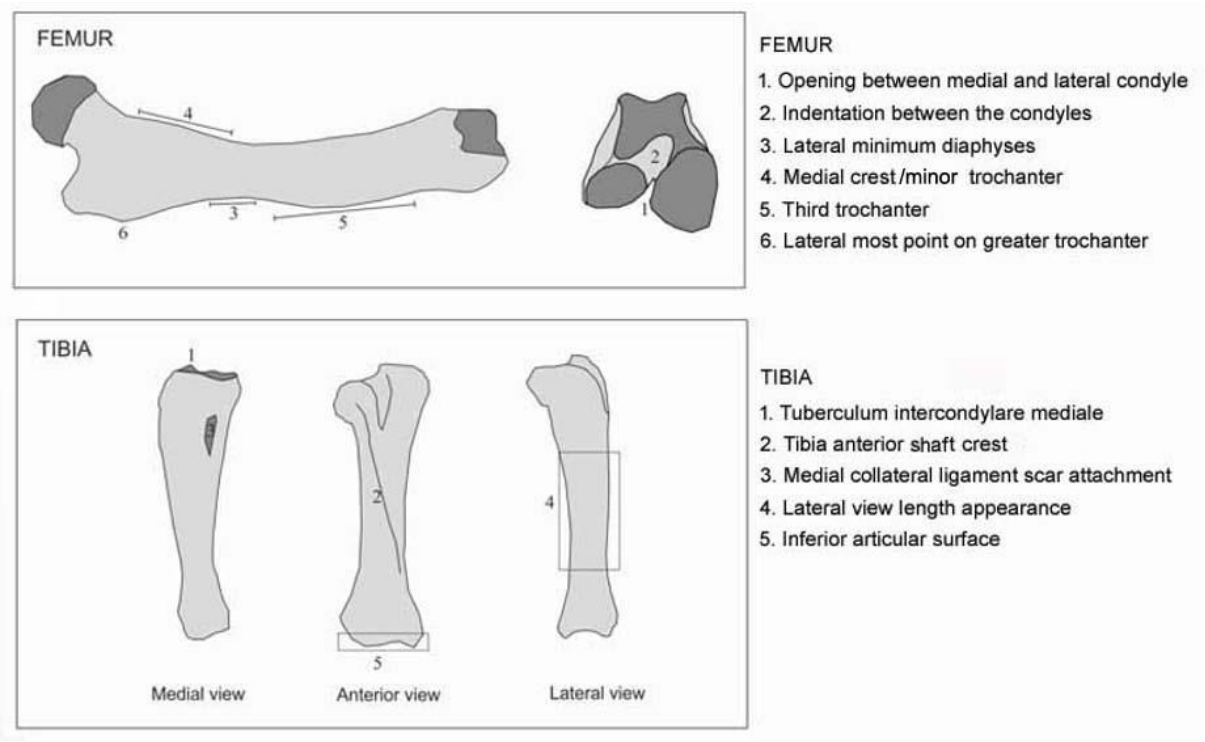

Figure 3.2. Distinctive features of the femur and tibia based on surface morphology assessment (modified from Ariens 1995). The figure shows specimens from the right side. Femur upper left corner: anterior view, upper right corner: distal view.

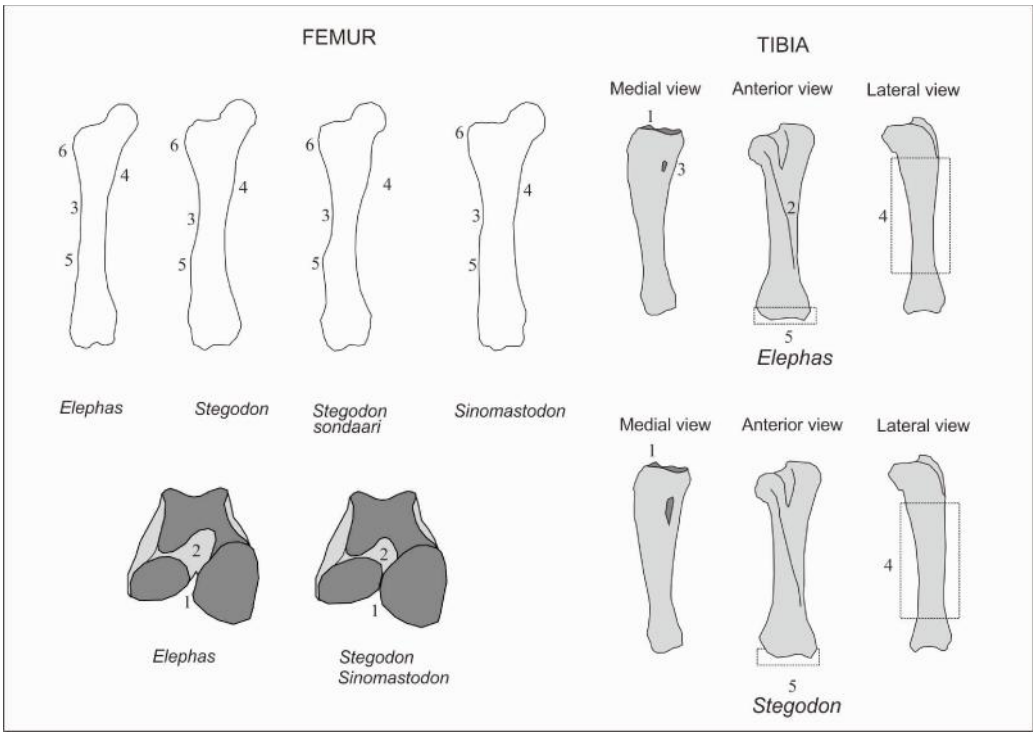

Figure 3.3. Sketch showing the differences between *Elephas* and *Stegodon* / *Sinomastodon* femurs and tibias, based on visual assessment of the surface morphology. All lengthwise figures are drawn to the same scale.

Table 3.5. Visually assessed morphological differences of femur surface morphology.

NO	SPECIMEN	SPECIMEN CODE	REFERENCE COLLECTION	OBSERVATION POINTS					
				1	2	3	4	5	6
				Opening between medial and lateral condyle	**Indentation between the condyles**	**Lateral margin of the diaphysis**	**Medial crest / Minor trochanter**	**Third trochanter**	**Most lateral point of the greater trochanter**
1	*Elephas maximus* 1	EM1	MGB-EM	Wide	Narrow, shallow	Straight	Weak	weak, short	More distally
2	*Elephas maximus* 2	EM2	MB-UGM-EM	Wide	Narrow, shallow	Straight	Weak	weak, short	More distally
3	*Elephas hysudrindicus*	EH	*MGB-EH	Wide	Narrow, shallow	Straight	Weak	weak, short	More distally
4	*Stegodon florensis* 1	SF1	MM14-F619	Narrow	Wide, deep	Concave	Strong	Strong, long	Proximal
5	*Stegodon florensis* 2	SF2	MM11-T23BF176	Narrow	Wide, deep	Concave	Strong	Strong, long	Proximal
6	*Stegodon florensis* 3	SF3	MGB DD4188	Narrow	Wide, deep	Concave	Strong	Strong, long	Proximal
7	*Stegodon sondaari*	SS	TT12-FF3A	Narrow	Wide, deep	Concave	Very strong	Very strong, long	Proximal
8	*Stegodon trigonocephalus* 1	ST1	*MGB-K-ST-FS	Narrow	Wide, deep	Concave	Strong	Strong, long	Proximal
9	*Stegodon trigonocephalus* 2	ST2	*MGB-K-ST-FD	Narrow	Wide, deep	Concave	Strong	Strong, long	Proximal
10	*Sinomastodon bumiajuensis*	SINO	MGB-M	Narrow	Wide, deep	Concave	Strong	Strong, long	Proximal
11	Bekasi femur	uBF	MGB-Bekasi	Narrow	Wide, deep	Concave	Strong	Strong, long	Proximal
12	Patiayam femur	uPT	MPT-FS	Narrow	Wide, deep	Concave	Strong	Strong, long	Proximal
13	Sangiran femur 1	uSang1	Reg225inv1388	Narrow	Wide, deep	Concave	Strong	Strong, long	Proximal
14	Sangiran femur 2	uSang2	Elp0183	Narrow	Wide, deep	Concave	Strong	Strong, long	Proximal
15	Sangiran femur 3	uSang3	Inv1712	Narrow	Wide, deep	Concave	Strong	Strong, long	Proximal
16	Sangiran femur 4	uSang4	Reg485inv1327	Narrow	Wide, deep	Concave	Strong	Strong, long	Proximal
17	Ngandong femur	uNG	*MGB-K-FNG	Wide	Narrow, shallow	Straight	Weak	weak, short	Very proximal

Table 3.6. Visually assessed morphological differences of tibia surface morphology.

No	SPECIMEN	SPECIMEN CODE	REFERENCE COLLECTION	OBSERVATION POINTS				
				1	2	3	4	5
				Tuberculum intercondylare mediale	**Tibia anterior shaft crest**	**Medial collateral ligament attachment scar**	**Lateral view length appearance**	**Distal articular surface**
1	*Elephas maximus* 1	EM1	MGB-EM	Small	Short	Small, shallow, smooth	Slim	Relatively flat
2	*Elephas maximus* 2	EM2	MB-UGM-EM	Small	Short	Small, shallow, smooth	Slim	Relatively flat
3	*Elephas hysudrindicus*	EH	MGB-EH	Small	Short	Small, shallow, smooth	Slim	Relatively flat
4	*Stegodon florensis* 4	SF4	MM05-1	Big	Long	Long, deep, robust	Robust	Relatively high relief
5	*Stegodon sondaari*	SS	TT12-FF18	Big	Long	Long, deep, robust	Robust	Relatively high relief
6	*Stegodon trigonocephalus* 3	ST3	MGB-K-ST-TS	Big	Long	Long, deep, robust	Robust	Relatively high relief
7	*Stegodon trigonocephalus* 4	ST4	MGB-K-ST-TD	Big	Long	Long, deep, robust	Robust	Relatively high relief
8	*Elephas* sp.	ESang5	ELP0983	Small	Short	Small, shallow, smooth	Slim	Relatively flat
9	*Stegodon* sp. Sangiran	SSang6	Reg1965 Inv187	Big	Long	Long, deep, robust	Robust	Relatively high relief
10	*Stegodon* sp. Patiayam	SPT	MPT-TS	Big	Long	Long, deep, robust	Robust	Relatively high relief
11	Ngandong tibia	uNG	MGB-K-TNG	Small	Short	Small, shallow, smooth	Slim	Relatively flat

3.3. Biometric Measurements

The biometric measurements that have been used in this study were taken from van den Bergh (1999). The biometric measurement parameters are shown in Figure 3.4. Eleven biometric measurements for the femur and five biometric measurements for the tibia were used. Of all the parameters, generally researchers compare the length and mediolateral thickness of bones to infer which bone is more robust or more gracile (van der Maarel 1932; Hooijer 1955; Hodgson et al. 2008). For the femur the total length measurement is F7 of van den Bergh (1999) and the mediolateral diameter of the femur shaft at the onset of the third trochanter is F1. For the tibia the total length measurement is T5 and the minimum mediolateral diameter of the tibia shaft is measurement T3 of van den Bergh (1999).

As can be seen from the biometric measurements of the femur (Table 3.7), the total length measurement (F7) separates the sample in three main clusters. There is one very short femur that is less than 500mm long, several middle sized femurs that are between 700-900mm long, and several long femurs of more than 1000mm length. *Stegodon sondaari* (SS) has a short femur, *Elephas maximus* 1 (EM1), *Elephas maximus* 2 (EM2), *Stegodon florensis* 1 (SF1), *Stegodon florensis* 2 (SF2), *Stegodon trigonocephalus* 1 (ST1) and *Stegodon trigonocephalus* 2 (ST2) are of intermediate size and *Elephas hysudrindicus* (EH) and the Ngandong femur specimen (uNG) are the longest.

For the femur's minimum transverse diameter of the diaphysis (F1) the measurements show four main clusters: minimum diameters of less than 100mm, between 100 and 120mm, 120 and 140mm, and more than 140mm. *Stegodon sondaari* (SS), *Elephas maximus* 1 (EM1) and 2, and *Stegodon florensis* 3 (SF3) have F1 measures of less than 100mm. Sangiran femurs 1 (uSang1), Sangiran femurs 2 (uSang2), Sangiran femurs 3 (uSang3), *Stegodon florensis* 1 (SF1), *Stegodon florensis* 2 (SF2), and *Sinomastodon bumiajuensis* (SINO) have F1 values of between 100-120mm. The Bekasi femur (uBF), Patiayam femur (uPT), *Stegodon trigonocephalus* 1 and 2, and Sangiran femur 4 have minimum diameters between 120 and 140mm. Specimens that have F1 values of more than 140mm are *Elephas hysudrindicus* (EH) and the Ngandong femur specimen (uNG).

The maximum length measurement for the tibia (measurement T5 of van den Bergh 1999) also breaks up into three size clusters: short ones of less than 300mm length, middle sized

tibias of between 400 and 700 mm length, and large tibias of more than 700 mm length. *Stegodon sondaari* (SS) has a short femur; *Elephas maximus* 1 (EM1), *Elephas maximus* 2 (EM2), *Stegodon florensis* (SF4) and *Stegodon trigonocephalus* are intermediate-sized; and *Elephas* from Sangiran (S6) and *Elephas hysudrindicus* (EH) have the longest tibias (Table 3.8).

For the minimum transverse diameter of the tibia shaft (T3) the data shows three main clusters. There are tibias less than 70mm in transverse diameter, a group of tibias with T3 values of between 70 and 100mm, and tibias with T3 values of more than 100mm. *Stegodon sondaari* (SS), *Elephas maximus* 2 (EM2), *Stegodon florensis* 4 (SF4), *Stegodon* Patiayam tibia (PT), and Sangiran 6 (S6) have T3 values of less than 70mm. *Elephas maximus* 1 (EM1), *Stegodon trigonocephalus* 1 (ST1) and *Stegodon trigonocephalus* 2 (ST2) have T3 values of between 70-100mm. Proboscidea that has T3 values of more than 100mm are *Elephas hysudrindicus* (EH), *Elephas* Sangiran 5 (ESang5) and the Ngandong specimen (uNG).

What these biometric measures show is that based on the size of its limb bones, Proboscideans from Indonesia have a wide range of sizes from small, medium to very large. Of all the specimens included in this study, the size of the Flores proboscideans are on average smaller than elephants from Java and Sumatra.

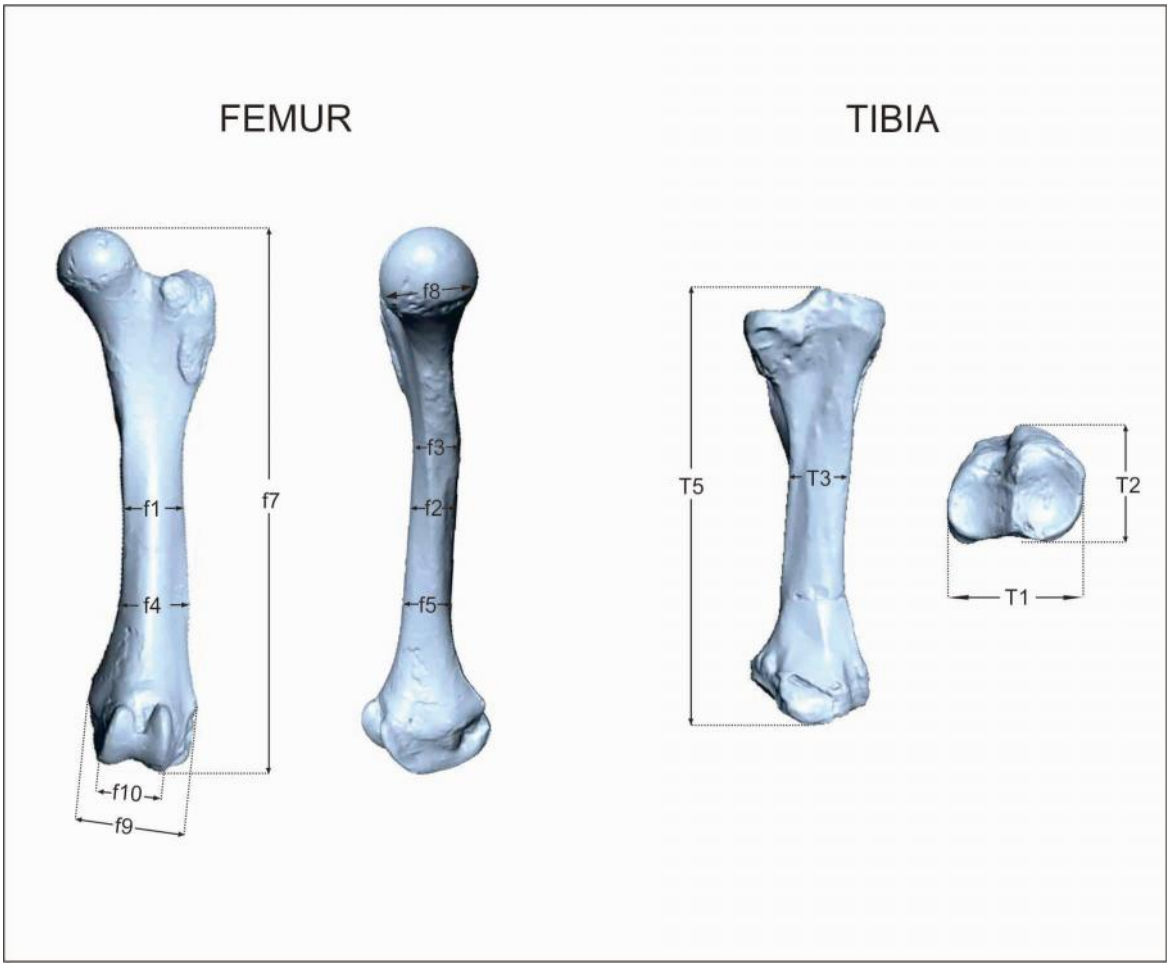

Figure 3.4. Biometric scaling measures of proboscidean femur and tibia. Measurement definitions are the same as used by van den Bergh (1999). **Femur**: F1: minimum transverse diameter of diaphysis; F2: anteroposterior diameter of diaphysis at level of minimum transverse diameter; F3: minimum anteroposterior diameter of diaphysis; F4: transverse diameter at distolateral tuberosities (the third trochanter); F5: anteroposterior diameter at the same level as F4; F6: minimum circumference of diaphysis; F7: total length of femur between caput and lateral condyle; F8: anteroposterior diameter of caput; F9: maximum transverse diameter of distal epiphysis; F10: maximum transverse diameter of distal condyles; F11: anteroposterior diameter of distal epiphysis, medial side. **Tibia**: T1: maximum proximal transverse diameter; T2: maximum proximal anteroposterior diameter; T3: minimum transverse diameter of diaphysis; T4: minimum anteroposterior diameter of diaphysis (opposite site of T3 but in the minimum location, not showing in the skets); T5: total length.

Table 3.7. Femur biometric measurements (in mm) for all specimens.

No	Specimen	Code	Measurement parameters														Index ratio
			parameters taken from van den Bergh (1999)											parameters added in the present study			
			F1	F2	F3	F4	F5	F6	F7	F8	F9	F10	F11	F12	F13	F14	F1/F7
1	*Elephas maximus* 1*	EM1	95	67	64	95	79	259	900	121	171	155	181	7	11.11	28.78	0.11
2	*Elephas maximus* 2*	EM2	92	53	52	94	62	244	817	102	153	133	146	7	11.67	29.87	0.11
3	*Elephas hysudrindicus**	EH	150	97	85	156	117	400	1251	159	254	250	239	12	11.11	31.97	0.12
4	*Stegodon florensis* 1	SF1	106	74	72	110	77	278	802	110	172	152	155	19	6.94	34.66	0.13
5	*Stegodon florensis* 2	SF2	104	71	64	113	75	273	778	113	166	149	180	19	6.94	35.09	0.13
6	*Stegodon florensis* 3	SF3	92	65	60	113	68	252	750	100	149	139	149	18	6.94	33.6	0.12
7	*Stegodon sondaari**	SS	52	42	32	65	41	141	467	63	99	73	91	13	12.5	30.19	0.11
8	*Stegodon trigonocephalus* 1	ST1	123	77	75	129	81	313	870	134	196	165	180	20	6.94	35.98	0.14
9	*Stegodon trigonocephalus* 2	ST2	134	78	77	145	92	330	870	138	197	177	183	20	6.94	37.93	0.15
10	*Sinomastodon bumiajuensis*	SINO	113	84	72	130	86	310	860	123	190	155	187	26	6.94	36.05	0.13
11	Bekasi femur	uBF	121	78	72	129	77	310	823	123	176	152	180	19	6.94	37.67	0.15
12	Patiayam femur	uPT	133	84	75	149	96	374	1047	128	245	216	207	23	7.78	35.72	0.13
13	Sangiran femur 1	uSang1	114	76	74	139	92	345	952	143	220	187	220	19	6.94	36.24	0.12
14	Sangiran femur 2	uSang2	103	68	80	122	72	289	874	126	175	162	193	20	6.94	33.07	0.12
15	Sangiran femur 3	uSang3	114	62	60	128	73	299	861	128	178	161	195	20	7.78	34.73	0.13
16	Sangiran femur 4	uSang4	136	82	127	154	93	381	995	141	232	185	227	26	7.22	38.29	0.14
17	Ngandong femur*	uNGF	159	108	95	177	126	433	1290	180	261	233	253	14	11.11	33.57	0.12

*Belong to (partial) skeletons.

Table 3.8. Tibia biometric measurements (in mm) for all specimens.

No	Specimen	Code	Measurement parameters								Index ratio T3/T5
			parameters taken from van den Bergh (1999)					parameters added in the present study			
			T1	T2	T3	T4	T5	T6	T7	T8	
1	*Elephas maximus* 1*	EM1	168	120	76	55	649	29	202	31.12	0.12
2	*Elephas maximus* 2*	EM2	148	103	61	46	515	23	182	35.34	0.12
3	*Elephas hysudrindicus**	EH	265	160	110	85	776	60	311	40.08	0.14
4	*Stegodon florensis* 4	SF4	159	127	66	55	467	88	203	43.47	0.14
5	*Stegodon sondaari**	SS	84	65	34	33	286	26	107	37.41	0.12
6	*Stegodon trigonocephalus* 3	ST3	172	128	78	60	470	88	233	49.57	0.17
7	*Stegodon trigonocephalus* 4	ST4	174	130	78	65	500	93	238	47.60	0.16
8	*Elephas* sp Sangiran	ESang5	243	177	110	83	741	56	308	41.57	0.15
9	*Stegodon* sp. Sangiran	SSang6	167	116	66	78	531	98	259	48.78	0.12
10	*Stegodon* sp. Patiayam	SPT	181	137	63	87	536	100	258	48.13	0.12
11	Ngandong tibia*	uNGT	245	150	118	86	785	61	298	37.96	0.15

*Belong to (partial) skeletons.

3.4. Sexual Dimorphism

Of all specimen included in this study, only of the two recent *Elephas* specimens the sex is known. *Elephas maximus* 1 is male and *Elephas maximus* 2 is female. Unfortunately, both of them are still in the growth stage, the male specimen more so than the female specimen.

Size and robustness are descriptive characteristics that are often used to evaluate the sex of mammal bones. Elephants are mammals that show clear sexual size dimorphism. In linear sizes, the males are about 20-40% bigger than female and can be nearly two times as heavy as the females (Haynes 1991; Sukumar 2003). In the extant modern African bush elephant (*Loxodonta Africana*), male elephants usually are 23% taller than females on average whereas for Asian elephant (*Elephas maximus*) males are around 15% taller than females (Larramendi 2015).

In postcranial bones, the sex of mammals usually can be identified based on the shape of the pelvis. Unfortunately, because its shape is wide and thin compared to the other postcranial bones, it is not common to find the pelvis in good condition in fossil forms. Among the fossil specimens only the *E. hysudrindicus* skeleton has a complete and well-preserved pelvis associated. Female elephants have larger pelvic apertures then males. Lister (1996) was able to distinguish between the pelvis of male and female individuals of *Mammuthus* based on distinct ratios between the height of the pelvic aperture and the width of the ilium shaft. In the Blora *E. hysudrindicus* individual, the pelvic aperture of the left pelvis has a diagonal dorso-ventral diameter of 422 mm and a minimum transverse diameter of the ilium shaft of 197 mm (Measurements 2 and 5, respectively, of Lister 1996), giving a ratio of 2.14. Lister (1996) found that this ratio is less than 2.4 in male mammoths and over 2.5 in females. The ratio of 2.14 in the *E. hysudrindicus* skeleton suggests that it was a male. This would be in accordance with the relatively large overall stature and tusk diameter, but the ratios should be checked with pelvis of male and female individuals of the more closely related extant Asian elephant for confirmation of the sex. In the various biometric and morphometric analyses, no distinction has been made between male and female individuals.

3.5. Age Estimation

When considering the age of fossil proboscideans, a distinction should be made between the actual age and the age estimates based on wear stages of the molar teeth and age estimates

based on epiphyseal fusion sequences. The actual age at death of *Elephas maximus* 1 and *Elephas maximus* 2 specimens are known from the information provided by the park rangers who facilitated the recovery of the skeletons.

For the age estimation based on molar teeth wear patterns we applied the method used by Jachmann (1988) and based on studies of the African Elephant. There is a difference in terminology in naming elephant molars as used by biologist and paleontologist. Palaeontologists commonly use the dp2, dp3, dp4, M1, M2 and M3 system (Hooijer 1980; van den Bergh et al. 2001) that is equivalent to the biologist's system of M1, M2, M3, M4, M5 and M6 (Lee et al. 2011). As it predominantly deals with fossil specimens, this study will use the first system. When estimating the relative age of an individual based on dental wear patterns as developed for the African elephant, it is customary to speak of African Elephant Years (AEY). Lee et al. (2001) refines the age estimation of Jachmann (1988) by calibrating the molar replacement scheme with known ages of individuals when they died. This age assessment scheme is presented in Table 3.9. The age estimation based on epiphyses fusion stages is based on the system developed by Herridge (2010) (see Table 3.10).

Table 3.9. Estimation of African elephants based on dental wear stages according to Jachmann (1988).

Age in years	**dp2**	**dp3**	**dp4**	**M1**	**M2**	**M3**
0-0.25	Present to wear	Present to wear, may be below gum line				
0.5	Worn	Present above gum line and 30% in wear				
1	Residual or gone	Up to 6 lamellae in wear	Visibly forming in alveolus			
2.5		7 lamellae in wear	Present, first lamellae starting to wear			
2.5		5 to 7 lamellae in wear	8 lamellae present and wear starting			
4		Few, if any lamellae remaining	8 lamellae in wear	Forming in alveolus		
5		Possible root visible	8 lamellae in wear	Visible but not in wear		
6			7 lamellae remaining	1 lamella in wear		

8			Variable (5-9)	5 lamella in wear		
10			2-5 lamellae in wear	4-7 lamellae in wear		
13				7-8 lamellae in wear	visible	
15				8 lamellae	1-6 in alveolus, 1-2 coming into wear	
18±2				5 lamellae	3 lamellae in wear	
20±2				4 lamellae	5-6 lamellae in wear	
22±2				3 lamellae remaining (or flat loops)	6-8 in wear	
26±2				2 remaining (or flat loops)	4-8 visible and coming	
28±2					7-9 in wear	Occasionally visible in alveolus
29±2					9+ in wear	1 in full wear
32±2					7-8 in wear	2-3 starting to wear
34±2					3 lamellae	3-6 visible and starting to wear
35±2					3-6 remaining in wear	5-7 in wear
38-41					2-3 remaining	5-8 in wear
42-44					1-2 may remain	10-11 in wear
45-46						9-11 in wear
47±2						8-10 in wear (overlap in ages between categories)
49±2						8-10 in wear
53±2						7-9 remaining
55±4						6-8 remaining
60-62						5-8 remaining
65-69						2-6 remaining

Individual *Elephas maximus* 1 (EM1) still has the M1 and M2, of which the M1 has the 8 posterior lamellae in wear and the M2 has the first 3 lamellae in wear, with the remaining lamellae still in the alveolus. Based on Jachmann's age assessment scheme, the age of EM1 is around 15 AEY years old (Table 3.11). In *Elephas maximus* 2 (EM2) the M1s are completely lost by wear and the succeeding M2s have 8 lamellae in wear, whereas the M3 is unworn and

still in the alveole. Based on Jachmann's scheme the estimated age of EM2 would be around 28 AEY old. These age estimates are in good agreement with the actual recorded ages at death of these two recent individuals, suggesting that the age estimation schemes developed for *Loxodonta africana* can also be applied for *E. maximus*.

The skeleton of *Elephas hysudrindicus* from Sunggun, Blora Regency, has 8 lamellae of the M3 in wear, so it can be inferred that this individual was around 49 AEY old. The associated mandible of the *Stegodon sondaari* partial skeleton still has the M2 and M3, with all lamellae of the M2 worn and the 5 anterior lamellae of the M3 worn. So the age of this individual of *Stegodon sondaari* can be inferred to be around 35 AEY based on Jachmann's scheme, although due to its very small body size the true age of this individual may have been less than 35 years. Since the total average lifespan of mammals correlates positively with body size, it is possible that dwarfed proboscideans such as *Stegodon sondaari* had shorter lifespans than their large-bodied relatives.

Since most postcranial elements of the studied assemblage are not associated with dentitions, the age estimates based on dentition cannot be used in these cases. As mentioned in Chapter two, Herridge (2010) developed a system to make relative age estimates based on elephant epiphyseal fusion successions in limb long bones (Table 3.10). The first limb bone epiphyses to fuse with the shaft is the distal part of the humerus; The next Stage 2 is reached when the proximal part of the ulna, the distal part of the femur, the proximal part of the tibia, and the distal part of the tibia fuse. In Stage 3 (fully adult) the proximal part of the humerus, the distal part of the ulna, and the proximal part of the femur fuse. After this all the limb bones are full-grown and no further growth takes place. So, although less accurate, the epiphyseal fusion scheme is more practical to apply in studies of isolated limb bones, or in partial skeletons with one or more of the long bones present. Of all the specimens in the studied sample, only two individuals are not fully full-grown. These are *Elephas maximus* 1 (EM1) in stage 1 and *Elephas maximus* 2 (EM2) in Stage 2 (Table 3.11).

As can be seen in Table 3.11, all fossil specimens are full-grown and belong to epiphyseal fusion Stage 3. It is unfortunate that no full-grown recent *Elephas* specimens were available for this study. It is possible that some morphological variation encountered in the various

analyses is due to the fact that the two recent *Elephas* specimens had not yet reached their full size. This should be kept in mind when analyzing the analytical results.

Table 3.10. Epiphyseal fusion scheme after Herridge (2010).

Stage		Humerus		Ulna		Tibia		Femur	
		Prox	Dist	Prox	Dist	Prox	Dist	Prox	Dist
1	First fused		V						
2	Early fusion			V		V	V		V
3	Late fusion	V			V			V	

Table 3.11. Relative ages of the fossil specimens in the studied sample, based on epiphyseal fusion stages based on the scheme of Herridge (2010).

No	**Specimen**	**Femur**		**Tibia**		**Herridge State**	**Age by teeth (AEY)**	**Actual Age**
		Proximal	**Distal**	**Proximal**	**Distal**			
1	*Elephas maximus* 1	Not fused	Not fused	Not fused	Not fused	1	±15	15
2	*Elephas maximus* 2	Not fused	Fused	Fused	Fused	2	±28	29
3	*Elephas hysudrindicus* EH	Fused	Fused	Fused	Fused	3	±49	-
4	*Stegodon sondaari*	Fused	Fused	Fused	Fused	3	±35	-
5	Ngandong specimen	Fused	Fused	Fused	Fused	3	-	-
6	*Stegodon florensis* 1	Fused	Fused	-	-	3	-	-
7	*Stegodon florensis* 2	Fused	Fused	-	-	3	-	-
8	*Stegodon florensis* 3	Fused	Fused	-	-	3	-	-
9	*Stegodon trigonocephalus* 1	Fused	Fused	-	-	3	-	-
10	*Stegodon trigonocephalus* 2	Fused	Fused	-	-	3	-	-
11	*Sinomastodon bumiajuensis*	Fused	Fused	-	-	3	-	-
12	Bekasi femur	Fused	Fused	-	-	3	-	-
13	Patiayam femur	Fused	Fused	-	-	3	-	-
14	Sangiran femur 1	Fused	Fused	-	-	3	-	-
15	Sangiran femur 2	Fused	Fused	-	-	3	-	-
16	Sangiran femur 3	Fused	Fused	-	-	3	-	-
17	Sangiran femur 4	Fused	Fused	-	-	3	-	-
18	*Stegodon florensis* 4	unknown	unknown	Fused	Fused	3	-	-
19	*Stegodon trigonocephalus* 3	unknown	unknown	Fused	Fused	3	-	-

20	*Stegodon trigonocephalus* 4	unknown	unknown	Fused	Fused	3	-	-
21	*Elephas* sp.	unknown	unknown	Fused	Fused	3	-	-
22	*Stegodon* sp. Sangiran	unknown	unknown	Fused	Fused	3	-	-
23	*Stegodon* sp. Patiayam	unknown	unknown	Fused	Fused	3	-	-

3.6. Ratio Tibia/Femur

The ratio tibia/femur analyses was applied to investigate the observations made on other large terrestrial mammals that showed shortening of the limbs that are thought to be the result of adaptations to island environments (Sondaar 1977). Only five individuals could be tested. Four of the five individuals have a similar T5/F7 ratio between 0,61 and 0.63. The exception is the youngest individual in the assemblage, *Elephas maximus* 1 (EM1), that stands out with a higher ratio of 0.72 (Table 3.12). Both EM1 and EM2 are still in the growth phase, although in EM2 only the proximal femur epiphysis was not yet fully fused, indicating that it was close to the full-grown stage. Therefore, it clusters with the other fully adult specimens. In EM1 all epiphyses of both tibia and femur are still not fused. It is possible that the length ratio would still change during further growth, which may explain the higher ratio in this individual. Again, this should be kept in mind when interpreting the data outcomes of the morphometric analysis. However, because the already small comparative sample size, it was decided to keep this specimen in the analysis.

Table 3.12. Ratio between the total length of the tibia and of the femur in single individuals.

No	Specimen	F7	T5	Ratio T5/F7
1	*Elephas maximus* 1	900	649	0.72
2	*Elephas maximus* 2	817	515	0.63
3	*Elephas hysudrindicus* EH	1251	776	0.62
4	*Stegodon sondaari*	467	286	0.61
5	Ngandong specimen	1290	785	0.61

3.7. 3D Scanning

A morphometric analysis requires precision shape data. Traditionally, this shapes data is generated from photographs and drawings. However, recent developments in software and technology now allow for morphometric analysis to be done in 3D graphics formats. The detailed information about the 3-dimensional shapes of specimens is needed in fossil material analysis. With 3D digital models on a computer screen the 3D landmark analysis can be done more precisely.

All of the limb bone specimens were surface scanned using a NextEngine 3D Scanner Ultra HD. The scanning process involved using three distance instrument settings (macro, wide and long) based on the context of the specimen. When the specimen is an isolated specimen the distance that was used was 'wide' or 'long'. However, when the specimen was part of a mounted and articulated skeleton all distance variations were used to catch the maximum point cloud as much as possible, and especially in blind spots such as where the bones articulated with the joints.

Once the scanning was complete for each specimen the data were imported into the 3D finishing software, Geomagic Studio (version 10). The 3D files from the NextEngine scanner are mostly not perfect in shape. Usually, there are blank areas that could not be scanned due to their hidden position and that could not be reached by the scanning laser beam. This results in 'holes' in the 3D file. With Geomagic software, these holes can be reshaped with precision. After completion the 3D files were exported as ply files (*.ply), and these were used for the acquisition of the 3D landmark coordinates using 3D Landmark software.

3.8. The 3D Landmarks

Landmark analysis is the measurement of data where the data is generated in the form of data point locations. A landmark point in this case is a spot on the surface of the object that is defined in such a way that it is equivalent for all the objects being compared (O'Higgins 2000). This study uses 3D landmark coordinates because some bones do not translate well to a two dimensional analyses, and this includes the tibia (Bonnan 2001). The data produced in a 3D analysis are three-dimensional coordinates (x, y, z). Digitisation of the landmark coordinates was done using the software *Landmark* (Version 3.6) developed by the Institute for Data Analysis and Visualization (IDAV) group at the University of California, Davis

(Wiley et al. 2005). The software is used to put the landmark points on the scans of the specimens and generate and extract the 3D point coordinates as a file with the *DAT extension. Each specimen's landmarks were then compiled in one file with a *TXT extension so that the landmark coordinate data could then be imported in the Geometric Morphometric (GM) software for further analysis.

The 3D coordinate landmarks are ranked into three types (Polly 2012), which are:

- Type I landmark

  Type I landmarks are the strongest type of landmarks. The points on the different 3D object are claimed to be homologue. These landmarks are well-defined and based on clear visibility, e.g. the meeting point of three sutures on the cranium. In the femur and tibia, only the nutrient foramen (a small hole in the bone for veins) can be used as landmark type I. Unfortunately due to its small size, the superficial openings of nutrient foramen are often obliterated after burial and fossilization. In this study, almost all of the specimens are fossilized. Therefore nearly all the nutrient foramen and all the other surface characteristics (e.g. muscle attachment scar) of the specimens are not clear. Therefore, no Type I landmarks could be used in this study.

- Type II landmark

  Type II landmarks are points that are claimed as homologous based on a significant geometric shape, e.g. the point on the surface of a tooth where the curvature is the sharpest. In this study, several protruding parts of the limb bones were used as landmark type II (e.g. the most lateral point on the greater trochanter of a femur and the highest tip of the condyles in a posterior view of the tibia).

- Type III landmark

  Landmark type III is a landmark that cannot be determined by its self, but requires other landmark points as auxiliary point to determine the position of the landmark type III point (e.g. the point exactly in the middle halfway between the onset of the medial crest and the termination of the medial crest on the femur).

A total of 34 landmarks were used to define the shapes of the femur (see Table 3.13) for the landmark definitions and Figure 3.5 for their location). A total of 24 landmarks were applied for the tibia (see Table 3.14 for the landmark definitions and Figure 3.6 for their location).

Most of the landmarks are taken from other studies, predominantly applied to recent bones. Because in this study most specimens are fossilized, some of the landmarks that are characterized by detailed surface shapes could not always be distinguished in fossils, due to localized surface abrasion of fossil specimens, for example obliterating muscle scars. For this reason most landmarks were devised to capture the overall shape of the specimens.

Before the landmark points were chosen for this study, first all the landmark points that were compiled from previous studies were applied to all the specimens to assess how well they could be applied. After this step, those landmark points were eliminated that could not be recognised in all fossil specimens. The landmark coordinates were checked for outliers in the GM software (see the next section). Specimens that were outliers were then re-examined and errors in landmark identification, and landmark number were corrected.

Table 3.13. Femur landmarks.

No	**Landmarks**	**Type**	**Source**
1	Most superior point of the femur head	II	Harmon, 2007
2	Head-neck border at neck midline	II	Harmon, 2007
3	Neck midpoint between head and greater trochanter	II	Harmon, 2007
4	Neck-greater trochanter border anterior to trochanteric fossa	II	Harmon, 2007
5	Most superior point of the greater trochanter	II	Harmon, 2007
6	Most lateral point on greater trochanter	II	Harmon, 2007
7	Pre-trochanteric tubercle	II	Bonneau, 2012
8	Most minimum diameter point on the lateral side	II	Modified from van den Bergh (1999)
9	Onset of third trochanter	II	This study
10	Third trochanter	III	This study

11	Third trochanter	III	This study
12	Termination of third trochanter	II	This study
13	Lateral constriction of the distal area	II	Smuts, MMS & Bezuidenhout 1994
14	Most posterior point of the distal lateral condyle	II	Bonnan, 2004
15	Maximal curvature of the lateral trochlea	II	This study
16	Maximal curvature of the central hollow of the trochlea	II	Bonneau, 2012
17	Maximal curvature of the medial trochlea	II	This study
18	Most posterior point of the distal medial condyle	II	Bonnan, 2004
19	Medial constriction of the distal area	II	Smuts, MMS & Bezuidenhout 1994
20	Point halfway between the medial constriction of the distal area and the point on the medial side of the shaft where the transverse diameter of the shaft is minimal	III	This study
21	Opposite point of the onset of the third trochanter	III	This study
22	Point on the medial side of the shaft where the transverse diameter of the shaft is minimal	II	Modified from van den Bergh (1999)
23	Distal onset of the medial crest	II	This study
24	Point halfway between the distal onset of the medial crest and the proximal termination of the medial crest	III	This study
25	Proximal termination of the medial crest	II	This study
26	Most inferior point on the caput - neck transition at its midline	II	Harmon, 2007
27	The most distal point of the lateral condyle	II	This study
28	The most distal point of the medial condyle	II	This study
29	The upper lateral corner of the lateral condyle on the posterior side	II	Modified from Figueirido & Janis, 2011
30	Medial upper corner of the lateral condyle on the posterior side	II	Modified from Figueirido & Janis, 2011
31	Inner upper corner point of the medial condyle at the posterior side	II	Modified from Figueirido & Janis, 2011
32	Posterior base inner corner point of the lateral condyle	II	Modified from Figueirido & Janis, 2011

33	Posterior point on the diaphyses minimum diameter	III	This study
34	Anterior point on the diaphyses minimum diameter	III	This study

Table 3.14. Tibia landmarks.

No	**Landmarks**	**Type**	**Source**
1	Tip of the proximal fovea for articulation with the femur condyles in posterior position	II	Smuts, MMS & Bezuidenhout 1994
2	Tip of the fovea for articulation with the femur condyle in anterior position	II	Smuts, MMS & Bezuidenhout 1994
3	The most anterior-ward point of the lateral fovea for articulation with the lateral femur condyle	II	This study
4	The most lateral-ward point of the lateral fovea for articulation with the lateral femur condyle	II	This study
5	The most posterior-point of the ridge separating the two articulation feveae, behind the first landmark point of the tibia	III	This study
6	The most posterior-ward point of the medial fovea for articulation with the femur condyle	II	This study
7	The most medial-ward point of the medial fovea for articulation with the femur condyle	II	This study
8	The most anterior-ward point of medial articulation fovea with the femur condyle	II	This study
9	Tuberositas tibiae	II	Smuts, MMS & Bezuidenhout 1994
10	The distal end of the anterior ridge of the diaphysis	II	This study
11	The most anterior point of the diaphysis at its minimun anteroposterior diameter	II	This study
12	The most medial point at the minimum anteroposterior diameter of the diaphysis	II	This study
13	The most posterior point of the diaphysis at the level of its minimum anteroposterior diameter	II	This study
14	The most lateral point of the diaphysis at the level of its minimum anteroposterior diameter	II	This study

15	Tip of the malleolus	II	Frelat, et al 2012
16	Most posteromedial point on the distal articular surface	II	Frelat, et al 2012
17	Most posterolateral point on the distal articular surface	II	Frelat, et al 2012
18	Most proximal point on the soleal line, often faintly marked tubercle just inferior to the fibular facet	II	Frelat, et al 2012
19	Most anterolateral point on the distal articular surface	II	Frelat, et al 2012
20	Most anteromedial point on the distal articular surface	II	Frelat, et al 2012
21	Most distal point of the proximal ligament attachment scar	II	Modified from Ariens, 1995
22	Ligament attachment proximalward point	II	Modified from Ariens, 1995
23	The most medial point of the diaphysis at the level of its minimum transverse diameter t	II	This study
24	The most lateral point of the diaphysis at the level of its minimum transverse diameter	II	This study

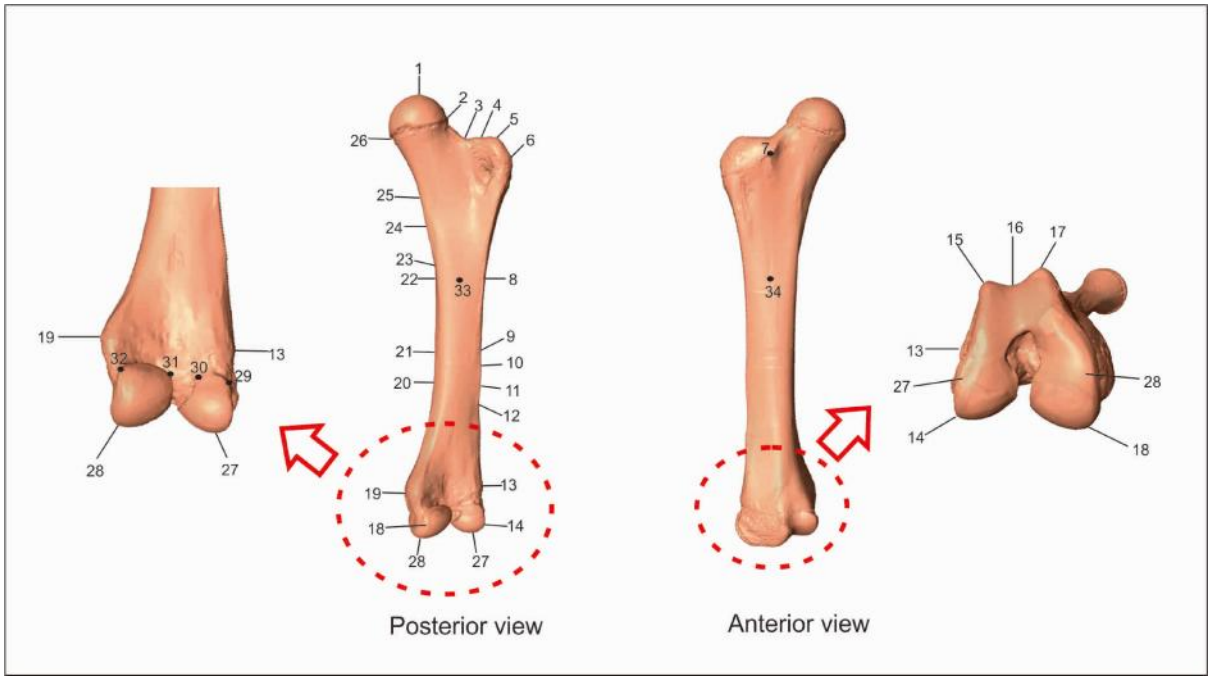

Figure 3.5. Landmark points of the femur. For definitions of these landmarks see Table 3.13.

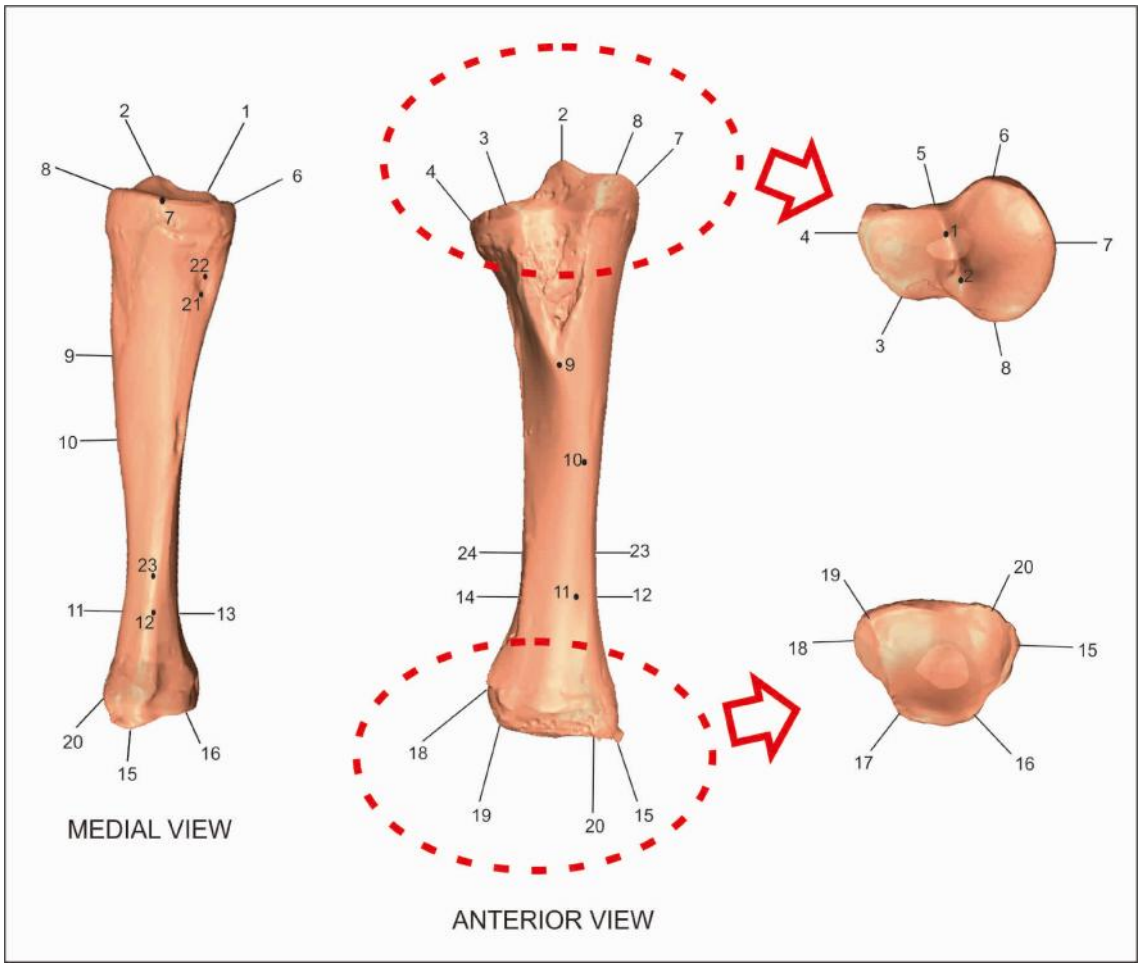

Figure 3.6. Landmark points of the tibia. For definitions of these landmarks see Table 3.14.

3.9. Statistical Methods

The statistical methods involved a series of steps. Firstly the data from the biometric measurements (see section 3.3) were analysed using a Principle Components Analysis (PCA) to see if any were significant for separating the identified specimens according to their known genera and species (Femur 1-10, Tibia 1-10). The biometric measurements that were important were then used in the GM analysis as independent variables. The new biometric measurements that were suggested by the GM analyses were converted into biometric measurements and then analysed using a PCA to see if they could improve the separation of genera and species. These new biometric measures were then tested with the unidentified specimens to see where they grouped with the identified specimens in the analysis.

The femur and tibia were analysed separately. To see if there is agreement within a specimen and between the two bones, a separate biometric analysis involved the specimens that were from a single individual. That is when the femur and tibia came from the same individual (Specimens in Table 3.13). The analytical methods are described in more detail below.

3.9.1. Principle Component Analysis (PCA)

The biometric measurements (Tables 3.7, 3.8) were analysed using a PCA using the palaeontological statistics software package PAST (version 3.10) (Hammer, Harper & Ryan 2001). The aims of PCA are to reduce the variables to retain only the most significant variables. Because a PCA assumes approximate normality of the data distribution, the data were transformed into normalised values to project the original data onto directions which maximize the variance before being used in PCA (Qian, Gabor, & Gupta 1994; Jolliffe 2002; Bonnan 2004). The normalized normal distribution is called Z-scored. The normalised values are obtained using the following equation (Gordon, 2006):

$$z = \frac{x_i - \mu_X}{\sigma_X}$$

Remarks:

- z : standard normal distribution score
- σ : standard deviation
- x_i : a value in the data set
- μ_X : the mean of the data set

The normalised data used in the PCA are shown in Table 1 and 2 of the Appendix A. PCA results in variables that are called principal components (PCs). Some of the values and features of a PCA that are used to interpret the result are:

- Eigenvalue

Each PC produced has a weight called an eigenvalue. PCs with larger eigenvalues are considered to be more important and representative of the entire state data. Only PCs within the cumulative eigenvalue limit up to 95% are considered.

- Loading

The principal components interpretation is based on the data of which variables are most strongly correlated with each PC. The most strongly influencing variable is the farthest from zero in either positive or negative direction (+/-). Which numbers are considered to be large or small is a subjective decision. The loading value that is traditionally chosen as an indicator of importance is 0.5 (+/-) (Stat 505 2016). If the value of the loading is more than 0.5 (+/-) this indicates that the biometric measurement parameter is important and has an influence in separating and clustering the specimens within the PCA scatter plot.

- Scree plot

The plot of eigenvalues in a scree plot can also be used as a tool to decide which of the PCs are important. The components may be regarded as insignificant after this curve starts to flatten out. In PAST software, the confidence interval shows 95% if bootstrapping has been carried out. Bootstrapping is a resampling technique used to obtain estimates of summary statistics. The expected eigenvalues under a ‘Broken Stick’ curve can also be plotted in PAST. In such a curve, the eigenvalues may indicate non-significance if they plot below the Broken Stick Curve (Jackson 1993).

3.9.2. Geometric Morphometics (GM)

To identify patterns of shape differences within and between the femur specimens, and within and between the tibia, 3D landmark coordinates can be analysed using the GM program, *morphologika2* (version 2.5), developed by O'Higgins and Jones (2006).

Identification of the variation in the analysis of GM is based on a complex of shape information and also independent of scale. The way *morphologika2* removes differences in orientation, position and scale is through Procrustes registration (O'Higgins 2000). Hammer and Harper (2006) stated that procrustes registration aligns landmarks from a number of specimens by subjecting them to scaling, rotation and translation (fig 3.7).

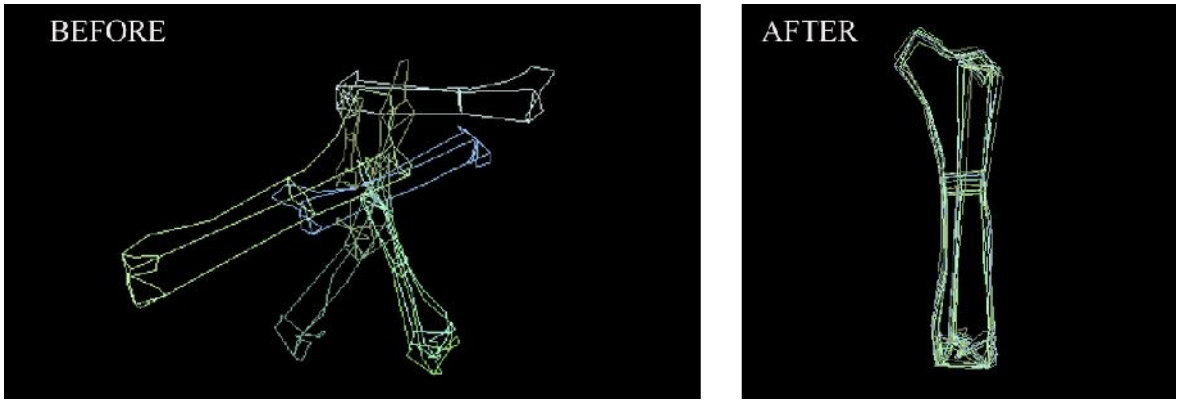

Figure 3.7. Before and after procrustes and tangent space projection for landmark 3D data of various femurs.

After Procrustes registration the following GM analyses were performed in *morphologika2*:

1. Principal Component Analysis (PCA): the principle patterns of variation occurring within a group of shapes, with each shape accorded scores according to these patterns of shape variation (PC scores). For deciding significance of the PCs the standard value of 0.05 was applied (Hammer & Harper 2006).
2. Wireframe images and Thin Plate Spline (TPS) deformation grids. These represent the visualizations of the analyses.
3. Multivariate Regression: the shape variations attributable to a particular aspect of individual difference, which is identified using independent variables.

These analyses are explained in more detail below:

Principal Components Analysis (PCA)

To perform a PCA in *morphologika2*, at first the coordinates in a 3D file should be extracted into a *.TXT file, which is the file type that can be read by *morphologika2*. The output of the PCA is a series of Principle Components (PCs), numbered PC1, PC2, PC3 and so on. Each PC has its own character. PC1 identifies the greatest variation, the information that contributes more than any of the other PCs to the overall variation. PC2 identifies the second largest variation but uses a different axis that intersects with PC1. PC3 takes the midpoint of PC1 and PC2. Higher numbered PCs usually do not show much variation because it only takes the remnants of information about the variation that is not used on previous PCs. In any analysis of PCA, *morphologika2* displays two values for each PC in the scatter plot graph. Each specimen is represented as a point in this graph where each point can be used to represent the differences and similarities aspects among the specimens based on their position in the scatter plot graph (Hayes 2009).

Wire Frame Images and Thin Plate Spline Deformation Grids

Morphologika2 program has the ability to construct 2d or 3d shapes called wireframes. *Morphologika2* program has the facility to analyse changes in the shape of a 3D data set. A slider function in *morphologika2* allows the user to see the changes in shape along the axis from the PCA scatter plot. The changing shape of wireframe can be seen as the slider is shifted from the negative side of the axis to the positive side of the axis and *vice versa* (Fig 3.8). Based on this sliding some significant changing features can be visualised and their relevance can be visually assessed.

To clarify the different shapes that appear along the axis of the PCA scatter plot, *Morphologika2* shows a thin plate spline deformation grid. This thin plate spline deformation grid has a function as an orientation point of changes in the shape of a reference wireframe comparing to a target wireframe that you want to compare in the PCA scatter plot (Hayes 2009) (see Figure 3.8).

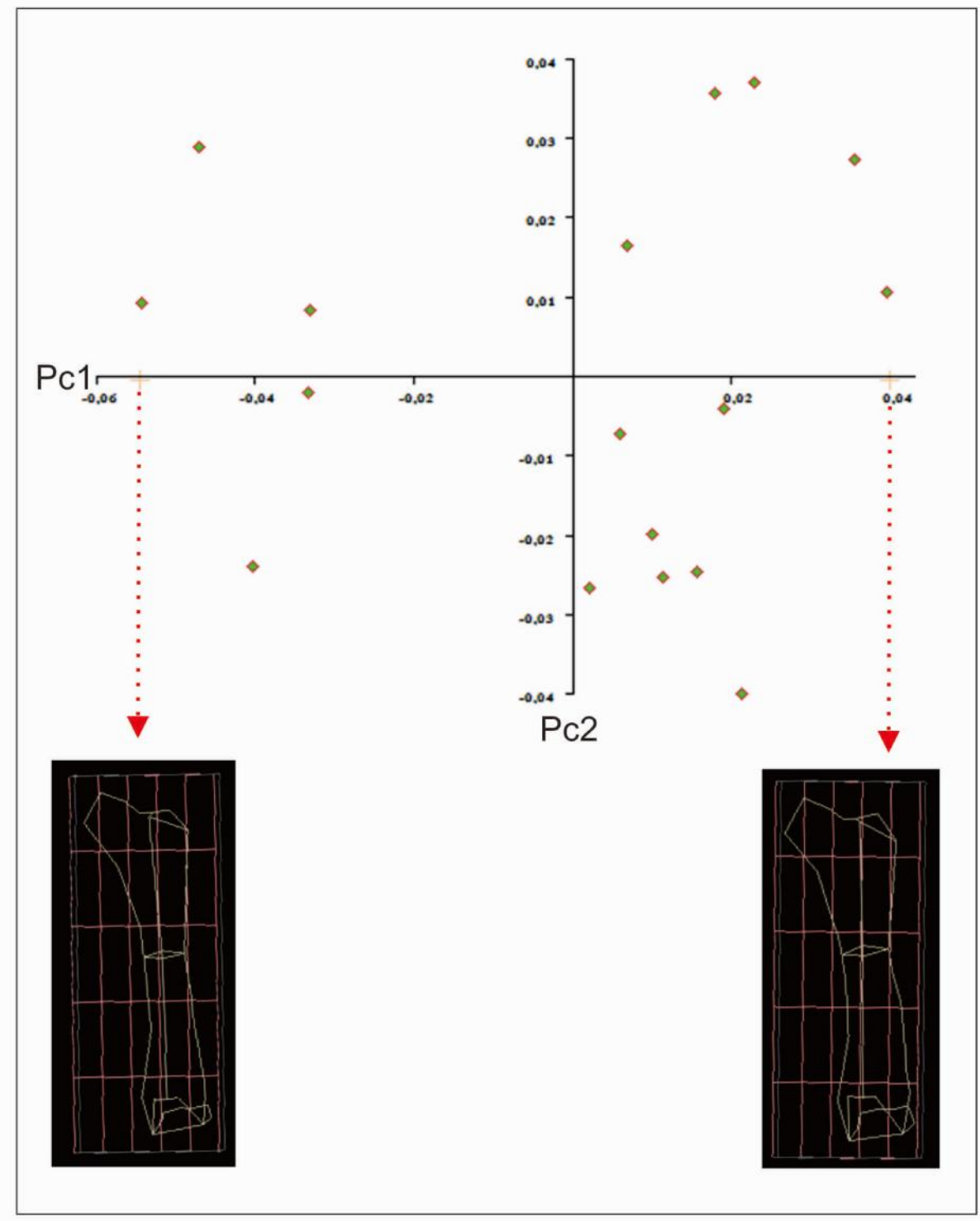

Figure 3.8. Wireframe diagrams with thin plate spline deformation grids in a PCA scatter plot.

Multivariate Regression and Combined Dependents

The visualisations via the wireframe diagrams and the thin plate spline deformation grids illustrate the shape analyses carried out by *morphologika2*. Partial forms that cause variations can be analysed through PCA analysis. This statistical analysis can be achieved by doing a multivariate regression within *morphologika2* against an independent variable, such as length, minimum diaphysis etc. Independent variables were analysed in the *morphologika2*, followed by regression against the dependent variables. The result of this multivariate regression is the significance level of the variable that is tested. If the probability is less than 0.05 then the overall variance is significant.

The multivariate regression results also give an indication to which each PC relates compared to the independent variable. These are the partial regression coefficients. For this analysis, the adjusted R^2 and *p*-values (significance limit is where *p*-value is less than 0.05) are used. The adjusted R-squared is a modified version of R-squared for the number of predictors in a model. The adjusted R-squared can be negative, but isn't always, while an R-squared value is between zero and 100 and shows the linear relationship in the sample of data. The adjusted R-squared is the best estimate of the degree of relationship in the basic population. This thesis used a small number of proboscidean specimens, and therefore the adjusted R-squared should be preferably more than the R-squared values.

As mentioned before, the adjusted R-squared value is usually not negative, but if the result is negative this is because too many landmarks have been used in the analysis, or there are not enough specimens. In this GM analysis many landmark points are needed to capture the shape, and because this study is analysing fossils, there are not many specimens. So the analyses will have negative adjusted r2 values. However, the reason for using GM is to explore the variation and see if there are new biometric parameters that can be used to identify genera in fossil proboscidea. Therefore the statistical analyses are done using the biometric measures in a PCA. So when a GM multivariate regression analysis is significant and has a PC with a significant correlation coefficient then this means that the significant PC may be useful in finding a biometric measure.

4. RESULTS

The results are presented as two experiments. The first experiment is the analysis of the identified femur and tibia specimens testing which variables can be applied to distinguish these elements based on morphology. The second experiment tests the results of the first experiment with the femur and tibia specimens that were found isolated and of which the identity (genus and species) is unknown.

Both experiments report the results of Principle Components Analysis (PCA) and Geometric Morphometrics (GM) analysis. In both experiments the PCA variables are from the visual assessment of the surface morphology and the biometric parameters and their measurements. The GM analyses are to see if there are other diagnostic features of the specimens that can be used to identify genera in proboscidean specimens. A second PCA was then undertaken with the new variables identified in the GM analysis, with these variables converted to biometric measures. The femur and tibia are analysed separately.

4.1. Experiment 1: Analyses of Identified Individuals

As discussed in Chapter 3 Materials and Methods (Chapter 3 section 3.1), the ten identified femur specimens are *Elephas maximus* 1 (EM1), *Elephas maximus* 2 (EM2), *Elephas hysudrindicus* (EH), *Stegodon florensis* 1 (SF1), *Stegodon florensis* 2 (SF2), *Stegodon florensis* 3 (SF3), *Stegodon sondaari* (SS), *Stegodon trigonocephalus* 1 (ST1), *Stegodon trigonocephalus* 2 (ST2) and *Sinomastodon bumiajuensis* (SINO).

4.1.1. The Femur of Identified Specimens

4.1.1.1. PCA of the Femur

The 11 biometric parameters taken from the 10 specimens were normalised (see Appendix A Table 1) and entered into a PCA to identify which may be diagnostic for identifying genera (*Elephas* and *Stegodon* or *Sinomastodon*). As discussed in Chapter 3 section 3.9.1, the percentage eigenvalues that are considered to be representative are those with a cumulative value of up to 95%. The results of the PCA (Table 4.1) show that the eigenvalues of Principle Component 1 (PC1) and Principle Component 2 (PC2) cover more than 95% of the total

variance (PC1 = 94.7%, PC2 = 2.8%). Therefore PC1 and PC2 can be considered to represent almost all of the variation in the data and PC1 and PC2 becomes the main focus in this PCA.

Table 4.1. Eigenvalue from all Principal Components of femur.

PC	Eigenvalue	% variance
1	10.4156	94.69
2	0.3046	2.77
3	0.1061	0.96
4	0.0731	0.66
5	0.0484	0.44
6	0.0201	0.18
7	0.0191	0.17
8	0.0085	0.08
9	0.0046	0.04

The significance level of a PC can be seen in the scree plot (see Chapter 3 section 3.9.1). The scree plot (Figure 4.1 shows that only PC1 is significant, because it has a value above the broken stick (dashed red line). The eigenvalue of PC2 is below the broken stick. Therefore, PC2 is considered non-significant (see Figure 4.1). The next step was to analyze the PCs further by examining their loading values for each variable.

The PCA shows that all the loadings for PC1 are less than 0.5. As mentioned before in Chapter 3 section 3.9.1, the boundary loading value that marks the relative importance of the PC's correlation is above +0.5 or below -0.5. A loading value of between -0.5 and +0.5 signifies that the component does not have a strong correlation with the other components. Although PC1 is significant (see Figure 4.1), all of the PC1 variables have a loading value that are similar and around 0.3 (see Table 4.2). This means all variables in PC1 share the same influence were on each component does not have a strong correlation with the other components.

As mentioned before, PC2 is non-significant with an eigenvalue of 2.8%. Despite its small eigenvalue, there is one variable in this PC that is important (all loading values are shown in

Table 4.2). PC2 has a loading value of **-0.58923** for F7 (total length). This means F7 has a strong correlation with each component in PC2.

Table 4.2. Loading values of the various femur parameters for PC1 and PC2 (important loading values are in **bold**).

Variables	PC1	PC2
F1	0.30385	0.22615
F2	0.29839	0.25041
F3	0.29805	0.33316
F4	0.29329	0.48902
F5	0.30679	-0.090703
F6	0.30853	0.096555
F7	0.29146	**-0.58923**
F8	0.3048	-0.044386
F9	0.30772	-0.11051
F10	0.30285	-0.29468
F11	0.30035	-0.26504

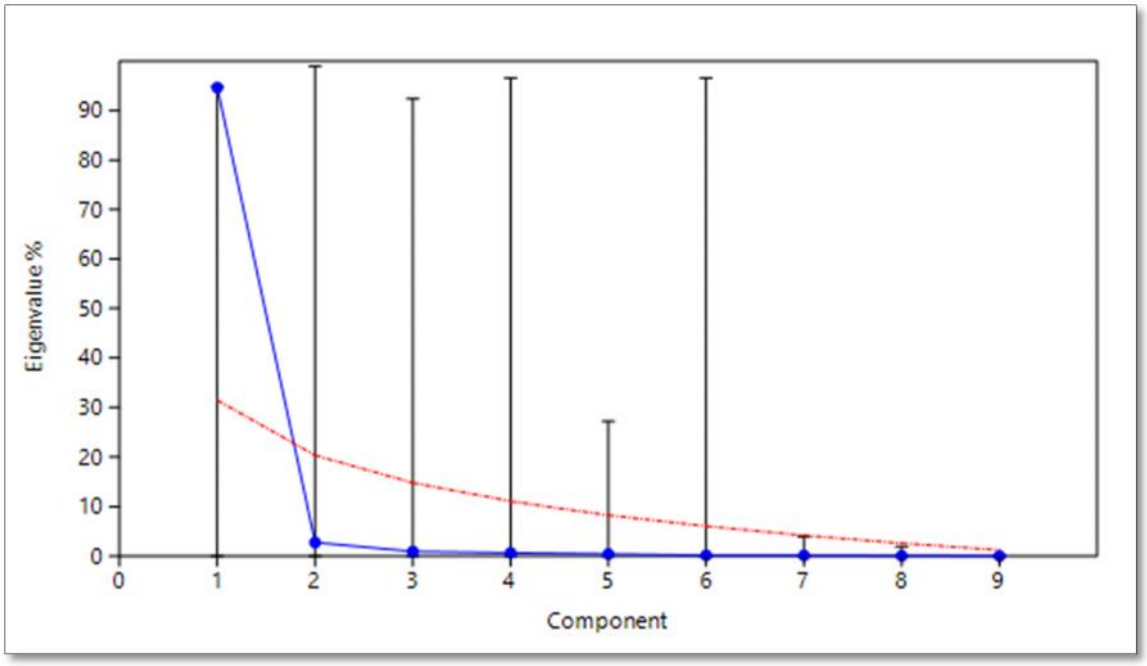

Figure 4.1. The scree plot of the PCs that define the variability of the femurs of identified proboscidean species.

The PCA scatter plot (Figure 4.2) shows the result of PC1 and PC2 for all femurs of identified specimens that were used in this analysis. The closeness of the position of each specimen in the scatter plot in relation to other specimens indicates the degree to which the measurements tend to be similar as the other specimens.

In the PC scatter plot (Figure 4.2), PC1 (x-axis) most specimens fall within the range between -2 − +3, except *Stegodon sondaari* (SS) and *Elephas hysudrindicus* (EH), which are on the opposite extreme values of the PC1 axis. PC1 divides the specimens into three clusters: low values (SS), intermediate values (EM1, EM2, SF1, SF2, SF3 ST1, ST2 and SINO), and high values (EH). This result is in agreement with the outcome of the biometric measurement analyses (see Chapter 3 Section 3.3), where the biometric measurements divided the specimens into three clusters, and these are the same specimens in each cluster as for PC1. SS represents a very short femur (it is from the dwarf species *S. sondaari*) that has a length of no more than 500mm. SS is isolated from the other specimens in PC1. The intermediate cluster in PC1 mirrors the intermediate-sized femurs that are between 700 − 900mm in length, and the single largest femur of EH of more than 1000mm length separates in PC1 as well. Amongst the femurs specimens, SS is by far the shortest, EH is the longest specimen, and the remaining specimens (EM1, EM2, SF1, SF2, SF3 ST1, ST2 and SINO) are all intermediate-sized. These results indicate that the clustering within PC1 is mostly based on size.

Within PC2 (y-axis) the scatter plot shows that *Sinomastodon* and all *Stegodon* except *S. sondaari* are on the positive side of the y-axis, while all *Elephas* specimens are on the negative side of the y-axis. Although SS has a slightly negative score, its value is closest to the cluster of *Stegodon* and *Sinomastodon* specimens with positive scores, so SS can be considered part of the *Stegodon Sinomastodon* group. Therefore it can be concluded that in PC2 the specimens can be divided into two main groups: the *Elephas* group and the *Stegodon-Sinomastodon* group (Figure 4.2). The joining of the dwarf *S. sondaari* (SS) with the *Stegodon-Sinomastodon* group, and the joining of the largest *E. hysudrindicus* (EH) with the *Elephas* group, indicates that PC2 is not clustering the specimens by size. If we look at the values of the loading value in PC2, we know that the F7 is indicated as the most important variable as compared to the other variables. These data indicate that the clustering of PC2 is largely based on parameter F7.

Although PC2's eigenvalue is not significant, PC2 has variables that can divide the specimen into two groups: the *Elephas* group and the *Stegodon-Sinomastodon* group. These results indicate that something correlated with parameter F7 has the potential to represent a diagnostic characteristic to separate the two taxonomic groups. The next step aims to determine these potential characters related to parameter F7. This is done by analysing the 3D coordinates in *morphologika2*, which is the Geomorphic Morphometric (GM) analysis program.

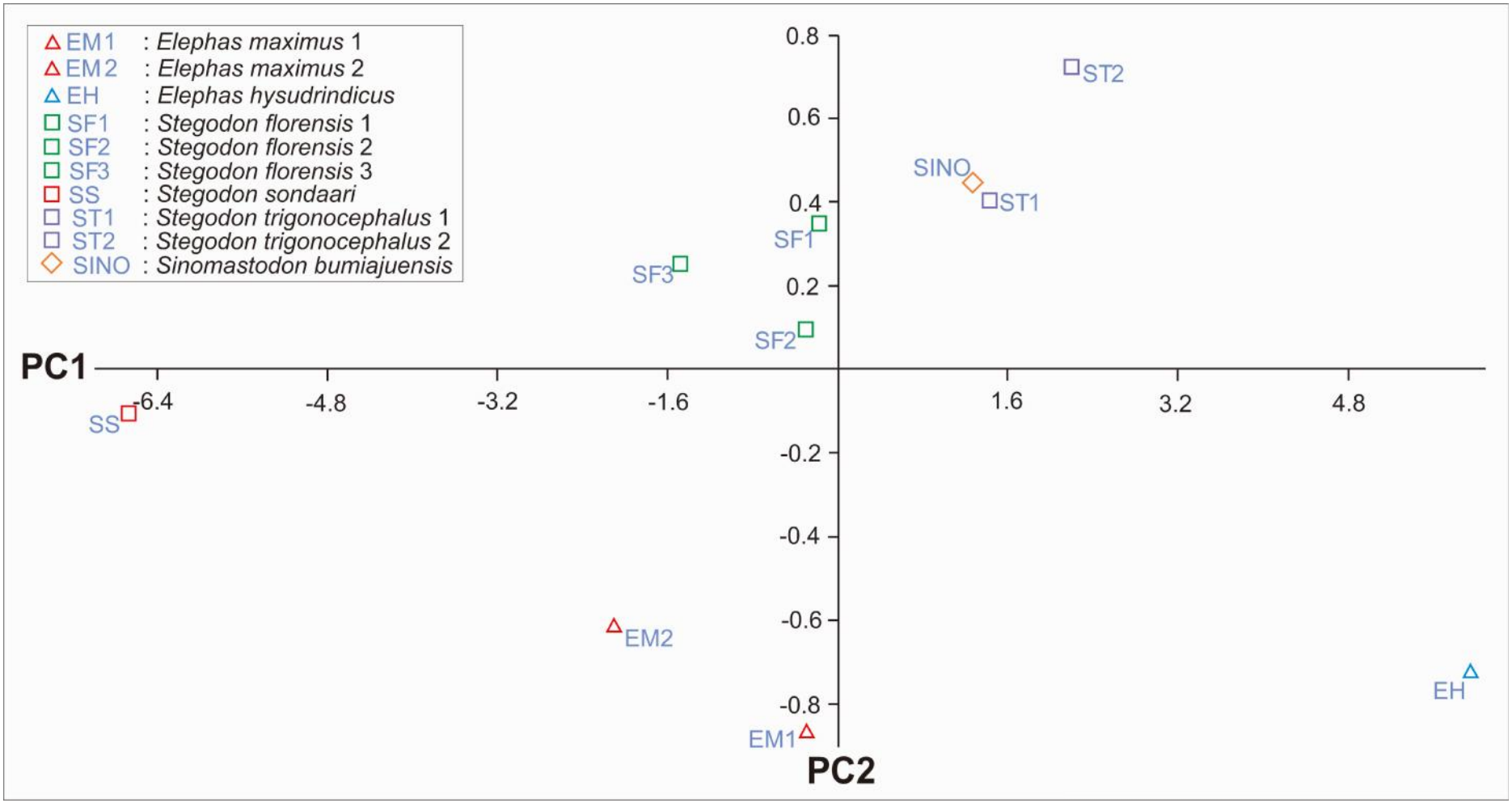

Figure 4.2. Results of the PCA of biometric parameters showing PC1 plotted against PC2 for all femur specimens of which the identity is known.

4.1.1.2. GM Analyses of the Femur

To further explore shape variations according to genera, 34 landmark coordinates of the identified specimens were analyzed using GM (See Chapter 3, section 3.8). The independent variable used in the multivariate regression analysis was genus. The one biometric measures that showed – based on the PCA – that they have the potential to be diagnostic (F7) were also used as independent variables to see if these variables agree with the GM genera results.

As can be seen in Table 4.3, the multivariate regression (MVR) by genera is 30.4% of the overall variance. The results are not significant (probability=0.24), but PC1 is significant as a partial regression coefficient (significance limit is where *p*-value is less than 0.05, see Chapter 3, section 3.9.2). The MVR by total length (F7) explains 14.56% of the overall variance, but again this is not significant (probability=0.55), and has no significant partial regression coefficients. What these results indicate is that the biggest variance in the specimens (PC1) is significantly related to their genus.

The GM scatter plot of PC1/PC2 is shown in Figure 4.3. In PC1 (x-axis) the specimens clearly separate into two groups, with all *Elephas* specimens in a group on the positive side of the x-axis, and the *Stegodon-Sinomastodon* specimens grouping on the negative side of the x-axis. Although it is not a significant partial regression coefficient, it can be seen in Figure 4.3 that in PC2 (y-axis) all specimens are located within the range -0.03 – +0.03, except specimen SINO that is isolated around a value of +0.06. This indicates that the *Sinomastodon* femur has some distinctive shape variable that distinguishes it from *Elephas* and *Stegodon* femurs. But because the *Sinomastodon* sample size is restricted to one specimen, it is difficult to statistically recognize that character.

Figure 4.3 also shows a comparison of the wireframes extracted from the minimum and maximum values of the specimens along the PC1 axis. The wireframes show that PC1 is separating the genera by their length of the third trochanter, by the femur torsion angle and something related to the minimum circumference (Fig 4.4). These features are considered as potential new independent variables that can be used to separate the specimens according to their genus.

Table 4.3. PCA of biometric measurements of the femurs, with as independent variables genus, F4 and F7. Only 2 partial regression variances are significant (shown in bold).

PC	% of total variance explained	Independent Variables							
		Genera				Total Length (F7)			
		MVR		Partial regression coefficients		MVR		Partial regression coefficients	
		Probability	% of the variance that explained by the selected PCs (PC1-7)	*p*-value of the slope	adjusted r^2	Probability	% of the variance that explained by the selected PCs (PC1-7)	*p*-value of the slope	adjusted r^2
PC1	39.49	0.24	30.40%	**0.0038**	**0.6243**	0.55	14,56%	0.2917	0.0279
PC2	18.94			0.4918	-0.0573			0.2155	0.0804
PC3	15.14			0.5853	-0.0818			0.1444	0.1497
PC4	9.76			0.5265	-0,0672			0.4378	-0.0394
PC5	4.76			0.5977	-0.0846			0.8631	-0.1206
PC6	3.87			0.4661	-0.0492			0.2612	0.047
PC7	3.32			0.8478	-0.1196			0.9706	-0.1248

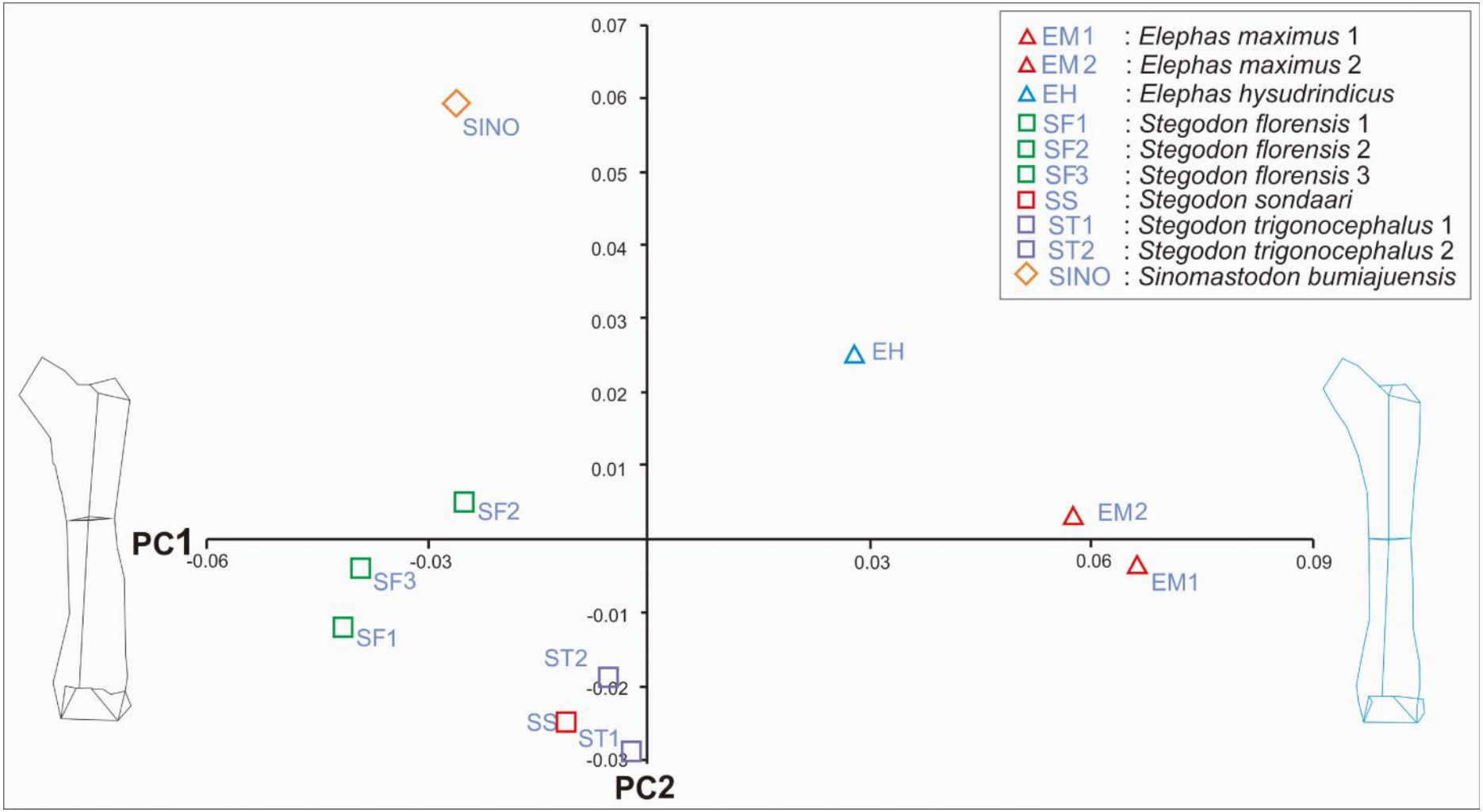

Figure 4.3. PCA results of the GM analysis of femur specimens of known identity. PC1 is a significant partial regression coefficient when the data is analysed with genus as the independent variable. Wireframes taken from the maximum values of specimens on the positive and negative of PC1 are shown. An overlay of these two wireframes that compares the output is shown in Figure 4.4.

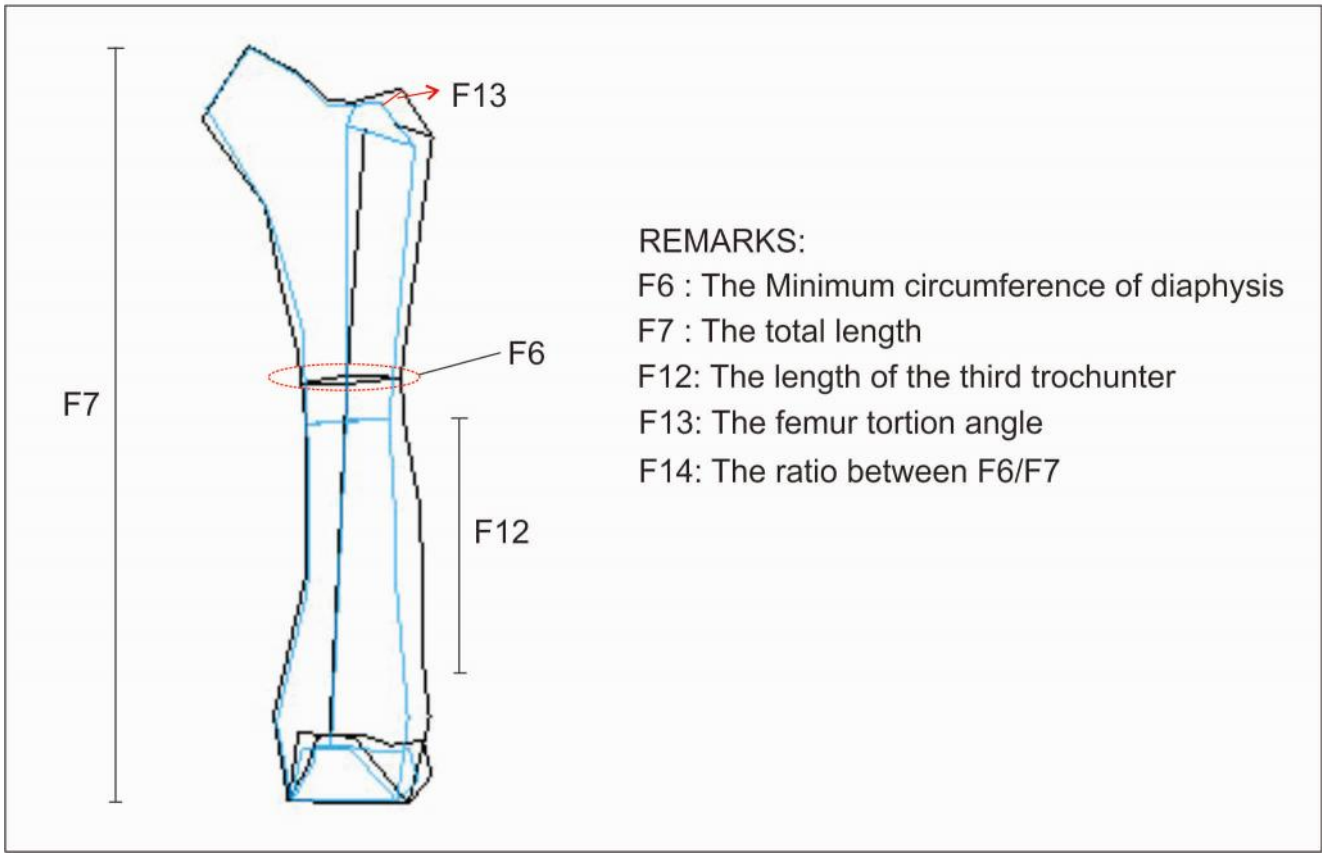

Figure 4.4. Minimum-maximum wireframe shape of the PC1.

The shape changes indicated by the wireframes resulting from the GM analysis indicate the existence of some new variables that could be used to identify genera amongst fossil femur specimens. To test these variables they were first turned into biometric measures. The length of the third trochanter (new parameter F12) is defined as the distince along the disto-lateral portion of the diaphysis from the proximal onset of the distolateral crest until its distal termination (Figure 4.5). New parameter F13 is the angle of femoral torsion measured by placing the posterior side of the femur on a flat surface with both distal condyles in contact with this flat surface. This position makes the shaft of the femur head forming an angle to the flat surface. This angle is then measured with a protractor as shown in Figure 4.5. This method was adapted from Han, Zhang and Shan (2014). The resulting angle value is then converted into an ordinary nominal by dividing the angle value by 360^{o}.

Some researchers have noted the relation of the total length and minimum circumference of femur with the elephant body mass (Christiansen 2007; Hutchinson et al. 2006; Kokshenev & Christiansen 2010). By comparing the minimum circumference with the total length. This formula is taken over here by creating a new variable (F14) defined as the ratio between the minimum circumference of the diaphysis (F6) with the total length (F7). The minimum circumference was measured with a measuring tape as shown in Figure 4.5.

The measurement values of the new femur biometric parameters (F12, F13, and F14) are listed in Chapter 3 Table 3.7. These values were then entered into a new GM analysis to see how they perform as independent variables in identifying the genera of the fossils. In GM the multivariate Regression (MVR) results when each variable is analysed as an independent variable is shown in Table 4.4. As can be seen, each new variable is statistically significant in identifying overall variance within the specimens. Not surprisingly, each new variable has PC1 as a significant partial regression coefficient (Table 4.4).

As can be seen in Table 4.4, the multivariate regression (MVR) with as independent variable the third trochanter length (F12) explains 33.09% of the overall variance (significant with probability=0.02). The MVR by angle of femoral torsion (F13) represents 26.69% of the overall variance (significant with probability=0.02). The multivariate regression (MVR) by the ratio between the minimum circumference (F6) and the total length (F14) is 27.41% of the overall variance (significant with probability=0.04).

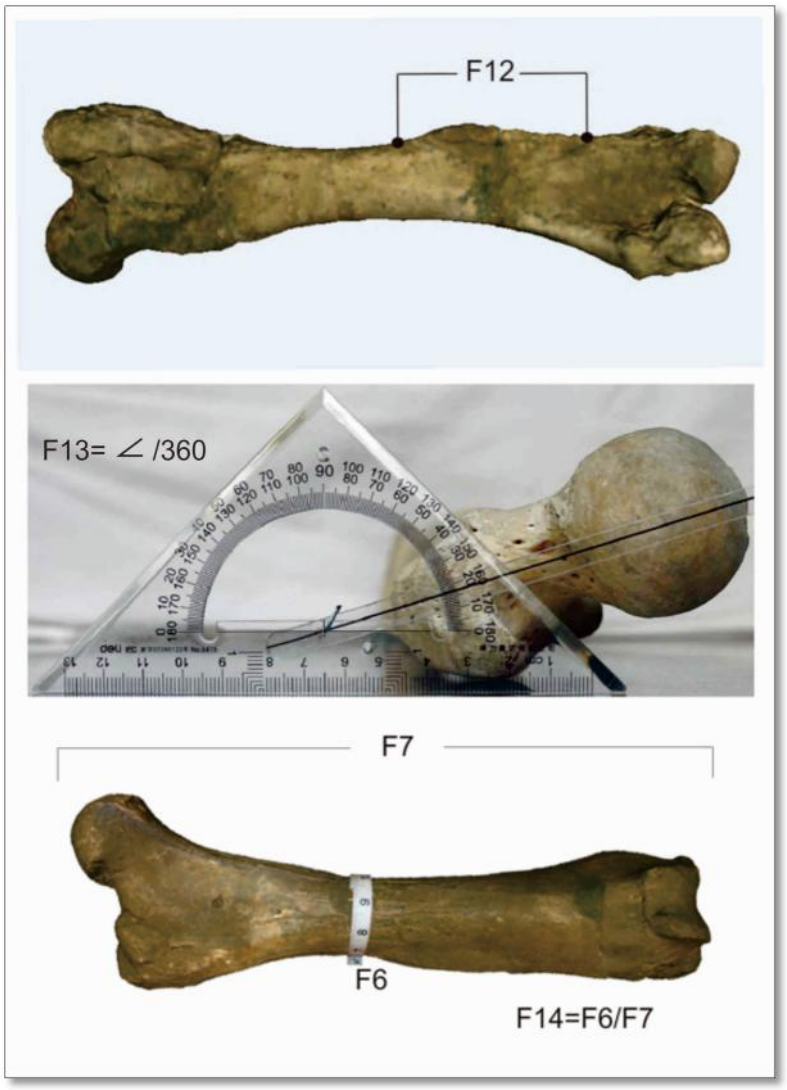

Figure 4.5. Methods to measure the new parameters F12, F13 and F14. F12 is the length of the third trochanter; F13 is the torsion angle of the femur, and F14 is defined as the ratio between F6 (minimum circumference of diaphysis) and F7 (total length). Top: dextral femur of *Stegodon sondaari*, posterior view; Middle: proximal view of *Elephas maximus* sinistral femur; Bottom: anterior view of *Stegodon* dextral femur.

Table 4.4. PCAs of the biometric measurements on identified femur specimens, including the new parameters F12-F14. Statistical scores are given for separate PCAs with as independent variables F12, F13, and F14. Significant scores and their statistical coefficients are in bold.

PC	% of total variance explained	New Independent Variables											
		Third trochanter length (F12)				Angle of femoral torsion (F13)				Ratio minimum diameter /total length (F14)			
		MVR		Partial regression coefficients		MVR		Partial regression coefficients		MVR		Partial regression coefficients	
		Probability	% of the variance that explained by the selected PCs (PC1-7)	*p*-value of the slope	adjusted r^2	Probability	% of the variance that explained by the selected PCs (PC1-7)	*p*-value of the slope	adjusted r^2	Probability	% of the variance that explained by the selected PCs (PC1-7)	*p*-value of the slope	adjusted r^2
PC1	39.49	**0.02**	**33.09%**	**0.0028**	**0.65**	**0.02**	**26.69%**	**0.0299**	**0.39**	**0.04**	**27.41%**	**0.0285**	**0.40**
PC2	18.94			0.4802	-0.05			0.8852	-0.12			0.1531	0.14
PC3	15.14			0.2132	0.08			**0.0382**	**0.36**			0.1802	0.11
PC4	9.76			0.9226	-0.12			0.5617	-0.08			0.6005	-0.09
PC5	4.76			0.6836	-0.10			0.9465	-0.12			0.81	-0.12
PC6	3.87			0.7217	-0.12			0.6911	-0.10			0.7131	-0.11
PC7	3.32			0.7195	-0.12			0.6104	-0.09			0.7424	-0.11

4.1.1.3. PCA of the Femur Including the New Variables (F12, F13, F14)

The three new variables were then tested on their influence on the other variables that were used previously in the biometric PCA. This test is done by combining the three new variables with the 11 initial femur biometric variables. The 14 biometric parameters taken from the 10 specimens were normalised (see Appendix A, Table 3). The 14 variables were introduced into a PCA to assess how they compare with the other biometric variables statistically.

The results of the PCA (Table 4.5) show that the eigenvalues of Principle Component 1 (PC1) and Principle Component 2 (PC2) cover more than 95% of the total variance (PC1 = 77.43%, PC2 = 18.91%). Therefore PC1 and PC2 can be considered to represent almost all of the variation in the data and PC1 and PC2 become the main focus in this PCA.

Table 4.5. Eigenvalues for all Principal Components of femur.

PC	Eigenvalue	% variance
1	10.8402	77.43
2	2.6471	18.91
3	0.1884	1.346
4	0.1750	1.2498
5	0.0564	0.403
6	0.0201	0.18
7	0.0191	0.17
8	0.0085	0.08
9	0.0046	0.04

The scree plot (see Figure 4.6) shows that only PC1 plots above the broken stick. However, PC2 plots just below and very close to the broken stick line, to the left of where the graph starts to flatten out. This could also indicate significance, because in scree plots all the components to the left of where the curve starts to flatten out may be regarded as significant (see Chapter 3 section 3.9.1). Therefore, PC2 is considered significant (see Figure 4.6). The next step to analyze the PCs further is by examining their loading values for each variable.

The PCA shows that all the loadings for PC1 are less than 0.5. This means all variables in PC1 share the same influence and show weak correlation with each component. As mentioned before, PC2 is significant with an eigenvalue of 18.91%. There are three variables

in this PC that are important (all loading values are shown in Table 4.6). So the pattern results are still similar as in the previous biometric PCA where the important value based on the loading value (above 0.5 either positive or negative direction (+/-)) was only associated with PC2.

The results show that the three new variables all have a loading value above 0.5, which means they all have a strong influence amongst these variables (Table 4.6). The loading values of F12, F13 and F14 are -0.55728, 0.52443 and -0.51149 respectively. These results demonstrate that the third trochanter length (F12), the angle of femoral torsion (F13) and the ratio between the circumference and the minimum total length (F14) can be considered as potential diagnostic variables to distinguish genera.

In the PC scatter plot (Figure 4.7), PC1 still divides the specimens into three clusters: low values (SS), intermediate values (EM1, EM2, SF1, SF2, SF3 ST1, ST2 and SINO), and high values (EH). This result is in agreement with the outcome of the biometric measurement analyses (see Chapter 3, section 3.3), where the biometric measurements divided the specimens into three clusters, and these are the same specimens in each cluster as for PC1. These results still indicate that the clustering within PC1 is mostly based on size.

Within PC2 (y-axis) the scatter plot shows the opposite axis values as compared to the PCA before adding the three new variables. *Sinomastodon* and all *Stegodon* except *S. sondaari* are on the negative side of the y-axis, while all *Elephas* specimens are on the positive side of the y-axis. In this PC2 *Stegodon sondaari* seems to be more isolated whereas *Stegodon*, in particular *Stegodon florensis*, form a tighter grouping. Therefore it can be concluded that the new variables have clear influences in the groupings and separate the specimens according to genera.

Table 4.6. Loading values for each variable on PC1 and PC2 (important values in **bold**).

Variables	PC1	PC2
F1	0.29943	0.000468
F2	0.29601	-0.038678
F3	0.29679	-0.054892
F4	0.29388	-0.089175
F5	0.29715	0.098335
F6	0.30229	0.03562
F7	0.27369	0.25697
F8	0.29602	0.086088
F9	0.29757	0.18829
F10	0.28964	0.1686
F11	0.28946	0.12559
F12	0.09845	**-0.55728**
F13	-0.12635	**0.52443**
F14	0.15547	**-0.51149**

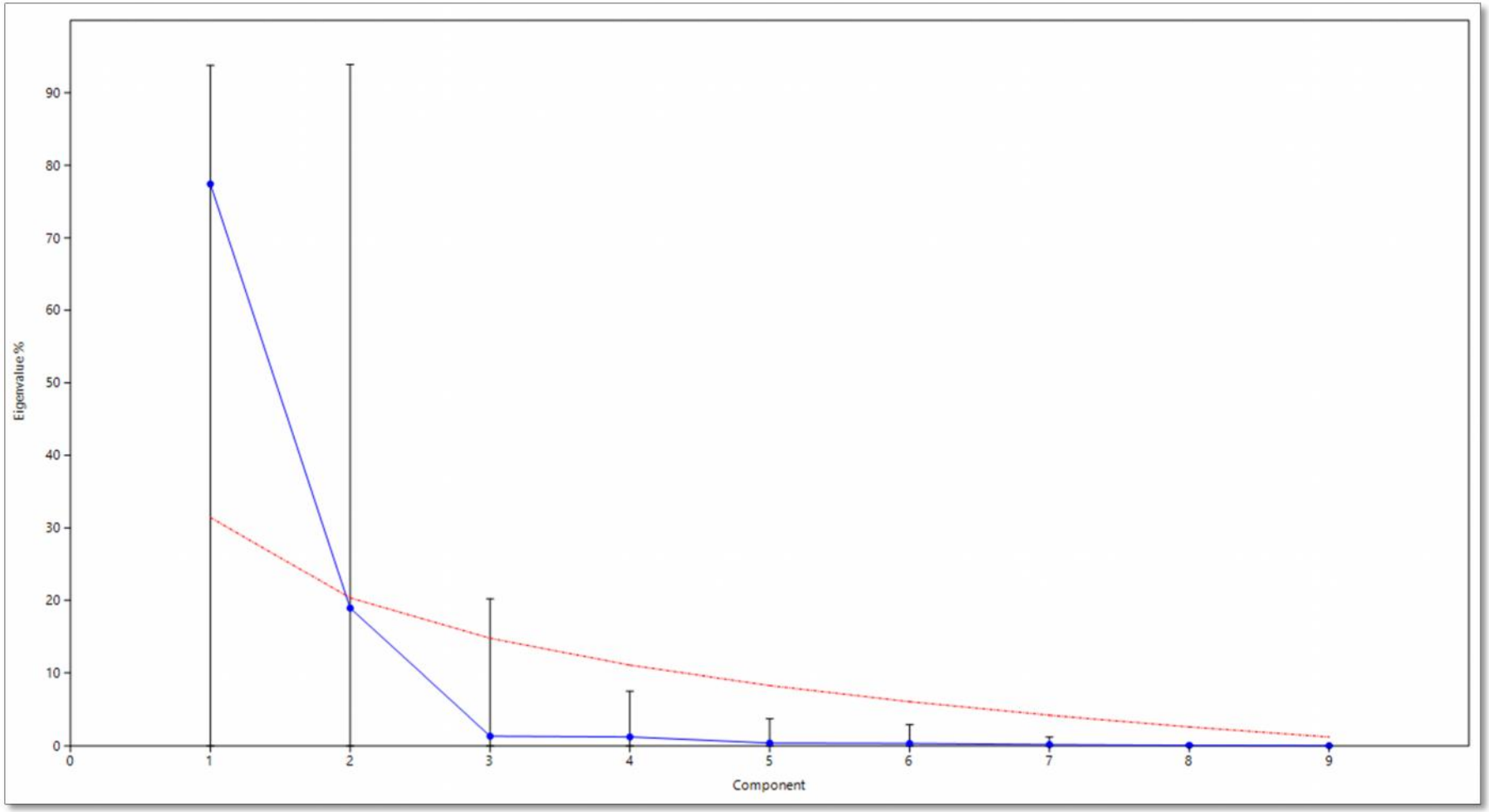

Figure 4.6. Scree plot of femurs PCA including the new variables (F12, F13, F14).

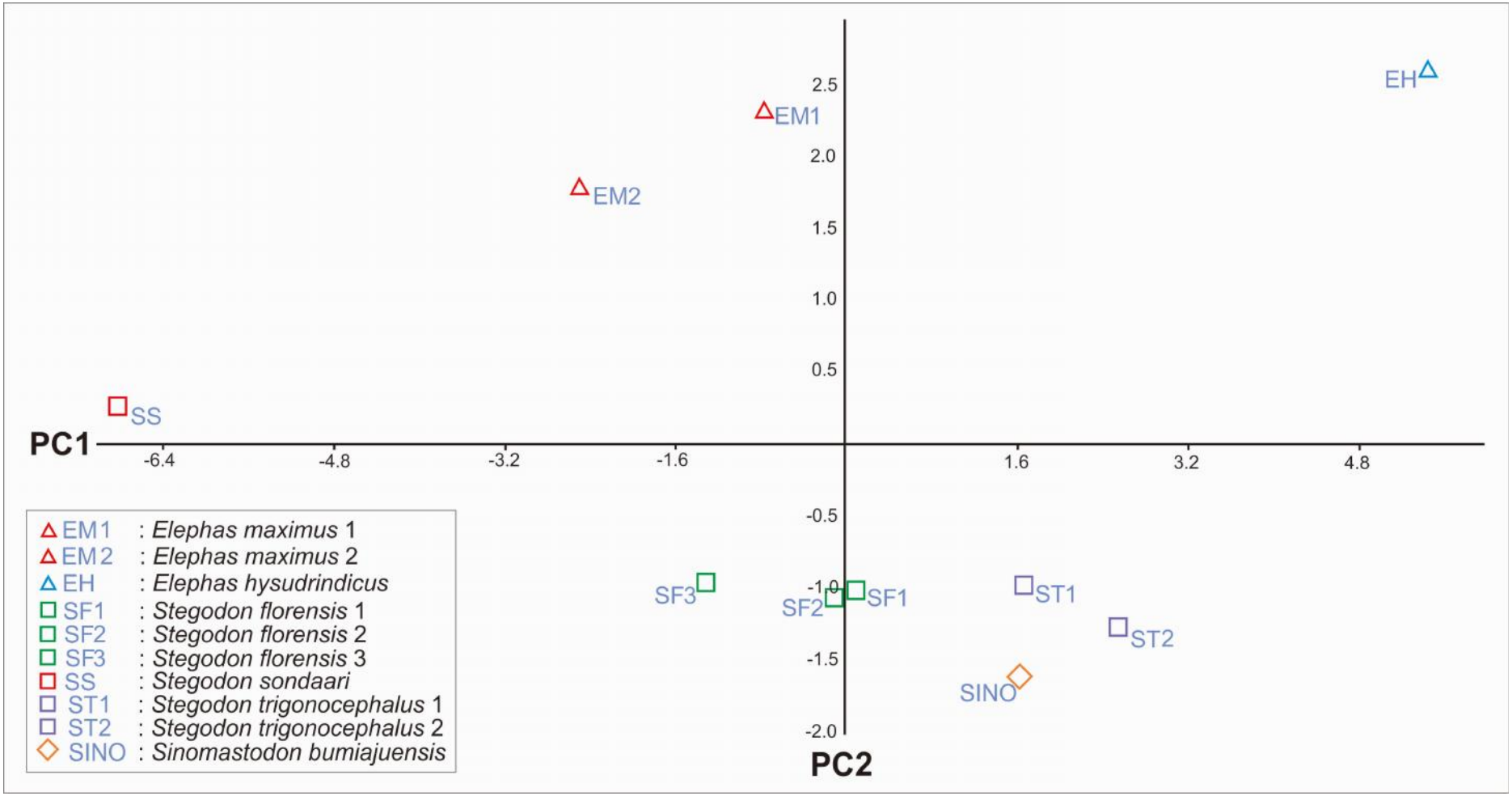

Figure 4.7. Results of the PCA based on 14 biometric parameters showing PC1 plotted against PC2 for 10 identified femur specimens.

4.1.2. The Tibia of Identified Specimens

As mentioned in Chapter 3, Section 3.1, the ten tibia specimens that were identified to either genus or species level based on associated fossils are: *Elephas maximus* 1 (EM1), *Elephas maximus* 2 (EM2), *Elephas hysudrindicus* (EH), *Stegodon florensis* 4 (SF4), *Stegodon sondaari* (SS), *Stegodon trigonochepalus* 3 (ST3), *Stegodon trigonochepalus* 4 (ST4), *Elephas* sp. Sangiran (ESang5), *Stegodon* sp. Sangiran (SSang6) and *Stegodon* sp. Patiayam (SPT).

4.1.2.1. PCA of the Tibia

The 5 metric parameters (measures) taken from the 10 specimens were normalised (see Appendix A Table 2) and entered into a PCA to identify which parameters may be diagnostic for identifying genera (*Elephas* and *Stegodon*).

The results of the PCA in the tibia metric parameters shows that the eigenvalue for PC1 and PC2 cover more than 95% of the variance (PC1 = 89.018%, PC2 = 7.2798%). As with the femur, from this it can be concluded that PC1 and PC2 can be considered to represent almost all of the variation within the data. From this stage PC1 and PC2 become the main focus of the PCA. The eigenvalues that result from this PCA are listed in Table 4.7.

Table 4.7. PCA eigenvalues for all PCs of the tibia.

PC	Eigenvalue	% variance
1	4.45091	89.018
2	0.363992	7.2798
3	0.133237	2.6647
4	0.0396277	0.79255
5	0.0122348	0.2447

The scree plot (Figure 4.8) shows that only PC1 is significant, and has a value above the broken stick (dash red line). The PC2 eigenvalue is below the broken stick and is non-significant. As with the femur results, the next step is to assess the PCs by analyzing their loading values for each variable.

The PCA shows that all the loading values for PC1 are less than 0.5, signifying no strong correlation with each component in this PC. All variables show loading values around 0.4 except variable T5 that has value less than 0.4. PC2 explains 7.3% of the variability but the variables have mostly - low eigenvalues, except T4 (minimum anteroposterior diameter of the tibia diaphysis). Although it explains only a minor amount of the variability T4 seems to be important as indicated by having a loading value of 0.8401, and therefore T4 has a strong correlation with each component (Table 4.8).

Table 4.8. Tibia loading values for PC1 and PC2 (important value in **bold**).

Variables	PC1	PC2
T1	0.46993	-0.07485
T2	0.4592	0.068451
T3	0.45392	-0.39916
T4	0.4066	**0.8401**
T5	0.2444	-0.35301

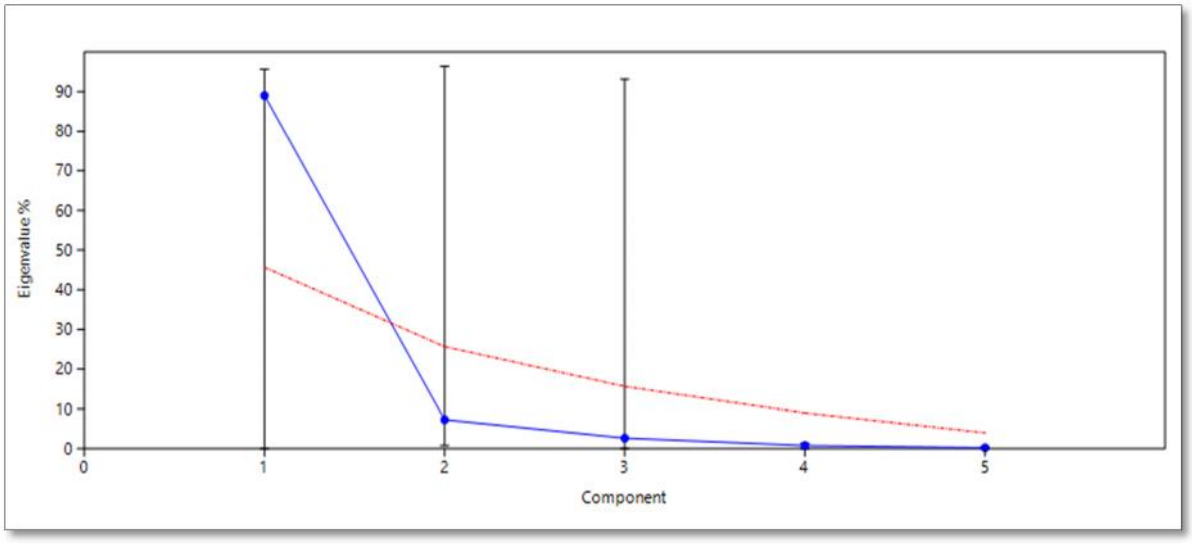

Figure 4.8. The scree plot of the identified tibias PCA.

The scatterplot for PC1 and PC2 are shown in Figure 4.9. As can be seen, PC1 (x-axis) shows that all specimen are located in the range of -2 to 1, except *Stegodon sondaari* (SS), *Elephas* sp. Sangiran (Esang5) and *Elephas hysudrindicus* (EH). SS has a value of around -4, while Esang5 and EH have values of more than 3 (see Figure 4.9). It can be concluded that PC1 divides the specimens into three clusters, a low value cluster (SS), a middle value cluster

(EM1, EM2, ST3, ST4, SF4, SSang6 and SPT) and a high value cluster (ESang5 and EH). These results agree with the biometric measurements, which showed that the pygmy *Stegodon sondaari* has a short femur, *Elephas maximus, Stegodon florensis* and *Stegodon trigonochepalus* are middle-sized, and *Elephas* Sangiran and *Elephas hysudrindicus* are the biggest (see Chapter 3, section 3.3). These results show the same pattern as the femur, with the clustering in PC1 being mostly based on size (Figure 4.9).

On PC 2 (y-axis) the scatter plot shows that all *Stegodon* specimens have values in the range of -0.1 to 1.5, which are all higher values than in *Elephas* specimens. The latter have values ranging between -0.8 to -0.2 (Fig 4.9). If we look at the loading values in PC2, it follows that the minimum anteroposterior diameter of the diaphysis (T4) is indicated as an important variable compared to the other variables. These data indicate that the clustering of PC2 is based on T4.

Although PC2's eigenvalue is not significant and has eigenvalue smaller than PC1, PC2 has a variable that, even though it is not very distinctive, it can still divide the specimens into two groups, namely the *Elephas* group and the *Stegodon* group. As mentioned before, these result indicate that some measurement correlated with T4 has the potential to become a diagnostic variable. As with the femur PCA, the next step now is to determine what this potential character related to T4 is, by applying the Geomorphic Morphometric (GM) program.

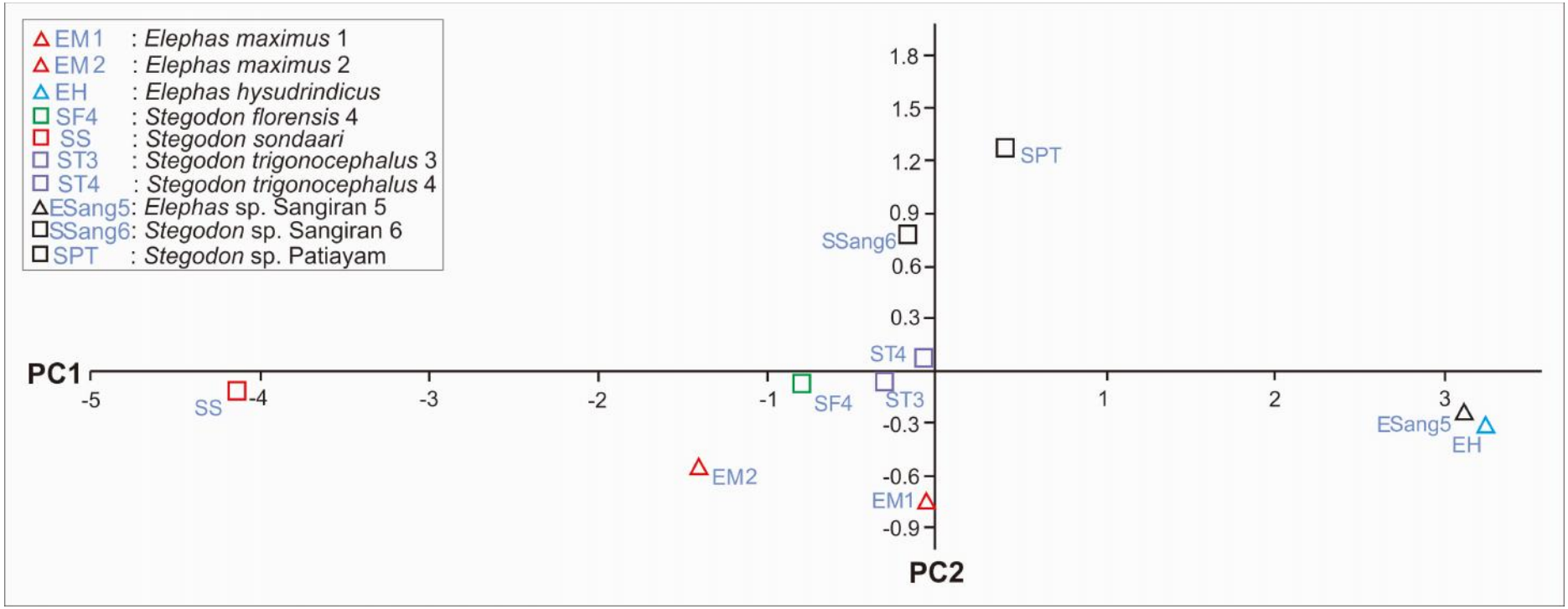

Figure 4.9. Results of the PCA based on biometric parameters showing PC1 plotted against PC2 for all tibia specimens of which the identity is known.

4.1.2.2. GM Analyses of the Tibia

To further explore shape variations according to genera, the 24 landmark coordinates of the identified tibia specimens were analysed using GM. The independent variable used in the multivariate regression analysis was genus. The biometric measure that has the potential to be diagnostic in the PCA (T4: minimum anteroposterior diameter of the tibia diaphysis) was also used as an independent variable to see if this agrees with the genera GM results.

As can be seen in Table 4.9, the multivariate regression (MVR) by genera explains 44.6% of the overall variance. The overall results are not significant (probability=0.07), but PC1 is significant as a partial regression coefficient (p=0.0001). The MVR using the independent variable T4 is not significant, and has no significant partial regression coefficients.

The GM scatter plot of PC1/PC2 is shown in Figure 4.10. In PC1 (x-axis) the specimens clearly separated into two genera groups, with *Elephas* specimens grouping in the negative x-axis and *Stegodon* specimens grouping in the positive x-axis. In PC2 (y-axis) all specimens are located within the range between values -0.03 and +0.01, except *Stegodon sondaari* (SS) that is isolated around 0.08. It indicates that *Stegodon sondaari* has something different in tibia shape that separates it from both *Elephas* and all other *Stegodon* tibias.

Figure 4.10 shows a comparison of the wireframes extracted from the minimum and maximum values of the specimens along the PC1 axis. The wireframes show that PC1 separates the genera by the size of the medial collateral ligament scar and by something related to the minimum circumference and total length (Fig 4.11). These features are considered as new variables that can be used to recognise the genera amongst tibia specimens.

Table 4.9. PCA of the biometric measurements of identified tibia specimens. Statistical scores are given for separate PCAs with as independent variables ‘identified genus’ and T4. Significant scores are in bold.

PC	% of total variance explained	Independent Variables							
		Genus				The minimum anteroposterior diameter of diaphysis (T4)			
		MVR		Partial regression coefficients		MVR		Partial regression coefficients	
		Probability	% of the variance that explained by the selected PCs (PC1-7)	*p*-value of the slope	adjusted r^2	Probability	% of the variance that explained by the selected PCs (PC1-7)	*p*-value of the slope	adjusted r^2
PC1	39.49	0.07	44.62%	**0.00013**	**0.8336**	0.32	8,98%	0.8586	-0.1203
PC2	18.94			0.55266	-0.0574			0.9414	0.2215
PC3	15.14			0.5822	-0.0811			0.2018	0.0918
PC4	9.76			0.8902	-0,1222			0.8730	-0.1212
PC5	4.76			0.7301	-0.1076			0.4759	-0.0523
PC6	3.87			0.6745	-0.0992			0.9998	-0.125
PC7	3.32			0.9198	-0.1235			0.9084	0.2402

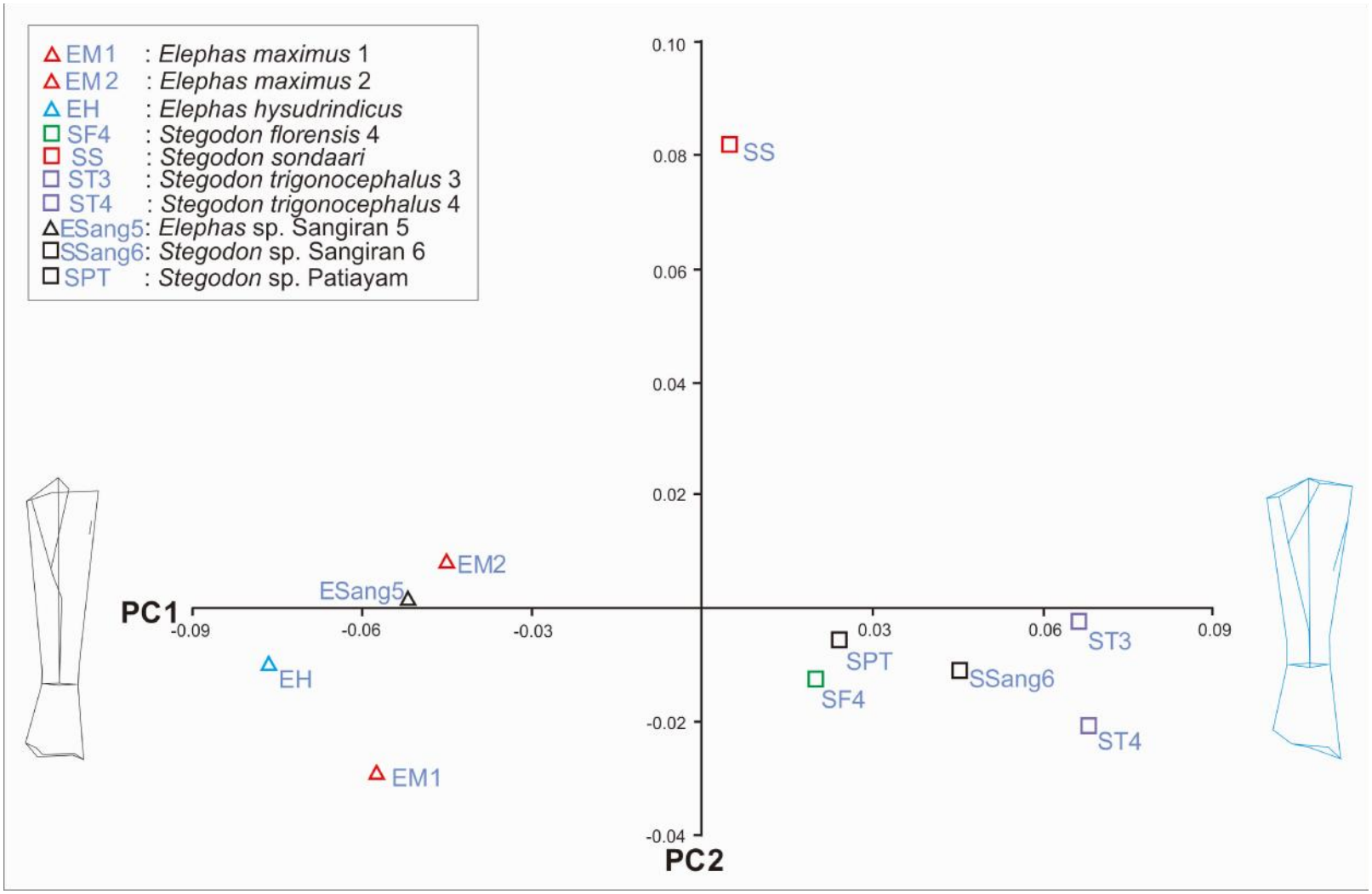

Figure 4.10. PCA scores of GM landmark analysis of tibia specimens of known identity, with genus as independent variable. Wireframes of the extreme values on PC1 are shown to the left and right. An overlay of these two wireframes is shown in Figure 4.11.

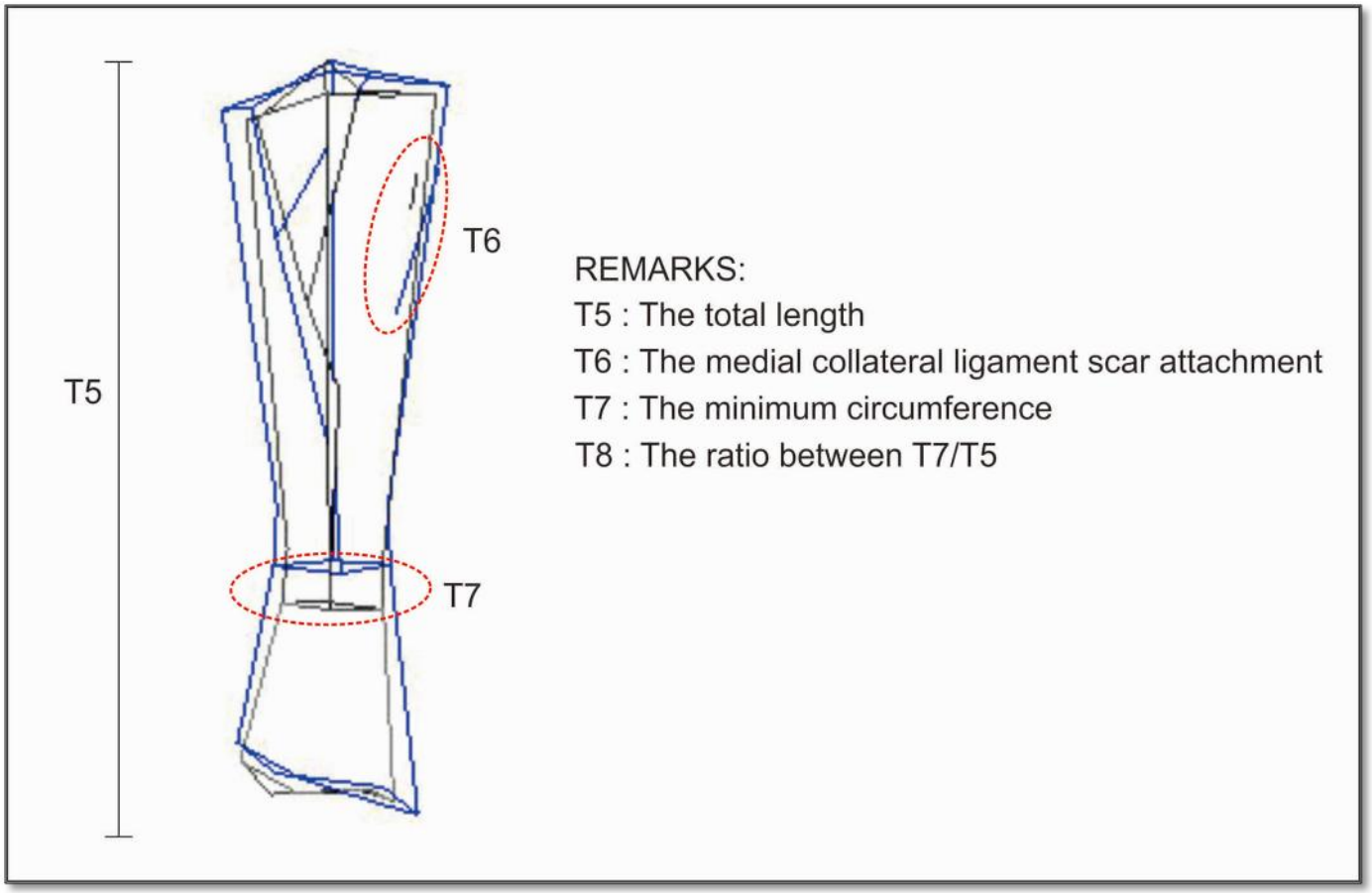

Figure 4.11. Minimum-maximum wireframe tibia shapes on PC1.

The observation of the overlaid wireframes from the GM analysis (Figure 4.11) indicates new variables that could be used to distinguish proboscidean tibia specimens on genus level. To test these new variables they were first converted into biometric measures. The length of the medial collateral ligament attachment scar (new variable T6) is measured along the length of the groove of the medial collateral ligament attachment scar that is located in the medioproximal part of the tibia (Figure 4.12). For the minimum circumference (T7), the measurement is manually taken with a tape measurement.

Similar as for the femur, some researchers noted that the diagnostic relation between the ratio of the total length and the minimum circumference of the tibia (Christiansen 2007; Hutchinson et al. 2006; Kokshenev & Christiansen 2010) by comparing the minimum circumference with the total length. This formula was also applied here by creating a new variable (T8) defined as the ratio between minimum circumference (T7) and the total length (T5). The new variable T8 is thought to better accommodate the observed biometric relation between minimum anteroposterior diameter of the tibia (T4) and the total length of tibia (T5) as was suggested by the GM landmark analysis.

The measurement results of the medial collateral ligament attachment scar (T6), the minimum circumference (T7) and the ratio between minimum circumference and total length (T8) are shown in Table 3.8 in Chapter 3. These results were first entered into a GM analysis to see how they perform as independent variables in identifying the genera of the fossils. The GM multivariate regression (MVR) results of each independent variable are shown in Table 4.9. Variable T6 has overall significance (probability=0.04), whereas T7 and T8 are not.

As can be seen in Table 4.10, the multivariate regression (MVR) by the medial collateral ligament attachment scar (T6) explains 31.95% of the overall variance. Minimum circumference (T7) explains 11.18% (not significant) and PC2 is a significant partial regression coefficient. The multivariate regression (MVR) by the ratio between minimum circumference and total length (T8) explains 34.59% of the overall variance, but this is not significant (probability=0.184. However, in PC1 T8 has a highly significant partial regression coefficient (p=0.006).

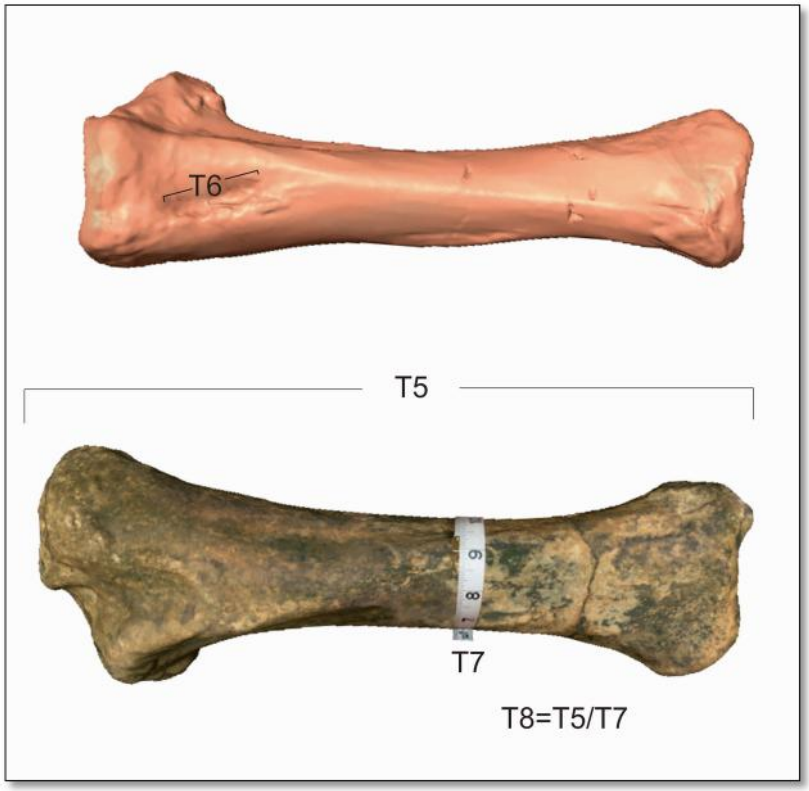

Figure 4.12. Methods to measure new tibia biometric parameters T6 and T7. New parameter T8 is the ratio between T7 and T5 (total length of tibia). Top: medial view of dextral *Stegodon* tibia; Bottom: anterior view of dextral *Stegodon* tibia.

Table 4.10. PCA of the biometric measurements of identified tibia specimens, including the new parameters T6-T8. Statistical scores are given for separate PCAs with as independent variables T6, T7 and T8. Significant scores and their statistical coefficients are in bold.

PC	% of total variance explained	**New Independent Variables**											
		The medial collateral ligament attachment scar (T6)				**The minimum circumference (T7)**				**The ratio between minimum circumference and total length (T8)**			
		MVR		Partial regression coefficients		MVR		Partial regression coefficients		MVR		Partial regression coefficients	
		Probability	% of the variance that explained by the selected PCs (PC1-7)	*p*-value of the slope	adjusted r^2	Probability	% of the variance that explained by the selected PCs (PC1-7)	*p*-value of the slope	adjusted r^2	Probability	% of the variance that explained by the selected PCs (PC1-7)	*p*-value of the slope	adjusted r^2
PC1	39.49			**0.018**	0.46			0.649	-0.095			**0.006**	0.58
PC2	18.94			0.4802	-0.05			**0.047**	0.330			0.551	-0.074
PC3	15.14			0.2132	0.08			0.264	0.045			0.356	-0.006
PC4	9.76	**0.04**	31.95%	0.9226	-0.12	0.24	11.18%	-0.123	0.885	0.184	34.59%	0.709	-0.105
PC5	4.76			0.6836	-0.10			0.253	0.053			0.512	-0.06
PC6	3.87			0.7217	-0.12			0.858	-0.120			0.98	-0.12
PC7	3.32			0.7195	-0.12			0.224	0.074			0.401	-0.025

4.1.2.3. PCA of the Tibia Using the New Variables (T6, T7, T8)

The three new variables were then tested on their influence on the other variables that were used previously in the biometric PCA analysis. This test is done by combining the three new variables with the five tibia femur biometric variables. The eight biometric parameters taken from the ten specimens were first normalised (see Appendix A table 4). The eight variables were introduced into a PCA to assess how they compare with the other biometric variables statistically.

The results of the PCA (Table 4.11) show that the eigenvalues of Principle Component 1 (PC1) and Principle Component 2 (PC2) cover more than 95% of the total variance (PC1 = 69.99%, PC2 = 25.52%). Therefore PC1 and PC2 can be considered to represent almost all of the variation in the data and PC1 and PC2 become the main focus in this PCA analysis.

Table 4.11. Eigenvalue from all Principal Components of femur.

PC	Eigenvalue	% variance
1	5.5982	69.99
2	2.0420	25.52
3	0.2100	2.62
4	0.0788	0.99
5	0.0472	0.59
6	0.0172	0.22
7	0.00597	0.07
8	0.000889	0.01

The scree plot (Figure 4.13) shows that both PC1 and PC2 are above the broken stick, and therefore PC1 and PC2 can be both considered significant. The next step to analyze the PCs further is by examining the loading values for each variable.

The PCA shows that all the loadings for PC1 are less than 0.5. This means all variables in PC1 share the same influence and show weak correlation with each component. As mentioned before, PC2 is significant with an eigenvalue of 25.52%. There are three variables in this PC that are important (all loading values are shown in Table 4.12). So the results show a similar pattern compared with previous biometric PCA, in which the important parameters

based on the loading values (above 0.5 either positive or negative direction (+/-)) are only associated with PC2. These important parameters with loading values of 0.61198 and 0.64569 are T6 and T8, respectively. These results demonstrate that the medial collateral ligament attachment scar (T6) and the ratio between the minimum shaft circumference and total length (T8) can be considered as potential diagnostic variables to distinguish between genera.

Table 4.12. Loading values for PC1 and PC2 (values> 0.5(-/+) are in **bold**).

Variables	PC1	PC2
T1	0.40933	-0.14892
T2	0.40912	-0.053657
T3	0.38727	-0.2124
T4	0.38787	0.1565
T5	0.36522	-0.33425
T6	0.1869	**0.61198**
T7	0.41924	0.04663
T8	0.14343	**0.64569**

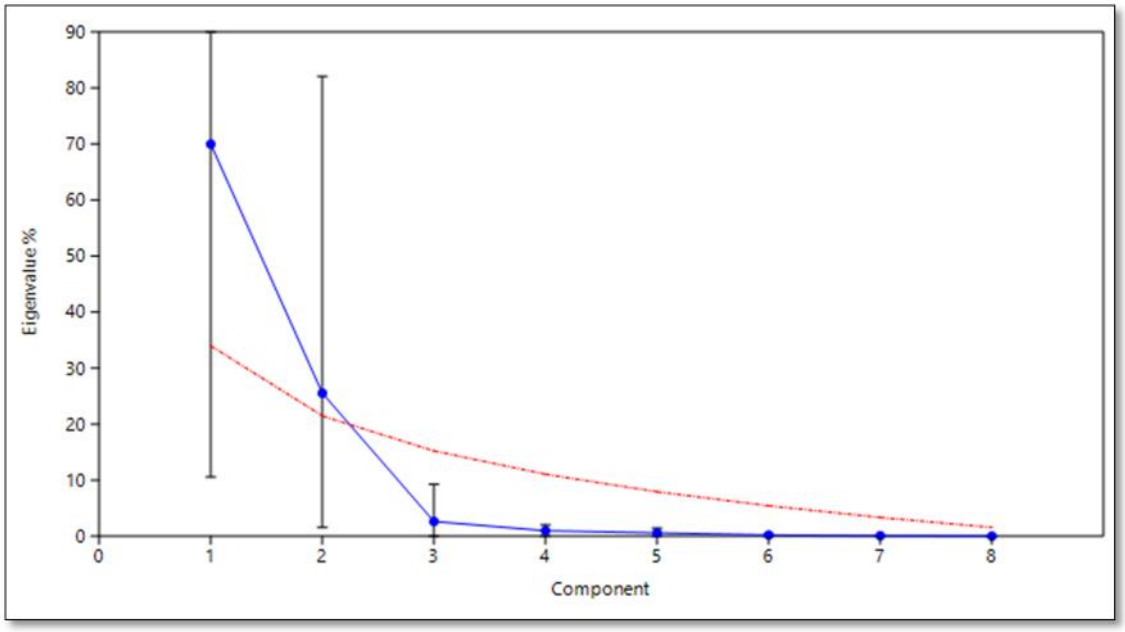

Figure 4.13. Scree plot of tibia PC eigenvalues based on PCA inclusive the new parameters T6-T8.

In the PC scatter plot (Figure 4.14), PC1 still divides the specimens into three clusters: low values (SS), intermediate values (EM1, EM2, SF4, ST1, ST2, SSang6 and SPT), and high values (EH). This result is still in agreement with the outcome of the biometric measurement analyses (see Chapter 3 Section 3.3), which divided the specimens into three size clusters that include the same specimens in each cluster as for the PC1 clusters. These results again indicate that the clustering within PC1 is mostly based on size.

Within PC 2 (y-axis) the scatter plot shows the same pattern as in the biometric PCA prior to adding the new variables. All *Stegodon* tibias except that of *S. sondaari* are on the positive side of the y-axis, while all *Elephas* specimens are on the negative side of the y-axis. In PC2 *Stegodon sondaari* turns out to be more isolated whereas all *Stegodon* except *S. sondaari* become tighter grouped along the positive Y-axis and are clearly separated from the *Elephas* Grouping with negative values. Therefore it can be concluded that the new variables have strong influences in the grouping and allow for separating the tibia specimens according to genus.

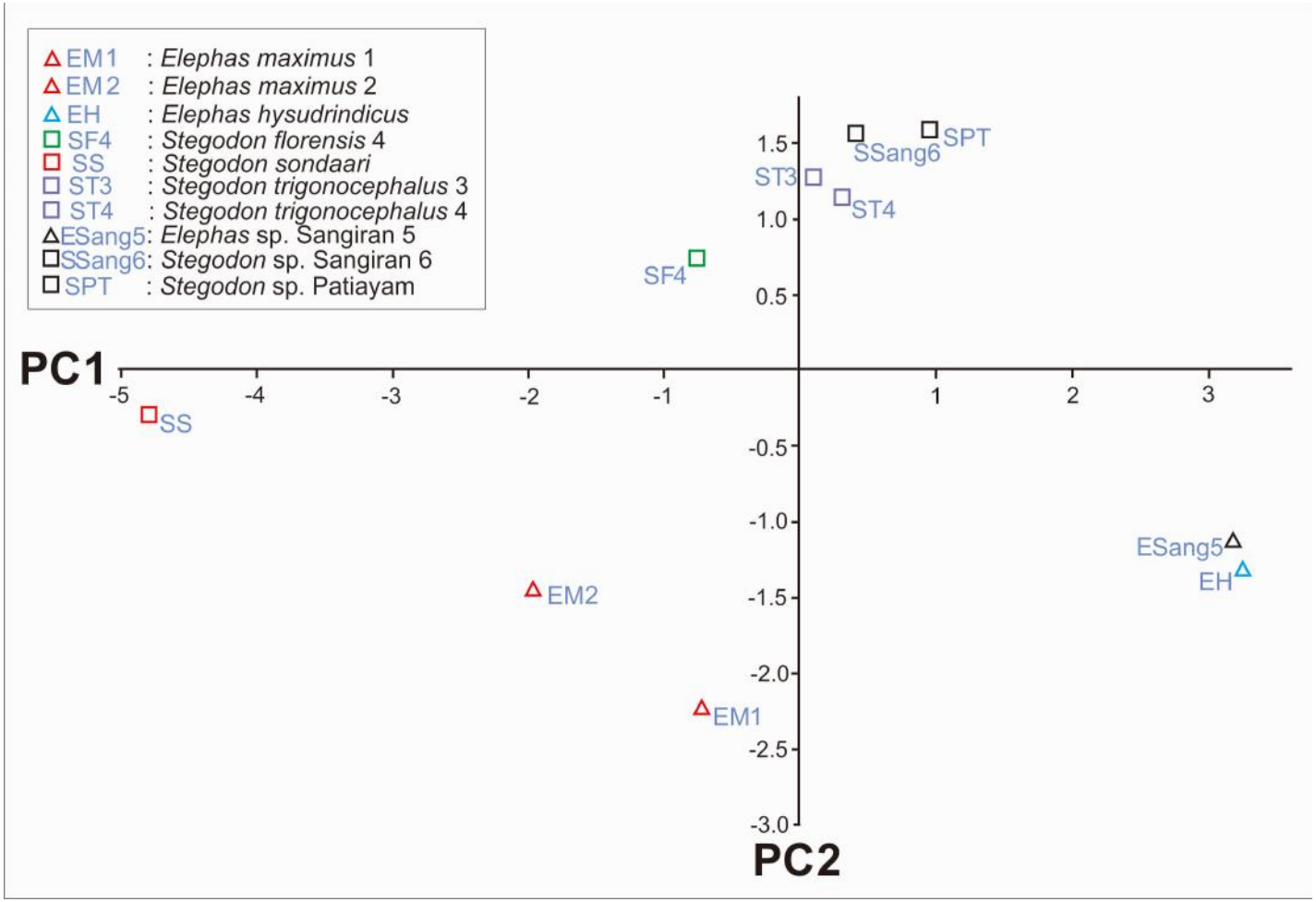

Figure 4.14. Results of the PCA based on 8 biometric parameters showing PC1 plotted against PC2 for 10 tibia specimens of known identity.

4.2. Experiment 2: Testing the New Parameters on Unidentified Proboscidean Taxa

In this experiment the results of Experiment 1 are applied on the limb bone samples including the unidentified specimens, to see how the new variables are able to separate the unidentified specimens according to genera. This involves analysing the unidentified specimens with the identified specimens and undertaking a PCA using the new variables. The tibia and the femur are analysed separately.

The new variables were not analysed in GM because the purpose of this study is to identify new diagnostic variables that can be applied manually in the determination of isolated femur and tibia specimens, and not to explore the functional morphological differences between genera. For Experiment 1 the GM analysis was used to investigate and identify the significant differences in shape that were not captured by the biometric measures undertaken in Chapter 3. Based on this GM assessment, new metric parameters were introduced and tested on their reliability to distinguish limb bones of specimens of which the genera had been identified based on associated fossils.

4.2.1. The Femur of All Specimens Included Unidentified Specimens

The measurements of 14 metric parameters (11 old and 3 new variables) measured on 17 femur specimens (10 identified and 7 unidentified specimens) were first normalised for size (see Appendix A Table 5) and entered into a Principle Components Analysis (PCA) to identify how the new variables separate the unidentified specimens into taxonomic groupings recognised in the previous experiment (*Elephas* and *Stegodon* or *Sinomastodon*).

As discussed in Chapter 3, the PCs can only be considered representative if their eigenvalues are included in the first cumulative 95%. The results of the PCA (Table 4.13) shows that the eigenvalues for PC1, PC2, PC3 and PC4 cover more than 95% of the total variance (PC1 = 73.92%, PC2 = 18.53%, PC3= 2.3134 % and PC4 = 1.6071%). PC1, PC2, PC3 and PC4 can be considered to explain almost all of the variance within the sample of measured femur specimens. But only PC1 and PC2 have significant scores in the scree plot, so it can be

concluded that PC1 and PC2 are the best choice to use in this analyses (Figure 4.15.) and become the main focus of further analysis.

Table 4.13. PCA eigenvalues of femur measurements, including femurs of unknown identity.

PC	Eigenvalue	%variance
1	10.3488	73.92
2	2.59422	18.53
3	0.32388	2.3134
4	0.225	1.6071
5	0.17619	1.2585
6	0.136936	0.97811
7	0.0910275	0.6502
8	0.0445423	0.31816
9	0.0203139	0.1451
10	0.0187102	0.13364
11	0.014147	0.10105
12	0.005081	0.036296
13	0.001064	0.0076018
14	0.00604428	0.00043173

The PCA loadings for PC1 are all less than 0.5 (Table 4.14). Although PC1 is significant none of the variables in PC1 is dominant in importance (all loadings are less than 0.5). This means all variables in PC1 do have a weak correlation with each of the other components, and again, PC1 mostly registers size differences.

PC2 explains 18.53% of the variance and has three significant loadings, all associated with the newly introduced variables F12, F13 and F14. These three variables contribute significantly in grouping the specimens. The loadings of F12, F13 and F14 are -0.55192, 0.56052, and -0.50924, respectively (see Table 4.14). This indicates that the third trochanter length (F12), the angle of femoral torsion (F13) and the ratio between the minimum circumference and the total length (F14) are strong diagnostic variables in grouping the femurs.

Table 4.14. PCA component loadings for PC1 and PC2 based on 14 biometric variables of the femur, including the three new variables F12-F14. All femur specimens (of both known and unknown identity) were included in the PCA. Significant loadings (> 0.5 -/+) are in bold.

Variables	PC1	PC2
F1	0.30308	0.0073974
F2	0.29288	0.039595
F3	0.25832	-0.12336
F4	0.30416	-0.060025
F5	0.29828	0.1332
F6	0.30956	0.015147
F7	0.28799	0.22068
F8	0.29709	0.091948
F9	0.30282	0.066699
F10	0.29483	0.13576
F11	0.29735	0.058654
F12	0.10502	**-0.55192**
F13	-0.071028	**0.56052**
F14	0.15493	**-0.50924**

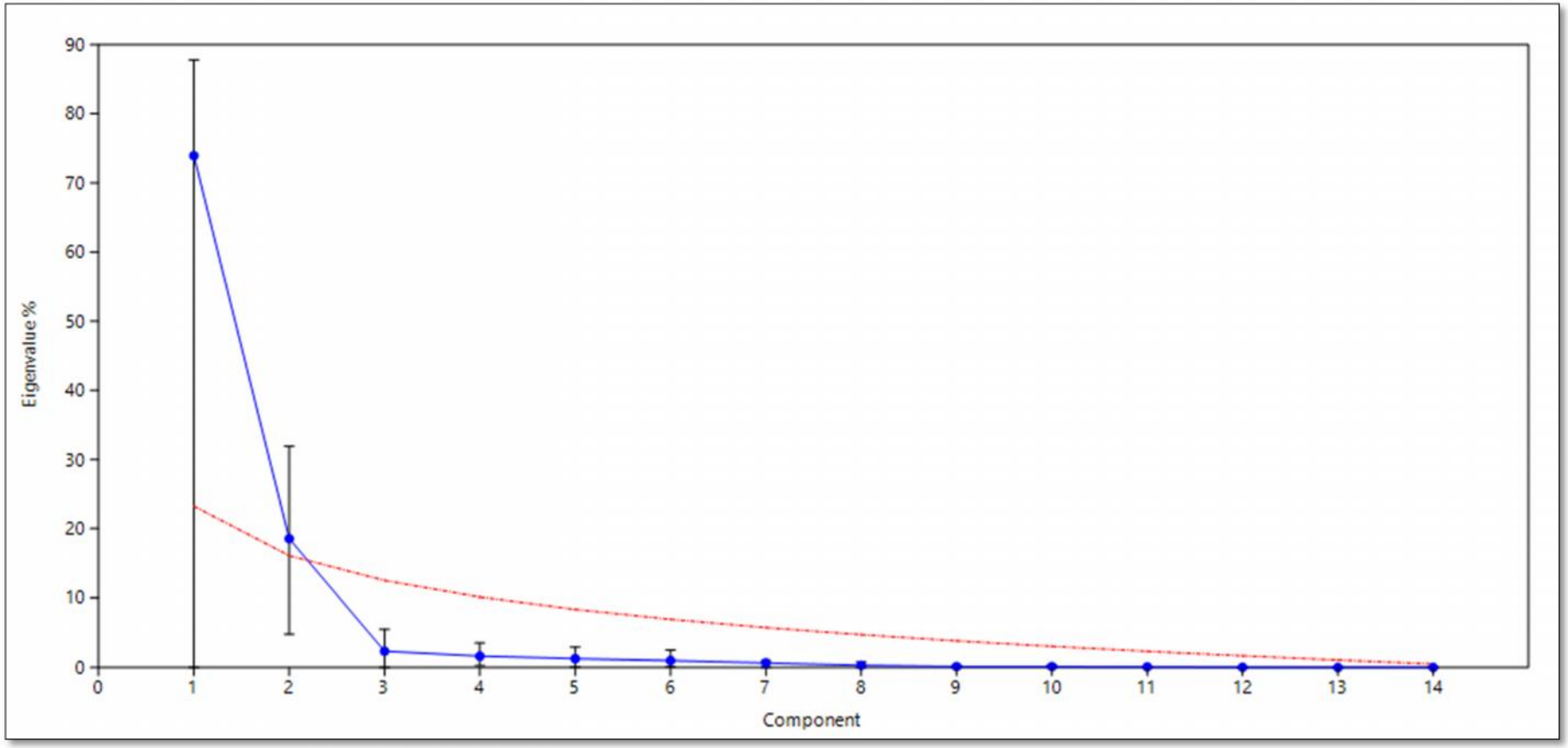

Figure 4.15. Scree plot of PCA based on 14 biometric variables, including three newly introduced variables. The analyzed sample included normalized values of both identified and unidentified femur specimens.

The scatter plot of PC1 and PC2, for all size-standardized specimens that were included in this PCA is shown in Figure 4.16. These results indicate that most femurs of unknown identity (those with a code starting with prefix ‘u’ in Table 3.2) cluster with one of the two groups that were recognised in Experiment 1 (*Elephas* and *Stegodon* + *Sinomastodon*). The exception is femur uSang4.

In Figure 4.16, PC1 divides the specimens into four clusters: Cluster 1 (SS); Cluster 2 (EM1, EM2, SF1, SF2, SF3, uSang2 and uSang3); Cluster 3 (ST1, ST2, uBF, uPT, uSang1, uSang4 and SINO) and Cluster 4 (EH and uNG). In PC1 it is interesting to notice that almost all unknown proboscidean femur specimens from Java cluster with the known specimens of *Stegodon trigonochepalus*1 and *Stegodon trigonochepalus*2 (ST1 and ST2). Specimens uSang2 and uSang3 are located in between the known *Stegodon* specimens from Flores (SF1, SF2 and SF3) and Java (ST1 and ST2). However, the two recent *Elephas maximus* specimens (EM1 and EM2) do not separate from the Flores *Stegodon florensis* specimens, and thus PC1 does not separate the femurs according to genera. The unknown Ngandong femur (uNG) shows a PC1 score close to EH (both uNG and EH represent large-sized femurs). It appears that PC1 still clusters the specimens predominantly according to their size (despite the fact that the values were size-normalized). Possibly, PC1 separates *Stegodon trigonocephalus* from Java from *Stegodon florensis* from Flores.

The femur scores on PC2 (y-axis) appear to separate the specimens much better according to their genus. All *Stegodon, Sinomastodon* (except the pygmy *Stegodon sondaari*, SS) and all unidentified specimens except uNG are on the negative side of the y-axis, while all *Elephas* specimens and uNG are on the positive side of the y-axis. Although the pygmy *Stegodon sondaari* (SS) is also on the positive side of the y-axis, its PC2 score is still far from the range of scores of the *Elephas* specimens, and its position is in between the *Stegodon* + *Sinomastodon* cluster and the *Elephas* cluster. So in PC2, SS also represents an isolated specimen, signifying that it is not only separated from the other *Stegodon* specimens based on its much smaller size (PC1), but is also morphologically distinct from the other *Stegodon* specimens.

The clustering of the unknown Ngandong femur with the *E. hysudrindicus* femur (EH) both in PC1 and PC2 suggests that apart of the similarity in size (both are large-sized femurs) in

PC1, the Ngandong femur also clusters with *E. hysudrindicus* in PC2, showing that it represents an *Elephas* femur.

The single known femur of *Sinomastodon bumiajuensis* (SINO) has the most negative score in PC2 among the known femur specimens. Interestingly, one unknown femur from Sangiran (uSang4) has an even more negative score in PC2 than specimen SINO. In PC1 uSang4 plots with the large *E. hysudricus* femurs suggesting that this femur might represent a larger sized *Sinomastodon* femur. However, care should be taken with this interpretation since only one *Sinomastodon* femur was included in the PCA.

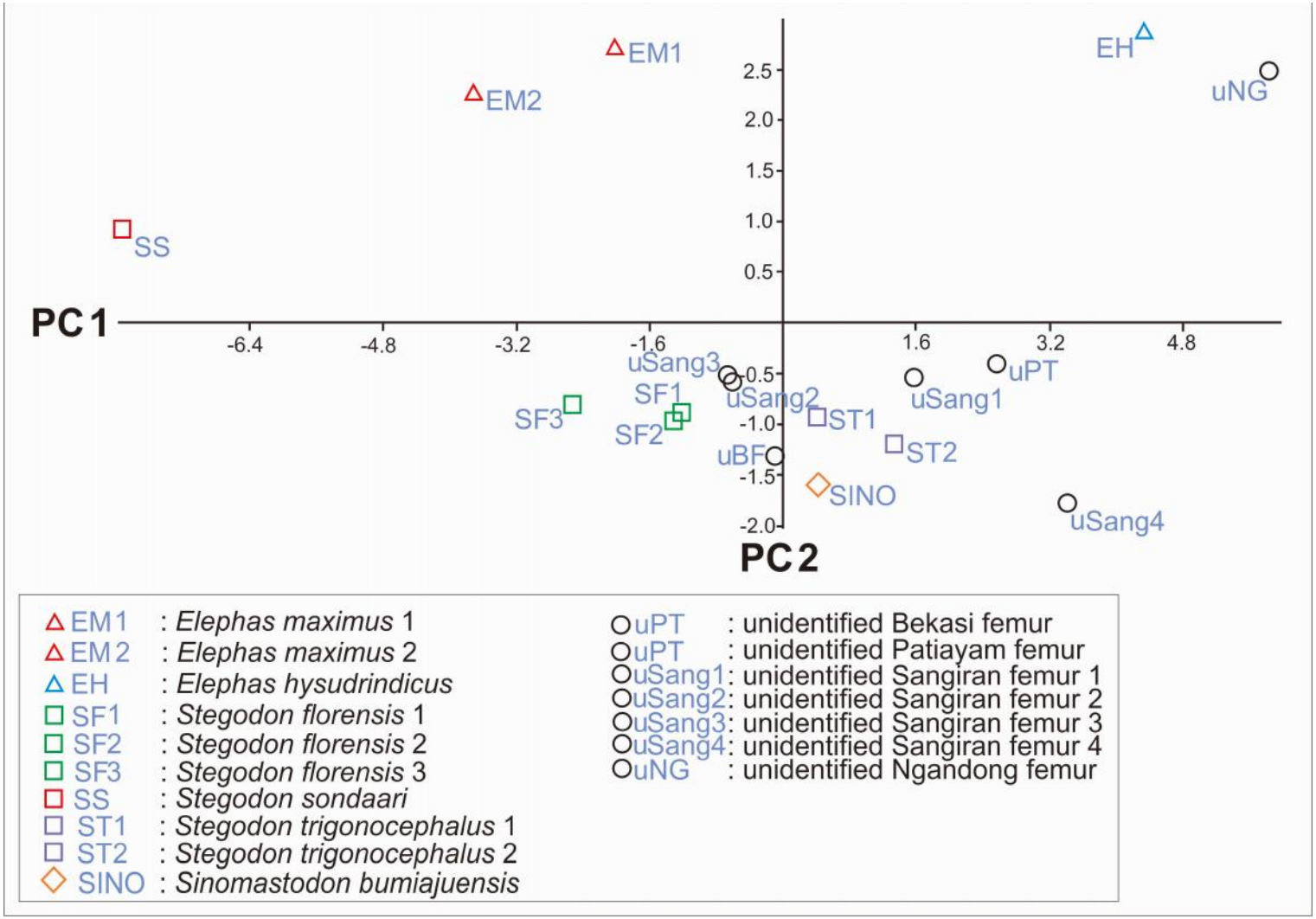

Figure 4.16. Scatter plot of PC1 and PC2 based on 14 variables measured on femurs of known and unknown identity. Loading values of both PCs are presented in Table 4.13.

4.2.2. The Tibia of All Specimen Included Unidentified Specimens

The 8 metric parameters (5 from old parameters and 3 from new parameters) taken from the 11 specimens (10 identified plus 1 unidentified specimens) were first normalised for size (see Appendix A Table 6) and entered into a Principle Components Analysis (PCA) to identify how the new variables are able to assign the unidentified specimen to genus (*Elephas* or *Stegodon*).

The results of the PCA shows that the eigenvalues of PC1 and PC2 cover more than 95% of the variance (PC1 = 69.36%, PC2 = 26.204%) (Table 4.15). Again, PC1 and PC2 becomes the main focus in this PCA. The loading values that result from this PCA are listed in Table 4.15.

Table 4.15. Eigenvalue of tibia.

PC	Eigenvalue	%variance
1	5.5488	69.36
2	2.0963	26.204
3	0.1790	2.2369
4	0.0757	0.9457
5	0.0694	0.8678
6	0.0158	0.1975
7	0.0143	0.1786
8	0.0008	0.0096

Based on the scree plot (Figure 4.17), PC1 and PC2 shows significant values. However, all the loadings for PC1 are less than 0.5. So this means the component does not have a strong correlation with each component (Table. 4.16). PC2 is significant and covers 26.2% of the variability. There are some variables in PC2 that are important. The loading value of T6 and T8 is **0.63**, and **0.66**, respectively. This demonstrates that the medial collateral ligament attachment scar (T6) and the ratio between minimum circumference and total length (T8) are confirmed as strong diagnostic variables to distinguish between genera.

Table 4.16. Loading values from each principle component (values> 0.5(-/+) in **bold**).

Variable	PC1	PC2
T1	0.41	-0.12
T2	0.41	-0.01
T3	0.39	-0.19
T4	0.39	0.15
T5	0.38	-0.30
T6	0.16	**0.63**
T7	0.42	0.06
T8	0.09	**0.66**

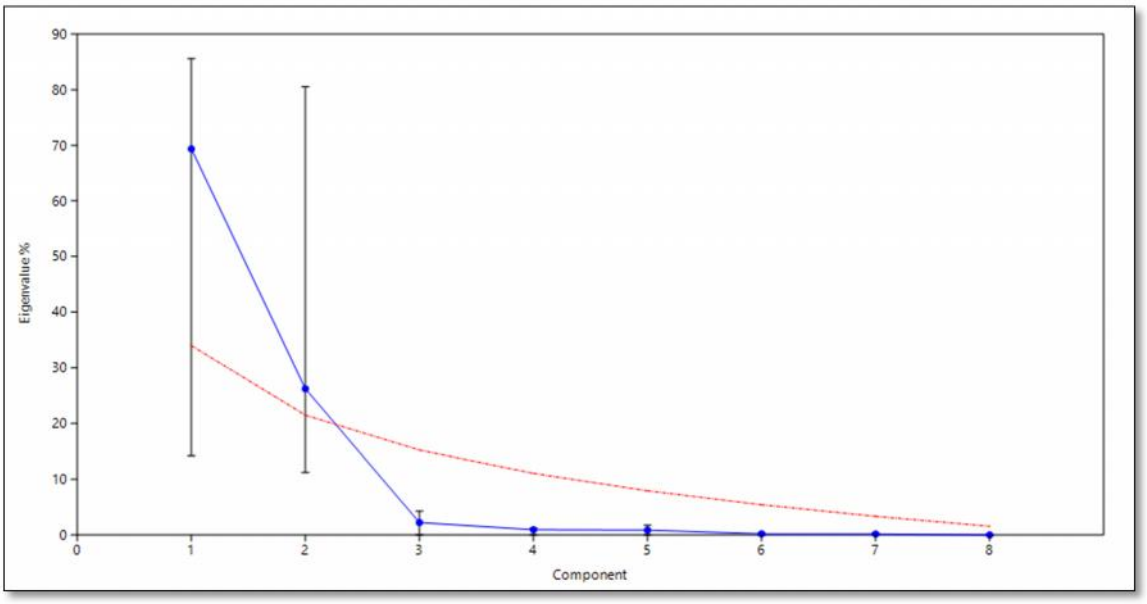

Figure 4.17. Scree plot of PCA on all tibias, including one unidentified specimen.

In a PC1-PC2 scatter plot, PC1 shows that PC1 divides the specimen into four clusters: first cluster (SS), second cluster (EM2), third cluster (EM1, ST3, ST4, SF3, SPT and SSang6) and fourth cluster (EH, uNG and ESang5). In PC1 the unidentified tibia from Ngandong (uNG) clusters where in femur Ngandong specimen also clustering with EH and ESang5) (Figure 4.18). This result indicates that the unidentified Ngandong specimen can be attributed to *Elephas*.

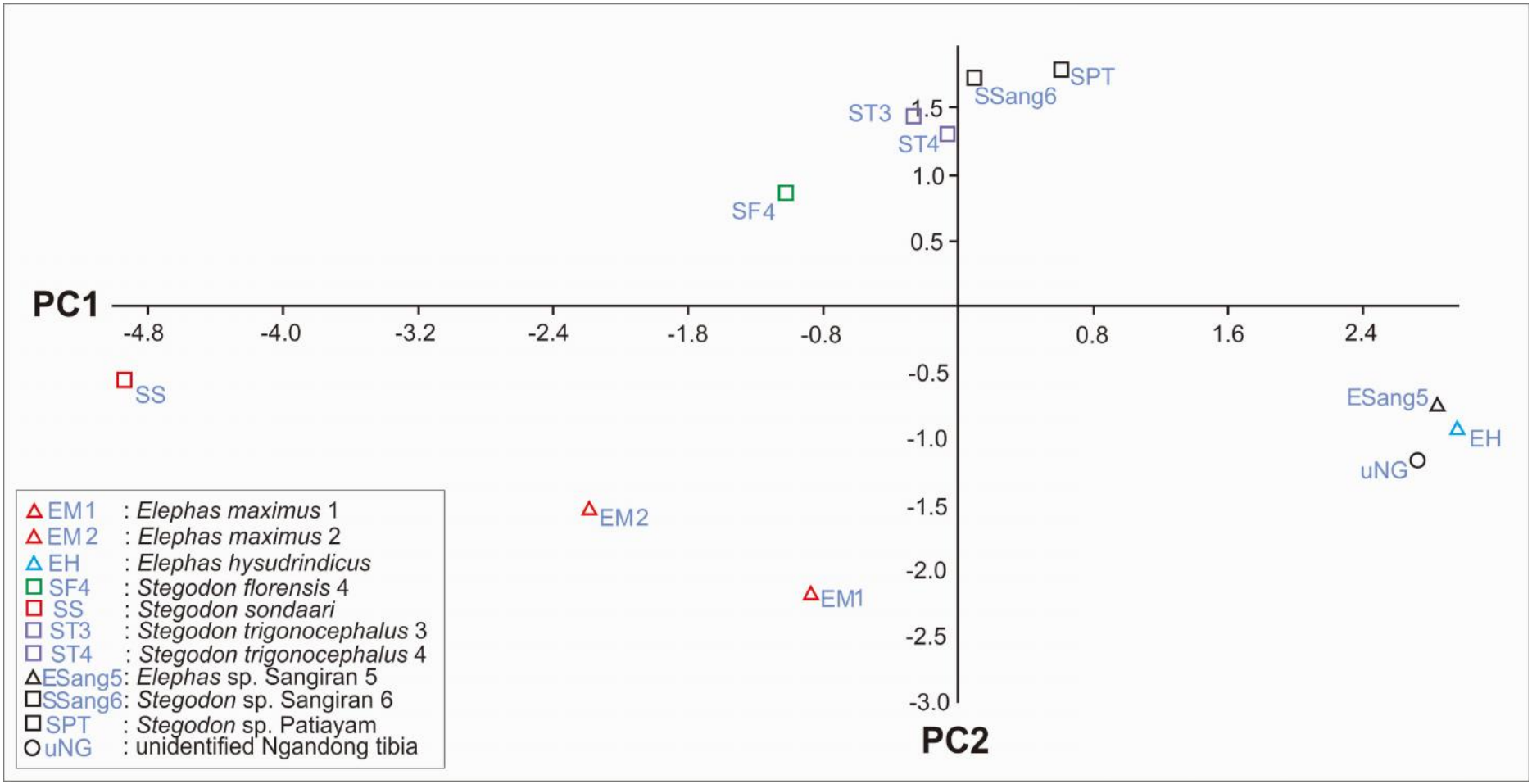

Figure 4.18. Scatter plot of PC1 versus PC2 based on a PCA with 8 variables, including three newly defined variables. Measurements of both tibias of identified and unidentified were included in the PCA.

4.3. Summary of Results

Experiment 1 was performed in order to find new variables to distinguish genera based on femur and tibia biometric parameters measured on limb bones of Proboscideans of known genus. For the femur, PCA with 11 ordinary parameters, was based on 10 identified specimens only. Despite the small sample size, the transverse diameter of the third trochanter (F4) and the total length (F7) were found to correlate weakly with genus. With these findings in mind, a PCA of 34 3D landmarks was performed in GM, with the independent variables of genus, F4 (transverse diameter of shaft at distolateral tuberosities of the third trochanter) and F7 (total length of femur between caput and lateral condyle). The GM analyses revealed that three morphological aspects contributed strongly to a separation of femurs by genus: 1) the length of the third trochanter; 2) the torsion of the femur shaft, and 3) the minimum circumference of the femur shaft. Based on these findings, three new variables were defined that were thought to capture the above-mentioned distinctive characteristics. These variables are: 1) the length of the third trochanter (new variable F12); 2) the angle of femoral torsion (new variable F13); and 3) the ratio between the minimum circumference and the total length (new variable F14).

A similar procedure for the tibia resulted in two new diagnostic variables: 1) the length of the medial collateral ligament attachment scar (new variable T6); and 2) the ratio between the minimum circumference of the tibia shaft (T7) and its total length (T8). Variable T7 alone did not produce significant results, but combined with the total length this variable can assist in recognising tibias by genus.

In Experiment 2 the newly defined diagnostic variables for femur and tibia were applied on the entire sample of femurs and tibias of both known and unknown identities, in order to test if the combined old and new variables were able to identify the genus of specimens of unknown identity. The PCA of size-normalized measurements revealed that all of the unidentified femur specimens grouped with either *Elephas* or with the cluster *Stegodon* + *Sinomastodon*. In the PCA PC1 was largely influenced by size, but PC2 separated the specimens according to genus, although *Sinomastodon* could not be distinguished from *Stegodon*. A femur from Ngandong of unknown identity clustered with *Elephas*, and also a single tibia of unknown identity from Ngandong clustered with *Elephas*.

In all femur and tibia PCAs the bones of the single pygmy *Stegodon sondaari* individual, although clustering with *Stegodon* specimens in general in PC2, was always found to have extreme scores in PC1 (size) and intermediate scores in PC2 (shape) between a cluster of combined large-bodied *Stegodon* + *Sinomastodon* specimens (for the femur only, since no tibia of *Sinomastodon* was available) and the cluster of *Elephas* bones.

One femur from Sangiran of unknown identity (uSang4) had the most extreme negative score on PC2, with as closest other femur a specimen of *Sinomastodon*, suggesting that uSang4 may belong to that genus, although more data would be required for a stronger result.

5. DISCUSSION

Knowledge of proboscidean genera and species, especially extinct proboscidea recovered from the Indonesian Archipelago is predominantly based on teeth and skulls. Some research has been undertaken with post-cranial material that found differences in the proboscidean genera and species. Hooijer (1955) distinguished between *Elephas* and *Stegodon* based on the degree of slenderness of the femur. This research examines a sample of extant and fossil proboscidean hindlimb bones (femur and tibia) from the Indonesian Archipelago to see if they can be distinguished on genus or species levels based on a set of diagnostic criteria. If it is possible to distinguish these elements based on morphology, the fossil femurs and tibias that have been found in isolation, can then be identified. The identification of morphological differences between taxa may also provide clues regarding differences in locomotion.

Ten proboscidean femurs and ten proboscidean tibias from identified species, and seven femurs and one tibia of unidentified proboscidea, were included in the analysis. Among these specimens, there were five associated femur and tibia specimens from single individuals that originated from three fossil and two recent skeletons. Mostly all of the specimens came from Java and Flores Island, except for the two recent skeletons that originated from Sumatra Island. One of these had been moved to Java Island and died there.

Firstly, the specimens were examined using a surface morphology assessment. Then 11 biometric measurements of the femur and five biometric measurements of the tibia were taken of all the specimens and the data results recorded. This data was entered into a Principle Component Analysis (PCA). The purpose of PCA is to reduce the variables in a group into several variables which are considered to have the most influence on all of the variables (Sharma 1995). So, from the 11 biometric measurements of the femur and five biometric measurements of the tibia, these were expected to reduce to just a few variables that have the most influence on all of the variables. The specimens were also analysed using 3D landmark coordinate data in Geometric Morphometrics (GM) analysis program, which was used to visualise the shape of each specimen and the differences between genera/species. Because the studied samples included pygmy proboscideans, the landmark coordinates of procrustes were registered in order to eliminate size as one of the most significant distinctive characters. Differences in shape that emerged between genera were then translated into a

number of new biometric parameters. Including these new variables in the PCA enhanced the distinction of genera into two groups, *Elephas* and *Stegodon* + *Sinomastodon* (for femurs only; no known tibia of *Sinomastodon* was available for comparison). Introducing the new variables and applying PCA biometric analysis on all the femur and tibia specimens, including those of unknown identity, resulted in the clustering of the unidentified specimens within either of the two groupings of known identity. Although *Stegodon* and *Sinomastodon* cannot be satisfactorily distinguished from each other, the inclusion of the new parameters can distinguish this group from *Elephas*.

5.1. Identified Femur Specimens

In the surface morphology assessment, six variables were observed (see Chapter 3). The femur of *Elephas* shows the difference at the distal articulation of the knee joint. All *Elephas* specimens have a wider opening between the medial and lateral condyles than in *Stegodon* and *Sinomastodon*, but demonstrate a narrower and shallower indentation between the condyles compared to *Stegodon* and *Sinomastodon*. The indentation between the condyles has the function of accommodating the anterior cruciate ligament (ACL) and posterior cruciate ligament (PCL) in the knee joint (see Figure 2.13 from Chapter 2).

From the surface morphology assessment, it was found that the lateral and medial borders of the central part of the diaphysis of *Elephas* tend to be straighter and more parallel compared to *Stegodon* and *Sinomastodon*, where the borders are slightly curved and converging. This is in accordance whit what was noted by other researchers (Christiansen 2007; Alexander et al. 1979), who found that the modern elephant has a more columnar femur shape compared to the archaic proboscideans. Furthermore, the *Stegodon sondaari* femur shape is more curved compared to all other specimens. In the medial crest/minor trochanter, the *Stegodon* specimens have a more robust and strong appearance, especially *Stegodon sondaari*, which has the strongest and widest minor trochanter compared to all other specimens (see Figure 5.1).

This study also showed that the distal femur is more robust in *Stegodon* than in *Elephas*, as expressed by the third trochanter which is wider flaring in *Stegodon-Sinomastodon* as compared to *Elephas*, which tend to be more gracile in appearance. In *Stegodon sondaari* it is

extremely wide compared to all *Stegodon* specimens, and even more so when compared with *Elephas* specimens.

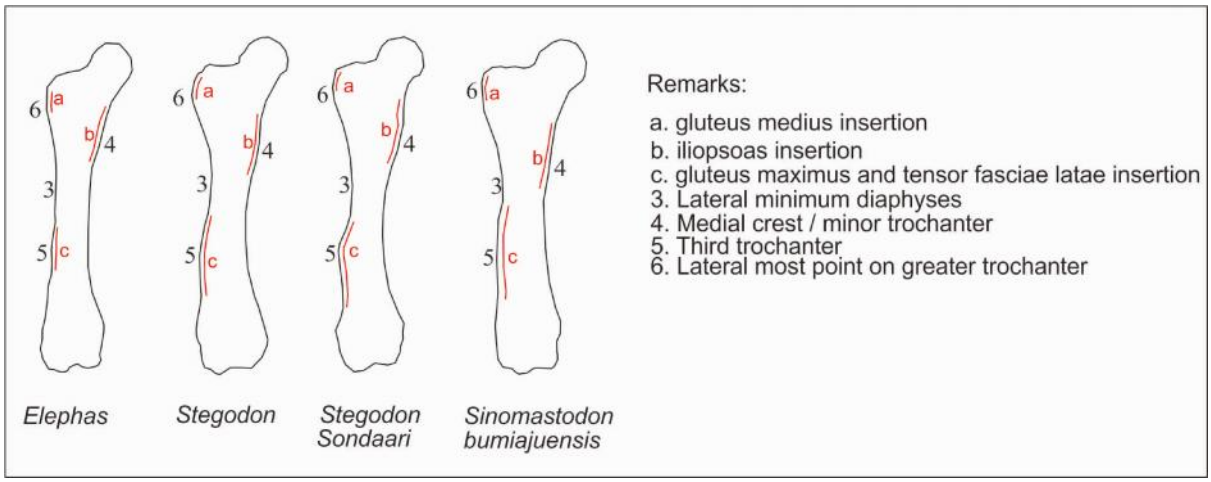

Figure 5.1. Simplification of three muscle attachment scars related to the surface morphology assessment variables (all femurs are scaled to the same size).

The medial crest/minor trochanter is the part of the femur where the iliopsoas muscles are attached (see Figure 5.1). Iliopsoas are the inner hip muscles that have a function in walking. Furthermore, they are also involved in the flexion and lateral rotation of the thigh (Schuenke et al. 2006). The third trochanter is the part of the femur where the two main muscles (the gluteus maximus [GMX] muscle and the tensor fasciae latae [TFL] muscle) are attached and have the function of supporting the load of body mass and influencing the coordination of the stride of vertebrates (Milne & O'Higgins 2012).

The most laterally protruding point of the proximal epiphysis is part of the major trochanter and its function is to keep the thigh in place and to prevent movement of the mid-sagittal body while standing. During walking, this muscle coordinates with the GMX muscle to support and keep the hips in place so that they do not move to the wrong side. In the most laterally protruding point of the proximal epiphysis of *Elephas*, the protruding point of the proximal epiphysis is located more distally than that compared with all of the *Stegodon* and *Sinomastodon* specimens. Distally inserted muscles use less energy and provide a more economical design for moving limb segments during locomotion (Milne and O'Higgins 2012; Kardong 2012). So, based on these hip muscle characteristics, either while standing or during movement, *Elephas* is more efficient in energy conservation compared to *Stegodon* and *Sinomastodon*.

In short, the surface morphology assessment of the femurs shows that all *Stegodon* and *Sinomastodon* specimens typically look more robust than *Elephas* specimens. Moreover, *Stegodon sondaari* shows very distinct shape characteristics that, apart from its small size, allow for distinction from other *Stegodon* species.

The biometric measurement data from the ten femurs of identified taxonomic affinity show that some variables (F7 = total length and F4 = transverse diameter at the third trochanter) have the potential to distinguish the genera. Parameters F7 and F4 were then analysed further using PCA and GM.

In the PCA results, only PC1 was significant. As mentioned in Chapter 4, all PC1 variables have a loading value that is almost the same, at around 0.3. This means that all variables in PC1 share the same influence in PC1. So, the level of significance of PC1 is affected by all variables because there are no variables that actually show a stronger influence than the other variables (all have a loading value of less than 0.5).

For PC2, which is not significant, the femur specimens appear to separate according to their genera. Within PC2, the total length variable has a loading value of more than ±0.5, and the transverse diameter variable at the third trochanter has a value close to 0.5. The other measurements are not significant for distinguishing genera.

The results show that the grouping of genera is primarily based on size (length) and not on differences in anatomy. The dataset in this research contains specimens of dwarfed *Stegodon* taxa that are small to extremely small compared to mainland taxa (both *Stegodon* and *Elephas* species); average-sized specimens, to which group the majority of studied specimens belong; and very large specimens of *Elephas hysudrindicus*. The inclusion of both dwarfed and large proboscidea specimens make size show up in PC1 in three clusters (small, medium and large) as a significant separator of specimens.

Although the PCA shows that the femurs are separated and grouped by size, the analysis also indicates that one variable related to the total length (F7) has the potential to distinguish genera among specimens. Based on these findings, F7 was chosen as diagnostic parameter to

be analysed further in GM to find other variables that could be potentially used to distinguish the genera.

From the wireframe analyses in GM, it could be inferred that the deformation shape significantly varies in the third trochanter region, in the proximal femur rotation and in the minimum diameter of the diaphysis that is also related to the length. As the aim of this study is to find new biometric variables, these deformation shape characteristics were then turned into measurement variables. The deformation shape in the third trochanter was measured by its length between the landmarks 9-12. The proximal femur rotation was measured by the width of the angle of the rotation of the femur head. And the deformation in minimum circumference, which is correlated to the length, as measured by the ratio between two. The codes of these new variables are the length of the third trochanter (F12), the rotation of the femur (F13) and the ratio between the minimum circumference and the total length (F14).

5.1.1. The length of the Third Trochanter (F12)

In this study, the third trochanter is a variable that allows for distinguishing between proboscidean genera. The shape and position of the third trochanter of mammalian femurs have been studied by some researchers (Koneval 2003; Milne & O'Higgins 2012). Koneval (2003) did a comparative study on the third trochanter shape in armadillos, while Milne and O'Higgins (2012) analysed the position of the third trochanter with respect to hindlimb locomotion function. The results of their research can be used for comparison in this study because the femurs in this study have a variety of shapes and positions of the third trochanter. This shape and position may provide clues regarding differences in their locomotion function.

As shown by the surface morphology assessment, the third trochanter of *Stegodon* and *Sinomastodon* is significantly more robust compared to *Elephas*. Hooijer (1955) also noted that the Java *Stegodon* had stouter limbs and feet than the living Asian elephant (*Elephas maximus*). The shape of the third trochanter of *Stegodon* and *Sinomastodon* flares out wider laterally (outward) compared to *Elephas*, in which the third trochanter forms only a straight crest parallel with the lateral distal part of the femur. The straight shape of the third trochanter in *Elephas* is congruent with its femur shape, which tends to be more column-like when compared to *Stegodon* and *Sinomastodon*. The third trochanter of *Stegodon sondaari* shows the relatively widest lateral flaring when compared to all other specimens (see Figure 5.2).

As discussed previously in the surface morphology assessment, the third trochanter is the part of the femur for GMX muscle attachment, and this muscle is one of the main muscles to play a role in locomotion. A wider shape of the third trochanter means that the attachment of the muscle to the third trochanter would be located further laterally from the centre of rotation in the head of the femur (see Figure 5.2). This implies that the energy required to move the bone would be greater (Bonnan 2004). Regarding the third trochanter as a place to attach the muscle, this would make the energy that is needed to move the femur through this point greater. In *Elephas*, the lateral distance of the hip joint to its third trochanter is closer than the lateral distance of *Stegodon* and *Sinomastodon*. This means that to move its hip, *Stegodon* and *Sinomastodon* required comparatively more energy than *Elephas*.

In *Elephas*, the onset of the third trochanter starts more distally and is less marked compared to the third trochanter of *Stegodon* and *Sinomastodon* (see Figure 5.2). Contrary with the lateral distance to the hip joint, the further or more distal the start of the third trochanter, the more efficient is the energy consumption to move the femur from this point. So, *Elephas* had more efficiency in energy consumption when the force was distributed to this point to move the limb compared to *Stegodon* and *Sinomastodon*, where the third trochanter had a position that was more proximal.

Overall, based on the combination of the lateral distance and the starting point of the third trochanter, it can be inferred that *Elephas* was the most efficient regarding energy requirements compared to *Stegodon* and *Sinomastodon*. Furthermore, *Stegodon sondaari* shows that it was the most profuse regarding energy consumption in locomotion due to its wide and proximal third trochanter. This could be a functional adaptation of *Stegodon sondaari* to deal with the environment in which it lived.

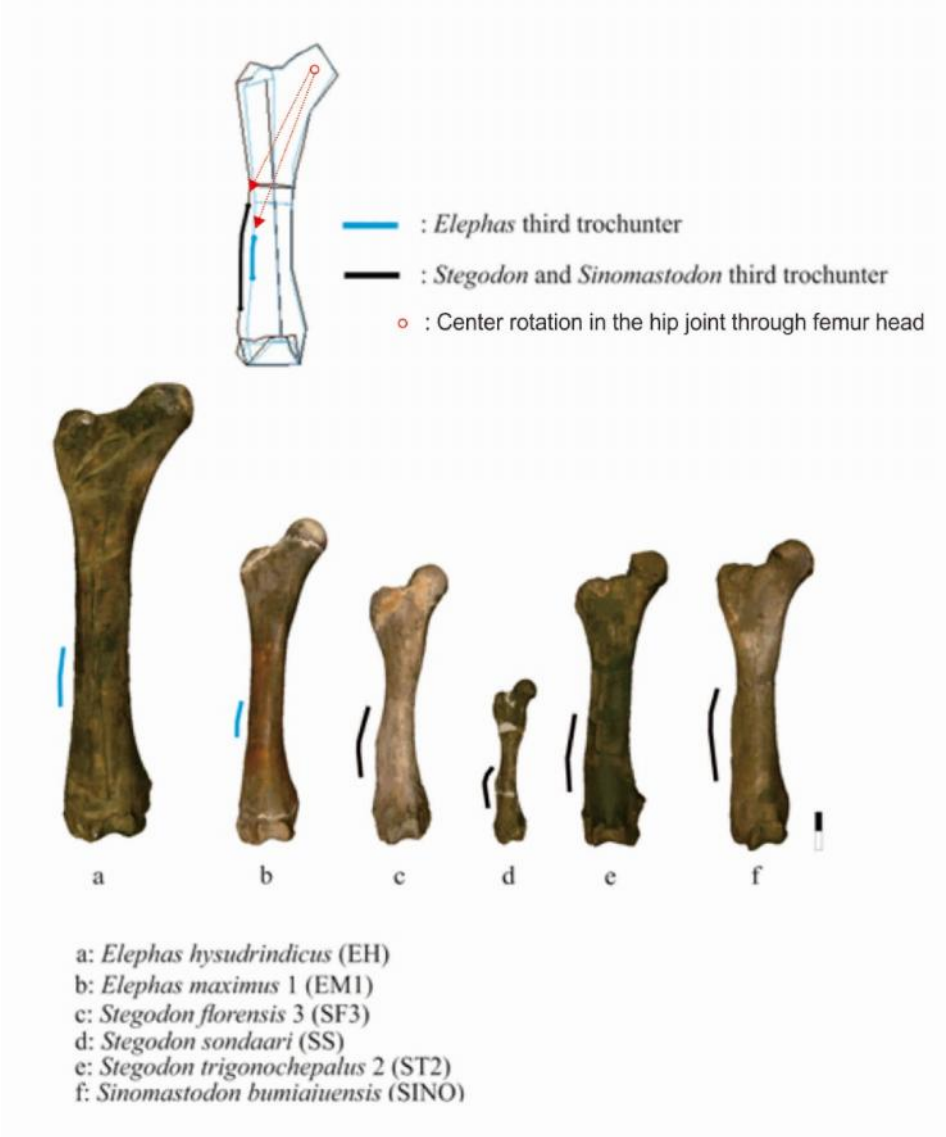

Scale = 10cm.

Figure 5.2. The third trochanter length proportion and it shapes in some specimens.

5.1.2. The Femur Torsion Angle (F13)

As shown in the results section, the angle between the plane passing through the greater trochanter and the femur head, and the plane passing through the distal condyles distinguishes *Stegodon* and *Sinomastodon* (except *Stegodon sondaari*) from *Elephas* (see Figure 5.3). The rotation angle of *Elephas* is wider than in *Stegodon* and *Mastodon*. In *Elephas*, the femur angle is around 40-45 degrees. In most *Stegodon* (except *S. sondaari*), and in *Sinomastodon*, this angle is around 25-26 degrees. *S. sondaari* has an exceptionally high angle of around 45 degrees. This is possibly the reason why *S. sondaari*, apart from its much smaller size, also represents an outlier in the PC scatter plots when it comes to shape difference.

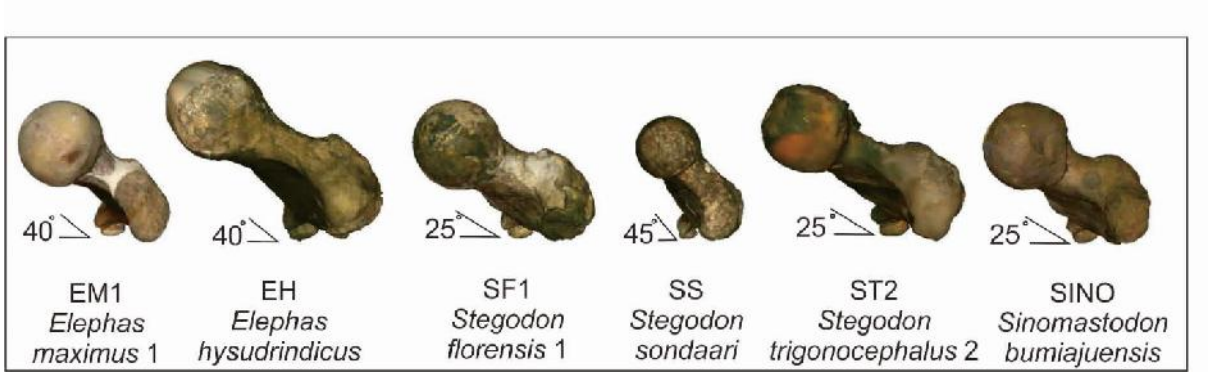

Figure 5.3. The femur rotation angle from some specimens (all oriented in dorsal view at the head of the femur great trochanter shaft).

A comparison with the rotation of the human femur is made to explain proboscidean femur rotation. The proximal femur is an essential locomotor component that is part of the hip joint. This angle has a direct effect on limb posture, both in humans and animals (Harmon 2007). The angle rotation of the femur is important in the context of adaptation in locomotion because it influences the amplitude of femur rotation in the hip joint (Tibar & Leunig 2012). However, this must be linked to the pelvis shape, especially in the head of the femur socket in the proboscidean pelvis (Smuts & Bezuidenhout 1994).

Femur rotation is influenced by how the proximal femur joins the femur shaft. Figure 5.4 shows how the femur rotation affects the horizontal amplitude of the hip joint movement in a posterior direction. A wider angle of femur shaft rotation (as in *Elephas*) correlates with a smaller amplitude in backward hip joint movement. In other words, the wider the angle rotation, the more rigid the hip joint. Whereas a medium wide angle rotation (as in *Stegodon*) shows the femur movement to be more complex. Considering the studied specimens, almost all *Stegodon* and *Sinomastodon,* except the extremely dwarfed *S. sondaari,* have an angle rotation that is smaller than in *Elephas* (see Figure 5.4). This implies that almost all *Stegodon* and *Sinomastodon* individuals could accommodate a hip movement that was more complex than in *Elephas*. As was mentioned previously, *S. sondaari*'s femur rotation shows a different pattern that is the opposite trend to the other *Stegodon* species. *S. sondaari* has an angle of rotation of the femur that is wider than any of the other *Stegodon* or *Elephas* specimens. This suggests that *S. sondaari* had a different hip adaptation with a clearly distinct femur rotation compared to the other *Stegodon* species. Unfortunately, no well-preserved pelvis of *S. sondaari* is available for study.

If the wide angle of the femur is indeed correlated to the shape and position of the third trochanter, it seems that the wider angle of the femur would place the distance of the third trochanter closer to the centre of rotation (hip joint), as shown by the *Elephas* femur in Figure 5.4, and further away in *Stegodon*. The exception is *Stegodon sondaari*, which shows a femur rotation angle that is wider than *Elephas*. This angle structure places the third trochanter closer to the hip joint and allows for the reduction of waste energy and provides a more effective locomotion. Based on these observations, the rotational angle of the femur is thought to represent an important morphological adaptation in locomotion, with the most extreme adaptation occurring in *Stegodon sondaari*. However, a detailed study of the pelvis would be required to verify this hypothesis.

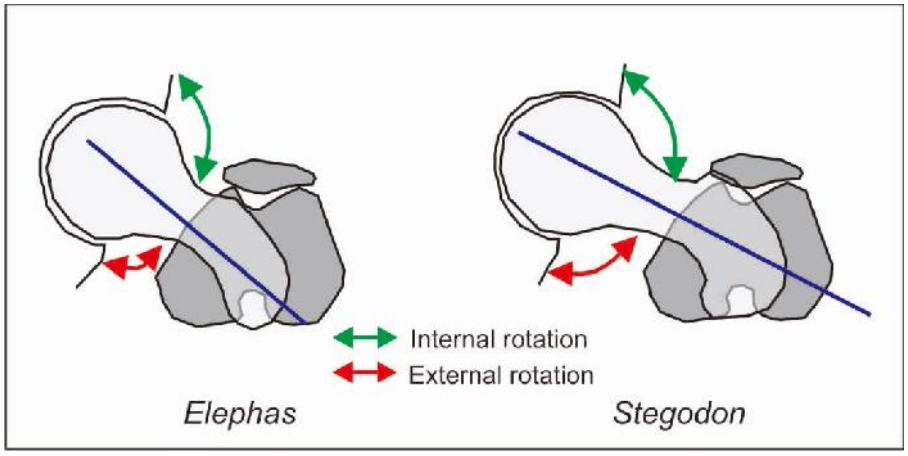

Figure 5.4. Articulation of the proboscidean femur and pelvis. The angle of the femur (blue lines) influences the extent of rotational movement of the femur (modified from Tibar & Leunig 2012).

5.1.3. The Ratio Between Minimum Circumference and Total Length (F14)

The minimum circumference/length ratio in *Elephas* has a smaller value than in *Stegodon* and *Sinomastodon*. The *Elephas* ratio is below 30, but in all of the *Stegodon* and *Sinomastodon* specimens, the ratio is larger than 30. This means that the femurs of *Stegodon* and *Sinomastodon* are more robust compared to *Elephas*. Hooijer (1955) also measured and compared the femurs of *Stegodon trigonocephalus* and *Elephas maximus*. Although he did not measure the minimum circumference, he measured the ratio of the length of the femur against the mediolateral minimum diameter. His reasoning was based on the notion that the mediolateral minimum diameter grows faster in size than the anterior-posterior diameter. This is why the cross section of a proboscidean's femur shows an oval shape. More recently,

various researchers prefered to measure the minimum circumference in the same place as the mediolateral minimum diameter, because this can be used as a more accurate predictor of body mass (Christiansen 2004; Campione & Evans 2012).

The value of the minimum circumference is linearly correlated with the mediolateral minimum diameter because both are measured at the same place on the femur shaft. This is why the results of this study agree with Hooijer's findings that the length/minimum diameter ratio of the femur of *Stegodon trigonocephalus* is much bigger than that of *Elephas maximus*.

5.2. Identified Tibia Specimens

The surface morphology assessment of the tibia shows a similar pattern as for the femur analysis. All *Stegodon* specimens typically look more robust than *Elephas* specimens. Five distinctive features were recognised based on surface observations. The tibia of *Elephas* shows a difference at the articulation of the knee joint. All *Elephas* tibias have a small tuberculum intercondylare mediale, which contrasts with *Stegodon* specimens that have a big tuberculum intercondylare mediale. The tuberculum intercondylare mediale functions as an insertion point for the ACL in the tibia. The bigger tuberculum intercondylare mediale on *Stegodon* indicates that the ACL of *Stegodon* is more robust than in *Elephas*. This result fits in with the distal shape of the femur which also indicates that the ACL of *Stegodon* is more robust than *Elephas*. Another knee ligament that is indirectly observable is the medial collateral ligament (MCL) attachment scar. The MCL attachment scar in *Stegodon* is deeper and more robust than in all *Elephas* specimens. This robusticity of the MCL is congruent with the other ligaments in the knee that, as stated previously, are also more robust compared to *Elephas*.

The length of the anterior shaft crest is relatively shorter in *Elephas* than in *Stegodon* specimens. The anterior shaft crest characteristically is most prominent in the proximal two-thirds of the tibia shaft, becoming more smooth and rounded distally. The result of the shape of the anterior shaft crest can also be observed in the lateral view. The anterior shaft crest is a place for attachment of the fibrous connective tissues in the leg. It appears that *Stegodon* again seems to be more robust in the appearance of its lower hindlimbs compared to *Elephas*. The indentation between the condyles has the function of accommodating the ACL and PCL in the knee joint. Like in humans, the ACL and PCL in proboscideans also have a function in

the control of flexion and extension of the knee joint (Weissengruber et al. 2006). The narrower and shallower indentation between the condyles in *Elephas* compared to *Stegodon* and *Sinomastodon,* implies that the ACL and PCL of *Elephas* are smaller and shorter than in *Stegodon* and *Sinomastodon*. This relates to the function of the ACL and PCL in controlling the flexion and extension of the hindlimb, so this tibia characteristic also indicates that *Stegodon* and *Sinomastodon* could bend their knees more easily when compared to *Elephas*.

The biometric analysis of the ten tibias of the identified taxa showed that the mediolateral minimum diameter (T4) has the potential to distinguish between genera. T4 was then analysed further in PCA and GM.

The PCA results in PC1 were found to be significant. As with the femur analyses, all variables in PC1 share almost the same influence. Similarly to the femur specimens, the PCA results of the tibia also showed three significantly separated clusters in PC1 that corresponded with the size groups: small, medium and large. The small-sized group includes *Stegodon sondaari* only; the medium-sized group includes all other *Stegodon* specimens and the two not full-grown recent *Elephas* specimens; and the large-sized group includes *Elephas hysudrindicus* only. For PC2, although not significant, the specimens appear to be separated by genera. Within PC2, the mediolateral minimum diameter (T4) has a loading value of more than ±0.5. The other measurements are not significant for distinguishing genera. These results show that the grouping is primarily based on size (length) and not on homology of anatomy.

Landmark coordinates were introduced and all data were scaled by procrustes registration in order to analyse the minimum diameter and other shape characteristics in GM, to explore potential other variables that might be better able to distinguish between genera. The GM analysis showed that the maximum shape deformations occur in three aspects of tibia morphology: 1) the length of the medial collateral ligament attachment scar; 2) the minimum circumference; and 3) the ratio of length and minimum circumference. These deformation shape characteristics were then converted into measurement variables. The shape deformation of the medial collateral ligament attachment scar is defined by its length (measurement T6). The shape deformation of the minimum circumference is measured as the minimum circumference of the tibia shaft (measurement T7). This minimum circumference is then compared to the total length as a ratio (T8=T7/T5).

After re-analysing with PCA, from these three new variables, only T6 and T8 were shown to make a significant contribution in the separation of genera (see Table 4.12). The minimum circumference (T7) alone, although not showing significant separation between genera, is required for the ratio (T8).

5.2.1. The Medial Collateral Ligament (MCL) Attachment Scar (T6)

The MCL attachment scar (see Figure 5.5) variable was adapted from Ariens (1995). He compared the MCL attachment scar of *Stegodon trigonocephalus* to the MCL attachment scar of *Mammuthus primigenius* in order to recognise the differences between these distantly related taxa. Like *Elephas*, *Mammuthus* belongs to the Elephantidae family and is more closely related to *Elephas* than either of them are to *Stegodon*, which belongs to the distinct family Stegodontidae (Shoshani & Tassy 2005).

Ariens (1995) found that the MCL of *Stegodon trigonocephalus* was deeper and more robust compared to that of *Mammuthus primigenius*. The results of the present study are similar to his findings. In this study, it was observed that the MCL attachment scars of *Stegodon trigonocephalus*, *Stegodon florensis* and *Stegodon sondaari* are deeper and more robust compared to *Elephas maximus* and *Elephas hysudrindicus*.

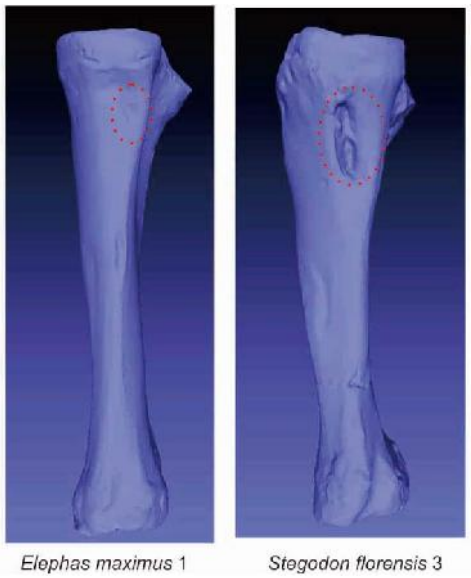

Figure 5.5. The medial collateral ligament (MCL) attachment scar (inside red dashed line).

Based on modern proboscidean phylogenetic classifications (see Figures 2.1 and 2.7), *Elephas* is more closely related to *Mammuthus* than to *Loxodonta*. This has been corroborated by DNA analysis (Rohland et al. 2010). The divergence of Stegodontidae and the lineage

leading to the Elephantidae is thought to have taken place much earlier and the oldest *Stegodon* remains from China are ~9Ma old (Saegusa, Thasod & Ratanasthien 2005). This explains the similarity in the characteristic of the MCL attachment scar of *Elephas* and *Mammuthus* and their distinctiveness from *Stegodon* in this aspect. Both *Elephas maximus* and *Elephas hysudrindicus* resemble more *Mammuthus* than *Stegodon*.

The primary function of the MCL is to act as a static stabiliser of the medial aspect of the knee. It prevents the femur and tibia from being separated on the medial side of the knee (Zhang, Brian & Wang 2015). The more robust MCL suggests that *Stegodon* had a more complex movement so that the knee joint required extra strength to prevent dislocation.

5.2.2. The Ratio Between Minimum Circumference and Total Length (T8)

The result of the ratio between the minimum circumference and total length of the tibia shows that the tibia of *Stegodon* is more robust than in *Elephas*, with the exception of *Stegodon sondaari*, which has a ratio value close to *Elephas*. Hooijer (1955) compared length/width ratios of the tibias of *Stegodon trigonocephalus* and *Elephas maximus*. He noted that the tibia of *Stegodon trigonocephalus* was more robust compared to that of *Elephas maximus*. The current study confirms Hooijer's observations. The exception is *Stegodon sondaari*, which has a ratio closer to *Elephas* than to *Stegodon*. The comparatively slender tibia of *S. sondaari* may be influenced by dwarfing and could signify a specific environmental adaptation.

5.3. Assigning Unidentified Femur and Tibia Specimens to Genus

5.3.1. Unidentified Femurs

The additional new significant morphometric parameters were applied together with existing biometric parameters in a PCA of the entire femur sample, including specimens of unknown species, in order to test the ability to assign the unknown species to a genus. The new parameters were: length of the third trochanter (F12), rotation of the femur (F13) and ratio between the minimum circumference and the total length (F14).

The PCA showed that of the seven unidentified femurs, six belong to the *Stegodon* + *Sinomastodon* group and one (the Ngandong specimen) closely aligns with *Elephas hysudrindicus*. In the PCA scatter plot, the unidentified femurs from Bekasi, Patiayam and

Sangiran share the same location with the identified *Stegodon* femurs in PC2 (see Figure 5.6). *Sinomastodon bumiajuensis* also shares the same location with *Stegodon* because almost all of the biometric values are quite similar to *Stegodon*. Only the length of its third trochanter (F12) is different (see Table 3.7 in Chapter 3). In *Stegodon*, F12 is around 19-20mm, while in *Sinomastodon bumiajuensis* it is around 26 mm, which means it is longer than in *Stegodon*. This PCA suggests clear differences, but because only one specimen of *Sinomastodon* was analysed, these findings are only considered to be a preliminary indication that both *Sinomastodon bumiajuensis* and *Stegodon* can be separated. More *Sinomastodon* femurs are required to verify this.

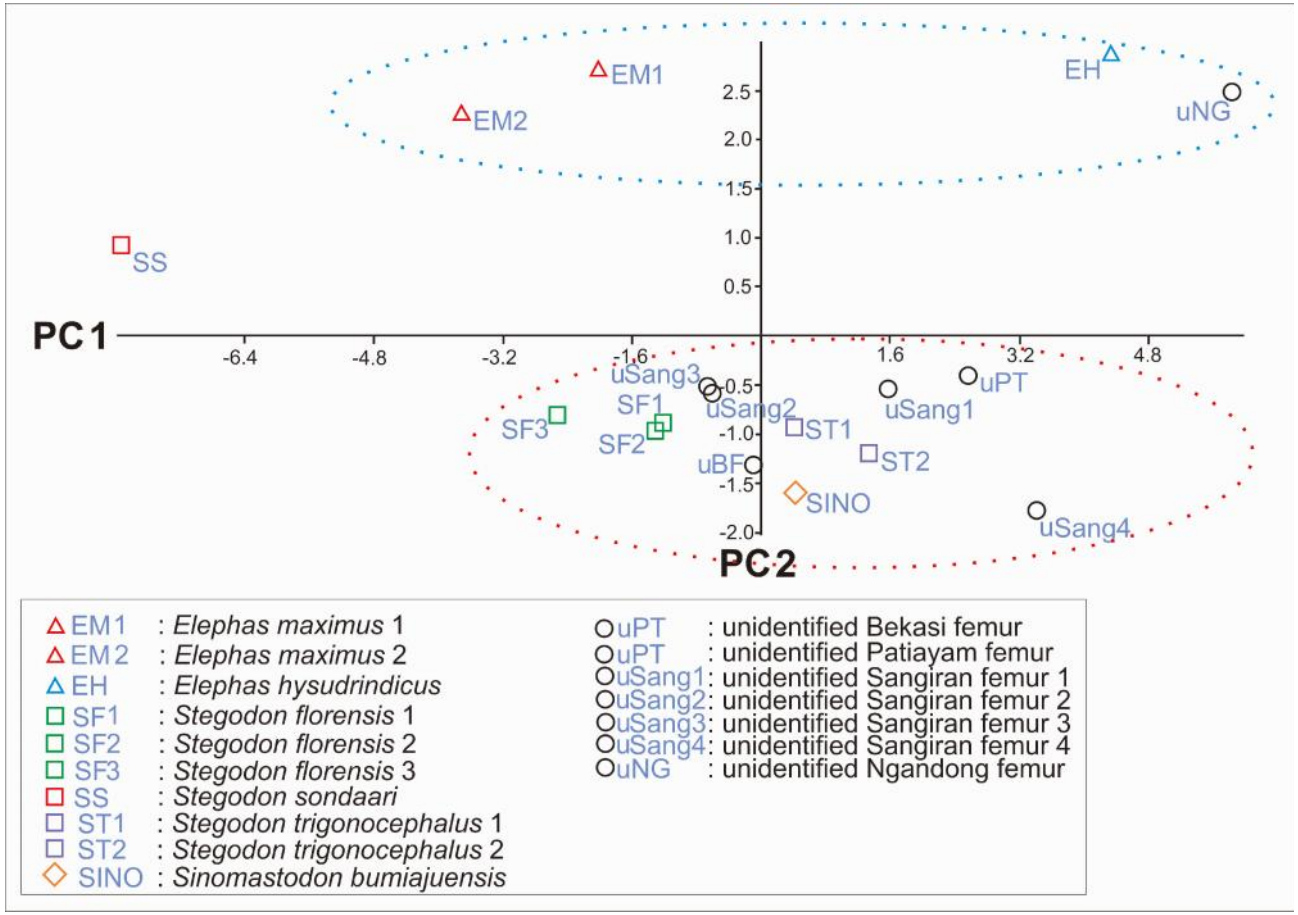

Figure 5.6. Scatterplot of PC1 and PC2 from identified and unidentified femurs with clustering by genera indicated (*Stegodon* + *Sinomastodon*: red dotted line; *Elephas*: blue dotted line). The very small-sized *S. sondaari* femur forms a separate intermediate group in PC2 between the larger *Stegodon* + *Sinomastodon* group and the *Elephas* group.

5.3.2. Unidentified Tibias

The PCA result of the analysis, for which both the identified tibias as well as the single unidentified specimen are included, supports the assumption that the length of the medial ligament attachment scar (T6) and the ratio between the minimum circumference and total length (T8) are significant enough to distinguish the genera among specimens. The minimum circumference (T7), taken separately, is not significantly distinct, but combined with T8 (the ratio between these two parameters) the result is a distinctive parameter to separate the genera from each other. The scatter plot (see Figure 5.7) shows that the Sangiran tibia-2 and the Patiayam tibia share the same location with tibias that were identified as *Stegodon* in both PC1 and PC2 (see Figure 5.8).

The unidentified tibia (uNG) that originated from the same skeleton as the Ngandong femur that belonged to *Elephas,* also show a similar pattern as the femur PCA results. Like the Ngandong femur, the Ngandong tibia also clusters with the *Elephas hysudrindicus* and *Elephas* Sangiran (ESang5) specimens, so that they can be safely attributed to the genus *Elephas*. The age of fossils from the Ngandong terrace is late Middle Pleistocene or early Late Pleistocene (Indriati et al. 2011). The clustering of the Ngandong specimens on PC1 and PC2 with the specimen from the Blora *E. hysudrindicus* skeleton, further supports this assumption.

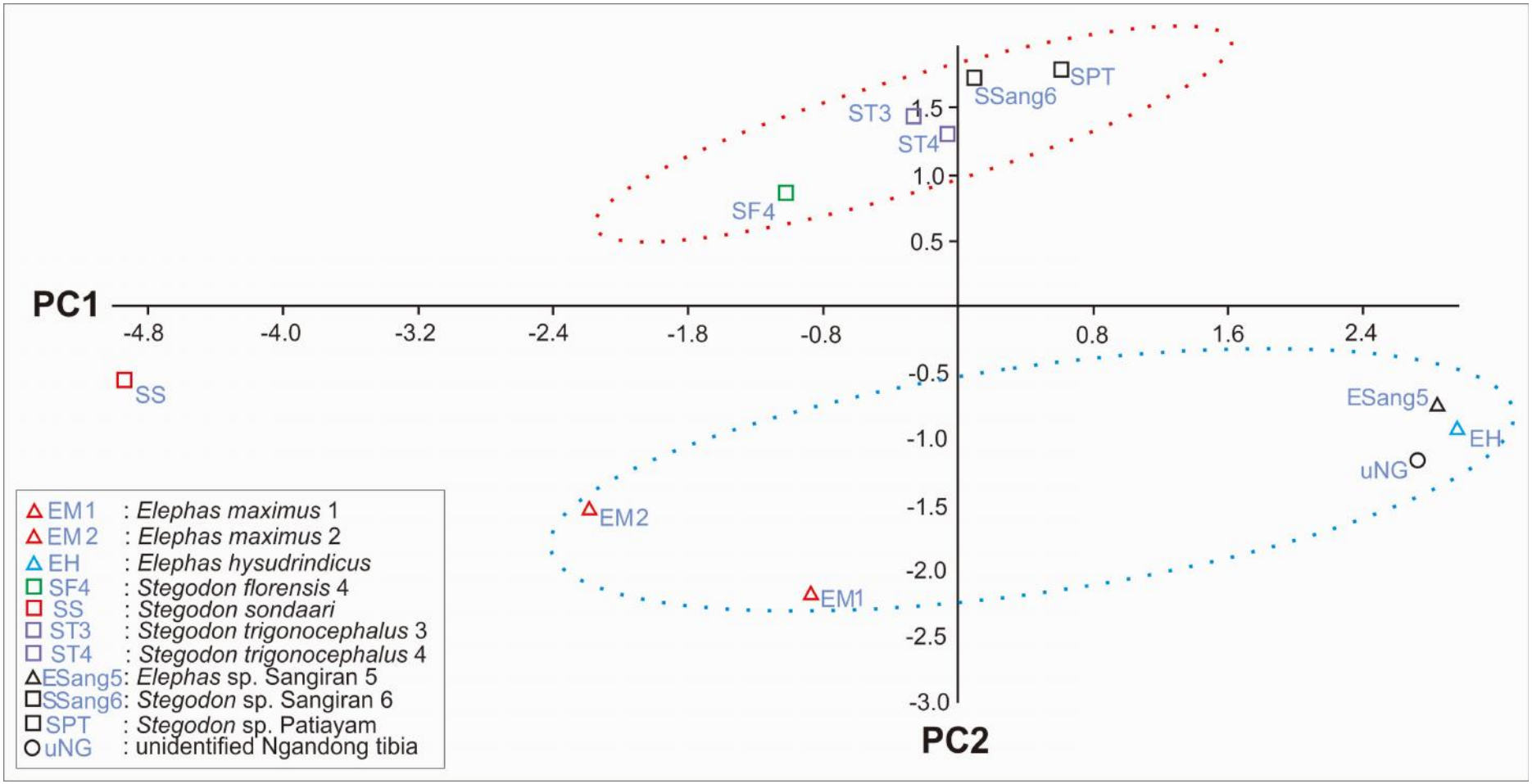

Figure 5.7. Scatterplot of PC1 and PC2 of identified and unidentified tibia with clustering by genera indicated (*Stegodon*: red dotted line; *Elephas*: blue dotted line).

5.4. Sexual Dimorphism

This study only included three specimens of which the sex is known. The recent *Elephas maximus* 1 (EM1) is male and *Elephas maximus* 2 (EM2) is female. Among the fossil specimens, only the *E. hysudrindicus* skeleton is indicated as male, based on its pelvis shape and large tusks (van den Bergh & Kurniawan 2010; also see Chapter 3.4).

So far, no distinctive characteristic has been published for determining the sex of elephants by the femur and tibia. Only size and a degree of robustness are assumed to distinguish males from females (Athanassiou 2012). The robustness grade regarding sex dimorphism should be done in full-grown adults because, at that time, the size and the shape presumably do not change. The sexual dimorphism analysis could not be investigated further because two out of the three specimens of known sex (EM1 and EM2) were not yet full-grown. A larger sample of full-grown individuals would be required for such an analysis.

5.5. Insular Dwarfism

For all kinds of Indonesian dwarf proboscideans, the conclusion of a dwarfed state is mostly based on teeth (van den Bergh et al. 2001), due to the frequent lack of post-cranial finds. Fortunately, a partial skeleton, including the mandible, one tusk, one tibia and one femur of a single *Stegodon sondaari* individual, has been excavated at Tangi Talo. This *Stegodon sondaari*'s age at death was estimated based on the wear stage of its teeth and by the fusion of the epiphyses of both its femur and tibia. All its epiphyses were already fused, so it can be inferred that this specimen represents a full-grown adult. This adult condition contrasts with its small size compared to the other large-sized adult *Stegodon* specimens. In our studied sample *Stegodon sondaari* shows an extreme dwarf size in all biometric measurements. Some researchers believe that this is because of its evolutionary adaptation for dealing with the isolated environment of an island (van den Bergh et al. 2001; Van der Geer et al. 2010; Gibson, Atkinson & Gordon 2009).

On islands, the lower limb bones of big mammals tend to become relatively shorter, in response to insular environmental selective pressures (Sondaar 1976). This characteristic was examined in the five individuals of the specimens in this study by comparing the total length

of the tibia with the total length of the femur (see Chapter 3, Table 3.12). The result of the ratio of tibia length to femur length from the five individuals showed no significant differences that would indicate that *Stegodon sondaari* had a relatively shorter tibia compared to the other species. The same result has also been found in *Palaeoloxodon falconeri,* the extreme dwarf proboscidea from Malta Island in Europe (Herridge 2010). Herridge analysed if there was a trend of shortening of hindlimbs in *Palaeoloxodon falconeri*, regarding the adaptation to an insular island, and the result also showed that this change did not occur.

However, if we look at its shape, *Stegodon sondaari*'s femur shows more bending compared to all the other *Stegodon* specimens (see Figure 5.2). So, when the tibia is articulated to the femur in life, the appearance of the hindlimb tends to be shorter due to its bending, and its hindlimb tends to be shorter with regard to its centre of gravity compared to the straight femur of *Elephas*. This may signify an adaptation of *Stegodon sondaari* to the rough terrain of Flores Island.

5.6. Locomotion Implications

Proboscideans have, in the past, encompassed an enormous diversity in shape and size, as well as adaptational differences in response to changing environments. The limbs of the Proboscidea show adaptive differences with taxonomic significance. The elephant forelimbs support the body and the hindlimbs provide both support and propulsion (Shoshani & Eisenberg 1982). Extant proboscideans differ markedly from other large mammals in that their limbs are kept near columnar during all forms of locomotion as an adaptation to dealing with their heavy body mass (Christiansen 2007). Another adaptation for keeping a near columnar position during locomotion is that the pelvic girdle is attached directly and fused to the sacral region of the vertebral column. Consequently, the waist region is more rigid.

The results of the surface morphology assessment, biometric measurement analyses and GM analysis show that there are differences in the hindlimb long bone morphology of *Elephas* compared to *Stegodon* and *Sinomastodon,* and especially with *Stegodon sondaari*. The *Stegodon* femur has characteristics which can be distinguished from *Elephas*. *Stegodon* has a robust femur characterised by a larger third trochanter, and a great trochanter and lesser trochanter that are more laterally extended compared to *Elephas*, but which have a lower value in femur angle rotation, with the exception of *Stegodon sondaari*, which has an angle of

rotation that is even larger than in all *Elephas* specimens investigated. In *Stegodon*, the tibia is also characterised by being more robust, and with a greater medial collateral ligament attachment scar.

The two main muscles that function to support the loading of body mass and have influence on the coordination of the stride of vertebrates, are the GMX muscle and the TFL muscle (see Figure 5.8) (Milne & O'Higgins 2012; Shindo & Mori 1956). The GM is a large muscle of the buttock that connects the third trochanter of the femur to the ischium of the pelvis. The TFL is a thick and strong muscle that arises from the outer surface of the anterior spine of the ilium. The TFL connects the third trochanter to the ilium of the pelvis (see Figure 5.9). The TFL is the hip adductor that has the function of moving the hip forward, whereas the GM is the hip retractor that has the opposite function to the TFL, namely to move the hip backward.

This study found that the length of the third trochanter and the rotation angle of the femur, and the medial collateral ligament attachment scar of the tibia, represent important morphological differences that can be used to distinguish between genera. The length of the femur third trochanter in *Stegodon* and *Sinomastodon* are more robust than in *Elephas*. The wide angle of femur rotation in *Elephas* and *Stegodon sondaari* is greater than in *Stegodon* and *Sinomastodon*. The attachment scar of the medial collateral ligament of the tibia of *Stegodon* is more robust than in *Elephas*.

Elephas has a more advanced femur shape with its third trochanter not flaring outwards and with a proximal termination located more distally when compared to *Stegodon* and *Sinomastodon*. As discussed previously, a less flaring femur makes the lateral distal muscle attach closer to the centre of hip rotation and makes the energy used in locomotion more efficient. Distally inserted muscles use less energy and provide a more economical design for moving limb segments during locomotion (Milne & O'Higgins 2012; Kardong 2012). The different position of the insertion of the muscles to the third trochanter also has the effect of "unbending" the femur (Milne & O'Higgins 2012). The more distal the insertion of the muscles, the more unbending or stiff the femur becomes. This unbending femur is an adaptation of proboscideans for dealing with their heavy body mass to maintain effective energy during locomotion (Kokshenev & Christiansen 2010). All these features likely have had an influence on their locomotion function, as discussed previously. *Elephas* appears more

advanced with a more energy efficient locomotion when compared to *Stegodon* and *Sinomastodon*.

Elephants can walk, run and swim, but they don't trot, gallop or jump. Elephants cannot trot or gallop because of the almost vertical orientation of the bones of the limbs that are like columns/pillars (Shil et al. 2013). Elephant limbs are the archetype for columnar limb design. They have a more columnar/straighter hindlimb to avoid large muscular stress, and *Elephas* seems to have a more effective and energy efficient type of locomotion compared to *Stegodon* and *Sinomastodon*.

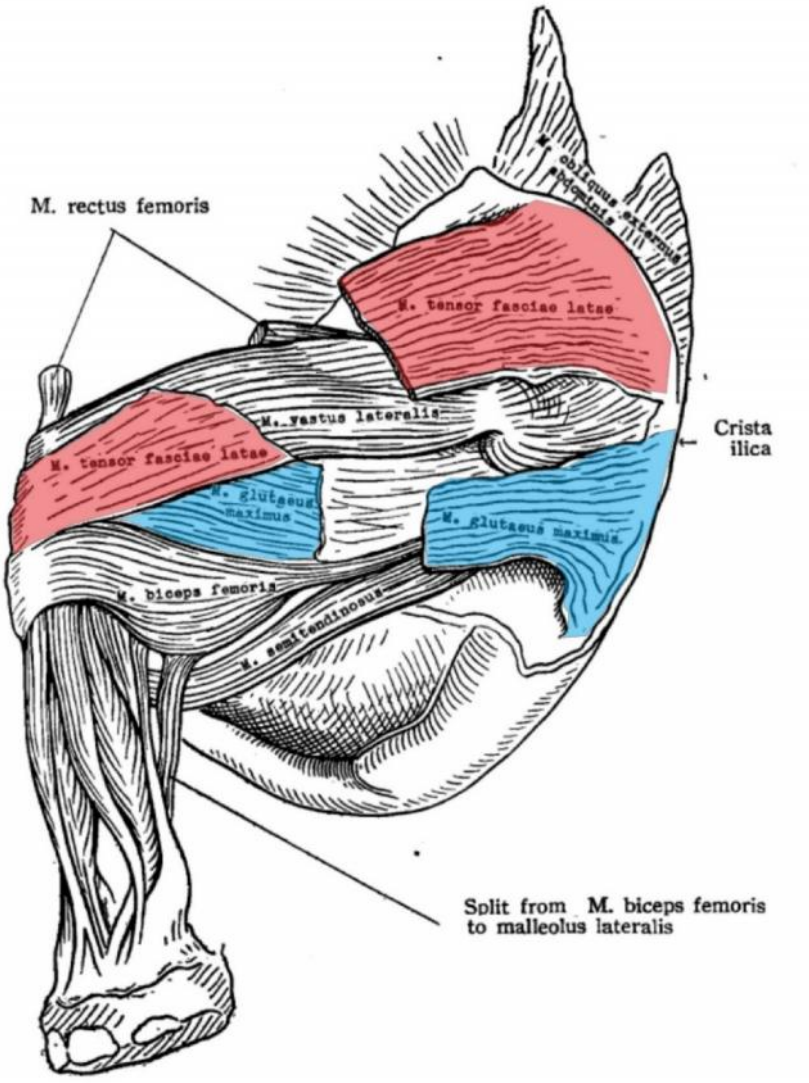

Figure 5.8. The position of the gluteus maximus (GMX) muscle and the tensor fasciae latae (TFL) muscle of the proboscidean thigh (modified from Shindo and Mori, 1956).

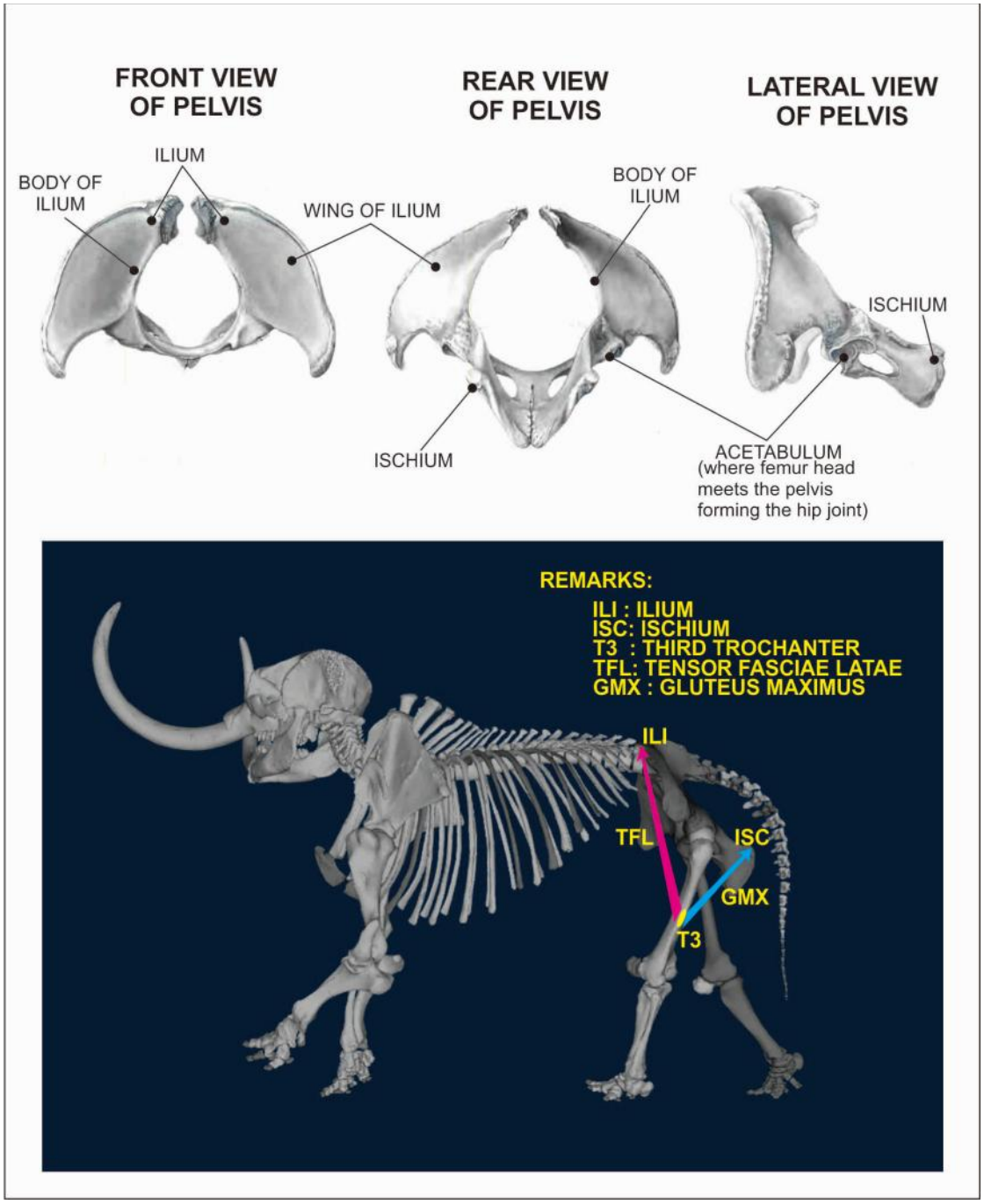

Figure 5.9. Simplification of the main muscle attachments of the GM muscle and the TFL muscle that connects the third trochanter of the femur with the pelvis. The pelvis figures are from Smuts and Bezuidenhout (1994). The proboscidean skeleton (a *Mastodon americanum* skeleton) has been taken from Museum of Paleontology University of Michigan (2014). The scheme of the main muscles that connect the third trochanter with the pelvis has been adapted from Milne and O'Higgins (2012).

5.7. Ancestry Aspect

When proboscidea share a common ancestry, the inherited locomotion type is also shared. This common elephantid pattern of locomotion provides a model from which evolution develops within proboscidea (Hutchinson et al. 2006). Regarding the object of this study, the movement pattern can be analysed by the hindlimb bone characteristics (femur and tibia), such as shape and muscle attachments. When the aim is to link morphological features to reconstruct ancestry aspects, we need to compare proboscidea in the terms of their hindlimb homology.

Fossils of the Asian elephant, *Elephas maximus*, share the same chronological age range as the woolly mammoth, *Mammuthus primigenius*, which lived in northern high latitudes and became extinct during the last glacial maximum (Osborn 1942). In the cladistic's framework, the family, Elephantidae, to which the woolly mammoth, Asian elephant and African elephant belong, all have a shared single ancestor (Thomas et al. 2000). The Asian elephant is more closely related to the extinct mammoth than to the African elephant (Shoshani 2002), which is supported by DNA research (Krause et al. 2006).

Ariens (1995) compared skeletal elements of *Stegodon trigonocephalus* with these of *Mammuthus primigenius*. The results showed that *Stegodon trigonocephalus* is more robust than *Mammuthus primigenius*. When Ariens' results were compared to the present study, the *Mammuthus primigenius* femur shape closely resembles *Elephas*. *Mammuthus primigenius* has a femur that is more columnar (Ariens 1995), similar to the *Elephas* specimens examined in this study. The position and shape of the third trochanter on its femur is also quite similar, in that the third trochanter is located more distally (see Table 5.1 and Figure 5.10).

a: *Mammuthus primigenius* / Wolly Mammoth (Alvarez-Lao et al, 2005)
b: *Elephas hysudrindicus* (EH) - in this study
c: *Elephas maximus* 1 (Em1) - in this study
d: *Stegodon florensis* 3 (Sf3) - in this study
e: *Stegodon sondaari* (SS) - in this study
f: *Stegodon trigonochepalus* 2 (St2) - in this study
g: *Sinomastodon bumiajuensis* (SINO) - in this study
h: *Mammut americanum* / American Mastodon (Hodgson et al, 2008)

Scale= 10cm

Figure 5.10. Femurs analysed in this study compared to the femurs of other proboscideans to see the similarity in the context of ancestry. The figure of *Mammuthus primigenius* was taken from Álvarez-Laó et al. (2005) and *Mammut americanum* was taken from Hodgson et al. (2008). All specimens are shown to the same scale.

Table 5.1. Comparison of femurs of genera investigated during this study with femurs of *Mammuthus primigenius* and *Mammut americanum.*

No	Observation points	*Elephas maximus*	*Elephas hysudrindicus*	*Stegodon trigonocephalus*	*Stegodon florensis*	*Stegodon sondaari*	*Sinomastodon bumiajuensis*	Woolly mammoth *Mammuthus primigenius**	American Mastodon *Mammut americanum#*
1	Opening between medial and lateral condyle	Wide	Wide	Narrow	Narrow	Narrow	Narrow	Wide	Wide
2	Indentation between the condyles	Narrow, shallow	Narrow, shallow	Wide, deep	Wide, deep	Wide, deep	Wide, deep	Narrow, shallow	Wide, deep
3	Lateral minimum diaphysis	Straight	Straight	Indented	Indented	Indented	Indented	Straight	Indented
4	Medial crest / minor trochanter	Weak	Weak	Strong	Strong	Very strong	Strong	Weak	Strong
5	Third trochanter	Weak, short	Weak, short	Strong, long	Strong, long	Very strong, long	Strong, long	Weak, short	Strong, long
6	Lateral most point on the greater trochanter	Very distal	Very distal	Proximal	Proximal	Proximal	Very proximal	Very distal	Proximal

Table 5.2. Comparison of tibias of genera investigated during this study with those of *Mammuthus primigenius* and *Mammut americanum.*

No	Observation points	*Elephas maximus*	*Elephas hysudrindicus*	*Stegodon trigonocephalus*	*Stegodon florensis*	*Stegodon sondaari*	Woolly mammoth *Mammuthus primigenius**	American Mastodon *Mammut americanum#*
1	Tuberculum intercondylare mediale	Small	Small	Big	Big	Big	Small	Small
2	Tibia anterior border crest	Short	Short	Long	Long	Long	Short	Long
3	Medial collateral ligament attachment scar	Small, shallow, smooth	Small, shallow, smooth	Long, deep, robust	Long, deep, robust	Long, deep, robust	Small, shallow, smooth	Long, shallow, robust
4	Lateral view length appearance	Slim	Slim	Robust	Robust	Robust	Slim	Robust
5	Distal articular surface	Relatively flat	Relatively flat	Relatively high relief	Relatively high relief	Relatively high relief	Relatively flat	Relatively high relief

*Data taken from Ariens (1995)

#Data from the observation of the 3D file from Museum of Paleontology University of Michigan (2014)

The tibia of *Elephas* has similar characteristics to those of *Mammuthus primigenius*. The MCL attachment scar of the tibia of *Elephas* has similar characteristics to those of *Mammuthus primigenius*, and both are characterised by a shallow MCL attachment scar (see Table 5.2).

When comparing the American Mastodon to the specimens of this study (see Figure 5.10), some features of its femur are quite similar to the femurs of *Stegodon* and *Sinomastodon* from Indonesia. All three have the third trochanter relatively proximal compared to the third trochanter in *Elephas*, and all have a slightly bent shaft compared to *Elephas* and the woolly mammoth. This suggests that the American *Mastodon*, *Stegodon* and *Sinomastodon* shared the more robust, sturdy limb bones of an archaic common ancestry, whereas *Elephas* and the woolly mammoth share a more advanced common ancestor that has more slender limb bones (see Figure 5.10).

This corroborates other cladistic studies that indicate that *Elephas* is more closely related to the *Mammuthus primigenius*/woolly mammoth compared to *Stegodon* and *Sinomastodon*. Based on the proboscidean's family tree, *Sinomastodon* is the most archaic proboscidean among the studied specimens that lived in Java during the early Pleistocene periods. In Java, *Sinomastodon* is succeeded by *Stegodon*, which ranged from the Early to Late Pleistocene. *Stegodon* partly overlaps with *Elephas hysudrindicus* (Hooijer 1955). Following the extinction of *Stegodon* in Java, only the modern species, *Elephas maximus*, survived and is still extant in Sumatra at present (see Figure 5.11).

5.8. Summary

This study indicates that the femur of *Stegodon-Sinomastodon* can be distinguished from *Elephas* based on its robustness and on the shape and position of its muscles attachments (e.g., the third trochanter). Similarly, the tibia of *Stegodon* is more robust than in *Elephas*. Based on these characteristics, in almost all unidentified specimens, either the femur or tibia, could be assigned to *Stegodon*. Only Ngandong specimens could be assigned to *Elephas*.

The results of this study also reveal that the combination of the femur rotation angle, and the different bone shapes and muscle attachments of the femur and tibia, suggest that there are differences in locomotion function between *Stegodon* and *Elephas*. The *Elephas* hindlimb is

designed to limit its movement and reduce energy consumption, while the *Stegodon* hindlimb is designed for strength in its locomotion. This characteristic seems to be an inherited character in elephantoid and stegodontid ancestries, and supports classification of *Elephas* and *Stegodon* into distinct subfamilies, the Elephantidae and the Stegodontodae.

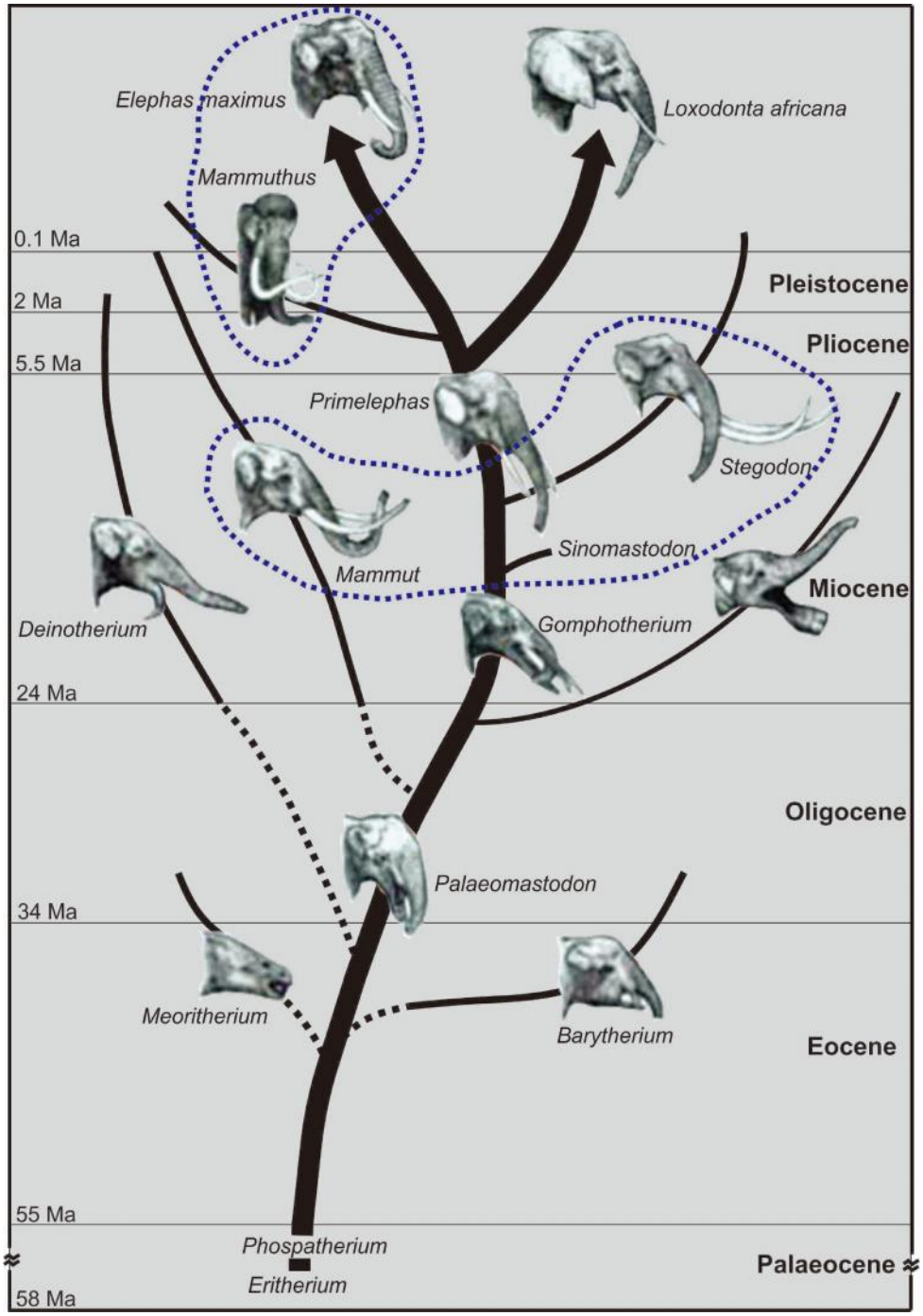

Figure 5.11. The proboscidean phylogenetic tree of proboscidean genera closely related groups based on femur and tibia morphology are encircled by blue dotted lines (figure modified from Shoshani, 2002).

Conclusions and Recommendations

The application of surface morphology assessment, biometric measurements and Geometric Morphometrics (GM) was combined to investigate differences in the shape of the femur and tibia of Indonesian proboscidea. This study shows that the femur and tibia of the genera *Elephas* and *Stegodon + Sinomastodon* can be distinguished from each other based on PCA on biometric variables that take into account these distinctive morphological characters.

GM was most effective in revealing additional shape differences of the femur and tibia that were not detected by Principal Component Analysis (PCA) on ordinary biometric measurements. For example, the length and curve of the femur third trochanter, the femur shaft rotation, and the ratio between total length and Minimum Circumference of the diaphysis (both for femur and tibia) were found to represent distinctive characteristics that are able to separate *Stegodon* from *Elephas*. These newly found distinctive features were translated into a new set of biometric parameters. The new variables are: the length of the third trochanter of femur (F12), the rotation of femur (F13), the ratio between the minimum circumference and total length of femur (F14), the length of the medial collateral ligament attachment scar on the proximal tibia (T6), the minimum circumference of the tibia diaphysis (T7) and the ratio between the minimum circumference and total length of the tibia (T8). When a PCA is applied using this new set of variables, the specimens cluster significantly according to genus in PC2, while PC1 predominantly separating specimens according to size (which is an important species-distinctive character). Using this new set of variables, isolated femur and tibia specimens of unknown identity could now be identified. Because only one *Sinomastodon* femur (and no tibia) was available for comparison, distinction from *Stegodon* was not significant, but significance may be reached with the availability of more *Sinomastodon* fossil material.

The main morphological differences between *Elephas* and *Stegodon* are that *Elephas* has more columnar and gracile hindlimb bones compared to *Stegodon*, and its femur shaft is more rotated. These differences are probably related to a more rigid but more energy efficient type of locomotion in *Elephas*. The combination of the surface morphology assessment, biometric measurements and GM analyses enhances our understanding of the differences in shape and function of proboscidean hindlimb bones, and provides us with more detail as compared to

classic biometric assessments only. In the future, a GM analysis and quantification of the other bones of the appendicular skeleton can provide a more complete picture of the morphological differences and adaptations in locomotion of proboscidea.

REFERENCES

Agenbroad, LD 2003, 'New absolute dates and comparisons for California's Mammuthus exilis', *the Second International Mammoth Conference: proceedings of a conference,* Roterdam, pp. 1-16.

Alexander, R, Jayes, A, Maloiy, G & Watuta, E 1979, 'Allometry of the limb bones of mammals from shrews (Sorex) to elephant (Loxodonta)', *Journal of Zoology*, vol. 189**,** pp. 305-314.

Álvarez-Laó, D, García, N, Mol, D & Martín, E 2005, 'A southern find of woolly mammoth at the El Padul site (Granada, South Spain)', *the Second World of Elephants Congress: proceedings of a conference*, Hot Springs, USA, vol.2 , pp. 6-8.

Andrews, CW 1904, 'Further notes on the mammals of the Eocene of Egypt. Part I', *The Geological Magazine,* vol. I, pp. 109-115.

Andrews, CW 1906, *A descriptive catalogue of the Tertiery vertebrate of the fayum, Egypt. Based on the collection in the British museum (Natural history), London,* British Museum, London.

Ariens, CM 1995, *Vergelijkend morfologisch onderzoek van postcraniale skeletdelen van Stegodon trigonocephalus en Mamuthus primigenius,* Nationaal Natuurhistorich Museum, Leiden.

Athanassiou, A 2012, 'A skeleton of *Mammuthus trogontherii* (Proboscidea, Elephantidae) from NW Peloponnese', *Quaternary International*, vol. *255*, pp. 9-28.

Audley-Charles, MG & Hooijer, DA 1973, 'Relation of Pleistocene migrations of pygmy stegodonts to island arc tectonics in eastern Indonesia', *Nature,* vol. 241, pp. 197-198.

Aziz, F & Morwood, M 2009, '1. Introduction: geology, palaeontology and archaeology of the Soa Basin, central Flores, Indonesia', in Aziz, F, Morwood M & van den Bergh, G (Eds.), *Pleistocene Geology, Palaeontology and Archaeology of the Soa Basin, Central Flores, Indonesia*, Pusat Survei Geologi, Badan Geologi, Bandung, Special Publication, pp. 1-18.

Aziz, F, Sondaar, PY, de Vos, J, van den Bergh, GD & Sujijono 1995, 'Early Dispersal of Man on Islands of Indonesian Archipelago: Facts and Controls', *Anthropological Science*,vol. 103(4), pp. 349-368.

Baigusheva, V & Titov, V 2010, 'The evolution of Eastern European meridionaloid elephants', *Quaternaire hors-série,* vol.3, pp. 13-16.

Bonnan, M 2001, The evolution and functional morphology of sauropod dinosaur locomotion, Phd thesis, Northern Illinois University.

Bonnan, M 2004, 'Morphometric analysis of humerus and femur shape in Morrison sauropods: implications for functional morphology and paleobiology', *Paleobiology*, vol. 30, pp. 444-470.

Bonneau, N, Libourel, P, Simonis, C, Puymerail, L, Baylac, M, Tardieu, C, Gagey, O 2012, 'A three-dimensional axis for the study of femoral neck orientation', *J. Anat*, vol. 221, pp. 465-476.

Brill, E 1935, *Koninklijk nederlandsch aardrijkskundig genootschap*, Tweede Serie Deel LII.

Brumm, A, van den Bergh, G, Storey, M, Kurniawan, I, Alloway, B, Setiawan, R, Setiyabudi, E, Grun, R, Moore, MW, Yurnaldi, D, Puspaningrum, MR, Wibowo, UP, Insani, H, Sutisna, I, Westgate, JA, Pearce, NJG, Duval, M, Meijer, HJM, Aziz, F, Sutikna, T, van der Kaars, S, Flude, S, Morwood, MJ 2016, 'Age and context of the oldest known hominin fossils from Flores', *Nature,* vol. 534, pp. 249-253.

Campione, NE & Evans, DC 2012, 'A universal scaling relationship between body mass and proximal limb bone dimensions in quadrupedal terrestrial tetrapods', *Bmc Biology*, vol.10, pp. 1.

Christiansen, P 2004, 'Body size in proboscideans, with notes on elephant metabolism', *Zoological Journal of the Linnean Society,* vol. 140**,** pp. 523-549.

Christiansen, P 2007, 'Long-bone geometry in columnar-limbed animals: allometry of the proboscidean appendicular skeleton', *Zoological Journal of the Linnean Society*, vol. 149, pp. 423–436.

Curray, J 2003, 'The many adaptations of bone', *Journal of biomechanics,* vol.36, pp.1487-1495.

Darlington, P 1957, *Zoogeography: the GeographicalDistribution of Animals,* J. John Wiley & Sons, Inc, New York.

de Vos, J 1997, 'Faunal Turnovers in Java In Relation to Faunas of the Continent. Association for Comparative Odontology', *Odontology,* Japan, vol. 1.

de Vos, J & Aziz, F 1989, 'The excavation by Dubois (1891-1900), Selenka (1906-1908), and the Geological Survey by the Indonesian-Japanese Team (1976-1977) at Trinil (Java, Indonesia)', *Journal of the Anthropological Society of Nippon,* vol. *97*(3), pp. 407-420.

de Vos, J & Sondaar, P 1982, 'The importance of the Dubois Collection reconsidered', *MQRSEA,* vol. 7.

Dubrovo, I 1977, 'A history of elephants of the ArchidiskodoneMammuthus phylogenetic line in the territory of the USSR', *Journal of the Palaeontological Society of India,* vol. 20, pp. 33-40.

Ferretti, MP 2003,'Structure and evolution of mammoth molar enamel', *Acta Palaeontologica Polonica*, vol. 48 (3), pp. 383-396.

Ferretti, M & Croiter, R 2001, 'Functional morphology and ecology of Villafranchian Proboscideans from Central Italy', *the World of Elephant International Congress: proceedings of a conference,* Rome, pp.103-108.

Fiedel, S 2009,'Sudden deaths, the chronology of terminal Pleistocene megafaunal extinction', In Haynes, G (Eds.), *American Megafaunal extinctions at the end of the Pleistocene*, Springer Netherlands, pp. 21-37.

Figueirido, B & Janis, CM 2011, 'The predatory behaviour of the thylacine: Tasmanian tiger or marsupial wolf?', *Biology Letters,* vol.7, pp.937-940.

Finlay, S & Cooper, N 2015, 'Morphological diversity in tenrecs (Afrosoricida, Tenrecidae): comparing tenrec skull diversity to their closest relatives', *PeerJ,* vol.3, pp.1-18.

Frelat, MA, Katina, S, Weber, GW & Bookstein, FL 2012, 'Technical note: a novel geometric morphometric approach to the study of long bone shape variation', *American Journal of Physical anthropology*, vol.149, pp.623-638.

Gaeth, A, Short, R & Renfree, M 1999, 'The developing renal,reproductive, and respiratory systems of the African elephant suggest an aquatic ancestry', *Proceedings of the National Academy of Science*, USA, vol. 96, pp. 5555-5558.

Gheerbrant, E 2009, 'Paleocene emergence of elephant relatives and the rapid radiation of African ungulates', *Proceedings of the National Academy of Sciences,*USA, vol. 106(26), pp.10717-10721.

Gheerbrant, E, Sudre, J & Cappetta, H 1996, 'A Paleocene proboscidean from Morocco', *Nature*, vol. 383(6595), pp.68-70.

Gheerbrant, E, Sudre, J, Cappetta, H, Iaroch"ene, M, Amaghzaz, M & Bouya, B 2002, 'A new large mammal from the Ypresian of Morocco: evidence of surprising diversity of early proboscideans', *Acta Palaeontologica Polonica,* vol.47(3), pp.493-506.

Gibbons, J & Clunie, F 1986, 'Sea level changes and pacific prehistory', *Journal of Pacific History,* vol.21, pp.58-82.

Gibson, RN, Atkinson, RJA & Gordon, JD 2009, *Oceanography and Marine Biology: An Annual Review,* CRC press. US.

Glover, I & Glover, E 1970, 'Pleistocene flaked stone tools from Timor and Flores', *Mankind*, vol.7, pp. 188-190.
Gohlich, U 1999, 'Order Proboscidea', *In: Rössner, G & Heissig, K (Eds.), The Miocene Land Mammals of Europe.* Pfeil, Munich, pp. 157–168.
Gordon, S 2006, *The Normal Distribution*, Mathematics Learning Centre, University of Sydney.
Gregory, WK 1912, 'Notes on the principles of quadrupedal locomotion and the mechanisms of the limbs in hoofed animals', *Ann. N. Y. Acad. Sci.*, vol.22, pp.267-292.
Hammer, O, & Harper, D 2006, *Paleontological Data Analysis*, Blackwell Publishing Ltd.
Hammer, Ø, Harper, DAT & Ryan, PD 2001, 'Past: Paleontological Statistics Software Package for Education and Data Analysis', *Palaeontologia Electronica*, vol. 4, pp.1-9.
Hammond, L & Kenchington, R 1978, 'A biometric case for revision of the genus Lingula (Brachiopoda: Inarticulata) from Queensland, Australia', *Journal of Zoology*, vol.184(1), pp.53-62.
Harmon, E 2007, 'The shape of the hominoid proximal femur: a geometric morphometric analyses', *J. Anat.*, vol.210**,** pp.170-185.
Han, M., Zhang, Y & Shan, T 2014, 'Femoral offset and its relationship to femoral neck-shaft angle and torsion angle', *Int. J. Morphol.*, vol.32(4), pp.1194-1198.
Hayes, S 2009, Seeing and Measuring the 2D Face, PhD thesis, University of Western Australia, Perth.
Haynes, G 1991, *Mammoths, Mastodonts and Elephants: Biology, Behavior and the Fossil Record*, Cambridge University Press, New York.
Herridge, V, 2010, Dwarf elephants on Mediterranean islands: A natural experiment in parallel evolution, PhD thesis, University College, London.
Hildebrand, M 1985, *Walking and running. In "Functional Vertebrate Morphology*, Harvard University Press, Cambridge.
Hildebrand, M 1995, *Analysis of Vertebrate Structure* (Vol. 4th Edition.), John Wiley and Sons Inc.
Hodgson, JA, Allmon, WD, Nester, PL, Sherpa, JM & Chiment, JJ 2008, 'Comparative osteology of late Pleistocene mammoth and mastodon remains from the Watkins Glen site, Chemung County, New York', *In (eds.) Mastodon Paleobiology, taphonomy, and paleoenvironment in the late Pleistocene of New York State: Studies on the Hyde Park, Chemung, and North Java Sites*, Palaeontographica Americana, vol.61, pp.301-367.
Hooijer, D 1955, 'Fossil Proboscidea from Malay Archipelago and the Punjab', *Zoologische Verhandelingen*, Leiden, vol.28, pp.163.
Hooijer, D 1964, 'Pleistocene vertebrates from Celebes: XII. Notes on pygmy stegodonts', *Zoologische Mededelingen*, vol.40(7), pp.37-44.
Hooijer, D 1974, 'Elephas celebensis (Hooijer) from the Pleistocene of Java', *Zoologische Mededelingen*, vol.48, pp.85-95.
Hooijer, D 1975, 'Quaternary mammals west and east of Wallace's Line', *MQRSEA*, vol.1, pp.37-46.
Hooijer, D 1980, 'Remarks upon the dentition and tooth replacement in elephants', *Netherland Journal Of Zoology*, vol.30(3), pp.510-515.
Hutchinson, J, Schwerda, D, Famini, D, Dale, R, Fischer, M & Kram, R 2006, 'The locomotor kinematics ofd Asian and African elephants: changes with speed and size', *The Journal of Experimental Biology*, vol.209, pp.3812-3827.
International Elephant Foundation 2014, *How are African and Asian elephants alike and different?* Available from: http://elephantconservation.org/downloads/Lessons/LessonOne.pdf. [10 October 2014].

Jachmann, H 1988, 'Estimating age in African elephants: a revision of Laws' molar evaluation technique', *Afr. J. Ecol*, vol.26, pp.51-56.

Jackson, DA 1993, 'Stopping rules in principal components analysis: a comparison of heuristical and statistical approaches', *Ecology*, vol.74, pp.2204-2214.

Janis, C 1988, 'New ideas in ungulate phylogeny and evolution', *Trends in Ecology and Evolution*, vol.3(11), pp.291–297.

Jolliffe, I 2002, *Principal Component Analysis* (Vol. Second Edition), Springer, USA.

Kardong, K 2012, *Vertebrates: Comparative Anatomy, function, evolution* (Vol. Six editon), McGraw-Hill, New York, USA.

Koneval, T 2003, Comparative hindlimb anatomy andfossoriality of three armadillos: Dasypus novemcinctus,Tolypeutes matacus, and Chaetophractus vellerosus (Mammalia, Xenarthra Cingulata, Dasypodidae), PhD thesis, University of Massachusetts, US.

Kokshenev, V & Christiansen 2010, 'Salient features in the locomotion of proboscideans revealed via the differential scaling of limb long bones', *Biological Journal of the Linnean Society*, vol.100, pp.16-29.

Krause, J, Dear, PH, Pollack, JL, Slatkin, M, Spriggs, H, Barnes, I, Lister, AM, Ebersberger, I, Paabo, S & Hofreiter, M 2006, 'Multiplex amplification of the mammoth mitochondrial genome and the evolution of Elephantidae', *Nature*, vol.439**,** pp.724-727.

Kretzoi, M 1950, 'Stegoloxodon nov. gen., a loxodonta elefántok esetleges ázsiai öse (Stegoloxodon nov. gen., a possible Asiatic ancestor of true loxodonts)', *Földtani Közlöny*, vol.80, pp.405-408.

Larramendi, A 2016, 'Shoulder height, body mass and shape of proboscideans', *Acta Palaeontologica Polonica*, vol. 61(3), pp.537-574.

Larramendi, A & Palombo, MR 2015,'Body size, biology and encephalization quotient of *Paleoloxodon* ex gr. *P. falconeri* from Spinagallo Cave (Hyblean plateu, Sicily)', *Hystrix, the Italian Journal of Mammalogy*, vol. 26(2), pp. 102-109.

Laursen, L & Bekoff, M 1978, 'Loxodonta Africana', *Mammalian Species*, vol.92, pp.1-8.

Lee, P, Sayialel, S, Lindsay, W & Moss, C 2011, 'African elephant age determination from teeth: validation from known individuals', *African Journal of Ecology*, vol.50, pp.9-20.

Leinders, J, Aziz, F, Sondaar, P & Devos, J 1985, 'The Age of the Hominid-bearing Deposits of Java-state of the Art', *Geologie en Mijnbouw*, vol.64(2), pp.167-173.

Linnaeus, C 1758, *Systema naturae per regna tria naturae, secundum classes, ordines, genera, species, cum characteribus, differentiis synonymis, locis. Regum animale. Class 1, Mammalia. Tenth edition* (Vol. 1), Laurentii Salvii, Stockholm, Sweden.

Lister, A 1996, 'Sexual dimorphism in the mammoth pelvis: an aid to gender determination', In Shoshani J & Tassy P (Eds.), *The Proboscidea: Evolution and Palaeoecology of Elephants and Their Relatives*, Oxford Science Publications, Oxford Univ. Press, pp. 254-259.

Mahboubi, M, Ameur, R, Crochet, J & Jaeger, J 1986, 'El Kohol (Saharan Atlas, Algeria): A new Eocene mammals locality in North Western Africa', *Palaeontographica*, vol.192(1-3), pp.15-49.

Maringer, J & Verhoeven, T 1975, 'Die Oberflächenfunde von Marokoak auf Flores, Indonesien. Ein weiterer altpaläolithischer Fundkomplex von Flores', *Anthropos*, vol.70, pp.97-104.

Markov, G & Saegusa, H 2008, 'On the validity of Stegoloxodon Kretzoi, 1950 (Mammalia: Proboscidea)', *Zootaxa*, vol.1861, pp. 55-56.

Martin, K 1884, *Ueberreste vorweltlicher Proboscidier von Java und Bangka*, Jaarb. Mijnw. Ned. Indië, vol.1884, pp.285-308

Martin, K 1887, *Fossiele Saugethierreste von Java und Japan*, Sammlungen des Geologischen Reichs-Museums, Leiden, vol.4(1884–1889), pp.1–24.

Matheus, PE 2003, *Locomotor adaptations and ecomorphology of short-faced bears (Arctodus simus) in eastern Beringia*, Yukon Palaeontology Program, Dept. of Tourism and Culture, Whitehorse, Yukon, Canada.

Matsumoto, H 1923, 'A contribution to the knowledge of Moeritherium', *Bulletin of the American Museum of Natural History*, vol.48, pp.97-140.

Medway, L 1979, 'The Niah excavations and an assessment of the impact of early man on the mammals of Borneo', *Asian Perspectives*, vol.20(1), pp. 51–69.

Miall, L & Greenwood, F 1878, *Anatomy of the Indian Elephant*, Macmillan and Co, London.

Milne, N & O'Higgins, P 2012, 'Scaling of form and function in the xenarthran femur: a 100-fold increase in body mass is mitigated by repositioning of the third trochunter', *The Royal Society Interface*, vol. 279(1742), pp. 3449-3456.

Mothe, D, Avilla, LS & Cozzuol, MA 2012,'The South American Gomphotheres (Mammalia, Proboscidea, Gomphotheriidae): Taxonomy, Phylogeny, and Biogeography', *Journal of Mammalian Evolution*, vol. 20(1), pp. 23-32.

Mosley, J, March, B, Lynch, J & Lanyon, L 1997, 'Strain magnitude related changes in whole bone architecture in growing rats', *Bone Joint Res.*, vol.20, pp.191-198.

Museum of Paleontology University of Michigan 2014, *Mammutidae*. Available from: https://umorf.ummp.lsa.umich.edu/wp/mammutidae2/. [12 October 2014].

Nilsson, O & Baron, J 2004, 'Fundamental limits on longitudinal bone growth: growth plate senescence and epiphyseal fusion', *Trends in Endocrinology and Metabolism*, vol.15, pp.370–374.

O'Higgins and Jones (2006). *Tools for statistical shape analysis*. Hull York Medical School. Available from: http://sites.google.com/site/hymsfme/resources. [6 August 2015].

O'Higgins, P 2000, 'The study of morphological variation in the hominid fossil record: biology, landmarks and geometry', *Journal of Anatomy*, vol.197(01), pp. 103-120.

Osborn, H 1936, Proboscidea: A monograph of the discovery, evolution, migration and extinction of the mastodonts and elephants of the world. Moeritherioidea, Deinotherioidea, Mastodontoidea, *The American Museum of Natural History*, vol.1, pp.1-804.

Osborn, H 1942, Proboscidea: A monograph of the discovery, evolution, migration and extinction of the mastodonts and elephants of the world. Stegodontoidea, Elephantoidea, *The American Museum of Natural History*, vol.2, pp.805-1631.

Pesquero, MD, Alberdi, MT & Alcalá, L 2006, 'New species of Hipparion from La Roma 2 (Late Vallesian; Teruel, Spain): a study of the morphological and biometric variability of Hipparion primigenium', *Journal of Paleontology*, vol.80(2), pp.343-356.

Pevzner, MA & Vangengeim, EA 2001, 'Age of some European localities with elephant remains determined by the biometric method', *the World of Elephant International Congress: proceedings of a conference*, Rome, pp.129-132.

Pocket Dentistry 2015, *Tusks and ivory*, www.pocketdentistry.com. Available from: http://pocketdentistry.com/2-tusks-and-ivory/. [10 June, 2015].

Pojeta, J & Springer, D 2001, *Evolution and the fossil record*, The Paleontological Sociaty, American Geological Institute.

Polly, P 2012, *A basic geometric morphometric analysis, step by step in R*, Indiana University.

Prothero, D & Sereno, P 1982, 'Allometry and Paleoecology of Medial Miocene Dwarf Rhinoceroses from the Texas Gulf Coastal Plain', *Paleobiology*, vol.8(1), pp.16-30.
Qian, G, Gabor, G & Gupta, R 1994, 'Principal components selection by the criterion of the minimum mean difference of complexity', *J. Multiv. Anal.*, vol.49, pp.55-75.
Rainboth, WJ 1991, *Cyprinids of South East Asia. Cyprinid Fishes: Systematics, Biology and Exploitation*, Chapman & Hall, London.
Ren, L & Hutchinson, J 2008, 'The three-dimensional locomotor dynamics of African (Loxodonta africana) and Asian (Elephas maximus) elephants reveal a smooth gait transition at moderate speed', *The Royal Society Interface*, vol.5, pp.195-211.
Rohland, N, Reich, D, Mallick, S, Meyer, M, Green, RE, Georgiadis, NJ, Roca, AL & Hofreiter, M 2010, 'Genomic DNA sequences from mastodon and woolly mammoth reveal deep speciation of forest and savanna elephants, *PLoS Biol*, vol.8, pp.1-10.
Roth, V 1992, 'Quantitative variation in elephant dentitions: implications for the delimitation of fossil species, *Paleobiology*, vol.18, pp.184-202.
Saegusa, H 1995, 'Phylogenetic Relationships of Stegodon and Sinomastodon (Proboscidea, mammalia) of the Mainland of East Asia', *International Symposium of Biogeography of Vertebrates in Indonesian Islands and adjacent Area & Comparative Anatomy of Early Hominids and other Mammals: proceeding of a conference*, Kashiwa, Japan.
Saegusa, H, Thasod, Y & Ratanasthien, B 2005, 'Notes on Asian Stegodontids, *Quaternary International*, vol.126-128, 31-48.
Sartono, S 1969, 'Stegodon timorensis: A pygmy specimen from Timor (Indonesia)', *Kon. Ned. Akad. Wet.* Amsterdam, vol.72, pp.192-202.
Sartono, S 1979, 'The discovery of a pygmy Stegodon from Sumba, East Indonesia: an announcement', *Mod. Quaternary Res. SE Asia*, vol.5, pp.57-63.
Scheid, RC 2012, *Woelfel's dental anatomy*, Lippincott Williams & Wilkins.
Schuenke, M, Schulte, E, Schumacher, U, Ross, LM & Lamperti, ED 2006, *General Anatomy and Musculoskeletal System (Thieme Atlas of Anatomy Series)*, Thieme Publishing Group.
Setiyabudi, E, Kurniawan, I, Aziz, F, Suryana, T, Octariani, H & Prasetyo, U 2012, Peninjauan lanjut di lokasi penemuan fosil gajah di daerah Setu, Kabupaten Bekasi, Jawa Barat, Internal field report, Museum Geologi, Badan Geologi. Bandung.
Sharma, S. (1995). *Applied multivariate techniques*: John Wiley & Sons, Inc.
Shil, S, Quasem, M, Rahman, M, Kibria, A, Uddin, M & Ahasan, A 2013, 'Macroanatomy of the bones of pelvis and hind limb of an Asian Elephant (Elephas maximus)', *Int. J. Morphol.*, vol.31**,** pp.1473-1478.
Shindo, T & Mori, M 1956, 'Musculature of Indian Elephant', *Okajimas folia anatomica japonica*, vol.28, pp.115-147.
Shoshani, J 1998, 'Understanding proboscidean evolution: a formidable task', *Trends in Ecology and Evolution*, vol.13(12), pp.480–487.
Shoshani, J 2002, *Proboscidea (Elephants)*, John Wileys and Sons, Ltd.
Shoshani, J & Eisenberg, J 1982, 'Elephas maximus', *Mammalian Species*, vol.182, pp.1-8.
Shoshani, J & Tassy, P 2005, 'Advances in proboscidean taxonomy & classification, anatomy & physiology, and ecology & behaviour', *Quaternary International*, vol.126-28, pp.5-20.
Shoshani, J, Walter, R, Abraha, M, Berhe, S, Tassy, P, Sanders, WJ, Marchant, GH, Libsekal, Y, Ghirmai, T & Zinner, D 2006, 'A proboscidean from the Late Oligocene of Eritrea, a "missing link" between early Elephantiformes and Elephantimorpha, and biogeographic implication', *PNAS*, vol.103(46), pp.17296-17301.

Smuts, MMS & Bezuidenhout 1994, 'Osteology of the pelvic limb of the African elephant (Loxodonta Africana)', *Onderstepoort Journal of Veterinary Research,* vol.61, pp.51-66.

Sondaar, P 1977, 'Insularity and and its effect on mammal evolution', *Hectht, MK. Goody, PC, Hecht, BM. (eds).Major patterns in vertebrata evolution,* Plenum, New York, pp. 671-707.

Sondaar, P 1981, 'The Geochelone faunas of the Indonesian Archipelago and their paleogeographical and biostratigraphical significance', *MQRSEA,* vol.6, pp.111-120.

Sukumar, R 2003, *The Living Elephants: Evolutionary Ecology, Behavior, and Conservation*, Oxford University Press, New York.

Stat 505 2016, *Interpretation of the principal components*. Pennstate EberlyCollege of Science.Available from: https://onlinecourses.science.psu.edu/stat505/node/54. [10 January 2016].

Thomas, M, Hagelberg, E, Jones, H, Yang, Z & Lister, A 2000, 'Molecular and morphological evidence on the phylogeny of the Elephantidae', *Proc. R. Soc. Lond. B Biol. Sci.*, vol.267**,** pp.2493-2500.

Tibar, L & Leunig, M 2012, 'Instructional hip: The pathoanantomy and arthroscopic management of femoracetabular impingement', *Bone Joint Res.,* vol.1, pp.245-257.

Todd, NE 2010, 'Qualitative Comparison of the Cranio-Dental Osteology of the Extant Elephants, Elephas Maximus (Asian Elephant) and Loxodonta africana (African Elephant)', *The Anatomical Record,* vol.293, pp. 62-73.

van Bemmelen, R 1949, *The Geology of Indonesia,* Vol. IA, Government Printing Office, The Hague.

van den Bergh, G, Awe, R, Morwood, MJ, Sutikna, T, Jatmiko & Saptomo, E 2008, 'The youngest Stegodon remains in Southeast Asia from the Late Pleistocene archaeological site Liang Bua, Flores, Indonesia', *Quatern. Intl.*, vol.182, pp.16-48.

van den Bergh, G, de Vos, J, Aziz, F & Morwood, M 2001, Elephantoidea in the Indonesian region: new Stegodon, findings from Flores. *the World of Elephant International Congress: proceedings of a conference,* Rome, pp.623-627.

van den Bergh, G, de Vos, J & Sondaar, P 2001, 'The late quaternary paleogeography of mammal evolution in the Indonesian Archipelago', *Palaeodiversity,* vol.171, pp.385-408.

van den Bergh, GD 1999, The Late Neogene elephantoid-bearing faunas of Indonesia and their palaeozoogeographic implications; a study of the terrestrial faunal succession of Sulawesi, Flores and Java, including evidence for early hominid dispersal east of Wallace's Line, *Scripta Geologica,* vol.117, pp.1-419.

van den Bergh, GD, Meijer, HJ, Due Awe, R, Morwood, MJ, Szabó, K, Van den Hoek Ostende, LW, Sutikna T, Saptomo, EW, Piper PJ, Dobney, KM 2009, 'The Liang Bua faunal remains: a 95k. yr. sequence from Flores, East Indonesia', *Journal of Human Evolution,* vol.57(5), pp.527-537.

van den Bergh, G D & Kurniawan, I 2010, A partial elephant skeleton and skull from the Menden Alluvial Terrace near Sunggu village, Solo River valley, east Central Java, Internal field report, UOW, Australia.

van der Geer, A, Lyras, G, de Vos, J & Dermitzakis, M 2010, *Evolution of Island Mammals: adaptation and extinction of placental mammals on islands*, Wiley-Blackwell, UK.

van der Geer, A, van den Bergh, G, Lyras, G, Prasetyo, U, Due, R, Setiyabudi, E & Drinia, H. 2016, 'The effect of area and isolation on insular dwarf proboscideans', *Journal of Biogeography*, vol. 43, pp.1656-1666.

van der Maarel, FH 1932, *Contribution to the knowledge of the fossil mammalian fauna of Java* (Vol. 15), Dienst Mijnbouw, Ned.-Indie.

van Heekeren, H 1958, 'The Tjabengè Flake Industry from South Celebes', *Asian Perspectives,* vol.2(2), pp.77-81.

Vergiev, S & Markov, G 2010, 'A mandible of Deinotherium (Mammalia - Proboscidea) from Aksakovo near Varna, Northeast Bulgaria', *Palaeodiversity,* vol.3, pp.241–247.

Villa, P, Soto, E, Santonja, M, Perez-Gonzales, A, Mora, R, Parcerisas, J & Sese, C 2005, 'New data from Ambrona: closing the hunting versus scavenging debate', *Quaternary International,* vol.126-128, pp.223-250.

Voris, H 2000, 'Maps of Pleistocene sea levels in Southeast Asia: shorelines. river systems and durations', *Journal of Biogeography,* vol.27, pp.1153–1167.

Wallace, A 1881, *Island life or the phenomena and causes of insular faunas and floras including a revision and attempted solution of the problem of geological climates*, Macmillan, London.

Weissengruber, G, Fuss, F, Egger, G, Stanek, G, Hittmair, K & Forstenpointner, G 2006, 'The elephant knee joint: morphological and biomechanical considerations', *J. Anat.*,vol. 208(1), pp.59-72.

Wiley, DF, Amenta, N, Alcantara, DA, Ghosh, D, Kil, YJ, Delson, E, Harcourt-Smith W, Rohlf FJ, St. John, K & Hamann, B 2005, 'Evolutionary morphing, *IEEE Visualization, proceedings of IEEE Visualization*, pp. 431-438.

Zhang, X, Brian, E & Wang, J 2015, *Structural and Functional features of Major Synovial Joints and Their Relevance to Osteoarthritis*. Intech. Available from: http://cdn.intechopen.com/pdfs-wm/48174.pdf. [3 Jaunary 2015].

APPENDIX A:

NORMALIZED DATA OF SPECIMENS

Table 1. Identified femur biometric measurement results with ordinary (11) measurement variables after changed to normality form.

No	Specimen	Specimen Code	Reference Code	Measurement parameters										
				F1	F2	F3	F4	F5	F6	F7	F8	F9	F10	F11
1	*Elephas maximus* 1	EM1	MGB-EM	-0.41	-0.25	-0.09	-0.75	0.06	-0,31	0.33	0.18	-0.09	0.00	0.31
2	*Elephas maximus* 2	EM2	MB-UGM-EM	-0.53	-1.15	-0.89	-0.79	-0.80	-0,53	-0.10	-0.55	-0.54	-0.50	-0.61
3	*Elephas hysudrindicus*	EH	MGB-EH	1.63	1.69	1.31	1.54	1.98	1,78	2.17	1.65	1.98	2.18	1.84
4	*Stegodon florensis* 1	SF1	MM14-F619	0.00	0.21	0.45	-0.19	-0.04	-0,03	-0.18	-0.24	-0.07	-0.06	-0.37
5	*Stegodon florensis* 2	SF2	MM11-T23BF176	-0.08	0.01	-0.09	-0.08	-0.14	-0,10	-0.31	-0.13	-0.22	-0.13	0.29
6	*Stegodon florensis* 3	SF3	MGB DD4188	-0.53	-0.37	-0.35	-0.08	-0.50	-0,42	-0.45	-0.63	-0.64	-0.36	-0.53
7	*Stegodon sondaari*	SS	TT12-FF3A	-2.01	-1.86	-2.22	-1.88	-1.86	-2,06	-1.94	-2.06	-1.89	-1.88	-2.05
8	*Stegodon trigonocephalus* 1	ST1	MGB-K-ST-FS	0.63	0.40	0.65	0.53	0.16	0,49	0.18	0.68	0.53	0.23	0.29
9	*Stegodon trigonocephalus* 2	ST2	MGB-K-ST-FD	1.04	0.47	0.78	1.13	0.72	0,74	0.18	0.84	0.56	0.51	0.37
10	*Sinomastodon bumiajuensis*	SINO	MGB-M	0.26	0.85	0.45	0.56	0.41	0,45	0.12	0.26	0.38	0.00	0.47

Table 2. Identified tibia biometric measurement results with ordinary (5) measurement variables after changed to normality form.

No	Specimen	Specimen Code	Reference Code	Measurement parameters				
				T1	T2	T3	T4	T5
1	*Elephas maximus* 1	EM1	MGB-EM	-0.16	-0.21	0.08	-0.53	0.71
2	*Elephas maximus* 2	EM2	MB-UGM-EM	-0.57	-0.77	-0.58	-1.03	-0.22
3	*Elephas hysudrindicus*	EH	MGB-EH	1.79	1.11	1.58	1.11	1.60
4	*Stegodon florensis* 4	SF4	MM05-1	-0.34	0.02	-0.36	-0.53	-0.56
5	*Stegodon sondaari*	SS	TT12-FF18	-1.86	-2.02	-1.77	-1.74	-1.82
6	*Stegodon trigonocephalus* 3	ST3	MGB-K-ST-TS	-0.08	0.06	0.17	-0.26	-0.54
7	*Stegodon trigonocephalus* 4	ST4	MGB-K-ST-TD	-0.04	0.12	0.17	0.02	-0.33
8	*Elephas* sp.	ESang5	ELP0983	1.35	1.67	1.58	1.00	1.35
9	*Stegodon* sp. Sangiran	SSang6	Reg1965 Inv187	-0.18	-0.34	-0.36	0.73	-0.11
10	*Stegodon* sp. Patiayam	SPT	MPT-TS	0.10	0.35	-0.49	1.22	-0.08

Table 3. Identified femur biometric measurement results with three new variables after changed to normality form.

No	Specimen	Specimen Code	Reference Code	Measurement parameters													
				F1	F2	F3	F4	F5	F6	F7	F8	F9	F10	F11	F12	F13	F14
1	*Elephas maximus* 1	EM1	MGB-EM	-0.41	-0.25	-0.09	-0.75	0.06	-0.31	0.33	0,18	-0.09	0.00	0.31	-1.48	0.95	-1.51
2	*Elephas maximus* 2	EM2	MB-UGM-EM	-0.53	-1.15	-0.89	-0.79	-0.80	-0.53	-0.10	-0,55	-0.54	-0.50	-0.61	-1.48	1.18	-1.16
3	*Elephas hysudrindicus*	EH	MGB-EH	1.63	1.69	1.31	1.54	1.98	1.78	2.17	1,65	1.98	2.18	1.84	-0.67	0.95	-0.47
4	*Stegodon florensis* 1	SF1	MM14-F619	0.00	0.21	0.45	-0.19	-0.04	-0.03	-0.18	-0,24	-0.07	-0.06	-0.37	0.47	-0.77	0.41
5	*Stegodon florensis* 2	SF2	MM11-T23BF176	-0.08	0.01	-0.09	-0.08	-0.14	-0.10	-0.31	-0,13	-0.22	-0.13	0.29	0.47	-0.77	0.55
6	*Stegodon florensis* 3	SF3	MGB DD4188	-0.53	-0.37	-0.35	-0.08	-0.50	-0.42	-0.45	-0,63	-0.64	-0.36	-0.53	0.31	-0.77	0.06
7	*Stegodon sondaari*	SS	TT12-FF3A	-2.01	-1.86	-2.22	-1.88	-1.86	-2.06	-1.94	-2,06	-1.89	-1.88	-2.05	-0.50	1.52	-1.05
8	*Stegodon trigonocephalus* 1	ST1	MGB-K-ST-FS	0.63	0.40	0.65	0.53	0.16	0.49	0.18	0,68	0.53	0.23	0.29	0.63	-0.77	0.84
9	*Stegodon trigonocephalus* 2	ST2	MGB-K-ST-FD	1.04	0.47	0.78	1.13	0.72	0.74	0.18	0,84	0.56	0.51	0.37	0.63	-0.77	1.47
10	*Sinomastodon bumiajuensis*	SINO	MGB-M	0.26	0.85	0.45	0.56	0.41	0.45	0.12	0,26	0.38	0.00	0.47	1.61	-0.77	0.86

Table 4. Identified tibia biometric measurement results with three new variables after changed to normality form.

No	Specimen	Specimen Code	Reference Code	Measurement parameters							
				T1	T2	T3	T4	T5	T6	T7	T8
1	*Elephas maximus* 1	EM1	MGB-EM	-0.16	-0.21	0.08	-0.53	0.71	-1.18	-0.46	-1.77
2	*Elephas maximus* 2	EM2	MB-UGM-EM	-0.57	-0.77	-0.58	-1.03	-0.22	-1.38	-0.79	-1.10
3	*Elephas hysudrindicus*	EH	MGB-EH	1.79	1.11	1.58	1.11	1.60	-0.19	1.33	-0.35
4	*Stegodon florensis* 4	SF4	MM05-1	-0.34	0.02	-0.36	-0.53	-0.56	0.70	-0.45	0.18
5	*Stegodon sondaari*	SS	TT12-FF18	-1.86	-2.02	-1.77	-1.74	-1.82	-1.28	-2.02	-0.77
6	*Stegodon trigonocephalus* 3	ST3	MGB-K-ST-TS	-0.08	0.06	0.17	-0.26	-0.54	0.70	0.05	1.15
7	*Stegodon trigonocephalus* 4	ST4	MGB-K-ST-TD	-0.04	0.12	0.17	0.02	-0.33	0.86	0.13	0.84
8	*Elephas* sp.	ESang5	ELP0983	1.35	1.67	1.58	1.00	1.35	-0.32	1.28	-0.12
9	*Stegodon* sp. Sangiran	SSang6	Reg1965 Inv187	-0.18	-0.34	-0.36	0.73	-0.11	1.02	0.48	1.02
10	*Stegodon* sp. Patiayam	SPT	MPT-TS	0.10	0.35	-0.49	1.22	-0.08	1.08	0.46	0.92

Table 5. Identified and unidentified femur biometric measurement results with 14 variables after changed to normality form.

No	Specimen	Code		Measurement parameters													
				F1	F2	F3	F4	F5	F6	F7	F8	F9	F10	F11	F12	F13	F14
1	*Elephas maximus* 1	EM1	MGB-EM	-0.76	-0.49	-0.44	-1.16	-0.19	-0.71	0.03	-0.17	-0.46	-0.30	-0.14	-1.94	1.29	-1.96
2	*Elephas maximus* 2	EM2	MB-UGM-EM	-0.88	-1.40	-1.05	-1.20	-1.05	-0.93	-0.41	-0.92	-0.89	-0.84	-1.04	-1.94	1.55	-1.57
3	*Elephas hysudrindicus*	EH	MGB-EH	1.42	1.47	0.62	1.10	1.73	1.34	1.90	1.32	1.52	2.04	1.37	-1.04	1.29	-0.83
4	*Stegodon florensis* 1	SF1	MM14-F619	-0.32	-0.03	-0.04	-0.60	-0.29	-0.43	-0.49	-0.60	-0.44	-0.38	-0.81	0.22	-0.69	0.12
5	*Stegodon florensis* 2	SF2	MM11-T23BF176	-0.40	-0.23	-0.44	-0.49	-0.39	-0.50	-0.62	-0.49	-0.58	-0.45	-0.16	0.22	-0.69	0.27
6	*Stegodon florensis* 3	SF3	MGB DD4188	-0.88	-0.62	-0.64	-0.49	-0.75	-0.81	-0.77	-1.00	-0.98	-0.70	-0.97	0.04	-0.69	-0.25
7	*Stegodon sondaari*	SS	TT12-FF3A	-2.47	-2.11	-2.06	-2.27	-2.11	-2.42	-2.28	-2.45	-2.18	-2.32	-2.47	-0.86	1.95	-1.46
8	*Stegodon trigonocephalus* 1	ST1	MGB-K-ST-FS	0.35	0.16	0.12	0.10	-0.09	0.08	-0.13	0.34	0.14	-0.06	-0.16	0.40	-0.69	0.59
9	*Stegodon trigonocephalus* 2	ST2	MGB-K-ST-FD	0.79	0.23	0.22	0.69	0.47	0.32	-0.13	0.49	0.16	0.24	-0.08	0.40	-0.69	1.28
10	*Sinomastodon bumiajuensis*	SINO	MGB-M	-0.05	0.62	-0.04	0.13	0.16	0.03	-0.18	-0.09	-0.01	-0.30	0.02	1.49	-0.69	0.61
11	Bekasi femur	uBF	MGB-Bekasi	0.27	0.23	-0.04	0.10	-0.29	0.03	-0.38	-0.09	-0.34	-0.38	-0.16	0.22	-0.69	1.18
12	Patiayam femur	uPT	MPT-FS	0.75	0.62	0.12	0.84	0.67	0.96	0.81	0.10	1.31	1.20	0.54	0.95	-0.30	0.50
13	Sangiran femur 1	uSang1	Reg225inv1388	-0.01	0.10	0.07	0.47	0.47	0.54	0.31	0.69	0.71	0.49	0.88	0.22	-0.69	0.68
14	Sangiran femur 2	uSang2	Elp0183	-0.44	-0.42	0.37	-0.16	-0.54	-0.27	-0.11	0.02	-0.36	-0.13	0.18	0.40	-0.69	-0.44
15	Sangiran femur 3	uSang3	Inv1712	-0.01	-0.81	-0.64	0.06	-0.49	-0.13	-0.18	0.10	-0.29	-0.16	0.23	0.40	-0.30	0.14
16	Sangiran femur 4	uSang4	Reg485inv1327	0.87	0.49	2.75	1.02	0.52	1.07	0.54	0.61	1.00	0.44	1.06	1.49	-0.56	1.40
17	Ngandong femur	uNG	MGB-K-FNG	1.78	2.18	1.13	1.87	2.19	1.82	2.11	2.14	1.69	1.62	1.73	-0.68	1.29	-0.27

Table 6. Identified and unidentified tibia biometric measurement results with eight variables after changed to normality form.

No	Specimen	Specimen Code	Reference Code	Measurement parameters							
				T1	T2	T3	T4	T5	T6	T7	T8
1	*Elephas maximus* 1	EM1	MGB-EM	-0.28	-0.29	-0.09	-0.63	0,52	-1.23	-0.56	-1.75
2	*Elephas maximus* 2	EM2	MB-UGM-EM	-0.67	-0.86	-0.68	-1.12	-0,35	-1.43	-0.89	-1.07
3	*Elephas hysudrindicus*	EH	MGB-EH	1.61	1.06	1.26	1.00	1,35	-0.19	1.22	-0.30
4	*Stegodon florensis* 4	SF4	MM05-1	-0.45	-0.05	-0.48	-0.63	-0,66	0.75	-0.54	0.25
5	*Stegodon sondaari*	SS	TT12-FF18	-1.91	-2.14	-1.75	-1.82	-1,84	-1.33	-2.11	-0.73
6	*Stegodon trigonocephalus* 3	ST3	MGB-K-ST-TS	-0.20	-0.02	-0.01	-0.36	-0,64	0.75	-0.05	1.25
7	*Stegodon trigonocephalus* 4	ST4	MGB-K-ST-TD	-0.16	0.05	-0.01	-0.09	-0,45	0.92	0.03	0.92
8	*Elephas* sp.	ESang5	ELP0983	1.18	1.64	1.26	0.89	1,12	-0.32	1.17	-0.06
9	*Stegodon* sp. Sangiran	SSang6	Reg1965 Inv187	-0.30	-0.42	-0.48	0.62	-0,25	1.09	0.37	1.12
10	*Stegodon* sp. Patiayam	SPT	MPT-TS	-0.03	0.29	-0.60	1.10	-0,21	1.15	0.35	1.01
11	Ngandong tibia	uNG	MGB-K-TNG	1.22	0.73	1.58	1.05	1,41	-0.16	1.01	-0.64

APPENDIX B:

SPECIMEN REMARKS AND FIGURES

Proboscidean 1

Specimen Code : EM1
Reference Collection : MGB-EM
Repository : Museum Geology Bandung
Genera and Species : *Elephas maximus*
Anatomy : Dextral
Geological Age : Recent

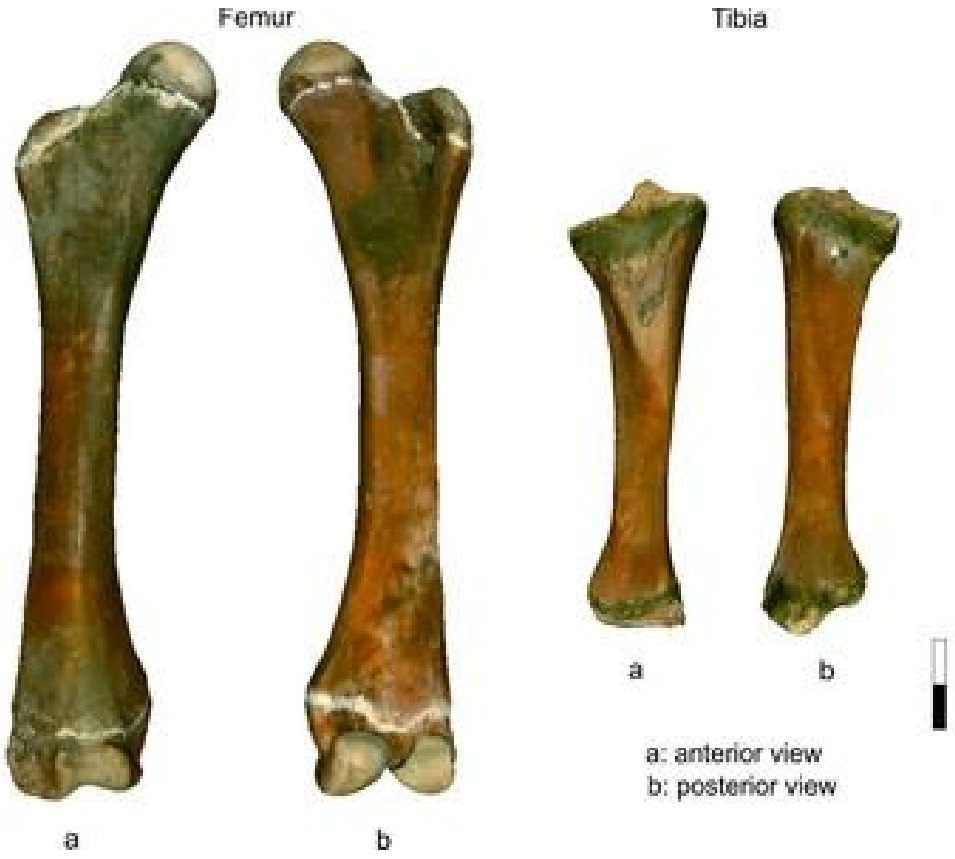

Scale = 10cm

Description:
These specimens are part of a full skeleton. They belong to a 15 year old male *Elephas maximus* from the Elephant Conservation Center in Waykambas, Sumatra. The femur preservation is good. The diaphysis is not fused with both epiphyses. The scar for muscle and tendon attachment is distinguishable. The tibia preservation is good. The diaphysis are not fused with the epiphyses. The scar for muscle and tendon attachment is distinguishable.

Proboscidean 2

Specimen Code : EM2
Reference Collection : MB-UGM-EM
Repository : Museum Biology, Gajah Mada University, Yogyakarta
Genera and Species : *Elephas maximus*
Anatomy : Dextral
Geological Age : Recent

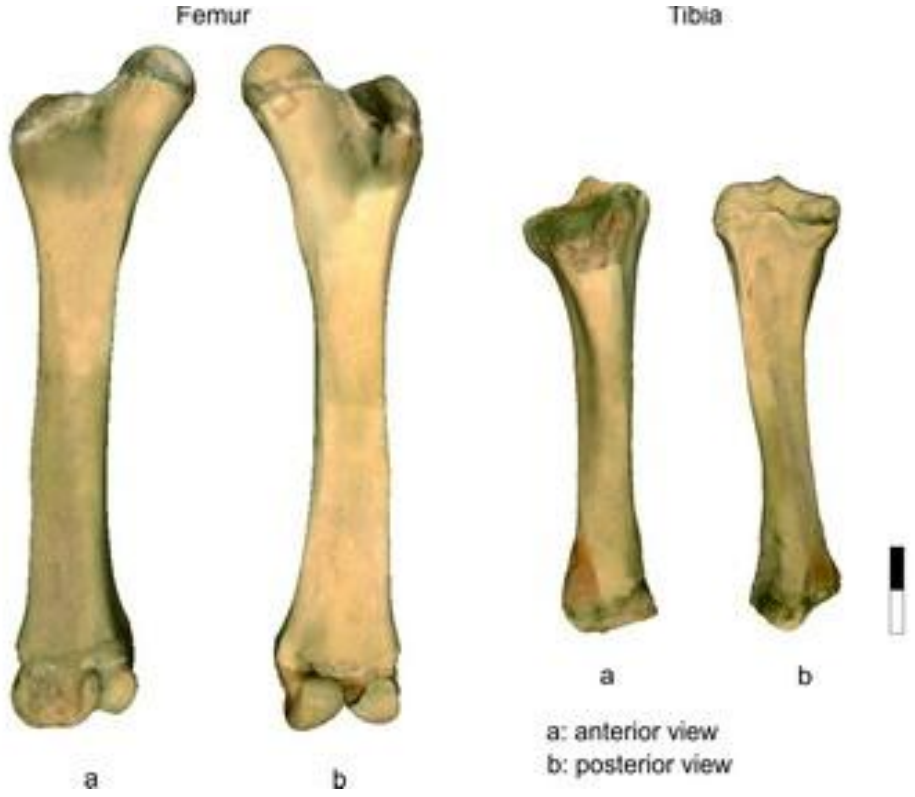

Scale = 10cm

Description:
This specimen is a part of a full skeleton. Its belongs to a 29 year old female *Elephas maximus* that was kept as a pet in the Mataram/Yogyakarta Kingdom. Its skeleton was donated to the Biology Museum of Gajah Mada University, Yogyakarta. The preservation of both femur and tibia are good. In the femur the diaphysis is fused with the distal epiphysis but not with the proximal epiphysis. The scars for muscle and tendon attachment still can be easily traced. In the tibia the diaphysis is not fused with both epiphyses. The scar for muscle and tendon attachment still can be traced.

Proboscidean 3

Specimen Code : EH
Reference Collection : MGB-EH
Repository : Museum Geology Bandung
Genera and Species : *Elephas hysudrindicus*
Anatomy : Dextral
Geological Age : Early Late Pleistocene

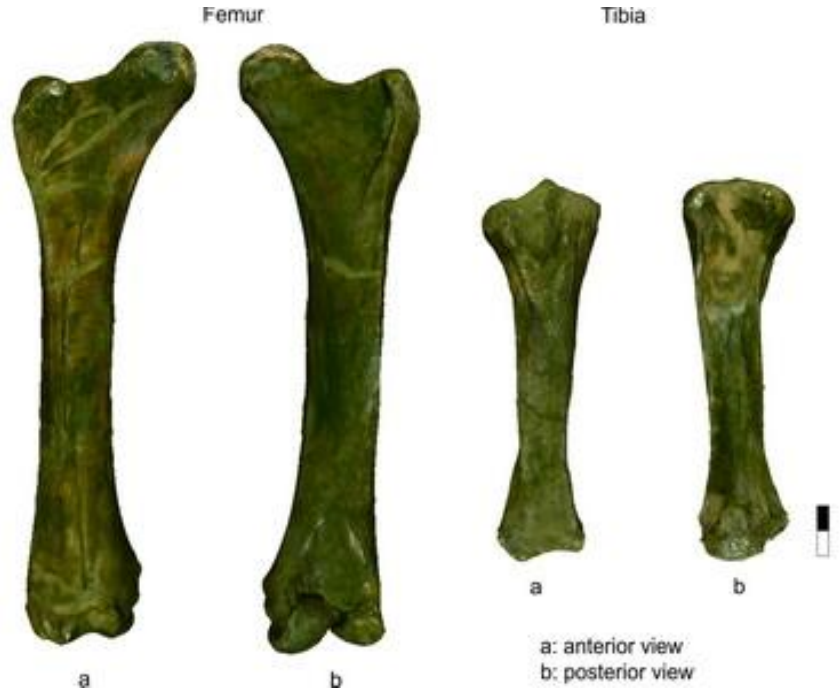

Scale = 10cm

Description:
This specimen belongs to an almost 90% complete of skeleton. Its comes from the river terrace of the Bengawan Solo River, located in the Sunggun Site excavation in Blora, Java. The preservation is moderate. The edges of both the proximal and distal epiphyses are slightly abraded. Some part in the diaphysis shaft had cracks but these have been restored with gypsum after excavation by a museum technician. The diaphysis is fused with the epiphyes. The scars for muscle and tendon attachment are not clear because the surface is slightly eroded. The tibia preservation is good. The diaphysis not fused with the epiphyes. Some location of the scar for muscle and tendon attachment are abraded while the groove that the place for medial collateral ligament attachment is recognizable. Based on the dental wear of its molars this individual was estimated to be 49 AEY old. The pelvis morphology and the large tusk size shows this to be a male individual.

Proboscidean 4

Specimen Code : ESang5
Reference Collection : ELP0983
Repository : Museum Sangiran
Genera and Species : *Elephas* sp.
Anatomy : Dextral
Geological Age : Upper Pleistocene
.

Scale = 10cm

Description:

This specimen comes from the Sangiran area. The geological age is unknown. The identification is only at the genus level (*Elephas*). The preservation is good and even the edges of the proximal and distal part are in good condition. Some parts of the diaphysis shaft have cracks but still preserve the original shape. The diaphyses are fused with the epiphyses. The scar for muscle and tendon attachment is clear and can be observed.

Proboscidean 5

Specimen Code : SF1
Reference Collection : MM14F619
Repository : Museum Geology Bandung
Genera and Species : *Stegodon florensis* 1
Anatomy : Sinistral (flipped to dextral view)
Geological Age : Middle Pleistocene

Scale = 10cm

Description:

This specimen is from the Matamenge excavation site, So'a Basin, Flores. This specimen is described as *Stegodon florensis* based on the teeth that were found together with this specimen. The preservation is good. No cracks were found but some parts of the edges have abraded. The abraded locations have been reconstructed using gypsum by a museum technician. The proximal and distal epiphyses are fused with the diaphysis. The scar for muscle, tendon or ligament attachment is not clear because the fossil surface is smooth due to the fossilisation process.

Proboscidean 6

Specimen Code : SF2
Reference Collection : MM11T23BF176
Repository : Museum Geology Bandung
Genera and Species : *Stegodon florensis* 2
Anatomy : Dextral
Geological Age : Middle Pleistocene

Scale = 10cm

Description:

This specimen is from the Matamenge excavation site, So'a Basin, Flores. This specimen is described as *Stegodon florensis* based on the teeth that found together with this specimen.The preservation is moderate. The surface areas of both the proximal and distal epiphyses are abraded. The cracks also found along the femur shaft, either longitudinally parallel to the length of the femur, as well as perpendicular to the length. These cracks represent excavation damage, and the broken parts have been restored with glue. Some parts of the distal condyle and in the proximal part of the femur head have been restored with gypsum (white colour) by a museum technician. The proximal and distal epiphyses are fused with the diaphysis. The scar for muscle and tendon attachment is not clear because the fossil surface is eroded.

Proboscidean 7

Specimen Code : SF3
Reference Collection : MGB DD4188
Repository : Museum Geology Bandung
Genera and Species : *Stegodon florensis* 3
Anatomy : Dextral
Geological Age : Middle Pleistocene

Scale = 10cm

Description:

This femur specimen is from Dozodalu site, So'a Basin Flores Island. Collected in 25 November 1997. The preservation is moderate. The proximal part are abraded. Sandstone are still attached in some places, especially at the condyle in the distal part. There is a large single crack perpendicular to the length of the femur shaft near the minimum circumference of the shaft. The proximal and distal epiphyses are fused with the diaphysis. The scar for muscle and tendon attachment is not clear.

Proboscidean 8

Specimen Code : SF4
Reference Collection : MGB-K-ST-TD
Repository : Museum Geology Bandung
Genera and Species : *Stegodon florensis* 4
Anatomy : Sinistral
Geological Age : Middle Pleistocene

Scale = 10cm

Description:

This femur specimen come from Matamenge Site in Ola Bula Formation, So'a Basin, Flores. The preservation is good. The surface part of both the proximal and distal epiphyses are abraded. Some parts of the diaphysis shaft have cracks but still preserve the original shape. The proximal and distal epiphyses are fused with the diaphysis. The scar for muscle and tendon attachment is not clear because the fossil surface is slightly eroded.

Proboscidean 9

Specimen Code : SS
Reference Collection : TT12-FF18
Repository : Museum Geology Bandung
Genera and Species : *Stegodon sondaari*
Anatomy : Dextral
Geological Age : Early Pleistocene - Middle Pleistocene

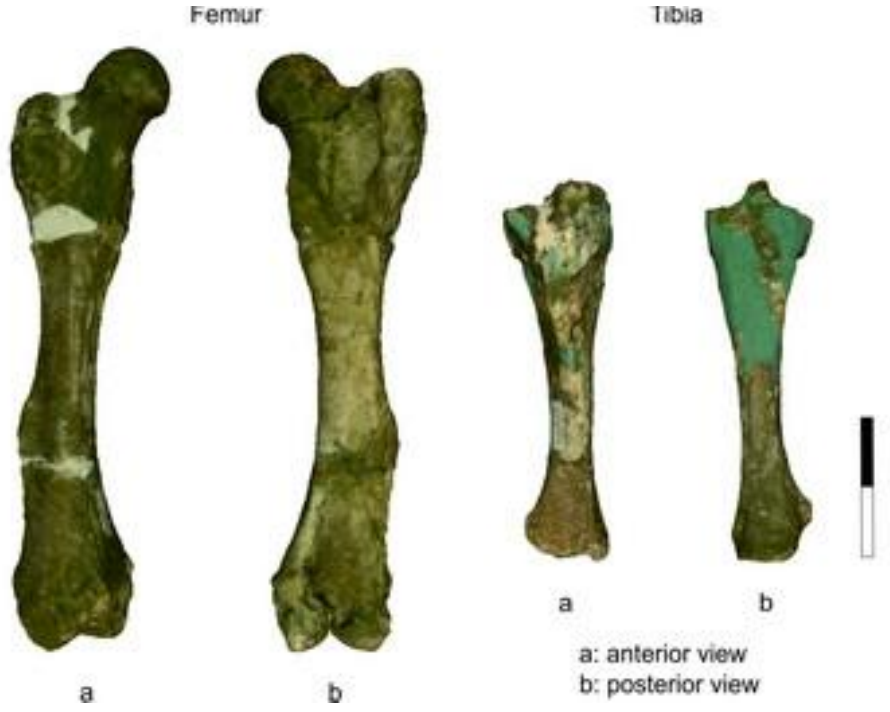

Scale = 10cm

Description:

These specimens are from a single individual from Trench F near Tangi Talo. Age 1.3 Ma (is slightly younger than the Tangi Talo main excavations). MGB Coll Nr. TT12-TF-F3 (femur) and TT12-TF-F18 (tibia). These specimens are described as *Stegodon sondaari* based on the teeth that were found associated with its teeth in the site. The preservation of the femur is moderate. The edges of both the proximal and distal parts are abraded. Some part in the diaphysis shaft had cracks but had been restore with the gypsum after excavation by a museum technician. The proximal and distal epiphyses are fused with the diaphysis. The scar for muscle and tendon attachment is not clear because the fossil surface is eroded. Regarding the tibia, its preservation is poor. The proximal and distal epiphyses are fused with the diaphysis. The scars for muscle and tendon attachment are not clear. The proximal part has a big hole in the posterior part and this gap was filled with green clay prior to 3D scanning.

Proboscidean 10

Specimen Code : ST1
Reference Collection : MG-K-ST-FS
Repository : Museum Geology Bandung
Genera and Species : *Stegodon trigonocephalus* 1
Anatomy : Sinistral (flipped to dextral view)
Geological Age : Late Pleistocene

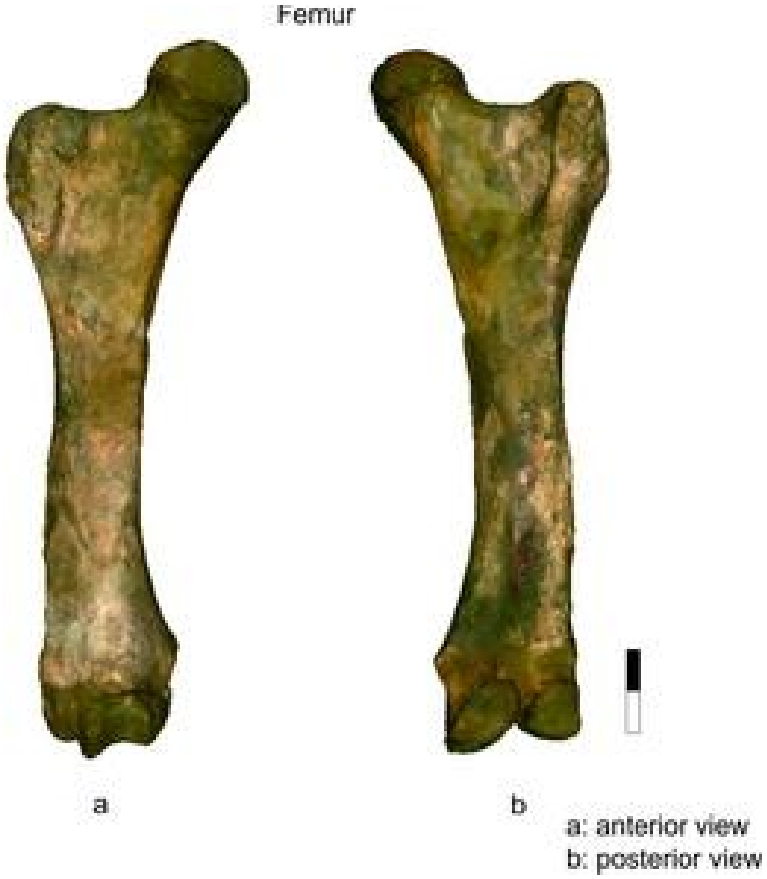

Scale = 10cm

Description:

This specimen is from the Dutch colonial era excavation at the Bengawan Solo terrace in East Java. It is described as *Stegodon trigonocephalus* based on the associated fossils where this specimen was found (von Koenigswald, 1935).The preservation is good. No cracks are found in this specimen, only the edge and head of femur are slightly eroded. The proximal and distal epiphyses are fused with the diaphysis. The scar for muscle and tendon attachment is not clear.

Proboscidean 11

Specimen Code : ST2
Reference Collection : MG-K-ST-FD
Repository : Museum Geology Bandung
Genera and Species : *Stegodon trigonocephalus* 2
Anatomy : Dextral
Geological Age : Late Pleistocene

Scale = 10cm

Description:

This femur specimen is from Dutch collection that excavated from the Bengawan Solo terrace in East Java. Descibed as *Stegodon trigonocephalus* based on the fossil association were this specimen was found (von Koenigswald, 1935). The preservation is moderate. The edges part either proximal and distal have abraded. Some part in the diaphysis especially in anterior distal part of shaft had big cracks but had been restore with the gypsum (dark colour) by Dutch technician in the past. The diaphysis had been fused with the epiphyses. The scar for muscle and tendon attachment is not clear because the fossil surface is slighty eroded.

Proboscidean 12

Specimen Code : ST3
Reference Collection : MGB-K-ST-TS
Repository : Museum Geology Bandung
Genera and Species : *Stegodon trigonocephalus* 3
Anatomy : Sinistral (flipped to dextral view)
Geological Age : Late Pleistocene

Scale = 10cm

Description:

This specimen is from Dutch colonial period, and discovered from the river terrace of the Bengawan Solo River in east Java, likely in Ngandong Site. The preservation is good. No cracks were found. The surface part of both the proximal and distal epiphyses are abraded. The proximal and distal epiphyses are fused with the diaphysis. The scar for muscle and tendon attachment is not clear because the fossil surface is slightly eroded.

Proboscidean 13

Specimen Code : ST4
Reference Collection : MGB-K-ST-TD
Repository : Museum Geology Bandung
Genera and Species : *Stegodon trigonocephalus* 4
Anatomy : Dextral
Geological Age : Late Pleistocene

Scale = 10cm

Description:

This specimen is from Dutch colonial period, and discovered from the river terrace of the Bengawan Solo River in east Java, likely in Ngandong Site.The preservation is moderate. The surface part of both the proximal and distal epiphyses are abraded. Some part in the diaphysis shaft had cracks but had been restore with the gypsum after excavation by a museum technician The diaphysis had been fused with the epiphyses. The scar for muscle and tendon attachment is not clear because the fossil surface slightly eroded.

Proboscidean 14

Specimen Code : SSang6
Reference Collection : Reg1965 Inv187
Repository : Museum Sangiran
Genera and Species : *Stegodon* sp. 4
Anatomy : Dextral
Geological Age : Unkonwn

Scale = 10cm

Specimen:

This specimen is a donation from the local villager Mr. Siswanto to Museum Sangiran. This specimen is discovered from Grogolan, Manyarejo in Sangiran area. The preservation is moderate. The surface part of both the proximal and distal epiphyses are abraded. Some part in the diaphysis shaft had cracks. The diaphysis had been fused with the epiphyses. The scar for muscle and tendon attachment is not clear because the fossil surface is slightly eroded.

Proboscidean 15

Specimen Code : SPT
Reference Collection : MPT-TS
Repository : Museum Patiayam
Genera and Species : *Stegodon* sp.
Anatomy : Sinistral (flipped to dextral view)
Geological Age : Early Pleistocene

Scale = 10cm

Specimen:

This specimen was donated to the Museum Patiayam by local villager Mr. Supeno. This specimen is discovered from Early Pleistocene Slumprit Formation in Slumprit hill, Patiayam region, Central Java. The preservation is good. The surface part of both the proximal and distal epiphyses are abraded. Some part in the diaphysis shaft had cracks but still preserve the original shape. The diaphysis had been fused with the epiphyses. The scar for muscle and tendon attachment is not clear because the fossil surface slightly eroded.

Proboscidean 16

Specimen Code : SINO
Reference Collection : MGB-M
Repository : Museum Geology Bandung
Genera and Species : *Sinommastodon bumiajuensis*
Anatomy : Dextral
Geological Age : Early Pleistocene

Scale = 10cm

Description:

This specimen is described as *Sinomastodon bumiajuensis* based on the teeth that were discovered associated this specimen in the Bumiayu excavation site, Central Java (van den Maarel, 1932). The preservation is good. The specimen was reported broken in the middle into two parts but has been fused by a technician. The broken position is in the minimum circumference where the crack can still be distinguished. Both epiphyses are fused with the diaphysis.

Proboscidean 17

Specimen Code : uBF
Reference Collection : MGB-Bekasi
Repository : Museum Geology Bandung
Genera and Species : Unidentified (Bekasi femur)
Anatomy : Dextral
Geological Age : Pleistocene

Scale = 10cm

Description:

This specimen was donated to the Museum Geology Bandung in 2012 by SMP 3 Setu, Bekasi, The junior high school institution near discovery site. It was discovered in a river terrace in Bekasi, West Java. No other teeth or bone were discovered together with this specimen. The genera is therefore unidentified. The preservation is good. In the middle of the femur shaft there is a crack that has been restored and filled with gypsum by museum technician. The diaphysis had been fused with the epiphyses. The scar for muscle and tendon attachment is not clear because the fossil surface is slightly eroded.

Proboscidean 18

Specimen Code : uPT
Reference Collection : MPT-FS
Repository : Museum Patiayam
Genera and Species : Unidentified (Patiayam femur)
Anatomy : Sinistral (flipped to dextral view)
Geological Age : Early Pleistocene

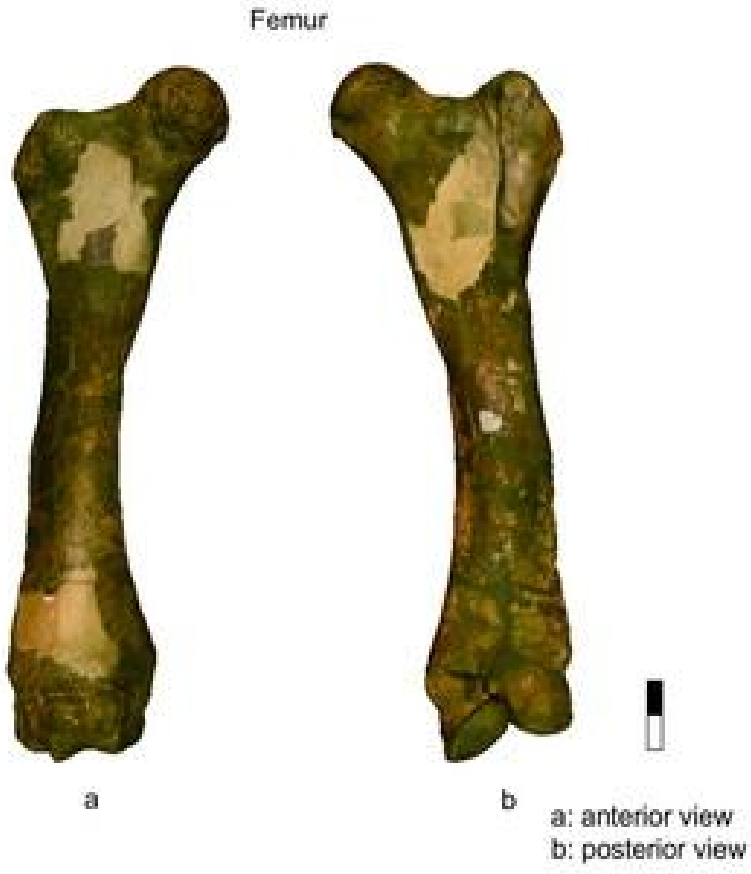

Scale = 10cm

Description:

This specimen was donated to the Museum Patiayam by local villager Mr. Karmijan, This specimen discovered from Early Pleistocene Slumprit Formation in Bukit Slumprit, Patiayam region, Central Java. The preservation is moderate. Some parts of the shaft have major damage specially in the proximal part, but have been restored with gypsum (white colour) by a Patiayam Museum technician. The epiphyses are fused with the diaphyses. The scar for muscle and tendon attachment is not clear because the fossil surface is slightly eroded.

Proboscidean 19

Specimen Code : uSang1
Reference Collection : Reg225inv1388
Repository : Museum Sangiran
Genera and Species : Unidentified (Sangiran femur 1)
Anatomy : Sinistral (flipped to dextral view)
Geological Age : Early Pleistocene

Scale = 10cm

Description:

This specimen is from the Sangiran area. No other fossils or teeth are associated with this specimen. The genera and the geological age is unknown because no documentation exist anymore. The preservation is good. No cracks are present in this specimen. The diaphysis had been fused with the epiphyses. The scar for muscle and tendon attachment is not clear because the fossil surface is slightly eroded.

Proboscidean 20

Specimen Code : uSang2
Reference Collection : Elp0183
Repository : Museum Sangiran
Genera and Species : Unidentified (Sangiran femur 2)
Anatomy : Dextral
Geological Age : Unknown

Scale = 10cm

Description:
This specimen also from Sangiran area. The genera and the geological age of this specimen also not clear. The preservation is moderate. Some parts in the middle of the shaft are cracked but have been restored with gypsum by a museum technician. The diaphysis had been fused with the epiphyses. The scar for muscle and tendon attachment is not clear because the fossil surface is slightly eroded.

Proboscidean 21

Specimen Code : uSang3
Reference Collection : Inv1712
Repository : Museum Sangiran
Genera and Species : Unidentified (Sangiran femur 3)
Anatomy : Sinistral (flipped to dextral view)
Geological Age : Unknown

Scale = 10cm

Description:

This specimen was donated to the Museum Patiayam by local villager Mr. Wasimin. This specimen is also from Sangiran. As with the other specimens from Sangiran, the geological context where this specimen was found is not clear. The preservation is moderate. The surface part of both the proximal and distal epiphyses are abraded. Some part in the diaphysis shaft had cracks but these have been restored with gypsum. The diaphysis had been fused with the epiphyses. The scar for muscle and tendon attachment is not clear because the fossil surface is slightly eroded.

Proboscidean 22

Specimen Code : uSang4
Reference Collection : Reg485inv1327
Repository : Museum Sangiran
Genera and Species : Unidentified (Sangiran femur 4)
Anatomy : Dextral
Geological Age : Early Pleistocene - Middle Pleistocene

Scale = 10cm

Description:

This specimen is discovered from Early Pleistocene - Middle Pleistocene Kabuh Formation in Pucung, Dayu, Gondangrejo Sangiran area. The preservation is moderate. The proximal edges are damaged and abraded. Some parts of the diaphysis shaft have cracks but have been restore with gypsum by a museum technician. The diaphysis had been fused with the epiphyses. The scar for muscle and tendon attachment is not clear because the surface is slightly eroded.

Proboscidean 23

Specimen Code : uNG
Reference Collection : MGB-K-TNG
Repository : Museum Geology Bandung
Genera and Species : Unidentified (Ngandong proboscidea)
Anatomy : Dextral
Geological Age : Early Late Pleistocene

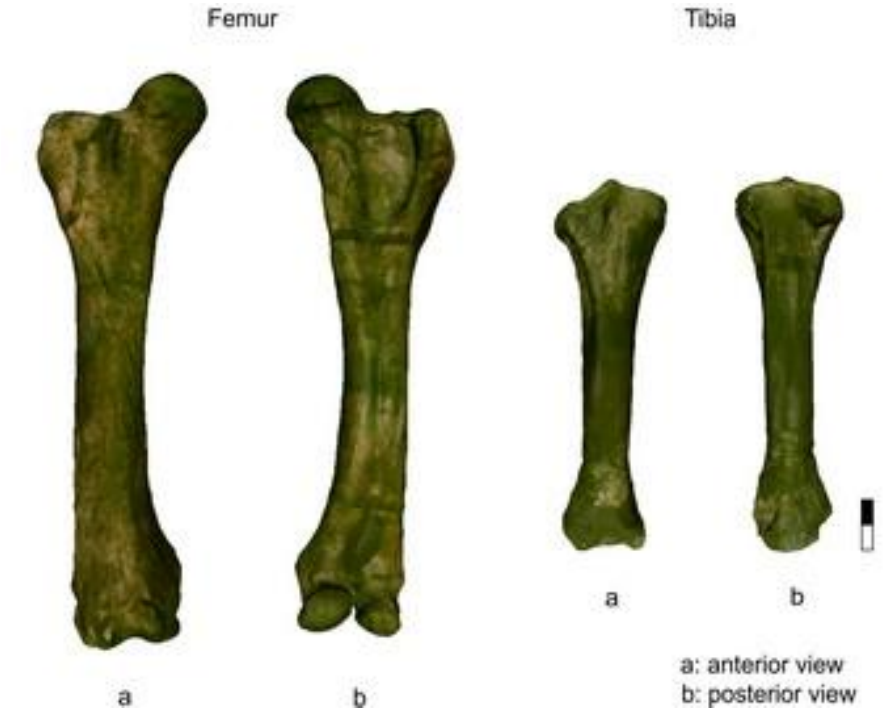

Scale = 10cm

Description:

This femur specimen is from the Dutch collection and was discovered in the Bengawan Solo river terrace at Ngandong, Central Java. The genus is unknown because documentation was destroyed during World War II. The preservation of the femur is moderate. The surface part of both the proximal and distal epiphyses are abraded. Some parts of the diaphysis shaft have small cracks. The diaphysis had been fused with the epiphyses. The scar for muscle and tendon attachment is not clear because the fossil surface is slightly eroded. The tibia is less well-preserved. The middle part of the diaphysis is damaged but restored with gypsum by a museum technician. The diaphysis had been fused with the epiphyses. The scar for muscle and tendon attachment is not clear because the surface is slightly eroded.